A Study of Classical and Novel Markers of Disease in Multiple Sclerosis

By

Ghaniah Z. Hassan-Smith

A thesis submitted to the University of Birmingham for

the degree of

DOCTOR OF PHILOSOPHY (PhD) IN MEDICINE

School of Infection and Immunity

College of Medical and Dental Sciences

University of Birmingham

February 2015

Abstract

Multiple sclerosis (MS) is a chronic inflammatory and degenerative condition of the Central Nervous System. Focal demyelinating lesions are its neuropathological hallmark, but widespread abnormalities found in otherwise "normal-appearing" tissue are better associated with disability outcomes. HMGB1 is a promiscuous sensor of cellular stress, acting as a link between sterile damage and innate immune mechanisms, with its extra-nuclear release producing diverse outcomes.

We report novel findings of significantly increased HMGB1 expression throughout the brain tissue of MS vs. non-MS patients, particularly in macrophages/microglia and oligodendrocytes (OGD). In addition, cerebrospinal fluid HMGB1 levels were increased in early-stage MS patients compared to non-inflammatory control patients. HMGB1 stimulation *in-vitro* upregulates expression of its receptors in an OGD cell line, potentially propagating chronic inflammation. Expression of the Leucine Rich Repeat and Ig-domain-containing molecules, AMIGO-3 and LINGO-1 is also significantly increased by HMGB1 stimulation *in-vitro*. These molecules demonstrate particularly intense immunoreactivity in human brain tissue taken at biopsy, at an early disease stage. Thus, exogenous HMGB1 may influence neurodegenerative processes via AMIGO-3 and LINGO-1 and blocking their function could have therapeutic value. Increased expression of HMGB1 in OGD, however, may highlight endogenous neuroprotective mechanisms in response to an unknown trigger.

For Zaki and Levizah

Acknowledgements

I extend sincere thanks to my supervisors, Dr Mike Douglas and Dr John Curnow, for their guidance and support over the period of study. The project would not have been possible without John's involvement and I am deeply indebted to him for this, and his mentorship. I am also grateful to Mike who, along with Dr Gordon Mazibrada, created this research post and provided an excellent learning environment. In addition, I benefitted greatly from Mike's breadth of knowledge in both scientific technique and clinical neurology and his respect for intellectual freedom was much appreciated.

I am also most grateful to Dr Gordon Mazibrada and Dr John Woolmore for the excellent training in clinical MS. Gordon was incredibly supportive in all aspects of the project, in particular pursuing all educational opportunities. Heartfelt thanks also to Dr Martyn Carey and Dr Santhosh Nagaraju for their patience in dealing with my (many) neuropathological queries, despite ever-present clinical commitments. Thanks also to Alex Sinclair for her support and mentorship.

Many thanks to the UK MS Brain Bank, Hammersmith Hospital and in particular to Professor Richard Reynolds and Dr. Djordje Gveric. Professor Margaret Esiri provided additional control tissue from the Thomas Willis Oxford Brain Collection, and I am most grateful to her for that. Many thanks also to Dr Peter Nightingale who was most helpful in reviewing statistical aspects of the project. Sincere thanks to Jane Steele's fantastic team at the HBRC; I have immense respect for Souad Messahel and Johanna Dieguez Navas, who went out of their way to help with the project. In addition, thanks to Lindsay Durant, Matt Edmunds, Marie Voice, Robert

Barry, Paul Tomlins and Seema Kalra from the Curnow Lab for their much-appreciated input on our collective 'journey'.

The project was only written up due to the help of a stellar supporting cast. Many thanks to my mother and father-in-law who were so generous with their time and help. My wonderful sister and her family offered unwavering support for which we are truly grateful. I would not have produced this document at all without the practical help of my parents and I sincerely thank them for this. More importantly, I thank them for their wisdom, kindness and inspiration, which have influenced me throughout my life.

This thesis is wholly dedicated to Zaki and to Levizah, for being the light of our lives.

Publications arising from the thesis

1. High sensitivity and specificity of elevated cerebrospinal fluid kappa free light chains in suspected multiple sclerosis. **Hassan-Smith G,** Durant L, Tsentemeidou A, Assi LK, Faint JM, Kalra S, Douglas MR, Curnow SJ. *J Neuroimmunol.* 2014 Nov 15;**276**(1-2):175-9.

Conference proceedings

1. High-mobility Group Box 1 (HMGB1) Expression Is Increased In The Normal-appearing Brain Tissue Of Multiple Sclerosis (MS) Patients Vs. Controls. **Ghaniah Z. Hassan-Smith** et al. E-poster oral presentation at ACTRIMS/ ECTRIMS, Boston, September 2014
2. The expression pattern of High-mobility group box 1 (HMGB1) in the normal-appearing brain tissue of Multiple Sclerosis (MS) patients and controls. **Ghaniah Z. Hassan-Smith**, Martyn Carey, Santhosh Nagaraju, Souad Messahel, Gordon Mazibrada Ana-Marie Gonzalez, S. John Curnow and Michael R. Douglas. Association of British Neurologists, May 2014

Table of Contents

List of Figures

Chapter 1

Chapter 2

Chapter 3

Chapter 4

Chapter 5

Chapter 6

List of Tables

Chapter 1

Chapter 2

Chapter 3

Chapter 4

Chapter 5

Chapter 6

Abbreviations

ATP	Adenosine Triphosphate
AL	Active Lesion
ALS	Amyotrophic lateral sclerosis
AMIGO	Amphoterin-induced gene and Open Reading Frame
Anti-MOG	Anti-Myelin-Oligodendrocyte
ANOVA	One-Way Analysis of Variance
BBB	Blood Brain Barrier
BCSFB	Blood Cerebrospinal Fluid Barrier
BDNF	Brain-derived neurotrophic factor
CAL	Chronic Active Lesion
CD	Cluster of Differentiation
CDMS	Clinically Definite Multiple Sclerosis
CIS	Clinically Isolated Syndrome
CNS	Central Nervous System
CSF	Cerebrospinal Fluid
DAB	3,3'-Diaminobenzidine
DAMP	Damage-associated molecular pattern molecule
DMT	Disease Modifying Treatments
DRGN	Dorsal Root Ganglion Neuron
DT	Diffusion Tensor
EAE	Experimental allergic encephalitis
EBV	Epstein Barr Virus
EDSS	Extended Disability Status Score
EEG	Electroencephalography
ELISA	Enzyme-Linked Immunoabsorbance Assay
EMG	Electromyography
FACS	Fluorescence-activated cell sorting
FasL	Fas ligand
FFPE	Formalin Fixed Paraffin Embedded
FLC	Free-Light Chain
GFAP	Glial Fibrillary Acidic Protein
GM	Grey Matter
H&E	Haematoxylin and Eosin
HIF-1α	Hypoxia Inducible Factor 1
HLA	Human Leucocyte Antigen
HMGB1	High Mobility Group Box 1
HSP	Heat Shock Protein
ICAM	Intercellular Adhesion Molecule 1
IFNγ	Gamma-Interferon
IHC	Immunohistochemistry
IL	Interleukin
JAK1	Janus kinase-1

Kv2.1	Potassium voltage-gated channel, Shab-related subfamily, member 1
LFB	Luxol Fast Blue
LINGO-1	Leucine-rich repeat and Ig-domain containing 1
LP	Lumbar Puncture
LPS	Lipopolysaccharide
LRRIg	Leucine-Rich Repeat with Immunoglobulin Domain
LT	Lymphotoxin
MAG	Myelin-Associated Glycoprotein
MAPK	Mitogen-activated protein kinases
MBP	Myelin Basic Protein
MHC	Major Histocompatibility Complex
MMP-9	Matrix metalloproteinase-9
MRI	Magnetic Resonance Imaging
MR	Mannose-Receptor
MS	Multiple Sclerosis
MSA	Multiple system atrophy
MT	Magnetisation Tensor
MTR	Magnetisation Tensor Resonance
mRNA	Messenger Ribonucleic Acid
NABT	Normal-Appearing Brain Tissue
NAGM	Normal-Appearing Grey Matter
NAWM	Normal-Appearing White Matter
NfH	Neurofilament Heavy isoform
NfL	Neurofilament Light isoform
NF-κB	Nuclear Factor Kappa B
NGF	Nerve growth factor
NgR	Nogo-66 Receptor
NLS1	Nuclear localization signal
NO	Nitric Oxide
NMDA	N-methyl-D-aspartate
NMO	Neuromyelitis optica
nNOS	Neuronal Nitric Oxide Synthetase
Nrf-2	Nuclear Erythroid-2 Related Factor 2
OCB	Oligoclonal Bands
OCP	Oral Contraceptive Pill
OGD	Oligodendrocytes
OMGP	Oligodendrocyte Myelin Glycoprotein
OND	Other Neurological Disease
ONID	Other Neurological Inflammatory disease
PAMPs	Pathogen-associated molecular pattern molecules
PAS	Periodic-Acid Schiff
PKR	Double-Stranded RNA Dependent Protein Kinase R
PLP	Proteolipid Protein
PMA	Protein Kinase C Activator 4-6-Phorbol12-Myristate 13-Acetate
PML	Progressive Multifocal Leukoencephalopathy
PPMS	Primary-Progressive Multiple Sclerosis

PRMS	Progressive-Relapsing Multiple Sclerosis
PRR	Pattern recognition receptors
PWM	Peri-lesional white matter
PCR	Polymerase Chain Reaction
PVDF	Polyvinylidene Diflorise
qPCR	Quantitative Polymerase Chain Reaction
RAGE	Receptor Glycation End Product
RCT	Randomised Control Trial
RhoA	Ras Homolog Gene Family, Member A
ROCK1	Rho-Associated, Coiled-Coil Containing Protein Kinase 1
ROS	Reactive Oxygen Species
RR	Annual Relapse Rates
RRMS	Relapsing-Remitting Multiple Sclerosis
RNA	Ribonucleic Acid
RT	Reverse Transcriptase
RTPCR	Reverse Transcriptase Polymerase Chain Reaction
SAH	Subarachnoid Haemorrhage
SDS-PAGE	Sodium Dodecyl Sulphate Polyacrylamide Gel Electrophoresis
SPMS	Secondary Progressive Phase of Multiple Sclerosis
STAT	Signal Transducer and Activator of Transcription
TBI	Traumatic Brain Injury
T2LL	T2-Lesion Load
Th1	T-helper cell 1
TLR	Toll Like Receptors
TMB	Tetramethylbenzidine
TNF-α	Tumour Necrosis Factor-Alpha
UPP	Ubiquitin-Proteasome Pathway
VCAM	Vascular cell adhesion molecule 1
VEPs	Visual Evoked Potentials
WML	White Matter Lesion
WT	Wildtype

1.

General Introduction

1.1 Clinical aspects of MS

1.1.1 History of MS

"17 October 1827.

"To my surprise (in Venice) I one day found a torpor or indistinctness of feeling about the Temple of my left Eye. At Florence I began to suffer from a confusion of sight. About the 6th November the malady increased to the extent of my seeing all objects double. Each eye had its separate visions. Dr. Kissock supposed bile to be the cause: I was twice blooded from the temple by leeches; — purges were administered; One Vomit, and I twice lost blood from the arm.. The malady in my Eyes abated, I again saw all objects naturally in their single state. I was able to go out and walk.."

Excerpt from the diaries of Augustus D'Este (1794-1848), illegitimate grandson of King George III. (Landtblom et al. 2010)

This description of relapses affecting the brainstem over weeks, followed by remission, is the earliest detailed description of MS– related symptoms recorded. It remains as informative for us now as it was likely to have been when presented to the physicians of the time, although our therapeutic armamentarium has certainly evolved over time. His detailed diaries describing the condition commenced in 1822; 16 years before the original depiction of neuropathological changes in the spinal cord occurring in MS by Scottish pathologist Robert Carswell (Carswell 1838). Others subsequently reported either clinical or pathological findings (Compston 1988), but it was Jean Martin Charcot who drew all of this information together using the clinicopathological findings in a single female

patient, in the seminal publication 'Histologie de la sclérose en plaques' (Charcot 1868). The clinical observations he described were particularly prescient, including a formal description of cognitive changes which we now believe are related to cortical changes in MS. Following this, clinical cases were reported by Eugene Devic (1858-1930), Josef Balo (1895-1979), Paulo Ferdinand Schilder (1886-1940) and Otto Marburg (1874-1948) which describe distinct but related conditions to MS. Oligodendrocytes- always difficult to stain for- were the last glial cell to be discovered using a new staining method created by the Spanish pathologist, Pio del Rio Hortega in 1921. In 1935, the first experiments in experimental allergic encephalitis (EAE) were carried out (Rivers & Schwentker 1935) and oligoclonal bands in the spinal fluid were discovered by Elvin Kabat in 1942 (Kabat et al. 1942). This confirmed the link between MS and the immune system and by the 1960s, ACTH was used to manage symptomatic relapses (MILLER et al. 1961). MRI was first used in the early 1980s, rapidly proving itself to be an invaluable biomarker for use in clinical trials and in 1993, the trials results for first injected disease-modifying drug, Betaferon were published (The IFNB Multiple Sclerosis Study Group 1993). Of all the neurological diseases, disease modification has been particularly successful in the management of MS, and has been aggressively pursued since these early studies. They are discussed in more detail in section 1.1.4 of this chapter.

1.1.2 Epidemiology

The mean age of onset is approximately 30 years with 70% of patients manifesting symptoms between ages of 20 and 40. Disease onset is rare before the age of 10 and after 60 years, forming a unimodal, age-specific onset curve. Between 80 and

100,000 patients in the UK have been diagnosed with MS, with approximately 2,500 people newly diagnosed each year. The distribution is not geographically uniform- the greatest incidence tends to be at the extremes of latitude in both northern and southern hemispheres. For example, the prevalence rate in England and Wales is approximately 100 per 100,000, whilst the northern areas of Scotland have a prevalence approaching 200 per 100 000. This strong latitudinal variation has been postulated to be due to sunlight, local microbial flora or even direct infection by specific viruses, though none have been directly proven (Hassan-Smith & Douglas 2011).

Women were previously thought to be two to three times more likely to develop MS than men. Despite extensive research, the reason for this difference was unclear, beyond the standard observations that women are generally more susceptible to autoimmune conditions, and that this predisposition may therefore be hormonally related. Several studies have suggested that oral contraceptive (OCP) use leads to a milder disease course (Gava et al. 2014; Sena et al. 2012). However, more recently, epidemiological data from a prospectively collected cohort failed to demonstrate sexual dimorphism. The authors stated that this difference could be ascribed to the method of data acquisition, and hence the female bias was likely to be untrue (Tintore, Brain 2015).

1.1.3 Risk factors for developing MS

***Genetic*:** Genetic influences on MS are clearly seen in twin studies, where the concordance rate for MS in monozygotic twins is as high as 30%, as compared to 1% for dizygotic twins. The risk of developing MS in first-degree relatives is about 1 in 40, which is 20 times higher than in the general population. For second degree

relatives, the risk falls to around 1 in 100- still approximately 10 times higher than the background rate. Genetically unrelated family members living in the same environment however, exhibit the same risk as the background population (Ebers et al. 2004; Dyment et al. 2004; Sadovnick et al. 1996). However, the converse is also true, as 70% of monozygotic twins are discordant for MS. This suggests that the genetic susceptibility of MS patients likely follows a polygenic heritability pattern. The best described genetic association through extensive genome-side association studies, is with the HLA haplotype DR2 (HLA-DRB1*1501). Despite a clear association, the relative risk of an individual HLA-DR2-positive individual developing MS remains low, and it remains impossible to accurately assess this on the basis of genetic susceptibility alone (Oksenberg et al. 2008; Sawcer et al. 2014).

***Environmental*:** Studies investigating links between environmental factors and MS are difficult to interpret, particularly as migration studies have highlighted that movement of individuals from a high-risk to a low-risk areas prior to puberty confers a degree of protection from developing the disease, and vice versa (Dean & Elian 1997). This suggests that the timing of exposure to environmental factors may be critical in determining subsequent risk - the so-called 'age-of-vulnerability' hypothesis. Reproducible evidence links Epstein-Barr virus (EBV) exposure, smoking and vitamin D levels to the development of MS and are the best established environmental risk factors at present. With respect to EBV, this demonstrates the only consistent association of MS with an infectious trigger. More than 99% of MS patients are EBV-seropositive, but interpretation is complicated by high background rate of infection in the general population which

can reach 95%. There is also dispute over the potential pathogenic mechanism involved in the association of EBV with MS, although immortalisation of autoreactive B cells and molecular mimicry with the CNS as the autoimmune target have been suggested as possible mechanisms (Levin et al. 2005). Recent studies have shown that smoking roughly doubles the risk of developing MS, although possible mechanisms are not clear (Hernán et al. 2001) (Hedström et al. 2009) (Pittas et al. 2009).

Lower serum levels of vitamin D have been associated with increased risk of MS and correlate with disability and brain atrophy in MS (Weinstock-Guttman et al. 2011). It is thought to exert immunomodulatory effects by influencing the number and/or activity of regulatory T lymphocytes. In this context, the previously described latitudinal gradient observed in MS natural history studies is thought to be a consequence of lower serum Vitamin D levels further away from the equator. However, a direct causal relationship is difficult to infer (Douglas et al, 2014).

1.1.4 Clinical presentation

Approximately 85% of patients present with a subacute neurological event, lasting over 24 hours and without evidence of fever, infection or encephalopathy. The symptoms peak in severity within 2-3 weeks and are followed by resolution over subsequent weeks. The first event is usually noted in young adults (aged 20–45 years old) and is termed a clinically isolated syndrome (CIS). One large study found that 46% of patients with CIS presented with long-tract symptoms and signs, 21% with optic neuritis, 10% with a brainstem syndrome and 23% with multifocal abnormalities (Confavreux et al. 2000). Once there is a second neurological event, patients fulfil the criteria for relapsing-remitting MS (RRMS),

hence the term dissemination of relapses in time. In contrast to RRMS, a proportion of patients never experience true relapses or remissions, but instead become gradually disabled over time, and are the 'primary-progressive MS' (PPMS) cohort. They commonly present with progressive limb spasticity and weakness and constitute 10-15% of the MS population (Rice et al. 2013).

Over time, typically 10-15 years, the majority of patients with RRMS find their relapses become less marked or even cease. Instead they note a progressive increase in their disability, usually with worsening gait or mobility due either to predominant ataxia or spasticity. These patients are termed as having entered the secondary progressive phase of MS (SPMS). It remains unclear whether early therapeutic intervention to minimise relapses in early disease truly slows or prevents the development of secondary progression (Filippini et al. 2013).

1.1.5 Diagnosis of CDMS

MS remains a clinical diagnosis following demonstration of typical signs and symptoms, and exclusion of MS-mimics.. Supporting ancillary MRI evidence is particularly useful as it is now possible to make a diagnosis of MS after one clinical event using the 2010 McDonald criteria (Polman et al. 2011). MRI changes are characterised by high signal white matter lesions on FLAIR/T2-weighted sequences, in regions typical for MS (periventricular, juxtacortical or posterior fossa). The most recent criteria do not typically require CSF analysis or neurophysiology (eg VEPs) to make the diagnosis. Basic CSF parameters are usually normal – with protein and glucose levels within the normal range. Some patients may exhibit a lymphocytic pleocytosis, but CSF cell counts are often normal. More strikingly, over 90% of MS patients will be positive for oligoclonal

bands (OCB) and are discussed further in chapter 5. CSF-specific OCBs are occasionally present in other neurological conditions, including syphilis and Lyme disease although the clinical picture would usually distinguish these conditions from MS.

1.1.6 Treatment

The aim of therapy in MS is either to treat related symptoms or modify the long-term outcome of disease (disease modifying treatments-DMT).

Symptom management: acute relapses are usually managed with high-dose methylprednisolone, reducing the duration of clinical symptoms, but there is no impact on long-term recovery (Hickman 2003). Actively managing chronic symptoms such as neuropathic pain, urge incontinence, fatigue, sexual dysfunction and spasticity-related symptoms, are optimally managed with multi-disciplinary input.

Disease modification- DMT: The injectable interferons ('Rebif', 'Betaferon' and 'Avonex') and glatiramer acetate (Copaxone) were introduced in the 1990s and are 'first- line' treatments in patients presenting with two or more relapses in the preceding two years, all reducing relapse rates by about 30%.

More recently, natalizumab (Tysabri), a monoclonal antibody to the vascular cellular adhesion molecule α4β1 was shown to reduce relapse rate by 68%, a more significant disease-modifying effect than first-line DMT (Polman et al. 2006). Other infused monoclonals also show efficacy in both clinical (relapse reduction) and paraclinical (e.g. MRI) outcomes. Alemtuzumab targets the CD52 antigen on lymphocytes/monocytes resulting in their profound depletion. Monoclonal

therapies targeting B-cells also demonstrate remarkable efficacy in clinical/paraclinical endpoints, such as Rituximab and the humanised Ocrelizumab which bind different epitopes of CD20. Daclizumab, another humanized monoclonal, antagonises CD25 and also appears to significantly reduce relapse rates.

The next generation of drugs are notable for their oral route of administration, with comparable efficacy. In addition, drugs such as dimethylfumarate potentially demonstrate novel, neuroprotective mechanisms of action by enhancing levels of nuclear erythroid-2 related factor 2 (Nrf-2) levels. This acts as a transcription factor for antioxidant response element targeting genes responsible for cellular repair with resultant reduction in neuro-axonal damage.

Uncertainty remains regarding the correlation between brain MRI parameters (e.g. number/volume of T2 (T2LL) or contrast enhancing lesions) and annual relapse rates (RR), with underlying disease progression and accumulation of disability. The apparent protection of DMTs against developing disability as stated in many clinical trials (Trojano et al. 2009; Goodin et al. 2012) may be influenced by relapse-related disability as the low rate of relapsing patients evolving annually into progressive MS is unlikely to be reflected in the short duration of most clinical trials (Hauser et al. 2013). When controlling for factors such as age, the benefit of DMTs appear to be lost on disability measures for example (Greenberg et al. 2013; Shirani et al. 2012). Recently, a direct correlation was shown between T2LL and relapse-rate (RR) in a pooled analysis of multiple RCTs, and combining T2LL and atrophy measures showed the strongest correlation with disability outcomes (De Stefano et al, 2013). Despite this, it remains unclear whether DMTs truly slow

disability accrual/death, although better outcome measures such brain atrophy have potential in refining our understanding. It is critically important to be clear on true clinical efficacy with the newer generation of MS drugs in particular, as they appear to have greater therapeutic potency but an increased risk of serious side effects, such as the development of Progressive Multifocal Leukoencephalopathy (PML) with natalizumab therapy (Bloomgren et al. 2012). In the end, the real interest lies in the long-term outcome data-comprising both efficacy and safety- of patients treated at the earliest stage with aggressive immunotherapy.

Regardless of the debate however, most neurologists would agree that current immunomodulatory therapy has revolutionized the management of relapsing MS patients (Evangelou 2012).

1.1.7 Prognosis

Although it is known that a diagnosis of MS will impact on overall life-expectancy (Scalfari et al. 2013), patients will generally live for 40 years or more following the diagnosis of the condition. Outcome data in treatment- naive CIS patients has been generated through a number of clinical trials (Beck et al. 1993), (Jacobs et al. 2000) (Comi et al. 2001). The probability of conversion to CDMS was 16.7%, 38% and 45% respectively in these trials although a more definite answer requires longer follow-up (Fisniku et al. 2008a). Prognostic markers are summarised in table 1.1, although younger age of onset, female sex and non-Caucasian ethnicity (Mowry et al. 2009) also influence prognosis.

Good Prognosis	**Poor prognosis**

Optic neuritis	'Multifocal' CIS
Isolated sensory symptoms	Efferent (motor/cerebellar) systems affected
Long interval to second relapse	High relapse rate in first 5 years
No evidence of disability at 5y	Substantial disability after 5 years
Normal MRI-brain	Abnormal MRI with heavy lesion load

Table 1.1. Clinical features influencing prognosis of patients presenting with CIS.

The presence of 10 or more lesions on baseline MRI-brain set patients at high risk of developing CDMS, although the relationship with subsequent disability at 20 years is not clear-cut (Fisniku et al. 2008b). CSF indices which help predict conversion include OCB positivity (Tintore et al. 2008), levels of CXCL13 (Brettschneider et al. 2010) and free-light chain (FLC) (Villar et al. 2012).

1.2 Pathological changes in MS

1.2.1 Macroscopic pathology

Externally, the meninges and brain surface appear relatively normal although mild cortical atrophy with widened sulci may be noted. Circumscribed, hardened light-grey areas may be seen on the unfixed surface, over the medulla, pons, corpus callosum, optic nerves and chiasm and distributed randomly on the surface of the spinal cord (Prineas, J; in Cook, S (Ed) 2001). Coronal slices of fixed brain demonstrate scattered plaques, often straddling subependymal veins through the lining of the lateral and fourth ventricles. Plaques containing multiple foamy macrophages display a characteristic 'chalky white' appearance. They are usually ellipsoidal in shape when viewed in three dimensions, measuring between 1 and 15mm in diameter. They can occur anywhere in the central nervous system (CNS) (BROWNELL & HUGHES 1962), although there is a predilection for regions

described above in addition to subpial and juxtacortical regions, with extension into the grey matter.

1.2.2 Microscopic pathology and staging of MS plaques

Once plaques are identified in post-mortem cases, the brain is then cut into blocks and those containing plaques can be sectioned for further microscopic analysis. They can be classified based on criteria as demonstrated in table 1.2:

Classification	CD68+ cells	Myelin: MBP+/ PLP+	Lesion border
Early active	Extensive; around and within lesion	Yes	Diffuse
Late active	Some; around and within lesion	Yes	Diffuse
Chronic active	Around the lesion	No	Diffuse to sharp
Chronic	Virtually absent	No	Sharp
Remyelinated	Absent	Yes	-

Table 1.2 Classification of MS plaques based on ICDNS criteria. CD68+ denotes activated macrophages/ microglia expressing CD68 on the cell surface. *MBP: myelin basic protein; PLP: proteolipid protein; LFB: luxol-fast blue*

Active plaques: Foamy macrophages containing myelin fragments are evident, and the lesion is characterised by progressive myelin destruction, variable perivascular inflammatory infiltrate comprising T-lymphocytes predominantly, reactive astrocytosis, and activation of microglial cells. Axons are often swollen and non-linear indicating damage with occasional demonstration of spheroids which represent neurodegenerative axonal retraction bulbs, (Trapp et al. 1998).

Chronic active plaques: Over time, plaques grow centrifugally and the centre of the lesion demonstrates increasing hypocellularity, with myelin stripped and cleared

by lipophages. Activated leucocytes at the lesion border can be seen although foamy macrophages filled with neutral lipids, but negative for MBP/LFB, can remain in tissue for months (Prineas, J; in Cook, S (Ed) 2001)). In addition, there are non-specific reactive astrocytic changes, increased number of microglia and lymphocytes and plasma cells in surrounding perivascular spaces.

Chronic plaques: Most MS plaques will become inactive with no evidence of recent demyelination/ active inflammation but an intense astroglial reaction, leading to the hardened, fibrillary plaques described by Charcot.

Remyelinated ('shadow plaques'): Varying degrees of remyelination occur in MS and, in specific areas such as the cortical grey matter, it appears to be fairly efficient in both animal models (Merkler et al. 2006) and human tissue (Albert et al. 2007). Despite this, failure of remyelination is a prominent feature in MS.

1.2.3 Immunopathogenesis

Traditionally, the CNS was viewed as an immune-privileged site due to the lack of a conventional lymphatic system and the fact that the blood brain barrier (BBB) and the blood-CSF barrier (BCSFB) appear impenetrable to cellular migration under resting conditions (Engelhardt 2008). However, it is now accepted that the CNS is also subject to immune surveillance, with continuous immune cell-mediated interactions behind both the BBB and the BCSFB (Wraith & Nicholson 2012). As stated earlier, both the BBB and BCSFB pose significant physical limitations to access and attention has thus turned to leucocyte entry via the choroid plexus for example (Engelhardt et al. 2001; Coisne et al. 2013). The immune mechanisms leading to demyelination and axonal injury in autoimmune

and virally-mediated animal models of inflammatory demyelinating diseases are extraordinarily complex. The innate and adaptive components of the immune system are both key mediators of damage, although may also serve protective functions (Bogie et al. 2014a; Schwartz & Raposo 2014). I will discuss salient aspects of both adaptive and innate immunity below.

Innate immunity

Tissue injury is mainly effected via activated macrophages which produce a plethora of toxic substances (Hendriks et al. 2005; Yamasaki et al. 2014; Bogie et al. 2014b), including lipolytic and proteolytic enzymes, reactive oxygen and nitrogen species' and excitotoxins. These cells can be activated in MS lesions by cytokines produced by activated T-lymphocytes, thereby initiating characteristic inflammatory, demyelinating processes. However, some studies have reported profound macrophage activation on a background of fairly mild T-cell infiltration, which may be limited to the perivascular space (Michael H Barnett & Prineas 2004; Marik et al. 1997). Thus, other mechanisms of activation may also be important in the pathological process. Stimulation of macrophages through innate immune mechanisms, e.g. toll like receptors (TLRs), is sufficient to induce demyelinating lesions (Felts et al. 2005). Of note, many endogenous ligands for TLRs may be present within multiple sclerosis lesions, one of which is HMGB1 (Andersson et al. 2008).

Adaptive immunity

The basic observation of inflammatory demyelination with associated or subsequent axonal degeneration is classically induced by MHC Class II restricted T-cells. It is thought that genetically susceptible individuals exposed to viral or other microbial infections trigger a CNS-specific cell-mediated immune response. Autoreactive T-cells (including both Th1 and Th17 phenotypes) are thought to be primed in the periphery, possibly via molecular mimicry to myelin proteins or by direct exposure to cognate antigen from draining lymph nodes e.g. cervical (see Chapter 5; section 5.1). Following access of these cells into the CNS and along with antibodies and complement, this can lead to selective destruction of myelinating oligodendrocytes and axons. Cytokines facilitate leucocyte extravasation and trigger inflammatory lesion development by upregulating chemokines, adhesion molecules and inducing MHC-Class II expression on endothelial and glial cells. Increased MHC-II expression on local and infiltrating cells, e.g. microglia and macrophages, allows interaction with the T-cell receptor and activation of the T-cell. Immune tolerance is normally maintained by mechanisms such as regulatory or suppressor cells, or clonal deletion of autoreactive T-cells.

Further focused tissue injury can be induced by MHC Class I cytotoxic T- cells (Cabarrocas et al. 2003; Huseby et al. 2001). These cells are primed to directly attack CNS-resident, antigen- laden target cells expressing MHC Class I molecules. Due to their ability to produce mediators such as matrix metalloproteases, granzymes and other elements that are capable of stromal destruction, these cells are able to traverse and invade the parenchyma.

Highly targeted tissue destruction is also induced by specific antibodies produced by B-cells, which recognize antigen or exact epitope expressed on the membrane

of target cells in the CNS (Linington et al. 1988). These antibodies still require a T-cell mediated pro-inflammatory environment, in order to open up the blood brain barrier and facilitate antibody access to the target tissue. Locally, effector mechanisms such as activated macrophages or complement, finally destroy the antibody- opsonized CNS targets (Lassmann 2008). In addition to their direct effects on lesional pathology, B-cells have also been implicated in chronic CNS inflammation, where soluble factors released from ectopic B-cell follicles in the meninges have been suggested as drivers of inflammation in later stages of the disease (Aloisi et al. 2010) (Magliozzi et al. 2007a).

1.2.4 Putative pathological subtypes in MS

In theory, the final common pathway for tissue injury in MS can be instigated by multiple immune mechanisms. An important aspect of MS research is to define which of these immune mechanisms are most relevant topathology and whether their relative contribution changes at different stages of the disease. The seminal publication by Lucchinetti et al (Lucchinetti et al. 2000) revealed four distinct patterns of acute MS lesions, obtained from patients who had died from a fulminant attack of MS leading to rapid death or else cerebral biopsy of patients presenting in a similar fashion. **Pattern I** lesions demonstrate perivascular T-cells and macrophages with preservation of oligodendrocytes but with no evidence of complement activation. **Pattern II** is similar to pattern I, but signs of complement system activation can also be seen. **Pattern III** lesions are more diffuse with inflammation, oligodendrocyte apoptosis and microglial activation. **Pattern IV** lesions demonstrate sharp borders and oligodendrocyte apoptosis, with a rim of normal appearing white matter and little evidence of active inflammation. The

presence of four lesional subtypes restricted to specific patients suggested therapeutic management could be individualised to their particular subtype; for example, pattern II lesions would be particularly amenable to plasmapharesis.

However, using similar early stage lesional tissue, Prineas et al disputed these findings, claiming that all of the patterns described above could be seen within the same patient. They concluded that these changes represented pathological evolution over time rather than distinct mechanisms unique to individuals per se (Michael H Barnett & Prineas 2004). Although they postulated a primary defect of oligodendrocytes (OGD) initiating MS pathogenesis, as OGD loss in 'pre-active' lesions preceded immune cell infiltration, it is not possible to extrapolate these observations universally. More recently, Lucchinetti et al have added further follow-up data to the biopsy series, demonstrating that those patients with specific pathological patterns in the initial study retained this pattern until re-biopsy or death, when their tissue was re-examined (Metz et al. 2014).

1.2.5 Metabolic insufficiency and axonal damage

Tissue damage following the release of oxygen and nitric oxide free-radicals also trigger mitochondrial dysfunction, and metabolic failure has been shown to play an important part in MS lesions (Witte et al. 2014). Neuropathological reports have suggested that in some highly aggressive pathological phenotypes, the pattern of tissue injury and demyelination demonstrate a hypoxia-like pattern of damage (Trapp & Stys 2009). Similar to classical hypoxic lesions seen in stroke, small calibre axons and neurons are disproportionately affected in MS lesions (Evangelou 2001). In addition, microarray studies have demonstrated widespread increased expression of hypoxia inducible factor 1α (Zeis et al. 2008), suggesting

that energy failure in the brain may also contribute to tissue damage in the progressive stage of the disease.

Given the significant metabolic demands placed upon axons in normal functioning, operating in the context of demyelination renders them particularly vulnerable to bioenergetic insufficiency. Depolarisation in this state leads to accumulation of Na^+ ions within the cytoplasm and metabolic processes are further compromised as ATP produced by mitochondria is required to clear these ions from the axoplasm. Inefficiency of this process can lead to classical 'conduction block' in demyelinated axons. Upregulation and redistribution of sodium channels along the axonal length restores conduction, but normal metabolic efficiency accompanying saltatory conduction is lost, further compounding the energy imbalance (Craner et al. 2004). Neuroprotective strategies have thus attempted to use Na^+channel blockers, and recent clinical trials have reported both negative (Kapoor et al. 2010) and positive (Arun et al. 2013) outcomes, as discussed in chapter 6, section 6.6.6.1

1.2.6 'Normal-appearing' brain tissue (NABT) in MS

The data presented above delineate the hallmarks of MS-related neuropathology; namely, inflammatory demyelinating lesions. However, recent work has suggested that MS is not, in fact, a collection of discrete lesions, but instead these represent the 'tip of the iceberg', appearing against a background of highly abnormal tissue (Chard & Miller 2009; Filippi & Rocca 2005). The key question then becomes; **are the focal lesions discussed above the primary pathology leading to subsequent global changes or is there an underlying, diffuse pathological process from which lesions then arise?** There need to be clear

definitions of 'normal-appearing brain tissue' (NABT), to determine whether these changes represent (i) entirely normal material adjacent to peri-lesional tissue only (ii) a diffuse intermediate between normal tissue and MS lesions, or (iii) whether normal tissue is surrounded by more extensive areas of abnormality which are not picked by conventional MRI or indeed histopathological techniques.

Novel MRI biomarkers

Increasingly sensitive MRI metrics derived from diffusion tensor (DT) and magnetisation transfer (MT) MRI have led the way in delineating pathological changes in NABT since the early 1990s (Feinstein et al. 1992), and have suggested that diffuse changes occur earlier in the disease course. In addition, the biochemical features of these changes can be further examined by proton MR spectroscopy, with an important recent study demonstrating that related metrics can be used to predict disability evolution (Llufriu et al. 2014). These techniques reflect diffuse axonal damage with consequent closer correlation with longer-term clinical outcomes, such as disability, than white matter lesions (Filippi et al. 1999; Werring et al. 1999; Filippi et al. 2001; Traboulsee et al. 2003). They also showed less of an association with short-term outcomes such as relapses (Gallo et al. 2005). Vrenken et al found that MTR changes occur predominantly in the peri-lesional white matter, although changes in NAWM were thought to represent subtle demyelination and axonal damage, as well as oedema, widening of the extracellular space, slow BBB leakage and leakage of fibrinogen into the parenchyma with microplaque formation (Vrenken et al. 2006). MTR indices in NAWM using a 7Tesla machine, was examined in relapsing MS patients (Mistry et al. 2014). The authors found that cortical lesions in this cohort were connected to

the remote NAWM in the same way as white matter lesions (WML) are, and that they were implicated in the generation of remote axonal damage underpinning diffuse NAWM change.

Neuropathological changes

Neuropathologists have always been aware that much of the so-called NABT is not normal at all, characterised by subtle and widespread abnormalities including diffuse astrocytic hyperplasia, perivascular cellular infiltration, patchy edema and variable axonal damage (Allen & McKeown 1979; Bjartmar et al. 2001; Barkhof 2002).

An important study by Kutzelnigg, and colleagues used a large collection of post-mortem tissue from patients with various MS subtypes (n=52) compared to controls (n=30) and found that new,focally active WML were most commonly observed in patients with acute and relapsing MS, whilst diffuse injury and cortical demyelination were characteristic of progressive MS, either primary or secondary (Kutzelnigg et al. 2005). NABT changes were described as "diffuse axonal injury with profound microglial activation..on the background of a global inflammatory response in the whole brain and meninges..". There was a weak correlation between focal WML load and both diffuse white matter injury and cortical lesions. They concluded that MS commences as a focal inflammatory disease, but over time diffuse inflammation accumulates globally, with associated axonal injury in the NAWM and subsequent cortical demyelination.

As described above, meningeal ectopic B-cell follicle-like structures may be driving chronic inflammation within a sealed BBB, down from the pial surface through both the grey matter and white matter beneath, leading to globally diffuse

abnormalities in the chronic phase of the disease (Serafini et al. 2004). However in an influential paper, Bo et al reported that there was no evidence of inflammation in cortical demyelinating lesions in a series of autopsy specimens from patients with progressive disease (Bo et al. 2003). They concluded that this provided evidence of primary neurodegeneration in MS, leading to the remote axonal dysfunction in the NAWM as alluded to in many of the MRI studies above. More recently however, Lucchinetti and colleagues demonstrated florid inflammatory cortical demyelination in, once again, an extensive series of brain biopsies from patients with tumefactive MS at very early disease stages (Lucchinetti et al. 2011a). They reported T- and B-cell perivenular infiltrates, lipid-filled macrophages, and neuronal pyknosis indicating neuronal death. They concluded their findings supported an 'outside-in' model of demyelination-commencing in the subarachnoid space and cortex and subsequently extending into the white matter. If this is true, one would speculate that cortical damage is likely to ensue around cortical lesions and into the normal-appearing grey and white matter, and the authors report this to be related to cytokine diffusion. Whilst the evidence is certainly compelling, there are a number of caveats to these findings, not least the fact that tumefactive MS samples often represent outliers, which could be associated with a higher incidence of meningeal inflammation and cortical disease due to mass effect and extensive breach of the BBB. In addition, distal axonal damage either from WML or the NABT may also contribute to the neurodegenerative changes observed, resulting in local glial activation and release of inflammatory mediators.

Other work has suggested that NABT changes are not directly influenced by adaptive immune responses. In close proximity to actively demyelinating lesions, microglial cells appear to be related to axonal pathology (Singh et al. 2013; Moll et al. 2011), underscoring the relevance of active inflammation and its effects on axonal damage (Trapp et al. 1998). However, clusters of activated microglia-characterised by upregulation of MHC-II molecules on their surface, are often found in the absence of overt demyelination, significant leukocyte infiltration, or obvious blood-brain barrier breakdown. They have been variably termed 'pre-active lesions' (De Groot et al. 2001), 'newly-forming lesions' (M H Barnett & Prineas 2004) or 'microglial nodules' (Moll et al. 2011). These nodules have also been suggested to reflect the early stages of pattern III lesions as described earlier, and essentially reflect pre-conditioned tissue which may precede the formation of a frankly demyelinating lesion (Marik et al. 1997). Evidence of their close association with oligodendroglial abnormalities such as apoptosis has also been reported (M H Barnett & Prineas 2004). Surprisingly, few studies have gone on to probe the molecular abnormalities underpinning these pathological observations, however.

Whilst investigating the MS patient antibody response to a wide variety of myelin-associated proteins, Van Noort et al discovered profound serum reactivity to Alpha B-crystallin, a small heat-shock protein (Van Noort et al. 2010), finding that it accumulates exclusively in stressed oligodendrocytes in the context of microglial nodules. They further demonstrated that a highly purified preparation of this molecule induced cultured microglia to produce immunoregulatory cytokines and chemokines, and more recently, a variety of antiviral factors (Bsibsi

et al. 2013a). The authors concluded that the oligodendroglial accumulation of the protein was the initiating factor, given its ability to activate microglia. The cue for this remains speculative, and the authors purported that OGD stress may result from inflammation itself, although intrathecal antibodies targeting OGD in addition to oxidative radicals, mitochondrial dysfunction and other neuroaxonal disturbances were also potential mechanisms of stress. Thus, they stated that the apparently protective, innate immune responses to Alpha B-crystallin accumulation might be in a precarious balance with the intensely damaging aspects of adaptive responses in MS, broadly in agreement with other NABT studies (Zeis et al. 2008).

It is important to continue the search for reliable markers of NABT changes. Thus, when considering outcome measures following treatment of patients in the relapsing phase of the disease, parameters assessing diffuse damage should also be taken into account in order to obtain an accurate a measure as possible of dynamic changes in the whole of the MS brain.

1.2.7 Oligodendrocytes

As described, OGD activity in NABT is of interest due to this purported balance between neuroprotection and damage. Macroglial cells in the CNS comprise astrocytes, ependymal cells, radial glia and OGD. Like all macroglial cells, OGD originate from tightly restricted periventricular germinal areas of the ectoderm, and are the last cell type to be generated in the CNS. Myelination increases exponentially in the first year of life but is not complete until 20-25 years of age. The myelin sheath is 80% lipid:20% protein and one oligodendrocyte can extend

its myelinating processes to ensheath 50 axons, wrapping around 1μm of myelin around each axon.

The function of myelin in the subcortical white matter is primarily to increase impulse speed, as saltatory propagation of action potentials occurs at the nodes of Ranvier in between OGD. Velocity increases linearly with axon diameter, with the insulating thickness proportional to the diameter of the fiber inside. In contrast, satellite oligodendrocytes are considered to be a part of the grey matter and are functionally distinct. They are characteristically positioned in apposition with neurons and thought to regulate their surrounding extracellular compartment (Ludwin 1984) (Lee et al. 2012).

1.2.7.1 Mechanisms of oligodendrocyte injury in the CNS

The profound metabolic demands placed upon OGD, largely due to the maintenance of multiple myelin sheaths, render them particularly vulnerable to damage in the CNS. CD4+ and CD8+ T-lymphocytes are activated following presentation of antigen by MHC molecules, generally expressed on macrophages/ microglia. Expression of MHC molecules in the CNS under physiological conditions is generally not detectable (Redwine et al. 2001), although OGD can express MHC I upon stimulation with pro-inflammatory cytokines such as IFNγ (Massa et al. 1993). However, whilst clonal expansion of CD8 T-cells is evident, the antigenic specificity of the expanded clones resulting in cell-mediated lysis remains unknown (Babbe et al. 2000). In addition, MHC class II expression on OGD could not be demonstrated in MS lesions, although are readily evident on macrophages/ microglia and astrocytes (Lee & Raine 1989). Thus, damage may result from toxic mediators secreted by a variety of cells (Berger et al. 1997) (Williams et al. 2007).

Figure 1.1 summarises the different cell types implicated in MS-related pathology and how they contribute to OGD damage and dysfunction.

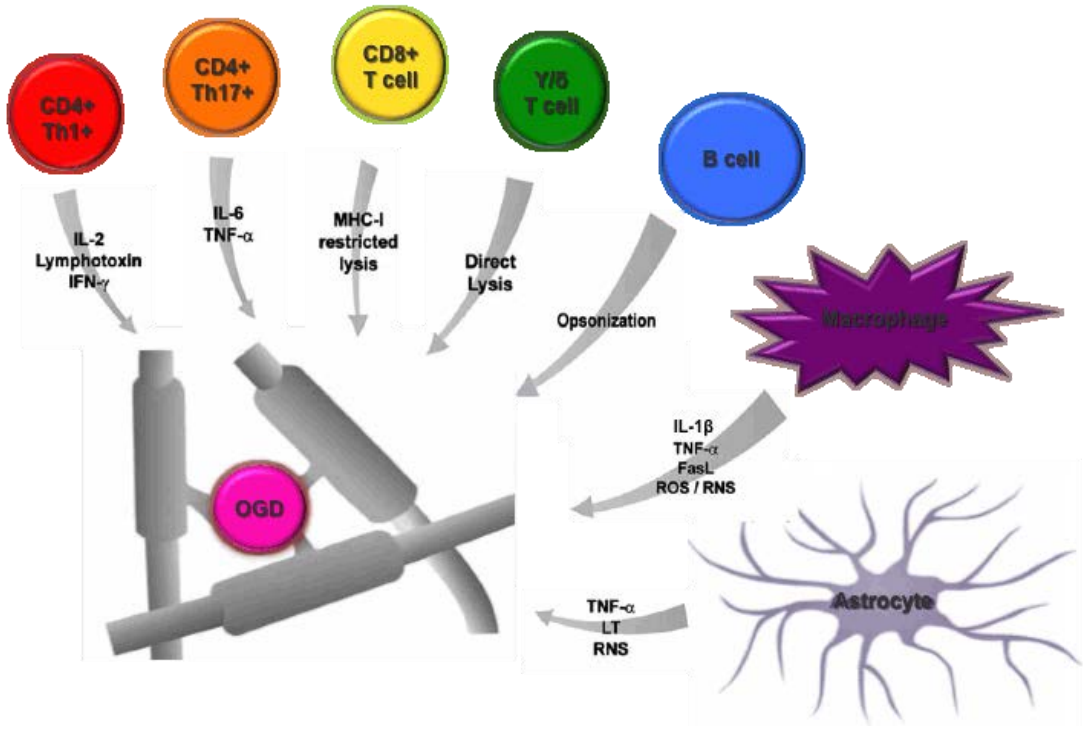

Figure 1.1. Cells mediating oligodendrocyte injury in the course of MS. Many cell types can injure oligodendrocytes. **CD4+ Th1 cells** can induce damage through mediators such as IL-2, IFN-g and LT, whereas damage resulting from Th17 T cells involves IL-17 itself as well as IL-6 and TNF-a. CD8+ T cells can cause direct injury by MHC class I-restricted cell lysis. B cell-mediated damage to oligodendrocytes can occur following antibody secretion and opsonization. Macrophages are a key cell type inducing oligodendrocyte damage by TNF-a,, ROS/RNS, FasL and other mechanisms. Finally, astrocytes were also shown to be harmful to oligodendrocytes by mechanisms involving TNF-a, LT, and RNS. *Adapted from* (Zeis & Schaeren-Wiemers 2008)

1.2.7.2 OGD as potential immune modulators

Recent work has suggested that oligodendrocytes are not just passive targets of inflammatory injury, but are in fact active participants of the neuroimmune networks involved in MS-related pathology (Zeis & Schaeren-Wiemers 2008). As discussed in chapters 3 and 4, the widespread changes in non-lesional brain tissue described in this thesis are increasingly recognised in MS generally (Zeis et al. 2008; Graumann et al. 2003). Zeis and Graumann et al found that upregulation of genes such as CXCL10, CCL3 and CCL5 as well as STAT-6 signalling pathways could

be seen in NAWM. Subsequent protein work using IHC also showed that these changes were particularly notable in OGD. In addition, M2-polarised microglia/ macrophages- thought to promote repair, versus the pro-inflammatory profile of M1-macrophages, drive differentiation of OGD precursors to aid remyelination (Miron et al. 2013).

This suggests that OGD are not simply victims of the immune-mediated processes occurring in MS, but instead appear to demonstrate a protective phenotype, acutely sensitive to inflammatory and metabolic challenges.

1.3 HMGB1 as a novel marker in MS

The high-mobility group (HMG) family of proteins, HMGB1 (previously HMG1), HMGB2 and HMGB3, were named due to their high electrophoretic mobility on SDS-PAGE gels. Their expression occurs mainly during development, and this thesis relates solely to HMGB1. Its unique properties linking sterile inflammation and damage as discussed below make it an ideal target to further develop our molecular understanding of pathological changes occurring in MS.

1.3.1 Structure and expression of HMGB1

HMGB1 is encoded on chromosome 13q12-13 and is composed of two DNA-binding domains- the HMG boxes –A and –B, and a C-terminal chain of aspartic and glutamic acids (figure 1.2).

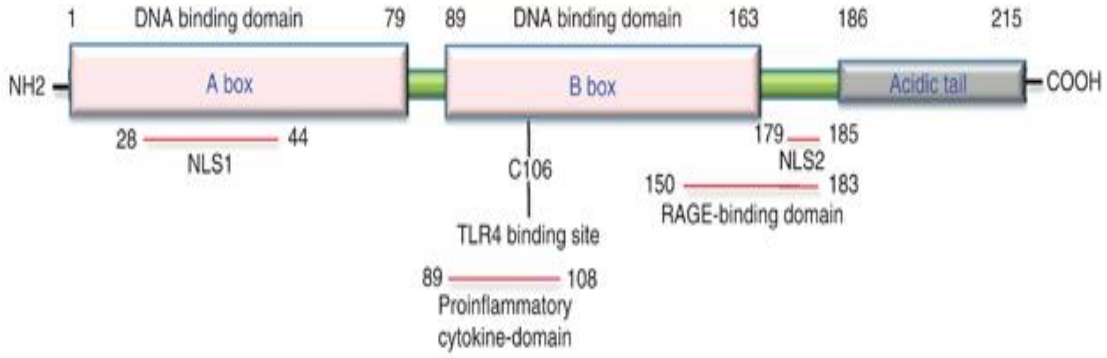

Figure 1.2 Structure of the HMGB1 protein. (**a**) HMGB1 is a 29-kDa non-histone protein of 216 amino acids. It is arranged in three domains made up by two positively charged DNA-binding structures (A and B box), and a negatively charged C-terminal acidic tail composed exclusively of 30 glutamic and aspartic acids. The latter is required for its transcriptional activity within the nucleus. There are two positively charged nuclear-localization signals, including amino-acid sequence segments 28–44 for NLS1 and 179–185 for NLS2. Amino acids 150–183 in the C-terminus of HMGB1 are responsible for RAGE binding. In addition, the cytokine activity of HMGB1 is located within the B box, and it can be antagonized by a truncated A box domain, although the latter's function is still not clearly defined. The cysteine in position 106 in the B box is required for HMGB1 to activate cytokine release, as shown by selective mutation.

Despite a molecular weight of 25kDa, it is detected at a position of 30kDa upon electrophoresis, probably due to its abundance of positively charged amino acids. It is highly conserved evolutionarily and abundantly expressed in most eukaryotic cells at approximately 10^6 molecules/ cell and has a vital role in nuclear homeostasis.

1.3.2 Nuclear role of HMGB1

HMGB1 was originally described by Johns and colleagues as a family member of the non-histone proteins (Goodwin et al. 1973) and its expression was accordingly thought to be restricted to the nucleus. Here, it binds to the minor groove of DNA (Yu & Spring 1977) and a strip of hydrophobic amino acids bulging from its inner surface interpolates between the bases, resulting in uncoiling and bending of DNA. The resultant local distortion of its helical structure enables distant molecules to

associate and form multiprotein complexes, which can have important biological functions. These include increased binding affinity of several transcription factors, including a uniquely important interaction with p53 (Jayaraman et al. 1998), and the RAG1 protein- responsible for V(D)J recombination (Bustin 1999).

However, knock- out mouse studies underscore the critically important role that HMGB1 plays in normal cellular physiology. Phenotypically, the mice are small and extremely lean (fat is virtually absent) with ruffled fur and long hind paws, but they die with 24 hours after birth due to a combination of hypoglycaemia, metabolic failure and defects in transcriptional control (Calogero et al. 1999)

1.3.3 Rediscovery of HMGB1 and its extranuclear function

Many nuclear proteins have been found to have extranuclear function, and the role of secreted HMGB1 was discovered serendipitously years after its initial discovery. Its multifunctional role was described in two important papers published at a similar time, but each following disparate lines of enquiry.

HMGB1 is expressed on the plasma membrane to facilitate neurite outgrowth

Interest in its role outside the nucleus was first raised following neuroscientific findings by Heikke Rauvala and colleagues who discovered a 30kDa protein, 'p30', secreted by neurons and which significantly enhanced neurite outgrowth (Rauvala & Pihlaskari 1987). Further characterisation of this molecule by the same group the following year showed that it was expressed on the membrane at the leading edge of developing neurones, and that a heparin-like structure was needed for the binding of p30 to advance neurite outgrowth through the surrounding ECM (Rauvala et al. 1988). The authors then added an addendum in

proof at the end of this paper, that subsequent review had shown sequence homology to HMG-1 as it was then known. They observed that,"'..the adhesive and heparin-binding properties of this protein as well as its localisation in the extracellular and cytoplasmic compartments strongly suggest that extranuclear mechanisms should be considered as the basis of the role of p30 in cell growth".

HMGB1 is secreted by activated macrophages and is important in innate immunity

During the same period but in an entirely different context, Wang et al reported that HMGB1 was critically important in innate immune mechanisms and identified it as an important pro-inflammatory mediator released by macrophages upon exposure to LPS, TNF and IL-1 (Wang 1999). They described its role as a delayed mediator of sepsis-related lethality in mice and that its attentuation, using polyclonal anti-HMGB1 antibodies, confirmed its functional relevance by improving mortality outcomes in mice. Serum ultrafiltration and subsequent SDS-PAGE analysis of patients with septicaemia also revealed higher HMGB1 levels in patients vs. healthy controls, and highest levels in those who died. They pointed out that whilst low levels of extracellular HMGB1 may be protective, akin to TNF and IL-1 (Leal et al. 2013; Chertoff et al. 2011), the delayed release in response to these prototypically early cytokines, produced high levels which were pathogenic. Unlike the brief, monophasic appearance of early cytokines, its late-onset kinetics and subsequent persistence highlighted its critically important role in propagating chronic inflammation as a damage-associated molecular pattern (DAMP). In addition, its potential as a biomarker for disease severity and blockade as a therapeutic intervention was also raised.

These two papers provided greater appreciation of its extra-nuclear function and thus demanded deeper understanding of (i) stimuli for release from the nucleus, (ii) mechanisms enabling release (iii) potential receptors and (iv) putative downstream signalling pathways to produce its pleiotropic actions. These will be discussed in more detail in the following sections.

1.3.4 Stimuli for release of nuclear HMGB1

Previously, it was thought that HMGB1 release from the nucleus occurred via two major pathways, either passively or actively. Whilst this is still accepted, our understanding of the mechanisms directing nuclear release have been greatly refined. In particular, it has become apparent that both post-translational and, critically, redox modifications direct the fate of HMGB1 molecules leaving the nucleus. As described earlier, myeloid cells secrete HMGB1 in response to a wide variety of stimuli including PAMPs such as LPS and endogenously derived inflammatory mediators such as TNF and IL-1. In addition, HMGB1 is actively released from a variety of other cells including myeloid dendritic cells (Ingrid E Dumitriu et al. 2005), natural killer cells (Semino et al. 2005), platelets (Rouhiainen et al. 2000), endothelial cells- where they significantly upregulate expression of VCAM/ ICAM (Fiuza et al. 2003), pituicytes (Wang et al. 1999), neurones and astrocytes (Hayakawa, Miyamoto, et al. 2012).

1.3.4.1 Microbial exposure

Although initial work focussed on its role in LPS-mediated responses, one of the most important roles of HMGB proteins have been their function as universal sensors of nucleic acids secondary to viral invasion, as DNA and RNA potently activate innate and adaptive immune responses. Interestingly, it also has a key

role in facilitating and potentiating viral infection within the nucleus (Moisy et al. 2012). HMGB1 directly stimulates enhanceosome formation by Epstein-Barr viral activators such as Rta and ZEBRA on their target gene, BHFL-1, by simply bending the DNA. This allows either nonspecific bowing of the helix to create a DNA conformation favourable for Rta binding to this region or by facilitating the binding of specific proteins such as ZEBRA (Mitsouras et al. 2002). The significance of this in MS patients has not yet been explored.

However, it is also important in viral clearance as it binds to multiple TLRs and other PRRs either at the membrane or in the cytosol, to activate innate and adaptive immune responses (Yanai et al. 2009). Stimulation of these receptors results in induction of type-I interferons (IFNs), proinflammatory cytokines, chemokines and inflammasome formation, resulting in secretion of IL-1β. Following various stimuli mimicking different types of viral insult, HMGB1 was shown to bind to all nucleic acids examined, thus acting as a master-sensor following nucleic acid exposure and orchestrating the subsequent specific responses via its downstream signalling pathways, as shown in figure 1.3.

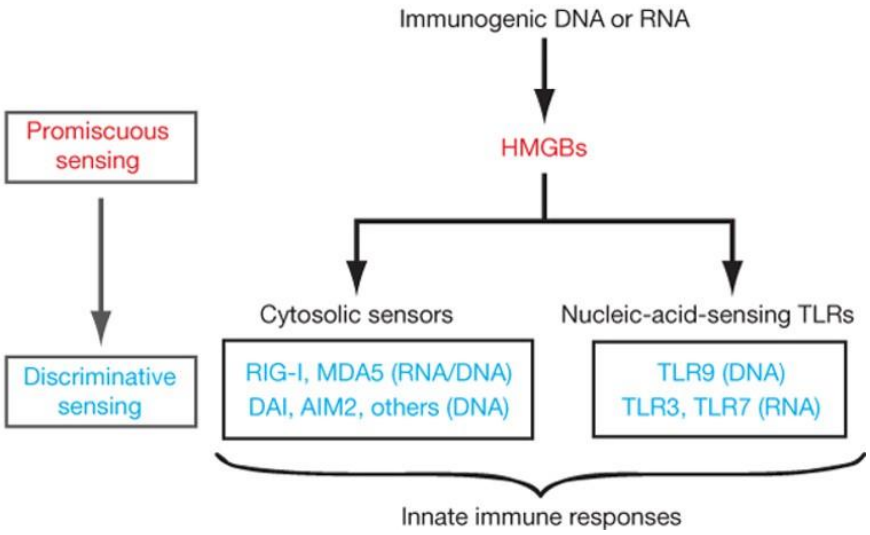

Figure 1.3. Schematic view of the hierarchy in the nucleic-acid-mediated activation of immune responses. All immunogenic nucleic acids bind HMGBs (promiscuous sensing), which is required for subsequent recognition by specific pattern recognition receptors (discriminative sensing) to activate the innate immune responses. *Adapted from Yanai et al (2009).*

The authors concluded that HMGBs serve an evolutionarily conserved role, able to sense invading particles prior to development of more discriminatory PRR for subsequent innate immune responses. Thus, the binding of nucleic acids to HMGBs enables a more efficient and targeted response of the appropriate PRR. IHC analysis suggested that HMGB1 was already present in the cytosol, as HMGBs were found to bind to some PRRs on the endosomal membrane and then released into the cytosol following membrane fusion. Lu et al went on to investigate mechanisms underlying release and found post-translational modifications were critically important; discussed below (Lu et al. 2012).

1.3.4.2 Necrosis

HMGB1 is a prototypic DAMP, signalling early tissue injury and necrosis exemplifies many aspects of HMGB1-related pathology. Simply put, it is clear that

the presence of a nuclear protein in the extracellular space implies cellular damage and various groups have demonstrated that HMGB1 can indeed leak passively following necrotic cell death (Degryse et al. 2001) and that its subsequent presence extracellularly was proinflammatory (Scaffidi et al. 2002). In this context, HMGB1 does not appear to be post-translationally modified (Lu et al. 2012) as release is almost instantaneous, and its extracellular presence initiates a cascade of inflammatory events predominantly via NFkB signalling as described below.

1.3.4.3 Inflammasome activation and pyroptosis

Pyroptosis describes programmed, necrotic cell death induced by caspase-1 and stimulates HMGB1 release by PKR (double-stranded RNA dependent protein kinase R)/ inflammasome activation.

HMGB1 secretion is markedly increased from macrophages upon exposure of to a variety inflammasome agonists, including polyinosinic:polycytidylic acid- a viral mimic, live E. Coli and DAMPs such as ATP (Lu et al. 2012). Genetic or pharmacological inhibition of inflammasome generation was associated with decreased HMGB1 expression in stimulated cell supernatants. This paper was critically important as it identified that HMGB1 released was hyperacetylated at the NLSs as already known, but also that its movement from the nucleus was under direct influence of PKR and inflammasome activation, to carry out further innate immune sensing functions (Yanai et al. 2009).

1.3.4.4 Apoptosis

Apoptosis describes programmed cell death and it was previously thought that HMGB1 was not released from apoptotic cells (Scaffidi et al. 2002). However, recent work has demonstrated that exposure to apoptotic bodies does induce monocytes to secrete HMGB1 in large quantities (Kazama et al. 2008). Curiously, however, it was found to be immunologically inert by failing to stimulate TNF release from neighbouring macrophages. Detailed analyses revealed the presence of a disulfide bond between cysteines 23 and 46. In addition, caspase cleavage and resultant ROS in apoptotic mitochondria go on to oxidise a specific cysteine at position 106 in the pro-inflammatory B-box domain of the HMGB1 molecule, suppressing its otherwise pro-inflammatory effect. Experimentally blocking the oxidation step at cysteine-106 reversed this non-inflammatory effect. This was a pivotal finding as it contributed to the explanation of why apoptosis was an immunologically tolerising event, and that HMGB1 was critical in mediating this (Kazama et al. 2008).

1.3.4.5 Autophagy

HMGB1 is critically important in autophagy (Tang et al. 2010) and this may have unique relevance to chronic CNS diseases given the inherently non-regenerative environment here (Frake et al. 2015) (Nixon 2013). A comparison of autophagic vs.apoptotic processes is shown in **figure 1.4.**

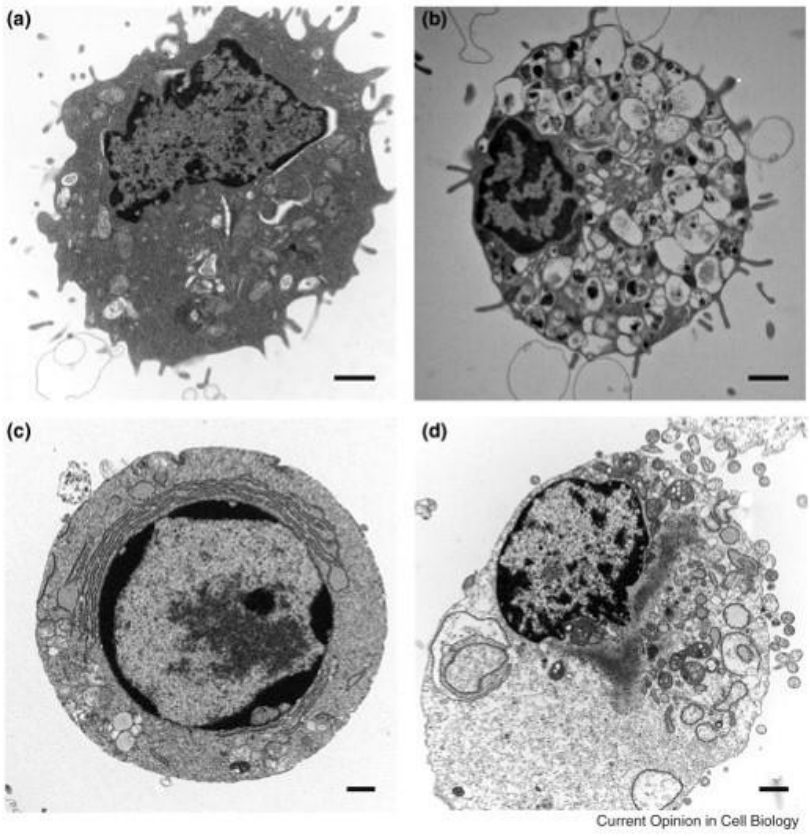

Figure 1.4. Morphological features of autophagic, apoptotic and pyroptic cells. (a) Normal, **(b)** autophagic, **(c)** apoptotic and **(d)** pyroptotic cells. Necrosis also stimulates autophagy by catabolising constituent molecules. Thus, vacuolation of the cytoplasm is observed in both autophagic cells (b) and in cells stimulated to undergo programmed necrosis (d). Conversely, ATP levels are preserved in normal (a) and apoptotic cells (c) consistent with fewer cytoplasmic phagosomes. *Scale bar=1 μm. Adapted from* (Edinger & Thompson 2004)

Neurons have uniquely large cytoplasmic expanses in their dendrites and axons, and so face distinct bioenergetic challenges in the disposal of dysfunctional proteins/cellular waste over time, particularly given their post-mitotic status. The specific protein involved is less relevant, as all aggregates are processed along a common pathway, implicated in many neurological diseases (**figure 1.5).**

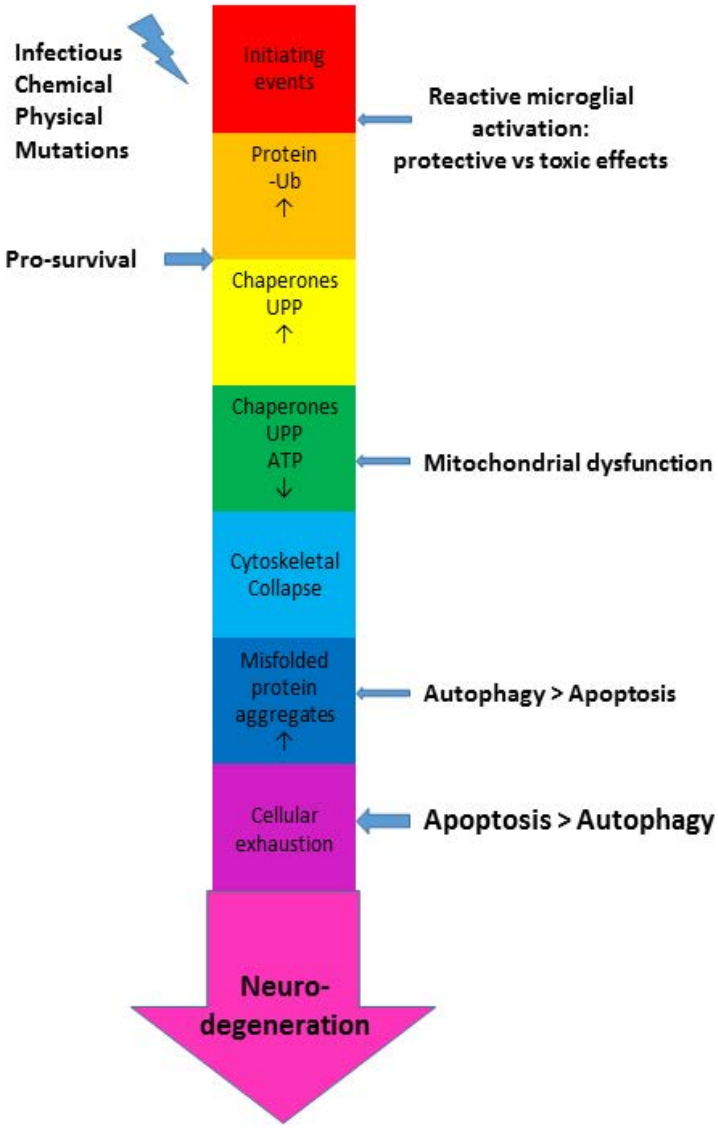

Figure 1.5. Timeline for neurodegeneration associated with protein misfolding. The CNS is subject to multiple insults, and these can activate resident glial cells which produce both protective (eg BDNF, VEGF) and toxic (NO, IL-6, TNFα) factors. If the latter predominates, the sustained cell stress leads to protein misfolding. Ubiquitination of these aberrant proteins and removal by the ubiquitin proteasome pathway (UPP) contains the damage and promotes cell survival. However, prolongation of this process places increased metabolic demands on the cell and eventually ATP levels decline secondary to mitochondrial dysfunction, leading to aggregation of ubiquitinated proteins. Autophagy enables cells to remove these aggregates from the cytosol, but a tipping point between pro-survival and pro-death pathways ultimately leads to neurodegeneration in some cells. Accordingly, autophagic clearance has been examined in Alzheimer's disease (Nixon et al. 2005; Salminen et al. 2013; W. Li et al. 2013), amyotrophic lateral sclerosis (Chen et al. 2012), Huntington's disease (Martinez-Vicente et al. 2010) and Parkinson's disease (Winslow et al. 2010), with defects arising at different stages of the pathway. *Adapted from* (Huang & Figueiredo-Pereira 2010)

Reactive oxygen species (ROS) are key stimuli inducing cellular autophagy, primarily generated via the mitochondrial electron transport chain and liberated by stimuli such as hypoxia, nutrient starvation and mitochondrial toxicity.

HMGB1 is an important regulator of autophagy, and its cytoplasmic translocation is stimulated directly by ROS (Tang et al. 2010). Inhibition of HMGB1 cytoplasmic translocation (using ethyl pyruvate) limited starvation-induced autophagy. Furthermore, they identified specific, intramolecular changes in HMGB1 critical for binding to Beclin1, displacing Bcl-2 to avert apoptosis and sustain autophagy. A summary of HMGB1's role in autophagy is shown in figure 1.6.

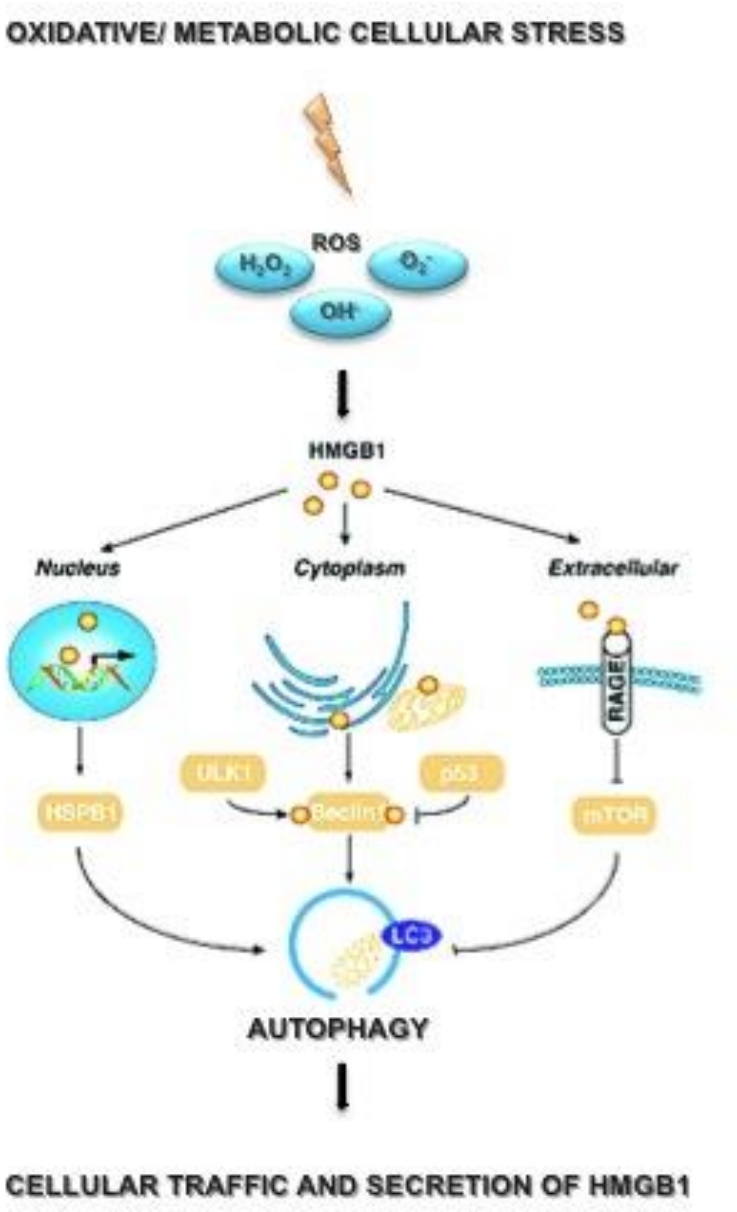

Figure 1.6. HMGB1-mediated autophagy pathways in response to stress. ROS are either a primary cause for damage/death via oxidative stress or a secondary signal to recruit and activate inflammatory cells. By inducing autophagy and releasing DAMPs such as HMGB1, cells are able to maintain homeostasis and promote survival. Pleiotropic mechanisms of HMGB1 in autophagy induction are illustrated; nuclear HMGB1 modulates the expression of heat shock protein beta-1 (HSPB1/Hsp27). Phosphorylated Hsp27/HSPB1 modulates the actin cytoskeleton, followed by mitophagy and/or autophagy promotion. Cytoplasmic HMGB1 with C23-C45 binding and displacing Beclin-1 from Bcl2/Bclxl, sustains autophagosome formation. Extracellular HMGB1 also triggers autophagy via interaction with the receptor glycation end product (RAGE), which initiates Beclin 1–PI3KC3 complex formation and inhibition of the mTOR pathway. *Adapted from* (Hou et al. 2013).

1.3.5 Mechanism of release

HMGB1 is secreted as a leaderless protein without an N-terminal signal peptide, akin to IL-1b and other DAMPs. It subsequently undergoes non-conventional lysosome-mediated exocytosis through the cytosol and into the extracellular space. Ultimately, the degree of stress that the cell is subjected to dictates the particular role that HMGB1 will adopt, related to its post-translational modifications as detailed in figure 1.6 and 1.7.

1.3.6 Post-translational modifications of HMGB1 and effects upon signalling pathways

Epigenetic modification: As discused earlier and shown in figure 1.1, acetylation is an important cue enabling HMGB1 to exit the nucleus (Sterner et al. 1979) (Bonaldi et al. 2003). The cues initiating acetylation remain poorly understood, but may involve modulation of histone deacetylases (Fu et al. 2004). Since then, methylation in neutrophils (Ito et al. 2007), phosphorylation (Oh et al. 2009) and redox-sensitive modifications (see below) have all been described.

Redox modification**:** HMGB1 is an excellent example of how one molecule can mediate a myriad of different cellular events, simply by redox modification of critical amino acids. In essence, increasing oxidative cellular stress results in a progressively pro-inflamatory phenotype and function as seen in figure 1.7. It is worth highlighting that different redox forms of the molecule can be found within the same subcellular compartment, indicating considerable functional plasticity. (Venereau et al. 2012).

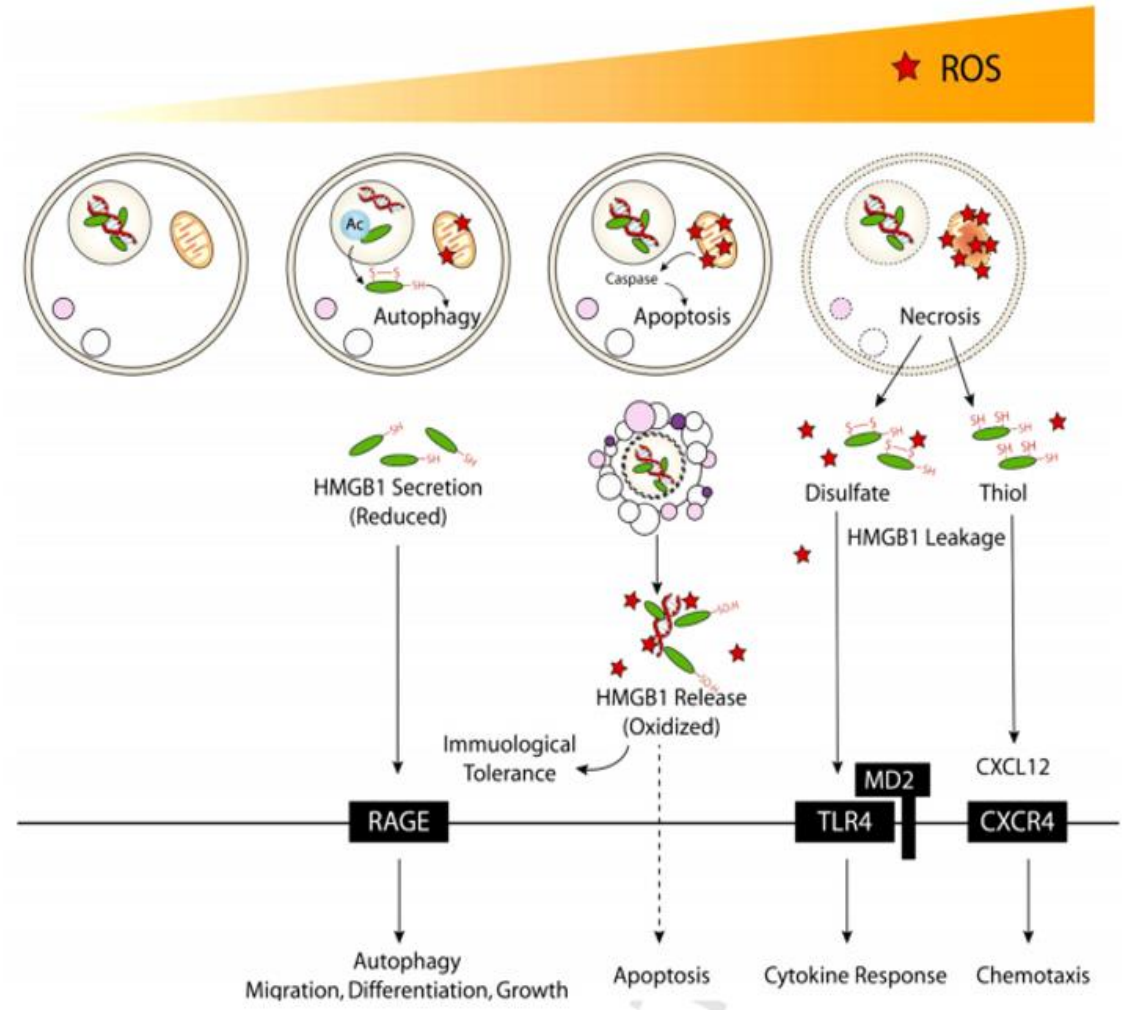

Figure. 1.7 The pathways of HMGB1 secretion or release in response to different degree of oxidative stress. Under resting conditions, HMGB1 is located primarily within the nucleus, protecting DNA structure and acting as a regulator of transcription. Modification of the amino-acid cysteine at key positions (23, 45 and 106) of the molecule determine subsequent HMGB1 function upon release**.** In its resting state within the nucleus, all of the cysteine residues are in their reduced form (Venereau et al. 2012). Upon mild metabolic stress, acetylated HMGB1 is released in a reduced form but with mutation of cysteine 106 and formation of a disulfide bridge between C23-C46, to stimulate autophagic pathways and augment cell function and survival. Progressive oxidative cellular stress stimulates redox-sensitive mitochondria to release molecules activating the caspase cascade to trigger apoptosis. As damage progresses with an increasingly inflammatory profile, this culminates in a conformation which stimulates MD2/TLR4 in the context of inflammasome activation and pyroptosis. Finally, at extreme levels of oxidative stress, severe mitochondrial permeability transition (MPT) or even the rupture of the mitochondrial membrane, promotes collapse and HMGB1 is leaked out of the cells in two forms: (1) Disulfate HMGB1 resulting in cytokine production via TLR4/MD2 interaction and (2) All thiol HMGB1, leading to chemotaxis via release and subsequent binding to CXCL12 and CXCR4. *Adapted from* (G. Li, Tang, et al. 2013)

1.3.7 HMGB1 receptors and intracellular signalling

When HMGB1 is released into the extracellular space, it binds to receptors to elicit specific responses. The number of receptors implicated in its subsequent signalling is growing, alongside our understanding of their synergistic interactions. The best established receptors comprise RAGE, TLR2, -4, -9 and CXCR4 (Yang et al. 2013).

RAGE: this was the first receptor identified which bound HMGB1 in rat brain extracts at amino acid residues 150-183 (Hori et al. 1995) (figure 1.1). Signalling through RAGE is important for maturation of immune cells, cellular migration and upregulation of surface receptors such as TLR4 and RAGE itself (Yang et al. 2007)(Rouhiainen et al. 2004; I E Dumitriu et al. 2005) and autophagy as discussed earlier. Neurite outgrowth was stimulated via RAGE, and subsequent work has shown the signalling pathways involved include cdc42/ Rac, concerned with both cytoskeletal regulation and cell migration (Huttunen & Rauvala 2004). HMGB1 ligation of RAGE also stimulates transcription of genes important in migration control including VCAM-1, ICAM-1,and the AMIGOs. AMIGO1 (Amphoterin-Induced Gene and ORF) was originally identified based on RAGE ligation by HMGB1 (Zhao et al. 2011; Kuja-Panula et al. 2003). These molecules will be discussed in further detail in section 1.3.6, below.

Ligation of RAGE can also result in activation of MAPKs e.g. p38, stress-activated protein kinase/c-jun N-terminal kinase and ERK1/2, leading to NFkB activation and production of pro-inflammatory cytokines.

TLR-4:Despite the central role that RAGE plays in HMGB1 function, it was shown that RAGE-knockout macrophages were still able to produce TNFα upon

stimulation by HMGB1. In contrast, TLR4-knockout macrophages were not able to produce TNFα upon the same exposure, introducing a role for TLR4 in the pro-inflammatory function of HMGB1 (Yang et al. 2010). This work showed that HMGB1 binds to TLR4-MD2 (using surface plasmon resonance), and that both binding and signalling require reduction of cysteine 106. This results in nuclear translocation of NfKB and production of TNFα. HMGB1 has also been shown to bind to TLR2 (Yu et al. 2006) secondary to LPS stimulation and TLR3 (Mina Son 2012) seondary to viral antigens or mimics to induce signalling via NFkB and leading to cytokine release.

The current dogma is that HMGB1 signalling takes place via RAGE in endothelial and somatic cells and via TLRs in myeloid cells (Andersson & Tracey 2011). The interaction, if any, between these respective receptor complexes is still not clear. Speculation that HMGB1 did not always operate alone and could form heterocomplexes with other molecules to trigger receptor activation is suggested by subsequent work, in particular concerning TLR9 and CXCR4. Tian et al demonstrated that HMGB1-DNA complexes activate TLR9 to augment maturation of immune cells as well as cytokine secretion (Tian et al. 2007). In addition, pivotal work by Schiraldi et al found that redox modification of HMGB1 also allows formation of a heterocomplex with CXCL12, associating with its cognate receptor CXCR4 to boost chemotactic activity (Schiraldi et al. 2012).

1.3.8 HMGB1 and adaptive immunity

Available data regarding the interaction of HMGB1 with lymphoid cells, in contrast to the myeloid lineage, is surprisingly limited. However, there is clear in-vitro evidence to suggest that it is secreted by activated natural killer cells to promote

DC maturation during the immune response (Semino et al. 2005; Semino et al. 2007). In addition, HMGB1 translocates and is secreted by human DC following LPS stimulation, acting as a pro-inflammatory cytokine. Thereafter, it plays an important role in promoting expansion, survival, and Th1 polarization of CD4+ (Ingrid E Dumitriu et al. 2005; Jube et al. 2012), and Th17-cells (He et al. 2012; Su et al. 2011; Shi et al. 2012), including when signals would otherwise result in suboptimal T-cell stimulation.

In contrast, human CD4(+)CD25(+)CD127(-)Tregs express significantly higher levels of RAGE on the cell surface than CD4(+)CD25(-)CD127(+)-conventional T-cells, while levels of TLR4 were similar.HMGB1 apparently induced migration and prolonged survival of Treg's and significantly increased IL-10 release and Treg suppressive capacity in a RAGE-dependent manner. Finally, they noted that HMGB1 directly suppresses IFNγ release from T-cells and inhibited their proliferation via TLR4 (Wild et al. 2012).

1.3.9 The role of HMGB1 in systemic disease

The vast majority of HMGB1 research has been linked to its role in systemic disease, and relate mainly to its extracellular, proinflammatory actions. Sepsis gained the most attention initially, given the original identification of LPS acting to trigger HMGB1 release from macrophages (Wang 1999) and other acute inflammatory diseases similarly reported its relevance such as in haemorrhagic shock and acute lung injury (Fan et al. 2007; Barsness et al. 2004). Attention rapidly turned to its role in potentiation of chronic inflammation e.g.in arthritis. It exemplifies why HMGB1 is thought to have a role in chronic inflammatory and autoimmune diseases; namely due to (a) identification of HMGB1 in serum or

other biofluids eg urine, synovial fluid (b) upregulation of HMGB1 expression in pathological tissue, including in the extracellular compartment (c) recapitulation of disease characteristics when HMGB1 is administered exogenously in vitro/ in vivo and (d) efficacy in ameliorating disease phenotype in animal models using HMGB1 blockade. Current studies in tumour biology have also yielded important insights into the role of HMGB1 in this disease process, and its relevance to many other diseases (G. Li, Tang, et al. 2013).

1.3.10 The role of HMGB1 in CNS disease

Despite its extranuclear role being originally identified in the brain, relatively little attention had focussed on the role of HMGB1 in the CNS. This is reflective of the usual limitations concerning experimental access to CNS tissue, where unlike a skin biopsy or synovial fluid aspirate, sampling of CNS material presents obvious difficulties. However, studies into several neurological diseases have successfully demonstrated the pathological importance of HMGB1. **Traumatic brain injury** (Laird et al. 2014) (Okuma et al. 2012), **CNS infection** (Tang et al. 2008; Asano et al. 2011) (Höhne et al. 2013a), **epilepsy** (Zurolo et al. 2011; Maroso et al. 2010), **ALS** (Casula et al. 2011), **Alzheimer's disease** (Takata et al. 2003; Takata et al. 2004), **Parkinson's disease** (Lindersson et al. 2004) (Gao et al. 2011) and, importantly, **stroke** (Kim et al. 2006) (Qiu et al. 2007) (Kim et al. 2012; Kim et al. 2006) (Hayakawa et al. 2010; Hayakawa, Pham, et al. 2012; Hayakawa, Nakano, et al. 2010; Hayakawa, Miyamoto, et al. 2012) have highlighted both detrimental and beneficial roles for HMGB1.

MS: HMGB1 expression has been examined in MS patients (Andersson et al. 2008)and will be discussed in detail in Chapters 3 and 4. However, this study

predominantly examined the expression pattern in active lesions only and did not consider changes that may be occurring in NABT.

1.3.11 Summary of HMGB1 function

HMGB1 is vital to both cell life and death, and has an important role in sensing increasing degrees of cellular stress. In response to significant levels of oxidative stress, it orchestrates predominantly innate and some adaptive immune mechanisms, with both chemotactic and cytokine-like functions. The latter is largely effected via TLR and RAGE-mediated NFkB signalling in macrophages to produce deleterious effects in the surrounding tissue. In conditions of lower levels of oxidative stress in somatic cells in particular, it also demonstrates protective properties, via activation of RAGE and non- NFkB signalling pathways. Given the sensitivity of HMGB1 in identifying cellular stress, and our understanding that NABT changes can reflect diffuse aspects of MS pathology it is possible that it could act as a marker of pathology in these regions. However, it has many other potential roles in MS also, from immune cell recruitment and cytokine release, to possible autophagic responses in resident cells exposed to the pathological environment in MS brain tissue. Thus, exploration of downstream molecular changes following HMGB1 stimulation is of particular interest as this may offer a more targeted approach to managing HMGB1-related pathology.

1.4 Leucine-rich repeat and Ig-domain containing (LRRIG) molecules

The leucine-rich repeat (LRR) sequence in proteins was discovered in 1985 and are solenoid-patterned, protein-ligand interaction motifs (Takahashi et al. 1985). They are present in a diverse range of proteins with heterogenous functions and sub-cellular locations (Kobe 2001). The number of LRRs is variable though are generally 20–29 amino acids in length. Structurally, each LRR consists of a β-strand and anα-helix connected by loops, in a repeating pattern arranged as a curved, horseshoe-shaped structure parallel to a common axis- see figure 1.7.

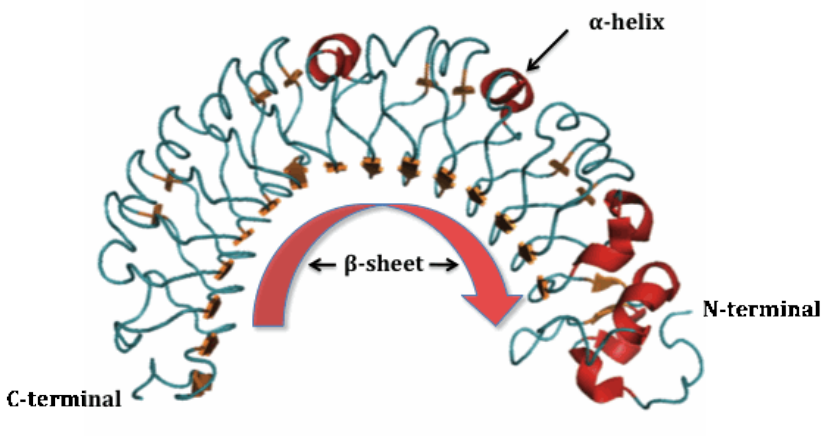

Figure 1.8. The three-dimensional structure of the LINGO-1 ectodomain: an illustration of typical structural features of a leucine-rich repeat molecule. The α-helices form the outer convexity of the horse-shaped molecule, whilst the inner β-helices form the exposed sheet to which ligands can bind, creating a large and versatile binding region. *Adapted from* (Loizou et al. 2014).

Some LRR proteins are anchored to the cell membrane and it is this group which frequently demonstrate brain-enriched expression, suggesting CNS-specific functions, and their importance in this context is increasingly recognised (de Wit et al. 2011; Chen et al. 2006). These include the neuronal cell surface Nogo-66 receptor (NgR) (Fournier et al. 2001; Thallmair et al. 1998) and its ligands e.g. oligodendrocyte myelin glycoprotein (Omgp) (Vourc'h et al., 2004) and LINGO-1

(Mi et al.,2004) as well as the AMIGO molecules (Chen et al.,2011; Kua-Panula et al.,2003). The latter two CNS-enriched families form a distinct class of LRR,type I-membrane proteins with a domain normally associated with adhesion molecules, the C2-type Ig-like domain; hence 'LRRIg' designation. The LRR domain differentiates these molecules from the Ig-like family of cell adhesion molecules, whilst the transmembrane domain distinguishes them from the family of secreted proteoglycans with LRRs. Our interest lies in the AMIGO family, primarily due to their close association with HMGB1 and to LINGO-1; a molecule extensively studied in the context of MS biology and for whom phase-2,anti-LINGO-1 clinical trials for MS treatment are underway.

1.4.1 AMIGO molecules

As mentioned earlier, neurite extension of embryonic neurons on a plate coated with HMGB1 or amphoterin as it was then known, induced gene expression of AMIGO-1 which was an unidentified molecule at the time. The upregulated transcript was subsequently named AMIGO (AMphoterin-Induced Gene and Open Reading Frame) and was cloned along with its homologues, AMIGO-2 and AMIGO-3. All the molecules demonstrated both homophilic and heterophilic biding with each other. The crystal structure of AMIGO-1 was recently elucidated and demonstrated that homophilic binding takes place via its LRR region. Subsequent BLAST searches using the AMIGO-1 ectodomain have further demonstrated sequence homology with Slit-proteins (axon guidance) and the Nogo-66 receptor (NgR1) (Zhao et al. 2014a). The latter is of particular interest with regards to AMIGO-3, as it was recently shown to mediate neurodegeneration via RhoA activation by acting at NgR1, analogous to LINGO-1 (Ahmed et al. 2013). AMIGO-1

and -2 did not demonstrate this function, despite the potential association at the NgR suggested by BLAST searches and instead, other researchers have demonstrated a clear role for them in CNS development, especially in the formation of fasciculated fibre tracts (Zhao et al. 2014b) and Andres, 2004) and LINGO-1 (Mi et al. 2004), as well as the AMIGO proteins (Chen et al. 2011; Kuja-Panula et al. 2003). Using a combination of reverse transcriptase PCR, in-situ hybridisation and IHC in mice, AMIGO-1 expression appeared to be CNS-specific, especially in hippocampal neurones. Both AMIGO-2 and AMIGO-3 displayed relatively more widespread tissue expression, though the latter was highly expressed in the CNS.

Functionally, AMIGO-1 has been found to associate closely with the Kv2.1 potassium channel and to directly affect central neuronal excitability via this association (Peltola et al. 2011), and also appears to regulate expression of Kv2.1 in the adult brain (Zhao et al. 2014b). The immunostaining pattern in mouse brain demonstrates striking co-localisation and clustering of both kv2.1 and AMIGO-1, in a characteristically punctate pattern, around the neuronal soma and proximal dendrites- see figure 1.8.

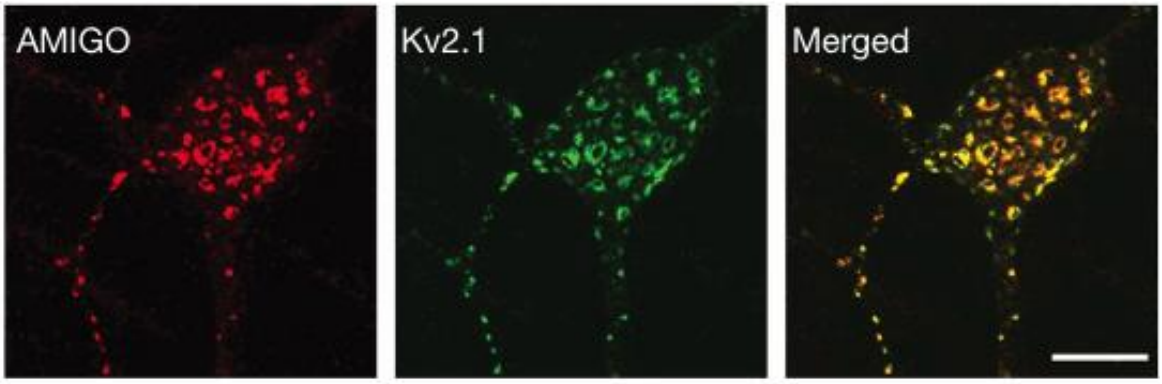

Figure 1.9. Colocalization of AMIGO and Kv2.1 in 24 days in vitro cultured hippocampal neurons. Single confocal plane from the basal surface of the cell. The classically punctate staining pattern around neuronal soma and proximal dendrites was evident. Scale bar = 10μm. *Adapted from* (Peltola et al. 2011).

The identification of AMIGO-2 ('alivin-1') was reported, coincidentally, at around the same time as Kuja-Panula et al published the original 'AMIGO' paper in 2003. It was found to be enriched in cerebellar granule cells and in a specialised region between CA1 and CA3 in the rat hippocampus (Ono et al. 2003b). More importantly, they noted that its mRNA transcription was dependent on neuronal activity, regulated by potassium chloride/ NMDA in culture media and tightly correlated to depolarisation-dependent survival. More recently, Laeremans et al reported that its hippocampal expression is in fact located in CA2 and CA3 of the Ammon's Horn; a region particularly resistant to neuronal injury/ toxicity (Laeremans et al. 2013). Thus AMIGO-2 was identified as an important cell survival- promoting factor. At a similar time, AMIGO-2 was also identified as a gene differentially expressed in human gastric adenocarcinomas (DEGA) in around 45% of tumour vs. control tissue from subjects with gastric cancer, highlighting a potential role in tumorigenesis (Rabenau et al. 2004), likely relating to its pro-survival functions (Ono et al. 2009a; Ono et al. 2003b).

1.4.2 Interaction between HMGB1 and AMIGO molecules

The interaction between HMGB1 and AMIGO-1 in particular has been studied recently (Zhao et al. 2011) but their exact relationship remains unclear. Antisense morpholino oligonucleotides specific for HMGB1 produced downregulation of HMGB1 expression as expected, but also of AMIGO-1 expression, as assessed by western blotting. High-resolution immunostaining in this study also demonstrated partial co-localisation of the proteins at the plasma membrane; suggesting that HMGB1 effects are not only on gene upregulation of AMIGO-1 but may have a more direct role in their interaction. Furthermore, injection of AMIGO-1 cRNA in the HMGB1 zebrafish knockdown morphants produced a rescue effect by increasing neuronal network development to around the same levels as with HMGB1 cRNA itself. The authors conclude that the expression and function of AMIGO-1 may be linked to HMGB1, at least in the context of forebrain development, and should be included in the signalling pathway through which HMGB1 regulates neural progenitors. Clearly, the physiological interaction of HMGB1 with AMIGO-1 may be distinct from a pathophysiological one, but given their close association, it seems plausible that AMIGO-1 may have a role in HMGB1-mediated inflammation, although whether in this context it has neurite outgrowth promoting or inhibiting properties is unknown. Recently, Chen et al (Chen et al. 2011) found that AMIGO-1 expression in rat and mouse brain was more widespread than previously suggested, with astroglial and oligodendroglial expression also seen; a difference presumed to be related to different AMIGO-1 antibody specificities. In neurones, they found that endogenous AMIGO-1 localised to the dendritic tree, responsible for forming synaptic connections. Interestingly, they reported that upon removal of the leucine-rich repeat molecules using DNA

manipulation, the molecule relocated to the axonal surface. However, elucidation of the crystal structure of the AMIGO-1 dimer has recently revealed that homophilic binding occurs through its LRR domains (Kajander et al. 2011). Thus it would appear that fasciculation of neurites and synaptogenesis require the LRR regions.

The association between HMGB1 and AMIGO-2 and -3 rests with their potential association with AMIGO-1, and little work has been done to explore any further link. LINGO-1 has no recognised connection to HMGB1, other than being from a similar family to the AMIGO molecules.

1.4.3 LINGO-1

LINGO-1 is the best characterised LRRIg molecule, in terms of cellular expression profile and function. Its potential role in MS has been comprehensively assessed in pre-clinical work, such that anti-LINGO-1 phase 2 trials are now underway following these findings.

It is established that as the nervous system matures, neuronal connections are stabilised, and the potential for structural remodelling or regeneration following injury becomes restricted. Postnatal structural plasticity is limited to "critical period"- a set developmental time window. Closure of the critical period coincides with myelination, and myelin-associated proteins are major factors in limiting structural plasticity in the adult CNS (although other myelin-independent mechanisms also exist). Inhibitory myelin-related proteins include Nogo66 (NogoA) (Chen et al. 2000), oligodendrocyte-myelin glycoprotein (Omgp) (Wang et al. 2002) and myelin-associated glycoprotein (MAG) (McKerracher et al. 1994; Schnaar & Lopez 2009). These three myelin proteins bind to the Nogo receptor

(NgR1) and inhibit neurite growth via two co-receptors containing p75 or TROY (Park et al. 2005; Shao et al. 2005; Wang et al. 2002).

LINGO-1 was initially discovered as a component of this NgR1complex, functioning as a natural inhibitor of neurite growth. It was also shown to be important in regulating oligodendrocyte differentiation and myelination, in the context of inhibitory myelin-related proteins (Mi et al. 2004; Mi et al. 2005). This inhibitory effect of myelin proteins on neurons is mediated by Ras homolog gene family, member A (RhoA) after binding with the NgR1 complex. RhoA itself is a small GTPase protein known to regulate the actin cytoskeleton in the formation of stress fibres, acting upon the effector protein ROCK1 (Rho-associated, coiled-coil containing protein kinase 1). LINGO-1, forms a ternary complex with the NgR1 and p75/TAJ/TROY to signal through the Rho-GTP cascade to inhibit CNS axon regeneration. Following activation of ROCK by RhoA (via RhoA kinase) this stimulates the actin-binding LIM kinase, which then stimulates cofilin (involved in the disassembly of actin filaments). Together, this results in reorganisation of the actin cytoskeleton of the cell. In the case of neurons, activation of this pathway results in growth cone collapse, thus inhibiting the growth and repair of neural pathways and axons. In addition to myelin-associated proteins, further constraints on axon regeneration are related to deposition of the glial scar, which also contains inhibitory ligands (e.g. semaphorins, ephrins, chondroitin sulphate proteoglycans (CSPG)). Some of the functional consequences of antagonism of this protein complex, via Anti-NgR1 antibodies (W. Li et al. 2004), soluble NgR1 (S. Li et al. 2004) and p75NTR antagonists, include the promotion of CNS axonal regeneration *in vivo* (Lee et al. 2003). In addition to its role in axon growth, LINGO-1 is involved in oligodendrocyte differentiation and remyelination, possibly

mediated through NGF and TrkA (figure 1.9) (Mi et al. 2005). Inhibition of oligodendrocyte differentiation requires its cytoplasmic domain, leading to downstream signalling via the RhoA pathway. Whether binding of LINGO-1 to a secreted or membrane-bound ligand, in *cis* or in *trans*, is required to initiate intracellular signalling is currently unknown. Importantly, LINGO-1 expressed on the axonal surface also inhibits oligodendrocyte differentiation and myelination, both in oligodendrocyte-neuron co-cultures and in transgenic mice overexpressing LINGO-1 (Lee et al. 2007a). This suggests that LINGO-1 signals from axon to oligodendrocyte to inhibit oligodendrocyte differentiation. The nature of this signal is not yet clear, but does not apparently involve the LINGO-1 binding proteins NgR1 and $p75^{NTR}$.

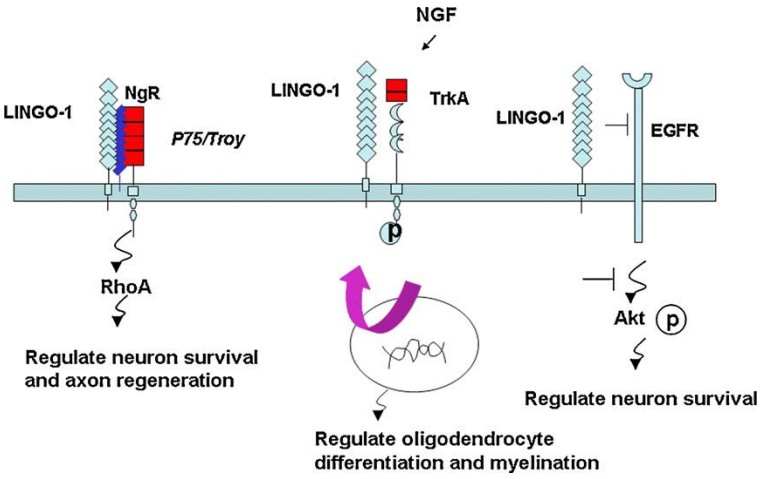

Figure 1.10. Putative signalling pathways for LINGO-1. *Reproduced from* (Rudick et al. 2008)

Furthermore, the NgR1-LINGO-1-p75/TROY complex may also participate in cell death following neuronal injury (Barker 2004; Bhakar et al. 2003; Florez-McClure et al. 2004). LINGO-1 antagonists or gene knock-out knock-out mice were found to promote OPC differentiation (Mi et al. 2005; Lee et al. 2007b), reduce apoptosis and promote survival of OGD and neurons, as well as enhancing recovery of

function after spinal cord injury (Ji et al. 2006). In addition, in vivo work has shown that attenuation of LINGO-1 activity promotes axonal remyelination, regeneration and functional recovery in an EAE model (Mi et al. 2007).

Its expression in human brain has also been studied, where Satoh et al found that LINGO-1 was expressed in neurons, reactive astrocytes and macrophages/ microglia but not in OGD, when using non-lesional and chronic actively demyelinating lesional tissue (Satoh et al. 2007). The lack of expression in OGD in this work is in stark contrast to the findings as discussed above by Mi et al, and this discrepancy has not been resolved thus far..

Despite LINGO antagonism leading to a significant increase in neurite outgrowth using *in vitro* assays, the importance of the protein *in vivo* is less clear, as LINGO-1 inhibition in CNS injury models as detailed above only led to delayed and then modest levels of regeneration (Lee et al. 2007b). This raises the possibility of functional redundancy, with alternative binding partners existing for NgR and $p75^{NTR}$.

1.4.4 AMIGO-3 blockade may enhance neuroregenerative processes more than LINGO-1

Recent work performed in the University of Birmingham suggests that specific members of the AMIGO family of proteins may function as alternative binding partners to LINGO-1 at the NgR (Ahmed et al. 2013). AMIGO3 levels were found to be significantly higher than those of LINGO-1 in the early phase following dorsal root ganglion neuron (DRGN) crush in rats and suppressed in the retina in a model of optic nerve regeneration. Functional outcome data showed that AMIGO3 interacts with NgR1-p75/TROY in both non-neuronal transfected cells and in brain lysates, with evidence of RhoA activation in response to CNS myelin extracts.

Knockdown of AMIGO-3 in primary DRG and retinal cultures in the presence of myelin resulted in disinhibited neurite outgrowth when stimulated with neurotrophic factors. This data suggests that AMIGO3 substitutes for LINGO-1 in the NgR1-p75/ TROY inhibitory signalling complex and mediates myelin-induced inhibition of axon growth acutely in the CNS itself. The authors concluded that antagonising AMIGO3 as opposed to LINGO-1 immediately after CNS injury may be a more effective therapeutic strategy for promoting CNS axon regeneration. The situation is likely to be complex, given much of the work regarding the AMIGO molecules has been related to roles in neurite outgrowth. However, the molecules may well have differing functions, depending on the pathological context,

1.5 Summary

The relationship between inflammation and neurodegeneration in MS remains unclear. This is partly due to apparent dissociation between focal lesions and diffuse inflammatory processes, which we know are prominent during the progressive phase of the disease in particular (Kutzelnigg et al. 2005). Global pathological changes are thought to better reflect disability outcomes than focal inflammatory lesions (Gallo et al, 2005), therefore greater understanding of the mechanisms responsible for widespread changes in MS brain tissue is important.

HMGB1 has been implicated in many diseases, and serves as a link between sterile injury and inflammation. HMGB1 expression is known to be increased in active MS lesions, predominantly in macrophages/ microglia (Andersson et al. 2008). If HMGB1 can be detected in the periplaque white matter, this may provide a molecular representation of inflammation spreading centrifugally from the lesion core out into the surrounding tissue. Other work has demonstrated that HMGB1 is also produced from activated plasma cells (Vettermann et al. 2011), which we know are present in ectopic B-cell follicular structures in the meninges of MS patients (Serafini et al. 2004). Thus, it is possible that secretion from both infiltrating macrophages and B-cells mean it may be detectable in the CSF also.

Exploring the link between the LRRIG proteins and HMGB1 in MS is a novel area of MS research. Given the myriad different roles that HMGB1 plays, blocking its action in vivo may have less predictable consequences. Focussing on associated markers such as AMIGO molecules, induced downstream from HMGB1 activation, may allow a more rational interpretation of findings.

1.6 Hypotheses underpinning thesis

1. The expression pattern of HMGB1 reflects damage-related changes emanating from the active lesion core into the peri-plaque region

2. HMGB1 is detectable in the subarachnoid space and CSF and levels are increased in MS patients vs. controls

3. Expression of molecular targets potentiating neurodegenerative pathways, such as LINGO-1 and AMIGO-3, are influenced by HMGB1 stimulation

1.7 Aims of thesis

1. To compare HMGB1 expression using neuropathological tissue from MS and non-MS control patients, in both lesional and non-lesional regions

2. Assess CSF HMGB1 levels in MS patients compared to non-MS controls

3. Explore the expression pattern of LRRIG molecules, including effects of HMGB1 stimulation

2.

General Methods

2.1 MO3.13 cell culture

2.1.1 MO3.13 cell line

This human-human hybrid cell line was developed using postmitotic CNS cells that expressed oligodendrocyte (OGD)-specific proteins and mRNA. The primary OGD cultures were originally obtained from surgical resections for intractable epilepsy, with the actual tissue used for primary cells taken distal to the electrically active site. The tumour parent for the MO cell line was RD- a rhabdomyosarcoma cell line from ATCC (Rockville, MD). An aminopterin-sensitive mutant of RD lacking hypoxanthine phosphoribosyltransferase (EC 2.4.2.8) by selection in 6-thioguanine was developed and designated RD.TG6. Primary glial cells were fused to adherent RD.TG6 cells by a phytohemagglutinin P-enhanced, polyethylene glycol- mediated procedure modified from Fournier (1981). Because of the lack of HPRT, the inhibition of de novo DNA synthesis by aminopterin results in death of all cells which are not fused to the RD.TG6 cells. However,growth of the hybridoma cells in the presence of aminopterin is permitted due to utilisation of the salvage pathway, allowing cells to incorporate exogenous hypoxanthine and to synthesise purines. Using a combination of flow cytometry, IHC, CNPase activity, Northern and immunoblotting, the hybrid clone M03.13 demonstrated membrane-bound immunoreactivity (IR) for galactosyl cerebroside and intracellular IR for myelin basic protein (MBP), proteolipid protein (PLP), and glial fibrillary acidic protein (GFAP). Serum deprivation or chronic treatment with a protein kinase C activator 4-6-phorbol12-myristate 13-acetate (PMA) increased OGD phenotypic markers with down-regulation of GFAP expression, demonstrating their potential utility for in-vitro OGD modelling experiments (Buntinx et al., 2004; McLaurin et al., 1995). Extrapolating data generated using this immortalised cell line to processes

occurring in primary OGD is subject to caveat, but it provides a window into how OGD may respond to the multiple stimuli presented in the context of MS pathology.

2.1.2 Cell proliferation

Frozen MO3.13 cells were obtained via a material transfer agreement between the University of Birmingham and Cedarlane Corporation, CELLutions Biosystems Inc. (Ontario, Canada), via the UK distributors, VH Bio (Gateshead, UK). All cell culture procedures were carried out under aseptic conditions in fume hoods. Cells were cultured in a high glucose formulation of DMEM (Sigma-Aldrich, Dorset, UK) supplemented with 10% Fetal Bovine Serum Gold (Sigma-Aldrich, Dorset, UK) and designated 'high serum media'. Although not an absolute requirement, we also added Penicillin/Streptomysin at 1X (Invitrogen: 15140-148). The cells were maintained in $75cm^2$ tissue-culture flasks (Greiner Bio-One, Frickenhausen, Germany) at 37^0C in a humidified atmosphere with 5% CO_2. Cells were passaged once 70% confluency was reached, at which point 2ml of Trypsin-EDTA solution (Sigma Aldrich, Dorset, UK) was added and the flask agitated by tapping on the bench. The approximate total cell count was generally $1x10^7$ following cell counting and was subsequently split 1:10, giving a concentration of approximately $1x10^6$cells/ ml. For experiments, 0.5ml cell suspension was added to 2ml of high serum media in each well and seeded into 6-well plates. Plates were left for 24h for adherence and the media was then replaced with a low-serum media, with 0.5% serum present instead of 10% and cells were left for a further 24h. As described earlier, serum reduction was employed as it has been reported that this led to the expression of the mature oligodendrocyte marker (GST-π) in this cell line (Haq et al. 2003).

2.1.3 Freezing down cells

Cells grown in TC flasks were trypsinised at 70% confluence, re-suspended in 10ml of high-serum media and centrifuged at 400g for 5 minutes. Media was aspirated and the pellet carefully re-suspended in 10% DMSO and 90% high serum media. Samples were aliquoted into cryovials and placed in 'Mr Frosty' Cryo Freezing containers (Nalgene, Hereford, UK), containing isopropanol and frozen at a rate of $1^{0}C$ $minute^{-1}$, or kept in liquid nitrogen for long-term storage.

2.2 RNA extraction

The RNEasy Mini kit (Qiagen, Hilden, Germany) was used. Samples were lysed in each well, using a buffer containing a highly denaturing guanidine-thiocyanate–containing buffer, which immediately inactivates RNAses to ensure purification of intact RNA. Following addition of the buffer to each well, the cell monolayer was disrupted by passing the lysate through a 20-gauge (0.9 mm) needle attached to a sterile plastic syringe ⩾10 times until a homogeneous lysate was achieved. 70% ethanol was added to provide appropriate binding conditions, and the sample applied to an Rneasy Mini spin column, where total RNA binds to the membrane and contaminants are washed away following a series of washing and centrifugation steps (≥8000g). RNA is then eluted in 30–100 μl water.

2.2.1 RNA quantification

The quantity of RNA was measured using NanoDrop ND-2000 Spectrophotometer (Thermofisher, Surrey, UK). The absorbance of 1μl of RNA at 260nm and 280nm and the OD_{260}/OD_{280} ratio indicates the RNA purity. Only OD_{260}/OD_{280} ratios in the range of 1.9- 2.1 were used. All measurements were made with respect to a blank consisting of nuclease free water. Once RNA concentration was determined,

samples were diluted using nuclease-free water to produce a standardized amount of RNA in 100µl.

2.3 Reverse Transcription (RT) reaction

We used the high capacity RT kit from Applied Biosystems (Warrington, UK) for the RT reaction. X2 RT mastermix was constituted using the reagents as outlined in table 2.1 in 1.5ml eppendorfs.

Reagent	**Volume/ sample (µl)**
10x RT buffer	2
25x dNTP Mix (100mM)	0.8
10x RT random primers	2
Multiscribe RT	1
Nuclease-free water	4.2
Total/ reaction	*10*

Table 2.1. Reverse transcriptase reaction volumes

Samples were then loaded into a thermal cycler (Bio-Rad, Hemel Hempstead, UK), for incubation at 25^0C 10 minutes (denaturing and annealing stage); 48^0C for 30 minutes (transcription); and 5 minutes at 95^0C (inactivation). Samples were then removed and stored at -20^0C until PCR was performed.

2.4 Relative Quantitative (real-time) PCR

Real-time PCR was performed using a Roche LightCycler480 system (Roche, Sussex, UK). GAPDH was used as the 'house-keeping gene', acting as the internal

reference for RNA expression in the samples used. Reactions were performed in duplicate, in 5µl volumes using white 384-well plates. The Lightcycler® 480 Probes Master (Roche, Sussex, UK) and Applied Biosystem "assay on demand" primer-probes (Applied Biosystems, Warrington, UK) for target and house-keeping (GAPDH) genes were used as shown in table 2.2. All reactions were multiplexed with primers specific for GAPDH RNA with VIC-labelled probes, whilst target genes had FAM-labelled probes.

REAGENT	**VOLUME (µl)/ WELL**
Mastermix	2.5
Nuclease-free water	0.2
Primer-probe reference	0.5
Primer-probe target	0.5
cDNA	1.3
Total/ reaction	*5*

Table 2.2 Real-time PCR reaction volumes

Reactions were as follows: 50°C for 2 minutes, 95°C for 10 minutes; then 40 cycles of 95°C for 15 seconds and 60°C for 1 minute. Data were expressed as cycle threshold (Ct) values (the cycle number at which logarithmic PCR plots cross the calculated threshold line) and used to determine ΔCt values (ΔCt = Ct of the target gene minus Ct of the housekeeping gene). Arbitrary units (AU) were calculated using the ΔCt [AU = 1000 x ($2^{-\Delta Ct}$)] whilst relative mRNA levels using treatment – control values, and were expressed as fold changes ($2^{-\Delta\Delta Ct}$).

2.5 Protein extraction

Cell monolayers were placed on ice and washed with cold, sterile PBS. 150µl of RIPA buffer (Sigma-Aldrich, Dorset, UK; supplemented with protease inhibitor cocktail (PIC; Roche, Sussex, UK)) was then added to each well of the 6-well plate. PIC is used to maintain protein integrity as once the cells are lysed, all the proteases are released and may alter the properties of the protein of interest due to unchecked degradation. Wells were scraped, lysates collected and placed at 4°C for 15minutes. They were then centrifuged at 8000g for 10minutes at 4°C and the clarified protein supernatants placed on ice.

2.6 Protein concentration assay

5µl of each of the clarified lysates was transferred to a 96-well plate, leaving the first 3 columns of the plate free. Bovine serum albumin (BSA) 5mg/ml was diluted in distilled water to establish a dilution series (0 mg/ml, 0.125 mg/ml, 0.25 mg/ml, 0.5 mg/ml, 0.75 mg/ml, 1.0 mg/ml, 1.5 mg/ml and 2.0 mg/ml). 5 µl of each protein standard was transferred, in triplicate, to the first 3 columns of the 96 well plate. Standard protein assay reagents using the BioRad$_{DC}$ kit (Bio-Rad, Hemel Hempstead, UK) were then added to each well using an automated pipette. The samples were incubated at 37°C for 10 minutes to facilitate the chromogenic reaction. The absorbance of each well was then read at 630 nm using the BioTek Synergy HT machine (BioTek, Winooski, USA). A standard curve was plotted from the known protein concentrations and used to calculate unknown protein concentrations from the samples.

2.7 Immunoblotting

For all molecules, 40µg of denatured protein was resolved on Novex® NuPage® 4-12% Bis-Tris protein gels under reducing conditions (Invitrogen, Paisley, UK).

The gels were run at 200V/115 mA for approximately 60 minutes. Proteins were then transferred to PVDF membranes using the Trans-Blot® Turbo™ machine (Bio-Rad, Hemel Hempstead, UK), for 10 minutes. Membranes were then washed and blocked in 10ml of 5% Marvel (milk) for 1 hour at room temperature with constant agitation. They were then incubated overnight at 4°C on an orbital shaker with primary antibodies. After generous washing, secondary antibody incubation was performed at room temperature with constant agitation. After washing again, immunoreactive bands were generated using the ECL detection kit (GE Healthcare, Bucks, UK) and visualised using the ChemiDoc™ XRS system. Densitometry was calculated using the in-built ImageLAB software, following β-actin band detection (see below). Membranes were then stripped to remove bound primary and secondary antibodies by incubating in stripping buffer (Tris-buffer 0.1%SDS, 1.5% glycine and 1% Tween-20 in pure water; addition of acid to a final pH of 2.2.) The membranes were then thoroughly washed and re-probed for HRP-conjugated β-actin 1:5000 (Genscript, New Jersey, USA) to act as a protein loading control.

2.8 Immunohistochemistry

We used the Bond Polymer Refine Detection system that utilises amplification techniques to prepare polymeric HRP-linker antibody conjugates.

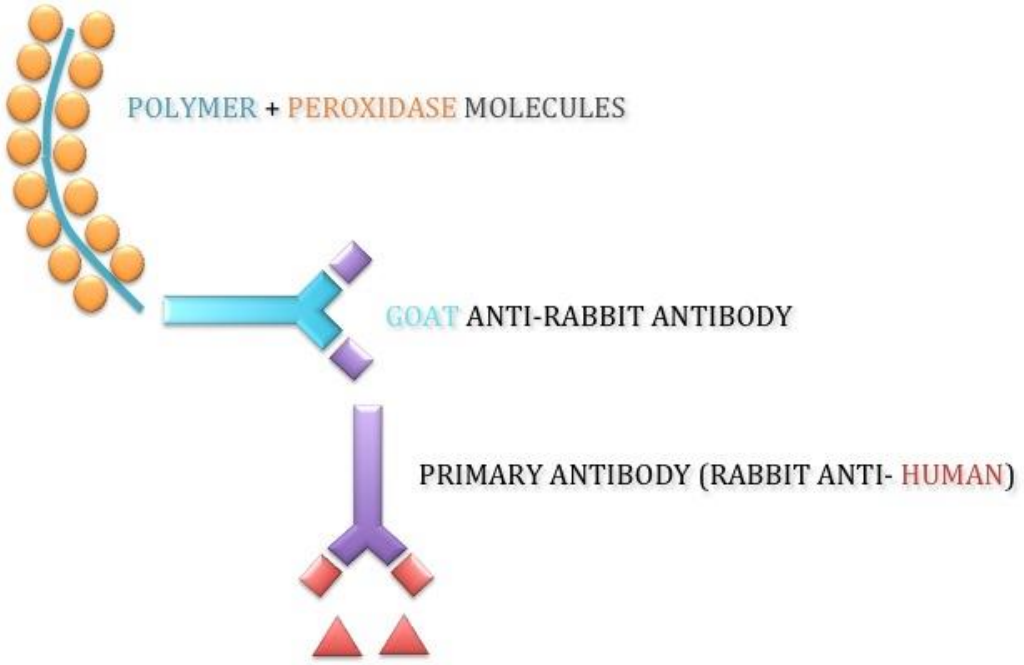

Figure 2.1 Schematic diagram illustrating the Bond Polymer Refine Detection system for immunohistochemical analysis in tissue. Amplification of signal generated from the antigen-antibody reaction is demonstrated with the use of polymer backbone technology with multiple molecules of peroxidase enzyme attached to this. An example of a rabbit anti-human antibody, with a corresponding anti-rabbit secondary antibody with a linked polymer backbone is illustrated. However, the Polymer Refine kit is a universal system with both anti-mouse and anti-rabbit secondary ('post-primary') antibodies with linked polymers included in the reaction mixture.

The detection system avoids the use of streptavidin and biotin, and thus eliminates non-specific staining as a result of endogenous biotin. The main purpose of this is to enhance the signal to noise ratio i.e. to enable specificity whilst maintaining a low level of background staining. Figure 2.1 illustrates the principle behind this.

8µm thick sections of formalin-fixed, paraffin embedded human brain tissue was obtained from the UK MS Brain Bank as outlined in Chapter 4. (Hammersmith Hospital, London, UK). Tissue slides were deparaffinised and treated with Epitope retrieval solution 1, pH 6(Leica Biosystems, Germany) at 98°C for 20 minutes. The

tissue was then washed and incubated with 1% hydrogen peroxide to quench endogenous peroxidase activity for 10 minutes. Primary antibodies were then used following optimization procedures and sections incubated for 30 minutes. 'Post-primary IgG linker reagent' localised mouse antibodies whilst 'poly-HRP IgG reagent' localises rabbit antibodies, and both were included in the post-primary mixture as a universal system enabling primary antibodies with different specificities to be used in the same run. This step lasted for 10 minutes, as did the subsequent chromogenic DAB reaction following washing steps. Once IHC was complete, haematoxylin (blue) counterstaining- allowing visualization of cell nuclei was also performed whilst still on the platform. Slides were then removed and progressively dehydrated with alcohol, cleared in xylene and mounted with a non-aqueous mounting medium for microscopy.

2.9 Immunocytochemistry (ICC)

Cultured MO3.13 cells in an 8-well chamber slide were washed with sterile PBS then fixed in 4% PFA for 15 minutes at room temperature (RT). After washing, they were blocked in 3% bovine specific albumin (BSA) for 20 minutes, and then incubated directly in the rabbit polyclonal anti-HMGB1 antibody for one hour at RT (Abcam, Cambridge, UK). Cells were washed and incubated in Alexa-Fluor-488-conjugated anti-rabbit secondary antibody for a further hour at RT, in the dark. After washing, the chambers were removed and the slide mounted in DAPI-containing aqueous mounting medium (Vector Laboratories, Cambridgeshire, UK) and stored in the dark at 4°C for subsequent microscopy.

2.10 Enzyme-Linked Iuhmmunoabsorbance Assay (ELISA)

2.10.1 Neurofilament-light chain assay

The ELISA was performed according to manufacturer's instructions and the principle outlined in figure 2.2.

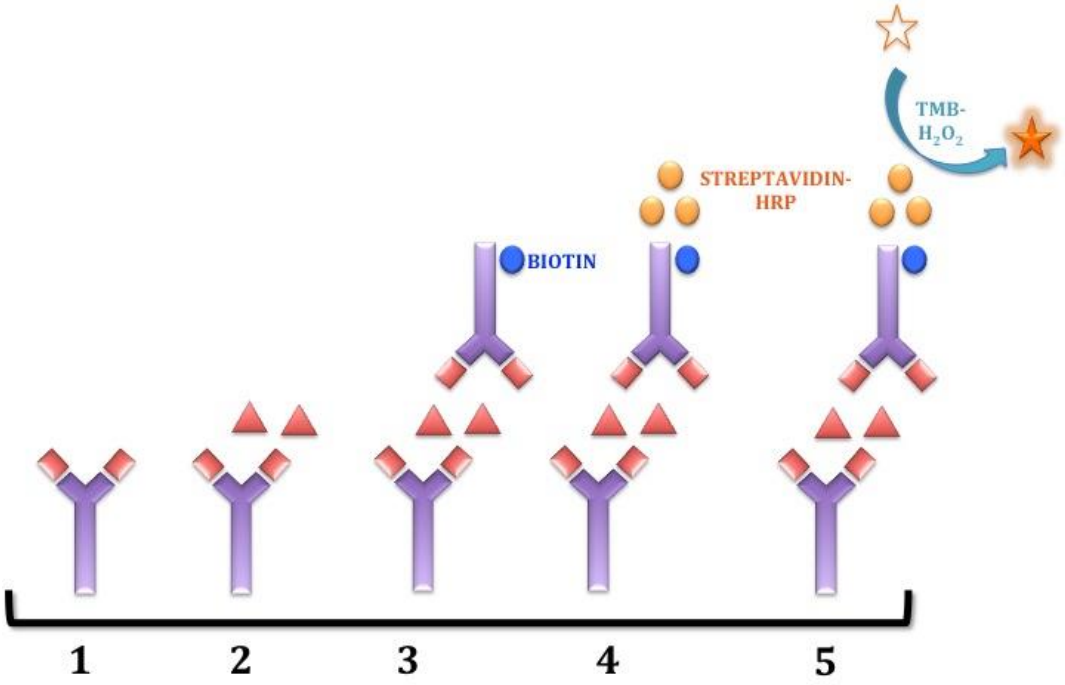

Figure 2.2. Principle for quantitative assay of Neurofilament-light chain in biological samples using the 'sandwich' ELISA technique. (1) plate is coated with a capture antibody (2) sample added and any antigen present binds to the capture antibody labelled with biotin (3) biotin-linked detecting antibody added (4) streptavidin-HRP added which binds to biotin-labelled antibody (5) substrate added and converted by HRP to detectable form.

In brief, the freeze-dried standards (purified bovine spinal cord with a purity > 98%) were reconstituted with 240 µL of sample buffer in a 1.5 mL Eppendorf vial to give a concentration of 40 ng/mL. The vial was gently swirled until thoroughly dissolved and then left at room temperature (RT) for 10 min. A series of eight Eppendorf vials were prepared, with the first vial containing 900 µL of sample diluent and vials 2 to 8, 600 µL of sample diluent. 300µL of the lyophilized standard was then added to the first vial to give a concentration of 10 µg/L. A doubling dilution using 600 µL in each step was performed and vial 8 was left only

with sample diluent to give the blank reading, corresponding to the following concentrations in ng/mL: 10000, 5000, 2500, 1000, 500, 100 and 0 ng/mL NfL. CSF samples were diluted 1:1 with sample diluent buffer to a total volume of 100ul. Wells to be used were washed with 300µl buffer x3, with removal by tapping the plate sharply against clean absorbant towels. 100µl standards/ samples were then added in duplicate and incubated for 1 hour at room temperature (RT; 20-25^{0}C) with agitation (800rpm). The wells were then washed x3 as described earlier, and 100µl tracer (biotin anti-NfL) added to each well and incubated for 45 minutes at RT with agitation as above. The wells were then washed again x3 and 100µl conjugated enzyme (streptavidin-HRP) added to each well. Following a 30 minute incubation at RT with agitation, the wells were washed x3 and 100µl tetramethylbenzidine (TMB) added as substrate to visualise the reaction, for 15 minutes at RT with agitation. 50µl 'stop' solution (8%v/v H_2SO_4) was added to each well to terminate the substrate reaction and absorbance read at 450nm using the BioTek Synergy HT machine (BioTek, Winooski, USA). The standard curves generated were analysed with 4 parameter logistic regression as recommended by the manufacturers, with values greater than the top part of curve capped to the maximum sensitivity of 10000ng/ml

2.10.2 HMGB1 assay

The assay was performed according to manufacturer's instructions, using digital multichannel pipettes to minimise pipetting error. In brief, the standards were

reconstituted and diluted as directed, corresponding to the following concentrations in ng/mL: 10, 5, 2.5, 1.25, 0.625, 0.313 and 0. CSF samples were diluted 1:1 with sample diluent buffer to a total volume of 100ul. 100ul standards/ samples were then added to the wells in duplicate and shaken briefly for 30seconds. The plates were then covered with adhesive foil and incubated for 24 hours at 37^0C. The following day, the incubation solution was discarded and plates washed x5 with 400ul of wash buffer, tapping the plate against clean absorbant towels in between washes. 100µl of enzyme conjugate was then added into each well, the plates covered with adhesive foil and incubated for 2 hours at RT. After washing x5 again, 100ul colour solution (a combination of TMB and buffer containing 0.005M hydrogen peroxide) was then added to each well and incubated for 30 minutes at RT. The reaction was stopped by the addition of 0.35M H_2SO_4 and absorbance read at 450nm using the BioTek Synergy HT machine (BioTek, Winooski, USA).

Using the goodness of fit test, linearity of the standard curve produced an R^2 of 1.0 and deviation from linearity using the runs test was not significant (p=0.3). Thus, interpolated values from the curve were calculated using linear regression.

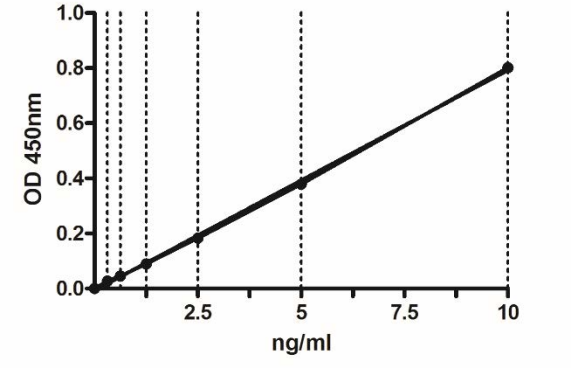

Figure 2.3. HMGB1 standard curve. (Y) axis: optical density (OD); (X) axis: concentration of HMGB1 (ng/ml). Dashed lines represent exact concentrations used in standard curve i.e. 0.313, 0.625, 1.25, 2.5, 5, 10ng/ml.

2.11 Statistical analysis

GraphPad Prism for Mac Version 5.0 (La Jolla, California, US) was used to perform statistical analysis. For in-vitro work, data was normally distributed and parametric tests were used. PCR data, statistical tests used both δC_t and fold-change values in statistical tests. Comparisons between multiple treatments were analysed using one-way analysis of variance (ANOVA) with Tukey's post-hoc multiple comparison test used to account for type 1 errors. Continuous data was expressed as mean and standard error of the mean (SEM). Statistical analysis of both neuropathological ex-vivo and CSF in-vivo human data used non-parametric testing. The data are represented as medians, with multiple comparisons performed using a Kruskal-Wallis test with Dunn's post-hoc correction. Two-group comparisons were performed using a Mann-Whitney *U* test for unpaired continuous measures. Spearman's rank correlation coefficient was used to evaluate the statistical dependency of two variables. The threshold for statistical significance was set at $p<0.05$.

3

Characterisation of early active lesional changes in a patient with clinically isolated syndrome, using classical and novel markers.

3.1 Introduction

The history of MS research commenced with the clinicopathological observations of the 19th century (Chapter 1; section 1.1). Neuropathological analysis of human tissue offers a window into pathological processes occurring in patients with disease. This chapter is concerned with the expression profile of HMGB1, an important mediator which potentially links inflammation and degeneration, in human MS tissue taken at biopsy. To our knowledge, examination of HMGB1 expression at an early time-point in a patient's disease using biopsy tissue, has not been performed before.

HMGB1 has pleiotropic roles, with much of the early literature based upon its important function in propagating pro-inflammatory loops following secretion by macrophages (Yang et al. 2013; Andersson & Tracey 2011; Fang et al. 2012). However, in recent years, the field of HMGB1 research has highlighted roles in diverse processes, from immune cell recruitment to autophagy. Research into a number of neurological disorders have also demonstrated an important role for HMGB1, linking neuroinflammation with degenerative processes (Gao et al. 2011; Fang et al. 2012; Kim et al. 2006); these studies have been discussed in detail in Chapter 1 (section 1.3).

HMGB1 expression has been examined in MS autopsy tissue, in addition to examination in spinal fluid using western-blotting techniques and comparison of the staining pattern in the murine model of MS, EAE (Andersson et al. 2008). The neuropathological component of the latter report used a large series of patients for immunohistochemical analysis, exclusively commenting on microglial/ macrophage cytoplasmic translocation in active lesions from both progressive and

'acute' MS patients- although the latter group are not clearly defined. They also reported that astrocytes did not demonstrate cytoplasmic translocation upon colocalisation with HMGB1, but did not comment upon expression in other cell types, such as oligodendrocytes (OGD), in either MS patients or controls. In addition, they did not consider the changes occurring in the normal-appearing brain tissue (NABT). As discussed in chapter 1, understanding molecular events taking place in these non-lesional areas in MS brain is critically important as it remains unclear as to whether lesions arise from these regions or the other way around. Interestingly, in situ hybridisation examining the spinal cord of relapsing EAE mice demonstrated that HMGB1 reactivity was widespread throughout the spinal cord, not just affecting lesional regions. They did not comment upon the significance of this in non-lesional regions, but concluded it suggested de novo HMGB1 synthesis during EAE relapses.

A study by Zeis et al also examined changes in non-lesional white matter regions using biopsy tissue (Thomas Zeis et al. 2009). They described a similar clinical presentation in a single patient who underwent stereotactic biopsy, with subsequent reporting of findings both in the active MS lesion and in the distal non-lesional tissue. They found that neuronal nitric oxide synthetase (nNOS) was upregulated in myelinated white matter with evidence of reactive-nitrogen species-mediated damage to OGD in these regions also, in the absence of overt inflammation. In addition, markers such as HIF-1α were upregulated in this region, suggesting OGD are held in a precarious balance of function and dysfunction in non-lesional tissue.

However, as stated earlier, the most striking findings in the study by Andersson et al were in the 'acute' and 'active' lesional tissue types, as opposed to 'chronic lesions' and non-MS control white matter, underlining its importance in active inflammatory processes. As will be detailed below, our biopsy tissue was taken from a patient with fulminant inflammatory demyelinating disease, such that the main differential prior to biopsy was of a neoplastic, gliomatous process. We would therefore predict that this type of tissue would exemplify the inflammatory aspects of HMGB1-related pathology described in highly active lesions by Andersson et al, thus enabling us to compare our findings directly with these. In addition, as noted by Zeis et al., abnormalities in non-lesional regions have also been observed in similar tissue types. Despite mounting evidence of its role in chronic neuroinflammatory and degenerative processes, detailed analysis of HMGB1 responses in early active MS brain lesions is novel and thus it would be of interest to investigate this using biopsy material.

3.2 Hypothesis

1. HMGB1 expression is increased in macrophages/ microglia of active lesional biopsy tissue.
2. Macrophages/ microglial expressing HMGB1 demonstrate evidence of cytoplasmic translocation
3. HMGB1 expression will be increased in peri-lesional regions, but this expression will decrease with increasing distance from the lesion border

3.3 Objectives

1. Perform a detailed characterisation of biopsy tissue from patient MS1 with a clinically isolated syndrome, using a range of established markers to delineate lesional and non-lesional regions.
2. Examine HMGB1 expression patterns to observe molecular changes occurring in active inflammatory lesions
3. Analyse HMGB1 expression in CNS-resident cells in regions distal to active inflammatory lesions

3.4 Methods

3.4.1 Neuropathological tissue preparation

Stereotactic brain biopsy was performed at University Hospital Birmingham (UHB) for diagnostic evaluation. Tissue was fixed in neutral buffered formalin and then embedded in paraffin. Five blocks of interest were selected by Consultant Neuropathologist, Dr Martyn Carey and supplied to the Human Biorepository Resource Centre (HBRC) following informed consent for participation in research studies, under local ethical approval of the HBRC Tissue Bank (LREC11/H1211/1). Of these, 4 blocks contained a mean tissue area available for analysis of 2.01cm^2, with the final block having a relatively smaller area of 22.42mm^2. These areas are far in excess the minimum often used to study biopsy material, where other studies have specified an area >1mm^2 is required as a minimum suitable area for analysis (Metz et al. 2014). Blocks were then sectioned at 8μm thickness using a steel microtome, with routine stains used to delineate lesion borders initially and further dedicated immunohistochemical stains to either verify this or to confirm identity of different cell populations in the different regions of tissue.

3.4.2 Analysis of neuropathological tissue

Biological tissue demonstrates limited natural contrast using light-microscopy. Staining is thus used to provide contrast in addition to highlighting interesting features. Haematoxylin and eosin (H&E stain) is a widely used histological stain. Hematoxylin is a basic dye, staining nuclei blue due to an affinity to nucleic acids. In contrast, eosin is acidic and stains cell cytoplasm pink. This enables identification of cell borders and morphological assessment based on factors such

as nuclear size and density of staining, in addition to cytoplasmic pattern of eosin staining. IHC was carried out using the Leica Bondmax automated stainer as described in chapter 2 (Leica Biosystems, Germany). Antibodies used were anti-MBP, -CD68, -CD3, -GFAP and –HMGB1 as described in table 3.1. Staining of sequential sections was performed in order to delineate the lesion border and cellularity.

Protein target	Antibody type	Source	Concentration used (μg/ml)
Myelin-basic protein	Mouse MC	Abcam	1
CD68	Mouse MC	Dako	5
CD3	Rabbit MC	Abcam	10
Glial fibrillary acidic protein	Rabbit PC	DAKO	0.3
HMGB1	Rabbit PC	Abcam	2.5
HMGB1 peptide control	-	Abcam	2.5
IgG isotype control	Rabbit PC	Abcam	2.5

Table 3.1. List of antibodies used in IHC experiments.

Stained sections were then mounted using xylene with glass coverslips. Preliminary microscopy was performed in order to assess staining success then whole slides were scanned using the Leica SCN400, and stored on the Digital Image Hub 'cloud' system, based at the University of Birmingham.

3.5 Results

3.5.1 Case report

This previously healthy 33 year old male patient presented with significant reduction in visual acuity in the right eye over a week. This was followed by progressive weakness affecting the left arm and leg, along with cognitive deficits including memory disturbance and he was admitted to his local hospital within

two weeks of symptom onset. Initial CT and MRI scans revealed a mass lesion in the parieto-occipital region suggestive of a malignant process and he was transferred to the Neurosurgical Unit at University Hospital Birmingham. Cranial nerve examination revealed reduced visual acuity with finger counting on the right and 6/9 on the left, with a left homonymous hemianopia. Peripheral nervous examination showed pyramidal signs on the left, with associated weakness of 2/5 and hemisensory alteration. Power and sensation were preserved on the right-hand side at this stage. Plantar responses were bilaterally extensor. Further MRI evaluation revealed a multifocal process with increased T2 signal in the right occipital lobe, spread across the splenium of the corpus callosum to the left (see Appendix 2, figure A1). Another discrete lesion in the left occipital lobe was noted, in addition to further moderately- sized lesions in the right frontal and parietal lobes, with patchy enhancement of the large right occipital and the callosal lesion. There was no significant mass effect. A stereotactic brain biopsy was performed the day after transfer from his local hospital, which demonstrated necrotic tissue with non- specific findings. A repeat biopsy demonstrated reactive astrocytes and some inflammatory changes, but again changes were non-specific and he was transferred to Neurology. Laboratory serum tests for rheumatic factors, ANA, ANCA, anti-cardiolipin antibodies, toxoplasma, syphilis, HTLV-1 and -2 and HIV were all negative. Initial CSF examination revealed no inflammatory cells although he had received steroid therapy (dexamethasone) whilst under the neurosurgeons. CSF analysis for herpes viruses, cytomegalovirus, varicella zoster virus, Enterovirus, EBV, Tropheryma whippelii, toxoplasma and acid-fast bacilli were all negative. CSF TB culture was also negative as were immunophenotyping of inflammatory cells. Oligoclonal band analysis was negative on two occasions

but subsequently positive. His clinical course was complicated by multiple medical problems and once stabilised, a third and final biopsy was carried out, which revealed changes described below. It supported evidence of a demyelinating process of recent onset and favoured a diagnosis of multiple sclerosis over ADEM, with no evidence of lymphomatous or neoplastic processes. He was treated with intravenous methylprednisolone, and soon after the final biopsy, he was commenced on Tysabri treatment and prednisolone was gradually tapered. In the subsequent 4 years, he developed classical RRMS.

3.5.2 Evidence of early active lesions consistent with MS

Figure 3.1 demonstrates florid perivascular cellular inflammatory infiltrate and throughout the parenchymal white matter. The region borders are ill- defined but despite fragmentation, there is preservation of myelin as shown by MBP staining, thus classifying this as an early active lesion. The predominant cell types are CD68-positive foamy macrophages, or lipophages, in 3.1C, with perivascular cuffing of CD3-positive lymphocytes in 3.1D, in addition to a few scattered lymphocytes in the parenchyma. There is a significant upregulation of GFAP reactivity shown in figure 3.1E, indicating astroglial activation, and their large bloated appearance denotes the presence of gemistocytes (3.1A and –E).

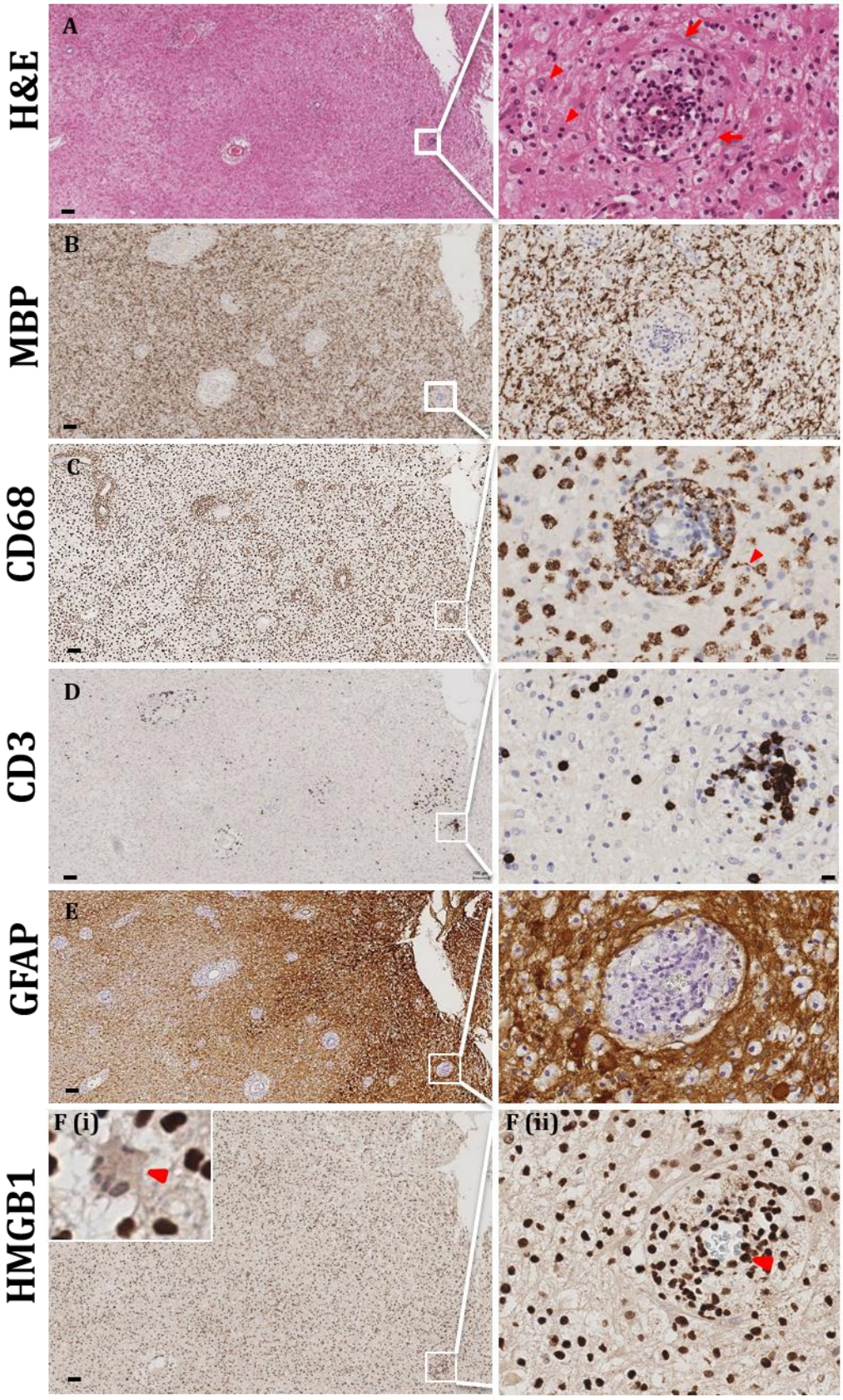

Figure 3.1. Characterisation of an early active lesion in FFPE biopsy tissue of a patient (MS1) with Clinically Isolated Syndrome (CIS), and corresponding HMGB1 expression pattern *(continued overleaf).*

Figure 3.1. Characterisation of an early active lesion in FFPE biopsy tissue of a patient (MS1) with Clinically Isolated Syndrome (CIS), and corresponding HMGB1 expression pattern. (A) H&E stain shows inflammatory cell infiltration over a large area, throughout the lesion. Inset illustrates perivascular inflammation as well as presence of hyperactivated/ gemistocytic astrocytes with evidence of multi-nucleation or large, pale nuclei (arrowheads). Extensive perivascular foot-processes are also evident (arrow). (B) anti-MBP IHC demonstrates that complete demyelination has not yet occurred at this stage of lesion evolution, although there is clear evidence of myelin fragmentation and peri-venous demyelination, demonstrated at higher magnification in the inset (C) shows significant anti-CD68-cell positivity throughout the lesions, representing activated macrophages/ microglia. Morphologically, the cells are predominantly foamy macrophages or lipophages (arrowhead). Inset shows higher magnification view of lipid-laden, perivascular macrophages. (D) anti-CD3-positive staining, denoting cells with a T-lymphocyte cell lineage, shows marked perivascular infiltration (inset) with dissemination into the parenchyma (arrowhead). € Widespread upregulation of anti-GFAP-positive cells on IHC, representing activated astrocytes. As noted on H&E, the bloated cells with pale cytoplasm, often displaying nuclear atypy or multinucleation and with extended processes, represent gemistocytes. (F) anti-HMGB1 IHC demonstrates strong, predominantly nuclear immunoreactivity most markedly in activated macrophages. Inset (i) shows multinucleate gemistocytes with little evidence of nuclear HMGB1 and very pale cytoplasmic staining, compared to intensely stained inflammatory cells around it. Inset (ii) shows perivascular staining at higher magnification, demonstrating likely HMGB1-positivity for perivascular lymphocytes also. *Scale bar= 100μm; inset scale bar=10μm*

3.5.3 HMGB1 immunoreactivity is evident in macrophages/microglia in early active MS lesions

In this context, anti-HMGB1 IR is clearly evident, predominantly in macrophage/ microglial cells, with intensely stained nuclei as shown in figure 3.1F, but also with some evidence of cytoplasmic translocation in these cells. Interestingly, astrocytic staining appears to be less marked compared to myeloid cells, with little nuclear staining evident in particular. However, faint cytoplasmic staining is evident, as shown in 3.1F(i), inset, although this non-specific pattern is frequently seen in this cell type *(M. Carey, personal communication)*. OGD staining is also evident, although number of olig2-positive cells were not counted.

3.5.4 HMGB1 immunoreactivity is evident in peri-lesional regions

Similar staining patterns in the active lesion are evident in different blocks from the same tissue biopsy. However, with the wide field of view from the scanned image, peri-lesional white matter tissue displaying normal MBP staining patterns, also demonstrates changes including CD68-positive cell reactivity and persisting CD3-positive peri-vascular cuffing. In particular, CD3-postive perivascular lymphocytes are also evident at the grey-white matter border, as shown in figure 3.2C, in the vicinity of layer VI pyramidal neurons. The border of the active lesion is highlighted by CD68-positive macrophages, which change morphologically into activated microglial cells into the peri-lesional WM.

HMGB1 staining is widespread, predominantly affecting myeloid cells as described earlier, but is also notably increased in oligodendroglial cells in the peri-lesional white matter. Astrocytes, once more, display little nuclear staining and only faint cytoplasmic reactivity. In addition, IR is prominent in the non-lesional

grey matter adjacent to the lesion as shown in figure 3.2D, which will be examined in more detail below.

Of note, three control methods were employed in order to delineate the possibility of non-specific HMGB1 immunoreactivity: (i) omission of the primary antibody, (ii) IgG isotype control (iii) using the specific peptide which the anti-HMGB1 antibody was raised against, as a blocking agent. The staining pattern using the range of controls was weak and suggested that the HMGB1 staining was antigen-specific (see Appendix 2, figure A2). The IgG control demonstrated clearly reduced staining but a few perivascular cells were shown to be positive, possibly reflecting IgG-positive B-cells. Although we did not stain for complement specifically, the presence of immunoglobulin when using the IgG control (figure 3.2E) demonstrates a probable pattern II lesional subtype (see Introduction; section 1.3.3.4).

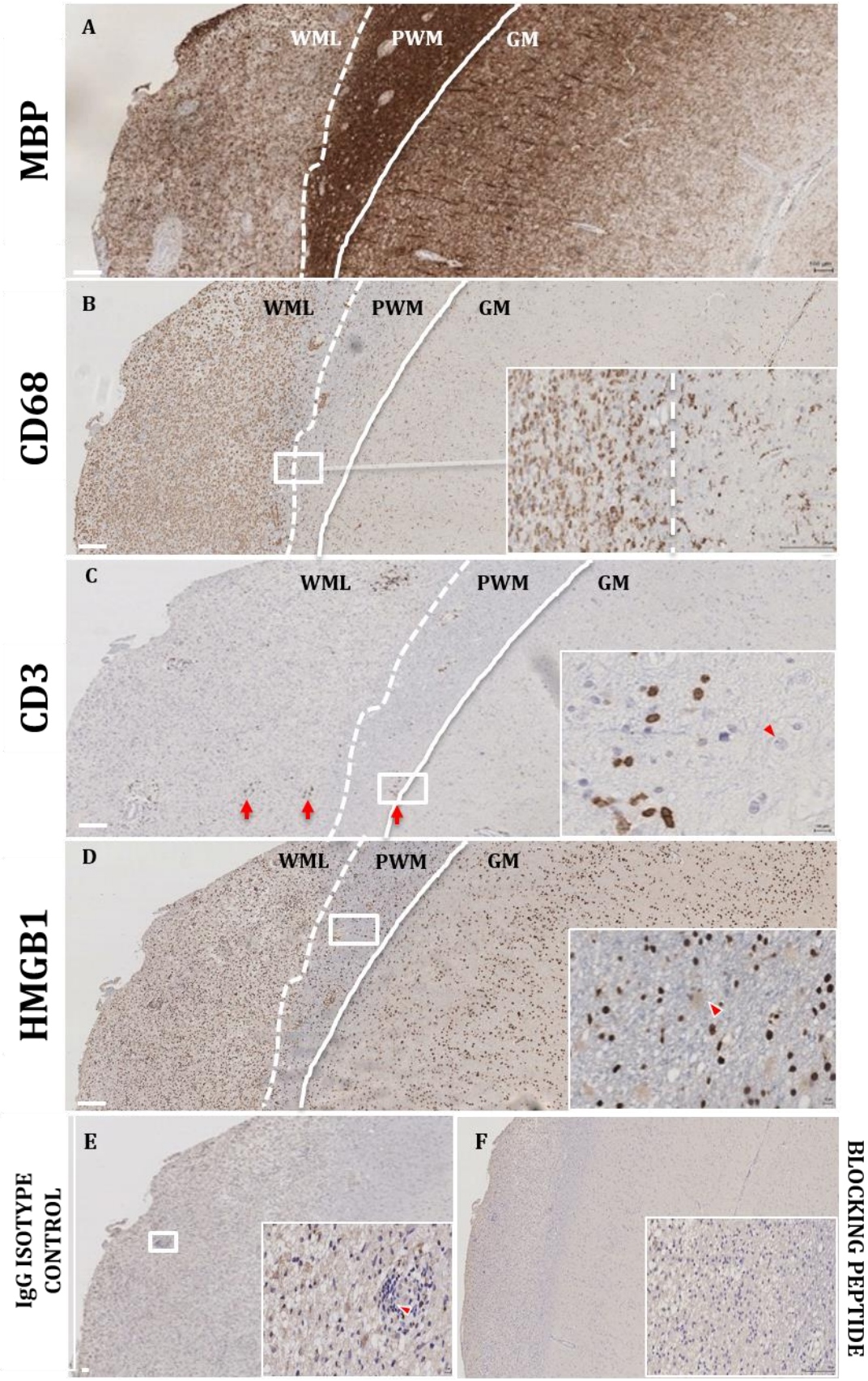

Figure 3.2. Early active, peri-lesional and non-lesional tissue in FFPE biopsy tissue of a patient (MS1) with Clinically Isolated Syndrome (CIS) *(continued overleaf)***.**

Figure 3.2 *(overleaf)*. **Peri-lesional and non-lesional tissue in FFPE biopsy tissue of a patient (MS1) with Clinically Isolated Syndrome (CIS).** (A) Anti-MBP staining highlights the white matter lesion by demonstrating myelin fragmentation, with the lesion border shown by the dotted line. The peri-lesional white (PWM) and grey matter (GM) borders are identifiable, with normal myelination patterns evident. (B) anti-CD68 IHC demonstrates massive macrophage infiltration within the WML. As shown in the inset at higher magnification, advancing lipophages form a border juxtaposed with cells of activated microglial morphology in the PWM (C) anti-CD3-positive staining shows multiple small blood vessels with lymphocytic infiltration throughout the tissue (arrows), including into non-lesional GM ((inset); arrowhead=neuron) (D) anti-HMGB1 IHC again demonstrates widespread increased immunoreactivity (IR) in macrophages within the WM. However, the wide field of view also demonstrates increased IR in CNS-resident cells in the adjacent, non- lesional tissue region, including in the GM. Inset shows gemistocytes with clear nuclei and pale cytoplasmic staining compared to other glial cells in the vicinity. (E) IgG isotype control antibody demonstrating limited IR although some perivascular cells are positive and likely to represent Ig-producing B-cells (arrowhead). (F) Blocking peptide specific to HMGB1 demonstrates virtually no IR. WML= white matter lesion; PWM= perilesional white matter; GM= grey matter; *Scale bar=100μm; inset scale bar=10μm except CD68=100μm.*

3.5.5 HMGB1 immunoreactivity persists into non-lesional regions

Non-lesional white matter was initially identified by being >7mm distance from the white matter lesion border on this block, in this plane (figure 3.3A). The white box shows a representative area here. MBP staining demonstrated a normal myelination pattern and minimal CD3-positive inflammatory cell infiltrates. A number of CD68-positive cells populated this region, as shown in figure 3.3B and these cells contribute to the intense HMGB1 IR in the non-lesional WM. However, oligodendrocytes appeared to be the predominant HMGB1-positive cell type. They were identified morphologically by parameters including size, roundedness and characteristic 'fried-egg' appearance, referring to the well-recognised artefactual regression of tissue immediately surrounding oligodendroglial cells (Greenfield's Neuropathology, Volume I; 8th Ed.). Again, astrocytes show evidence of faint HMGB1 cytoplasmic reactivity, in stark contrast to the staining pattern in other glial cells.

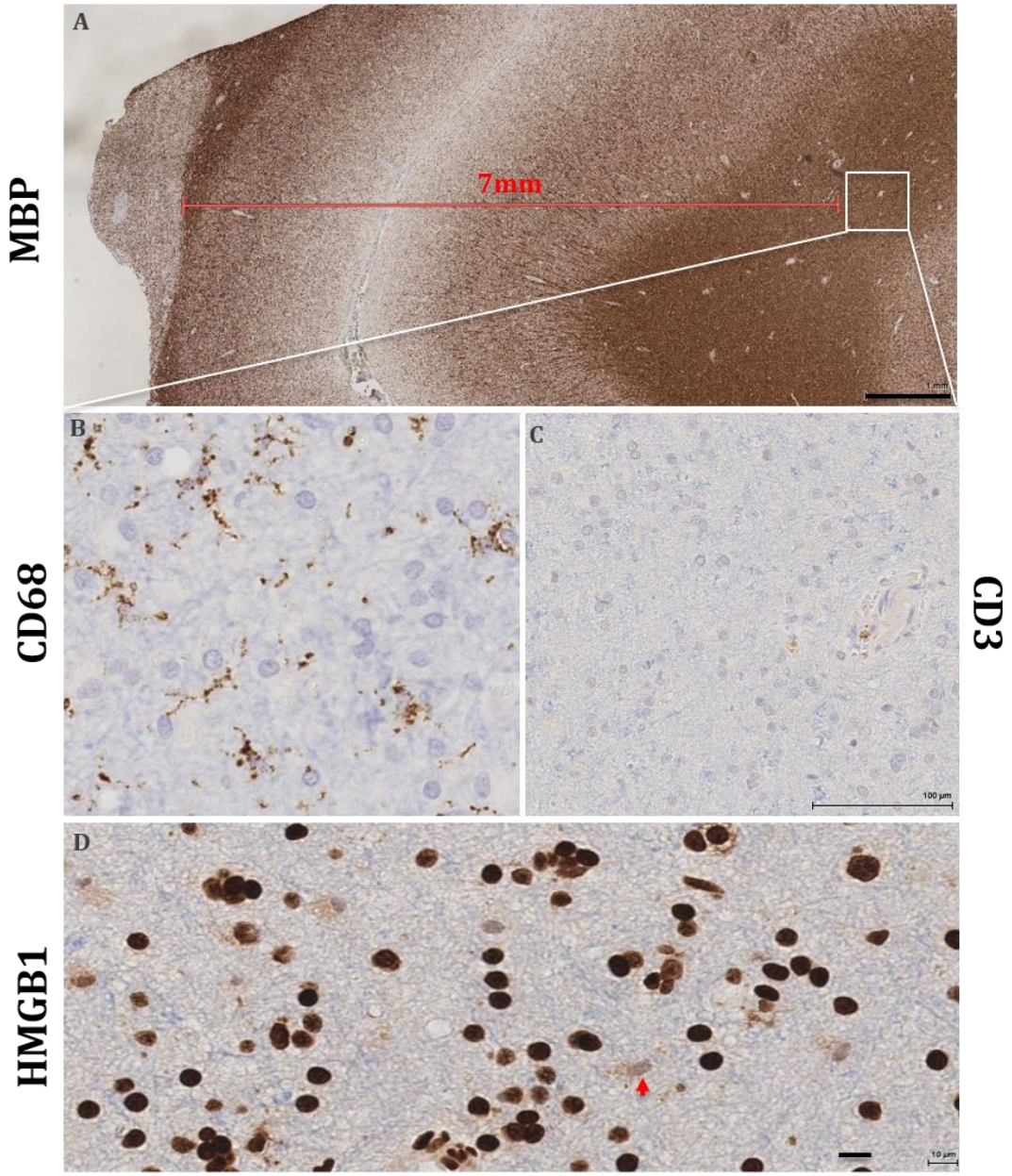

Figure 3.3. Demonstration of non-lesional white matter in FFPE biopsy tissue of a patient (MS1) with Clinically Isolated Syndrome (CIS). (A) Anti-MBP staining highlights the white matter lesion ('WML') described in figures (3.1) and (3.2) at the extreme left of the image. The cytoarchitecture of white matter and grey matter borders are clearly identifiable, with normal myelination patterns evident. The inset shows a representative region of non-lesional white matter and (B)-(D) demonstrate IR in this region for different markers, at higher power (B) anti-CD68 IHC demonstrates microglial infiltration (C) anti-CD3 IHC staining shows virtually no positive cells in this region (D) anti-HMGB1 IHC again demonstrates widespread increased immunoreactivity in CNS-resident cells. *Scale bar= 100µm; inset scale bar=10µm.*

3.5.6 Cortical regions remote from white matter lesions demonstrate specific HMGB1-positive expression patterns

Non-lesional: Anti-MBP IR in Figure 3.4A shows a normal myelination pattern but despite this, significant abnormalities are evident in all layers of the cortex. Some relatively normal pyramidal neurons can be seen as in figure 3.4C, but cells with condensed, pyknotic nuclei are widespread, in addition to changes suggestive of chromatolysis (figure 3.4D; circle). Other than a small number of scattered perivascular lymphocytes, there are few CD3-positive lymphocytes in the cortical parenchyma (figure 3.4E). However, they can clearly be seen in overlying meningeal vasculature, although no follicular-like structures were seen. Microglial cells with extended processes in close association with pyramidal neurons are seen with CD68-staining (figure 3.4F).

Anti-HMGB1 IR is widespread in the cortex and demonstrates significant IR in most neuronal nuclei, (figure 3.4G). Interestingly, satellite oligodendrocytes- in their classic configuration in apposition with neurons- show particularly intense IR. These were frequently adjacent to neurons with evidence of cytoplasmic translocation (figure 3.4I). In addition, dystrophic neurons with pyknotic nuclei also strongly expressed HMGB1. Other conformations of interest show intensely IR glial cells aligning longitudinally (figure 3.4H). Morphologically they are OGD, supported by lack of CD68 or CD3 reactivity in sequential sections and appear to group along blood vessels. Figure 3.4J further demonstrates neuronal cytoplasmic expression of HMGB1, with apparent membranous 'blebbing'. This may represent HMGB1 expression at the membrane near the soma or else may highlight evolving apoptotic change within neurons.

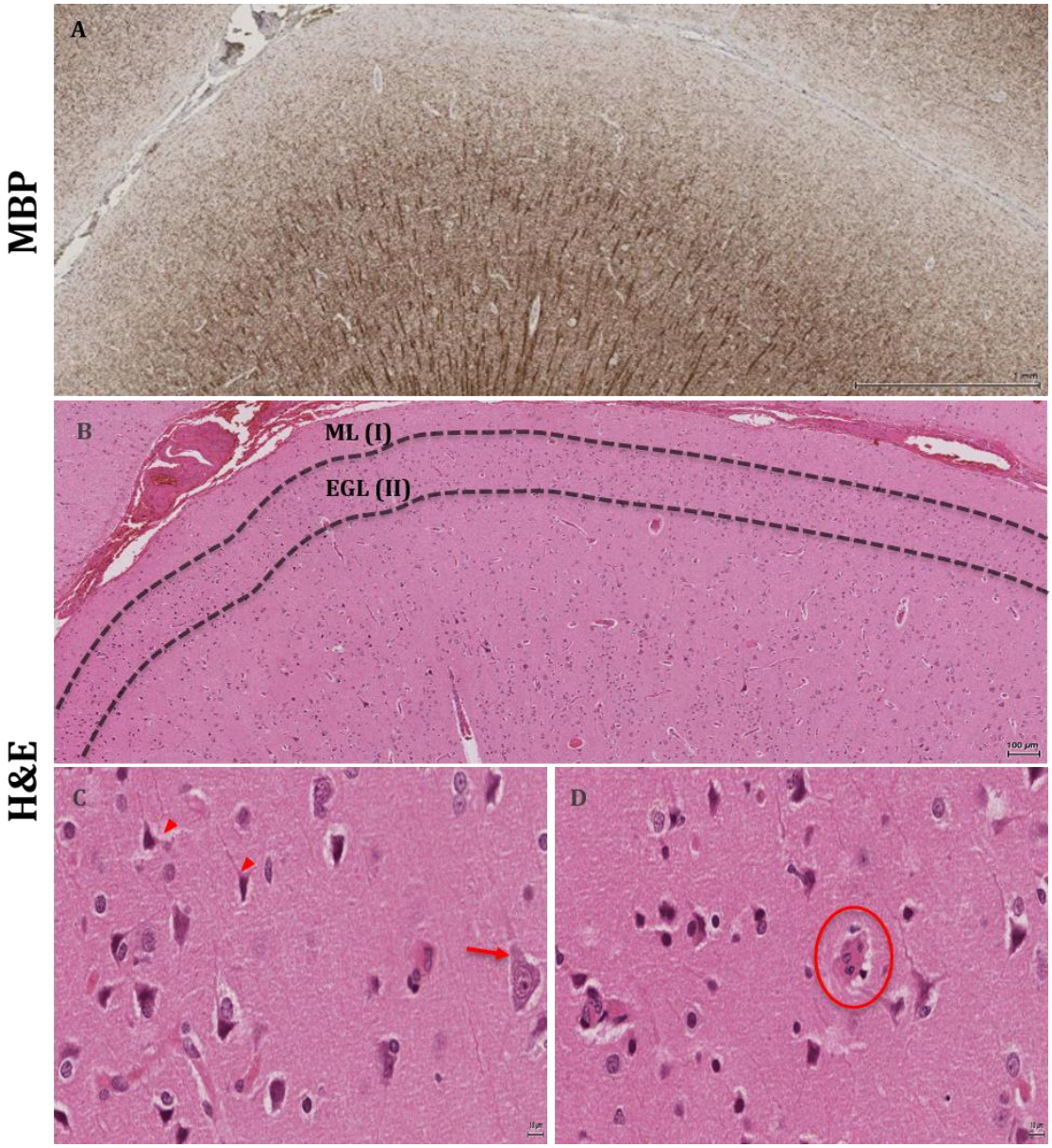

Figure 3.4. Demonstration of non-lesional grey-matter tissue in FFPE biopsy tissue of a patient (MS1) with Clinically Isolated Syndrome (CIS) (A-D). This region of grey matter is situated >5mm away from the active lesion border as shown in figure 3.2. (A) anti-MBP IHC demonstrates a normal myelin pattern in this region of the cortex. (B) H&E stain at low magnification demonstrating cortical layers of the grey matter, with overlying meningeal blood vessels (C) and (D) high magnification representation of neuronal changes. Pynknotic neurons are evident, with nuclear condensation and cytoplasmic retraction (arrowhead), whilst larger pyramidal neurons with normal morphology are also evident in the vicinity (arrow). There is also evidence of chromatolysis (circle). NB molecular layer (I) of pyramindal neurons is demonstrated next to the the external granular layer (II) to highlight cortical anatomy *(continued overleaf).*

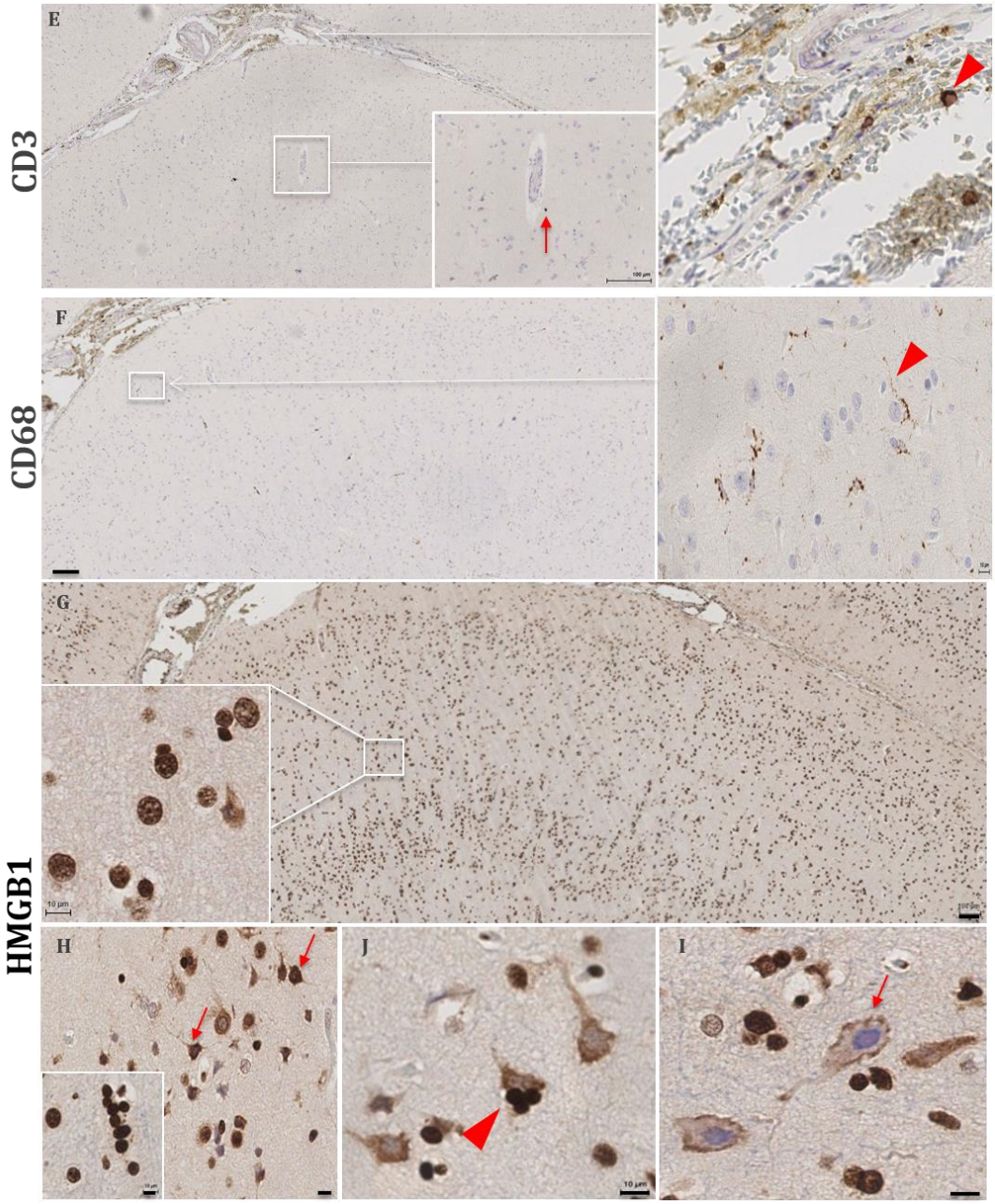

Figure 3.4 *(continued).* (E) anti-CD3: positive cells in the overlying meningeal vessels are seen (inset; arrowhead), occasional parenchyma cells seen near blood vessels (arrow). (F) anti-CD68 IHC demonstrates microglial activation in the cortex surrounding neurons (arrowhead) (G-J) anti-HMGB1 IHC (G) increased IR throughout the cortex, with granular layers demonstrating intense IR. Most neurons e.g. layer III demonstrate nuclear IR with characteristic chromatin staining pattern evident (inset) (H) markedly increased IR in dystrophic neurons (arrow), whilst strongly HMGB1-positive OGD also seen, possibly along vessels (inset) (I) neurons with evidence of cytoplasmic translocation into the soma and proximal dendrites demonstrated intensely stained OGD immediately adjacent to them, in their classical configuration (arrowhead). (J) other pyramidal neurons displaying cytoplasmic translocation are shown with apparent HMGB1-positive membranous 'blebbing'. *Scale bar= 100µm; inset scale bar=10µm.*

Lesional: Figure 3.5A, demonstrates a sub-pial type III cortical lesion in this biopsy tissue (Bo et al. 2003), with a significant inflammatory cell infiltrate in the meningeal vessels overlying it, as shown in figures 3.5B and 3.5C. Whilst there are few CD3-positive cells in the parenchyma, there are numerous CD68-positive cells throughout, which morphologically appear to be activated microglial cells, with no evidence of lipophages. A number of activated astrocytes are evident in the cortex, as shown in figure 3.5D, though the cells are not gemistocytic in appearance as seen in the white matter lesions, suggesting they may be performing an alternative function here. HMGB1 IR is evident in the external granular layer but IR is less intense overall and there is evidence of much more widespread cytoplasmic translocation. The high stromal background staining may be artefactual.

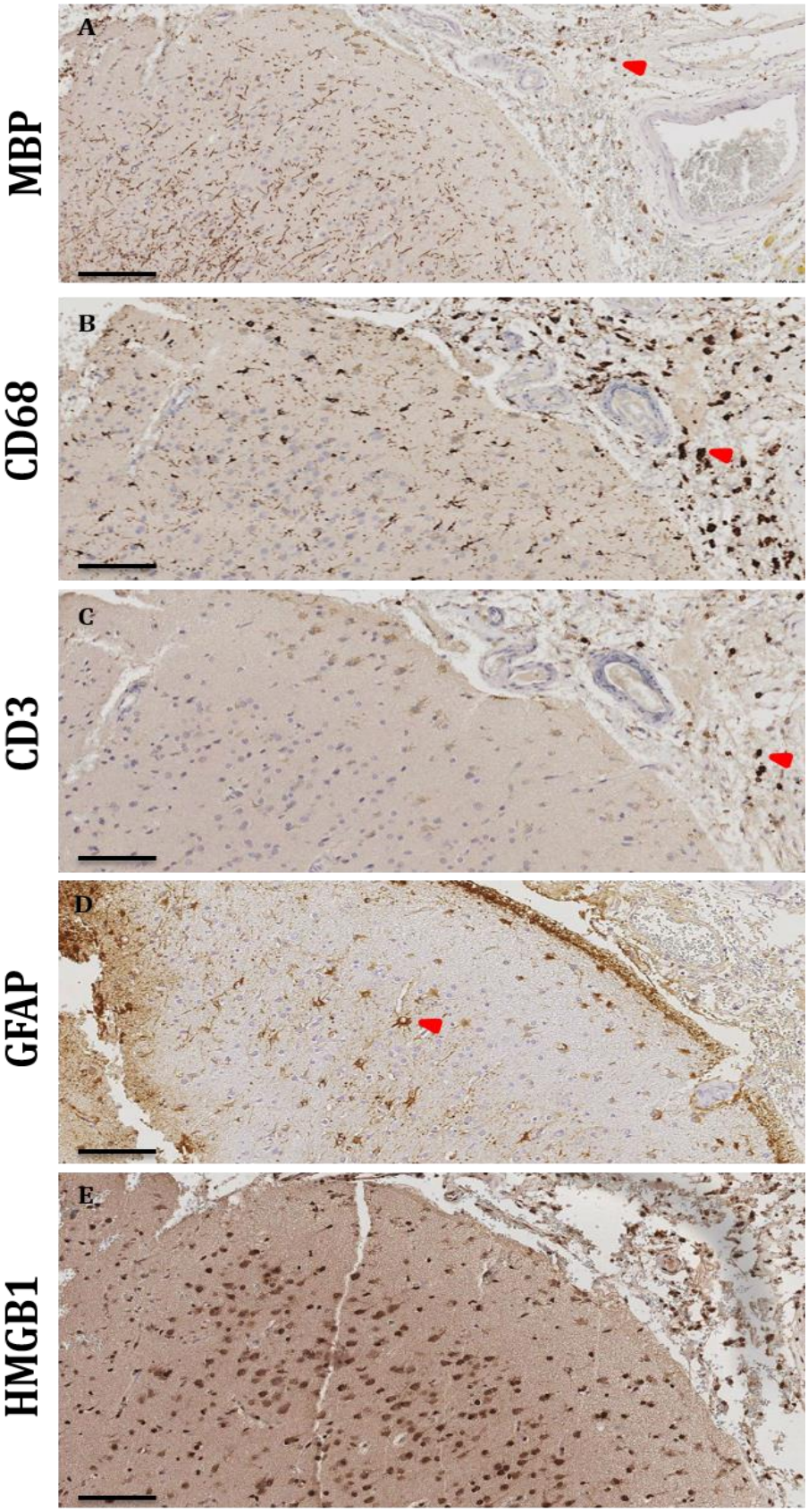

Figure 3.5. Type III demyelinating cortical lesions are evident in active lesional tissue blocks, with evidence of overlying meningeal inflammatory cells. *(continued overleaf)*

Figure 3.5 ***continued*****.** (A) Anti-MBP IHC demonstrates reduced immunoreactivity, consistent with a type III cortical lesion due to its sub-pial location. A few cells in the overlying meningeal blood vessels are also positive for MBP, suggesting myelin breakdown products are carried by these cells (arrowhead). (B) anti-CD68 IHC demonstrates many positive cells in the overlying meningeal blood vessel, which appear to be lipid-laden macrophages given the findings on anti-MBP staining as above (arrowhead). In addition, there are numerous CD68-positive cells in the molecular layer, which appear to be activated microglial cells, and down into the cortex below. (C) anti-CD3-positive staining shows scattered cells in the meninges (arrowhead) but few in the underlying cortex (D) ant-GFAP-positive cells are evident in the cortical parenchyma, representative of activated astrocytes (E) anti-HMGB1 IHC demonstrates widespread increase in cortical IR, particularly in neuronal cells with evidence of cytoplasmic translocation. *Scale bar= 100μm*

3.6 Discussion

3.6.1 Early active lesional changes demonstrate overlapping immunopattern II/III pathology

We have examined early active lesional changes using biopsy tissue from a patient who presented with a clinically isolated syndrome and subsequently developed RRMS. The changes found here are in accordance with established descriptions of early active white matter lesions (www.icdns.org). Based on preliminary analysis, the data presented here demonstrates features of pattern II pathology, given the evidence of perivascular T-cells, numerous macrophages with lipid proteins and relative preservation of OGD. However, especially in those blocks where we had a more complete area of the lesion, the borders were rather diffuse, with clear evidence of widespread microglial activation in the vicinity in addition to evidence of IgG positivity, although it is important to note that we did not stain for complement. Thus, our patient may represent a pattern II/ III overlap by the definitions posed by Lucchinetti et al and discussed in the General Introduction, section 1.3.3.4. This has important implications as discussed previously, as it may be explained by the concept of stage-specific vs patient-specific pathological heterogeneity (M H Barnett & Prineas 2004; Metz et al. 2014). In essence, the latter pattern suggests that some patients are likely to respond to specific therapies, for example immunomodulation with plasma exchange for patients with exclusive pattern II pathology, more predictably. However, if the changes are stage-dependent, technically all patients may benefit from this approach, but this would depend upon the stage of disease they present with (Barnett et al. 2009). This issue was addressed comprehensively by Metz et al, in a recent study, where 1321 surgical biopsy specimens with pathologically-confirmed MS were screened.

This study concluded that pathological heterogeneity was indeed limited to individual patients, and did not appear to be stage-specific when examined longitudinally over the course of a patient's disease. When examining these findings more closely, of the 1321 specimens initially screened, 79 were biopsied ⩾2 times or had autopsy material from the same patient, allowing longitudinal assessment of the individual patient's case. From this group, only 22 cases met the stringent inclusion criteria, which included presence of early active brain lesions from at least 2 time-points from the same patient, with reliable tissue staining and sufficient area for analysis (>1mm^2).

Importantly, 5 patients demonstrated type I, 14 patients demonstrated type II and only 2 patients demonstrated type III immunopatterns, with 1 overlap case (type II/III). In addition, 8 out of the 22 subjects had been exposed to some form of immunosuppression prior to biopsy, and 7 patients received steroids shortly after the first biopsy. Given that the median duration between the first and second biopsy/ autopsy was 50 days, it is possible that this treatment may have influenced the pathological findings. The same is true of our case also, as he had received dexamethasone therapy prior to biopsy sampling, and thus may have influenced our findings to a degree. It is impossible in clinical practice to withhold steroid therapy if it is clinically indicated, and this highlights inherent difficulties in drawing conclusions from material like this. However, in attempting to define true pathological heterogeneity, this is an important factor that must be considered carefully. The authors state that no correlation was identified between immunopattern and therapy given, but concede that small numbers precluded definitive conclusions. It is also of interest that the two patients demonstrating a type III immunopattern had a median EDSS of 7, vs 4 and 3 in patterns I and II

respectively, despite similar symptom duration prior to biopsy. However once again, they do not specify which of these patients had immunosuppression.

They also reported one case with an overlap between type II/III immunopatterns, possibly similar to our case. However, the authors describe this as an exceptional case as the other pattern II subtypes- the majority of cases- failed to show pathological overlap over time. Thus, although this work is of an exceptionally high standard given the number of samples screened and the stringent inclusion criteria, it is inevitably hard to draw definitive conclusions given the inherent bias in analysing tissue from this type of cohort. It appears that the final consensus has still not been reached therefore, and it is still possible that pathological heterogeneity may not be specific to individual patient.

3.6.2 Anti-HMGB1 IR may reflect pro-inflammatory activity in early active lesions

The HMGB1 staining pattern in the active lesion is in agreement with previously published work (Andersson et al. 2008), with massive HMGBI-positive inflammatory cell influx- predominantly of macrophages, into the active lesional tissue. Cytoplasmic translocation was evident in macrophages/microglia, supporting the contention that HMGB1 may be released into the inflammatory milieu of the developing active MS plaque. Release of NO and reactive oxygen species produce a highly inflammatory environment and based on available literature, it is probable that HMGB1 released from macrophages in this context is oxidised and post-translationally modified, and likely to produce tissue damage as a result (see figure 1.6). In this model, activated macrophages or other immune cells e.g. plasma cells (Vettermann et al., 2011) release HMGB1 which further activates macrophages via ligation of TLR-4, initiating NFkB signalling and pro-

inflammatory cytokine release such as IL-1β. which in turn stimulates macrophages to produce more HMGB1, and propagates the cycle of chronic inflammation and tissue destruction. Release of HMGB1 into the extracellular space could theoretically be measured in the CSF and this is considered in Chapter 5. We also know that HMGB1 can form a complex with CXCL12 (Schiraldi et al. 2012) potentially enhancing chemotactic activity and this may propagate the profound inflammatory cell infiltration following BBB breach. In this study, we also identified perivascular lymphocytes which also appeared to be HMGB1-positive although as discussed below, this would need to be examined in more detail, including using in-situ hybridisation techniques to ascertain production.

It is worth noting, however, that without characterising the phenotype of these macrophages i.e. M1 or M2, it is not possible to ascertain whether this is an entirely pro-inflammatory response based on these findings. Classically activated or M1 macrophages have cytotoxic and proinflammatory attributes as above whilst alternatively activated or M2 macrophages promote tissue repair by secreting anti-inflammatory cytokines and extracellular matrix molecules. Macrophages can be polarised in vitro by stimulating with IFN-γ or lipopolysaccharide (LPS), whilst M2 phenotype induction results from stimulation by cytokines such as IL4 (Vogel et al. 2013). Recent work has shown that macrophages within MS lesions express M1 markers as one might expect, including CD40, CD86, CD64 and CD32 (Vogel et al,2013). Interestingly, however, double-staining revealed 70% of the CD40-positive i.e. M1 macrophages also expressed the mannose-receptor (MR), an established marker of the M2 phenotype. This suggests that macrophages in active lesions in fact express an

'intermediate' activation status in response to endogenous signals. On balance however, current data suggests that the role of extracelllar HMGB1 in this context is likely to be destructive.

3.6.3 HMGB1 expression is evident in both peri-lesional white matter and in regions distal to the lesion border

Intense anti-HMGB1 IR was also shown to extend into the perilesional region. CD68+ HMGB1+ cells were clearly seen, with evidence of perivascular lymphocytic cuffing even into the lower layers of the cortex at the grey-white matter junction in figure 3.1D, suggesting that the fulminant inflammatory reaction in the active lesion causes widespread pathology including into the cortex.

What is also striking however, is the intensity of staining in the myelinated regions distal to identified white matter lesions, with distances of ≥7mm in those blocks with non-lesional tissue. This is less consistent with our original hypothesis that anti-HMGB1 IR reflects centrifugal diffusion from the lesion centre given the significant distance from the lesion border in this plane, although there are clear caveats to this interpretation (see below). In the study by Metz et al, the minimum area of tissue available for analysis needed to be $1mm^2$- a relatively large area and sufficient to draw conclusions about the question in hand i.e. pathological phenotype. In addition, over 1000 specimens were analysed and thus area for analysis would need to be relatively constrained in this context also. However, as I only reviewed the changes in a single patient, I was able to assess the changes over a larger area, with a mean of $2.01cm^2$ per block of tissue available for analysis (i.e. $>8cm^2$ total tissue area analysed). This was valuable when assessing tissue

changes overall, including in non-lesional regions, utilising the whole slide scanning technology in capturing the images.

In the white matter, strongly positive OGD are evident, although activated microglia also contribute to total number of HMGB1-positive cells. As discussed in more detail in the following chapter, OGD expression of HMGB1 or amphoterin in rodent brain has been reported in one previous study (M. M. Daston & Ratner 1994). This was particularly marked during CNS development, with relatively weak expression in the adult animal.

Interestingly, throughout the tissue in both lesional and non-lesional areas, astrocytes did not generally show evidence of HMGB1-positivity in the nucleus and only weak staining in the cytoplasm. This differential staining pattern, which is remarkably consistent, also suggests relative specificity of anti-HMGB1 IR. This pattern may be because astrocytes do produce HMGB1 but it is 'emptied' from the nucleus into the cytoplasm and extra-cellular space, thus producing falsely-reduced cellular staining. However, in agreement with Andersson et al (Andersson et al. 2008)- who asserted that astrocytes did not express HMGB1- it may be that HMGB1 is not expressed as highly as in macrophage/ microglial and oligodendroglial cells. It is known that astrocytes express toll-like receptors on their surface (Bsibsi et al. 2002), and so extracellular HMGB1 released by microglia, for example, may target TLRs on astrocytes and activate proinflammatory, or indeed anti-inflammatory (Nair et al. 2008), signalling in this way.

3.6.4 HMGB1 expression pattern in both non-lesional grey matter and in cortical lesions is striking

The changes in myelinated grey matter are revealing, with intensely stained HMGB1-positive neurons, predominantly in the nucleus. The intensity of staining suggests that HMGB1 may be performing specific functions related to transcriptional regulation, one of its best known functions in both health and disease. Further exploration of this is considered in Chapter 6, section 6.6.8. Some HMGB1-positive neurons clearly demonstrate cytoplasmic translocation from the nucleus, with others also showing possible early apoptotic changes or else appear to be frankly pyknotic and dying (figure 3.4G-I). Wallerian degeneration secondary to remote but connected white matter lesions is one potential explanation for these changes. Thus, increased HMGB1 reactivity in pyknotic cells may just be reflecting its condensation in preparation for cell death following trauma sustained distally to the neuronal soma. However, widespread presence of activated microglial cells was evident once again, and it is known that microglial activation can also trigger neurodegeneration via ligands acting at TLR4 (Lehnardt et al. 2002; Lehnardt et al. 2003), of which HMGB1 is an important example. The translocation evident may also represent autophagic activity in the face of metabolic insult, as we know that HMGB1 can translocate into the cytoplasm to augment the latter.

Interestingly, cytoplasmic translocation in neurons appeared to be accompanied by intensely IR satellite OGD, perhaps providing trophic support to neurons undergoing cellular stress (Lee et al. 2012). Of further interest were multiple examples of what appeared to be oligodendroglial-like cells lining up near to blood vessels. This phenomenon has been shown to occur in CNS injury, where OGD-precursor cells expressing MMP-9 accumulated peri-vascularly and were associated with BBB leakage prior to overt demyelination taking place (Seo et al.

2013). Further characterisation of these oligodendroglial-like cells is required to investigate this in the context of MS.

Although this was a preliminary assessment of changes in OGD cells in this study, our findings have highlighted a possible disturbance in their function through their intense expression of HMGB1 in non-lesional regions. However, given HMGB1 is expressed in adult rat brain, albeit weakly (M.M. Daston & Ratner 1994) it is difficult to conclude from this without corresponding non-MS control tissue.

Cortical lesions were identified independently of white matter lesions in some blocks, and were found to be infiltrated by CD68-positive activated microglial cells throughout the lesion, and in the overlying meningeal vessels. The latter also showed numerous CD3-positive lymphocytes, although there were very few in the cortical parenchyma proper. HMGB1 staining was less intense than in myelinated grey matter, and demonstrated widespread neuronal cytoplasmic translocation. Whilst others have found little evidence of active inflammation in the cortex (Bo et al. 2003), the results arising from analysis of the biopsy specimen from this single patient would tend to support the findings of Lucchinetti et al in a much larger study of similar patients (Lucchinetti et al. 2011b) with regard to evidence of inflammatory cortical demyelination. Their group and others (Magliozzi et al. 2007b) postulate that in the context of inflammation and breach of the BBB, toxic mediators in the CSF released from activated B-cells amongst others, penetrate the underlying cortical tissue and propagate damage, including to OGD (Lisak et al. 2012). HMGB1 is known to be released from activated plasma cells (Vettermann et al. 2011) and so it is possible that HMGB1 is one of these mediators, causing activation of microglial cells via TLRs or RAGE and effecting pro-inflammatory damage in the local tissue. Given its known propensity to

potentiate pro-inflammatory loops, HMGB1 may be important in perpetuating damage long after the initial wave of active inflammation has passed. The HMGB1 staining pattern may well reflect this resultant abnormality, although as discussed below, a larger cohort and comparison with non-MS control biopsy tissue would be required to characterise this fully in our hands. In addition, the possibility that HMGB1 is acting to promote neuroprotective responses cannot be ruled out (G. Li, Liang, et al. 2013), particularly as characterisation of M1/M2 macrophages was not done.

3.7 Limitations of study

The main limitation to drawing conclusions from this body of work is that it describes findings in a biopsy specimen from a single patient. It would have been helpful to compare the staining patterns found in this CIS patient with non-neurological biopsy brain tissue, in addition to other non-MS, neurological disease and this type of tissue is currently being processed for this purpose.

Comparative material would give an idea whether the apparently increased HMGB1 expression is specific to MS, or whether it reflects other, procedural factors such as the speed of fixation given the smaller size of these specimens compared to the whole brain, as used in post-mortem analysis. Furthermore, biopsy specimens do not have issues regarding post-mortem interval (PMI) time and the potential degradation of antigens in this period. However, as De Groot et al reported, PMI had less impact on IR of a panel of inflammatory markers in brain tissue than formalin fixation itself, which was most likely to mask epitopes (De Groot et al. 2001). These and related issues will be discussed in Chapter 4.

Additional criticisms include the possibility that studies examining biopsy material from similar patients are not representative of typical MS patients due to their unusually aggressive clinical presentation. However, it has been highlighted that studying extreme representations of disease can often offer insights into disease-specific pathomechanisms that would not otherwise be identifiable (Calabresi 2011).

Other potential confounders include demographic factors such as the patient's young age and also the biopsy process itself producing artefact. Regarding the latter, although Lucchinetti et al described very similar findings to ours with respect to neuronal dystrophy (Lucchinetti et al. 2011b), but most neuropathologists are aware that neuronal abnormalities such as pyknosis can result as an artefact of biopsy and do not reflect a neurodegenerative event per se (*M. Carey, personal communication*). However, we also observed changes suggestive of chromatolysis which may reflect Wallerian degeneration, possibly secondary to remote white matter lesions.

With regard to classification of non-lesional tissue; it is difficult to ascertain how far from active lesional changes any part of the tissue is. Although we measured >7mm away from the lesion border, it is possible that another lesion above or below the apparently non-lesional tissue in this plane affected our assessment. However, the presence of normal myelin staining patterns and paucity of lymphocytic perivascular cuffing would support the contention that these areas are not actively inflamed, despite increased CD68-positive cells as reported before (Thomas Zeis et al. 2009).

3.8 Conclusion

It is rare to obtain neuropathological tissue sampled at the earliest stages of MS. However we were able to perform a detailed description of changes occurring in early active lesional (EAL) biopsy tissue, using a number of conventional stains and IHC analyses. Preliminary analysis demonstrated a pattern II/III pathology, suggesting that not all patients demonstrate unique subtypes only. At this earliest stage of MS, we have also demonstrated HMGB1 expression in biopsy tissue for the first time and confirmed its expression in EAL. A predominantly nuclear expression pattern was observed in macrophages/microglia, OGD and neurons, with evidence of cytoplasmic translocation in lesional macrophages. The tissue alterations and changes in HMGB1 expression in non-lesional regions are striking in this tissue type and suggests a more widespread alteration in MS tissue. It is tempting to speculate this may have preceded active lesion formation (Thomas Zeis et al. 2009), but requires further verification. Therefore, we wished to carry out an extended study, examining lesional and non-lesional areas using autopsy tissue in both MS patients and non-MS control subjects. These findings will be discussed in the following chapter.

4

Post-mortem study of HMGB1 expression patterns in MS and non-MS control patients

4.1 Introduction

As discussed in chapter 3, immunohistochemical (IHC) analysis of brain tissue offers an insight into potential pathogenetic mechanisms of MS. Studies examining HMGB1 expression using immunohistochemistry (IHC) in human

neuropathological tissue have been performed in patients with other neurological diseases such as epilepsy/ cortical malformation (Zurolo et al. 2011; Maroso et al. 2011; Maroso et al. 2010), alcoholism (Crews et al. 2013; Zou & Crews 2014) and amyotrophic lateral sclerosis (Casula et al. 2011).

Neuropathological examination of HMGB1 expression in MS patients and controls has been reported by Andersson et al (2008). In this study, the autopsy MS tissue comprised six patients with 'acute' MS, seven patients with RRMS, 18 with SPMS and 11 patients with PPMS. The authors did not provide clinical details for the patients classified as having 'acute' MS. They found that HMGB1 immunoreactivity (IR) was marked in the nucleus and cytoplasm of microglial/ macrophage cells within active lesions, and identified these cells morphologically. The methodology of how they collected the data regarding number of macrophage and microglial cells/mm^2 is not clear; for example number of frames sampled. They also do not comment on IR in other cell types, except astrocytes where co-localisation analysis revealed that HMGB1 immunoreactivity (IR) was not identified. They reported that the staining pattern in control white matter was nuclear, although do not provide pictorial evidence to demonstrate the cellular staining pattern in all cells here. This is of interest as some of the cells in the chronic active lesional tissue image demonstrated in figure 1 of this study appear to be OGD morphologically. Given that this is a critically important cell in MS-related pathology as well as my findings described in chapter 3, it would have been useful to compare expression patterns between MS and non- MS patients. In addition, in the animal study, HMGB1 mRNA levels are especially high in the grey matter of the spinal cord, although they do not comment on this specifically. However, the high levels overall are postulated to reflect de novo synthesis due to continuing

loss from the cytoplasm, and use the IHC analysis to demonstrate this dynamic process by the cytoplasmic localisation in macrophage/ microglial cells. They also describe diffuse extracellular staining in the protein analysis of rat spinal cord using immunofluorescence techniques, although these images are not presented.

Furthermore, the HMGB1 expression pattern in non-lesional regions was not specifically assessed. Identifying the presence of HMGB1 in non-lesional tissue is important as it may reflect a more global disease process, as has already been discussed in Chapter 1. Understanding changes taking place in the normal-appearing brain tissue (NABT) is fundamentally important in MS research, as we increasingly understand that these areas may demonstrate endogenous mechanisms whereby the brain limits new lesion formation. They also give an insight into how it may be that these mechanisms fail in order to produce the characteristic lesional changes of MS pathology. However, whilst there is increasing evidence implicating NABT changes in MS pathology, our understanding of the molecular changes occurring in these regions is incomplete. Given the unique role of HMGB1 in propagating inflammation in the context of neurodegeneration (Gao et al. 2011; Fang et al. 2012), this potentially allows an insight into disease mechanisms in MS that have not been explored before.

The present study is the only comprehensive assessment of HMGB1 expression in MS brain tissue which includes non-lesional regions and highlights an important role of HMGB1 in this context. The main goal of the study is to further our understanding of disease processes occurring in these regions and thus consider how these observations could be exploited therapeutically.

4.2 Hypothesis

The hypothesis underpinning this chapter is that HMGB1 expression reflects more widespread processes than immune cell infiltration alone, and that expression will be increased in both lesional and non-lesional regions. Given the findings in chapter 3, we hypothesize that OGD demonstrate increased immunoreactivity in both peri-lesional and non-lesional regions in MS brain.

4.3 Aims

Using immunohistochemistry:

1. Assess HMGB1 expression in non-MS control tissue
2. Assess HMGB1 expression in active lesions in patients with chronic MS
3. Compare HMGB1 expression in non-lesional MS brain tissue with non-MS control brain tissue
4. Evaluate evidence for cytoplasmic translocation of HMGB1 in CNS tissue

4.4 Methods

4.4.1 Post-mortem brain tissue

The majority of autopsy material was supplied by the MS Society Tissue Bank at Imperial College, London, using a UK-wide prospective donor scheme with full ethical approval (08/MRE09/31+5). Two non-MS control cases were supplied by

the Oxford Brain Bank, University of Oxford (07/H0606/85). One non-MS control case was supplied by the Neuropathology department, University Hospital Birmingham, following research ethics consent under local guidelines. Storage of the tissue at the University of Birmingham was approved by local research ethics committee approval (LREC 11/H1211/1).

For the UK MSBB tissue, a summary clinical history for each case was prepared by MS neurologists. The clinical and post-mortem details of the MS and control cases used in this study are given in Table 4.1, including age at death, post-mortem delay, sex and type of MS.

Upon receiving the post-mortem brains at the UK MSBB, the material for this study was fixed in 4% formalin for 4 weeks and then the entire brain was divided into multiple blocks. The blocks were numbered in a standard fashion by the brain bank. The brain was divided into anterior (A) and posterior (P) halves at the level of mamillary bodies. One centimetre thick coronal slices were then cut through the brain with the first slice anterior to the mamillary bodies named A1, and the second A2 etc. The first slice posterior to the mamillary bodies was named P1 and so on. Each slice was then cut into 2 by 2 cm blocks identified by letters (A–E) in a vertical plane, with A as the left superior block, and by numbers in the horizontal plane (1–5) with 1 as the left superior block. For this study, 22 blocks were used for analysis from 20 patients, taken from anatomically-defined regions within the frontal lobe (13/21), parietal lobe (2/21), occipital lobe (3/21) and temporal lobes (4/21). Control blocks were predominantly taken from the frontal lobe, apart from 2 blocks, from the Oxford Brain Bank which were sampled from the temporal lobe. The hippocampus and parahippocampal gyri themselves were avoided when analyzing HMGB1 and LRRIg immunoreactivity due to its unique

anatomy when compared to other regions of the brain, in either control or MS patients. The blocks used for this study were fixed in formalin and embedded in paraffin. Sections were then cut at a thickness of 8μm and used for initial lesion characterisation at the tissue bank and then and for subsequent analysis by other researchers, including our group. Confirmation of the diagnosis of MS in each case was provided by experienced neuropathologists based at Imperial College London using a variety of markers and stains. These included H&E, Luxol Fast-blue (LFB)/ MHC Class II and LFB/ periodic-acid Schiff (PAS) and other immunohistochemical markers such as anti-myelin-oligodendrocyte (anti-MOG) antibody to further delineate myelination patterns. Once lesions were identified using the above techniques, they were classified as 'active lesional', 'chronic active lesional' and 'normal-appearing white matter'. The latter blocks were at least 1cm in all directions away from identified white matter lesional zones. The UK MSBB kindly donated all of the original diagnostic slides to us for characterization purposes, in addition to the FFPE sectioned material.

	AGE	SEX	MS SUBTYPE	DISEASE DURATION	PMI (H)	CAUSE OF DEATH
MS						
	57	M	PR	33	21	MULTIPLE SCLEROSIS
	50	M	SP	NK	24	BRONCHOPNEUMONIA
	73	M	PP	52	20	LEFT VENTRICULAR FAILURE, BRONCHOPNEUMONIA
	77	F	SP	21	7	BRONCHOPNEUMONIA
	39	F	SP	21	18	BRONCHOPNEUMONIA
	53	M	SP	NK	46	ASPIRATION PNEUMONIA; MULTIPLE SCLEROSIS
	44	F	SP	19	20	URINARY TRACT INFECTION; SEPSIS
	53	M	SP	33	14	SEPTICAEMIA DUE TO UTI
	77	M	SP	39	19	BRONCHOPNEUMONIA; MYOCARDIAL INFARCTION
	59	F	SP	42	8	BRONCHOPNEUMONIA; HEART FAILURE
	59	M	SP	39	22	MULTIPLE SCLEROSIS
	72	M	SP	43	11	BRONCHOPNEUMONIA; MULTIPLE SCLEROSIS
	55	M	SP	20	19	MULTIPLE SCLEROSIS
	60	F	SP	34	10	ADVANCED SIGMOID COLON CANCER; MULTIPLE SCLEROSIS
CONTROL						
	93	F	N/A	N/A	9	BRONCHOPNEUMONIA/ CVA
	82	M	N/A	N/A	21	NK
	78	F	N/A	N/A	33	MYELOID LEUKAEMIA
	67	F	N/A	N/A	33	ACUTE ARRHYTHMIA, INTESTINAL OBSTRUCTION
	71	F	N/A	N/A	24	ACUTE BRONCHITIS
	85	F	N/A	N/A	48	NK

Table 4.1. Details of MS and control cases. *PR= progressive relapsing; SP= secondary progressive; PP= primary progressive; NK= not known*

4.4.2 Immunohistochemical analysis

IHC analysis was performed as described in Chapter 2, Materials and Methods, and was carried out using the Leica Bondmax automated stainer. Antibodies used were anti-MBP, -CD68, -CD3, -GFAP and –HMGB1 as described in table 3.1. HMGB1 staining in particular was extensively optimised in order to achieve an acceptable balance between signal: noise, especially as staining in all non-MS control samples. Sequential sections were used to delineate lesion borders and cellularity by staining with H&E, MBP and CD68 in order to verify presence of 'active' and 'chronic active' lesions in-house. This was also useful for confirming the absence

of active inflammatory demyelination in the 'normal- appearing white- matter' tissue blocks in our hands, as well as in non-MS control tissue.

4.4.3 Image processing and selection of areas for analysis

All stained sections were scanned using the Leica SCN400, and stored on the Digital Image Hub 'cloud' system, based at the University of Birmingham. In some of the 'active lesion' blocks, the original inflammatory, demyelinating lesion as identified on the diagnostic slides supplied by the UK MSBB was not clearly evident in our sections. This was likely to be due to their small size within the block, and may have already been sampled by the tissue bank. In all of these cases however, significant CD68 infiltration- which morphologically appeared to be activated microglia or macrophages- were apparent in the immediate vicinity and thus it was possible locate where the lesion was originally situated. In these cases, they were not used for assessment of active lesions but were included when analysing immunoreactivity scores for 'non-lesional' regions. In identifying the latter, regions $\geqslant$ 1500μm were used from the lesion borders in active and chronic active lesional blocks to delineate non-lesional tissue for image acquisition. In addition, anti-MBP staining was used in order to identify cortical lesions and the same distance measurement was used to delineate non-lesional grey-matter.

Thus for each section, regions were identified as (i) active/ chronic active lesion (ii) chronically demyelinated white matter (without significant inflammatory cell infiltrate) (iii) peri-lesional regions (within 300μm of the lesion border) (iv) non-lesional white matter $\geqslant$ 1500μm from the lesion border (v) non-lesional grey matter (vi) demyelinated grey matter. Images were then captured using the Leica

'Slidepath' software in each of these regions to fully ascertain the pathological changes occurring across the tissue in each section.

4.4.4 HMGB1 immunoreactivity scoring (IR) analysis

IR scoring was performed for HMGB1 stained sections, using active/ chronic active lesional and normal-appearing white matter tissue blocks from MS patients and controls. The regions used for semi-quantitative scoring were (a) non-lesional white matter and (b) non-lesional grey matter. Images were captured at x10, x20 and x40 magnification using the Leica Slidepath software and IR scoring was performed using x40 magnification images. The average area covered by each image was 45,656 μm^2 and the images were coded to maintain blinding.

IR scoring was assessed as previously described (Vandeputte et al. 2002; Geurts et al. 2003; Ravizza et al. 2006; Casula et al. 2011), with both immunostaining intensity and frequency of cells combined to produce a semi-quantitative 'IR score'. Staining intensity was evaluated using a scale of 0–3 (0: –, nil; 1: ±, weak; 2: +, moderate; 3: ++, strong IR). The approximate proportion of cells showing HMGB1 reactivity at the stated intensity (1) single to 10%; (2) 11–50%; (3) >50% was also scored to give information about the relative number ('frequency' score) of positive cells within the HMGB1 specimens. The product of both of these measures then gave rise to the composite "IR score' as shown in figures

Four assessors independently scored the material, one of whom was myself. The other three assessors included two neuropathologists at University Hospital Birmingham (Dr Martyn Carey and Dr Santhosh Nagaraju) and one senior neuroscientist with extensive experience in the assessment of neuropathological tissue, from the University of Birmingham (Dr Ana Maria Gonzalez). These three

assessors were entirely blinded to any clinical details. Semi-quantitative anti-HMGB1 IR scoring showed an inter-rater consistency of 0.8 which was deemed acceptably similar in order to use median values for calculation of comparative IR scores for each patient.

4.4.5 CD68 quantification

Two-dimensional cellular quantification analysis using sectioned material is subject to certain limitations, related to section thickness and size of objects counted, as reviewed in the discussion of this chapter, and we did not routinely assess this using a microcator. However, in this aspect of the study, we simply wished to ascertain whether anti-CD68 IR changed between the different lesion types and between controls. 6 non-overlapping fields from non-lesional tissue as defined above, at x20 resolution, were used per section; x3 from non-lesional white matter and x3 from non-lesional grey matter. Each field covered an area of approximately 200,000 μm^2. An unbiased counting frame was placed over the whole field and positive cells were identified and counted manually. Average values per section for both grey matter, white matter and combined data was recorded. ImageJ software was used to verify total number of cells using haematoxylin staining and thus proportion of CD68-positive cells from this number was calculated.

4.4.6 Assessment of cytoplasmic translocation

Using the Leica Biosystems' Tissue IA software, cellular nuclei are first located on the basis of counterstain and shape. A decomposition algorithm is then used, based on the Voronnoi tessellation method, to delineate cell and hence cytoplasmic boundaries. Any further calculations e.g. assessing amount of DAB

stain in the nucleus vs. cytoplasm are thus determined by the algorithm. With regards intensity, it is accepted that DAB reactivity is not a stoichiometric reaction, in that 'amount' of DAB cannot be extrapolated to 'number' of HMGB1 molecules in a linear fashion. Having said that, the Leica IA software has devised various techniques to quantify the DAB colour, by utilising a histogram model with a range of 0-255, where 0=black and 255=white. Intensity of pixels in each cell compartment (i.e. nucleus or cytoplasm) is measured and average intensity calculated based on positive readings. For example, average cytoplasmic staining intensity is calculated as the following:

Mean cytoplasmic staining intensity =

$$\frac{\text{mean total staining intensity of cytoplasmic+ve pixels in all cytoplasmic+ve cells}}{\text{number of cytoplasmic positive pixels in all cytoplasmic positive cells.}}$$

Absorbance is calculated in a similar way, but also takes into account the background tissue threshold, i.e. the designated cut-off for positive staining in tissue. Although effects of light absorbance (e.g. from glass slides) or the non-stoichiometric nature of the DAB stain are not accounted for in this algorithm, it enables quantification of immunostaining in different cellular compartments.

Neuronal nuclei are unique as compared to glial nuclei as they are larger and, because of their prominent nucleolus, are more heterogenous. We used these differences to generate two algorithms for 'neurons' and 'glia'. This allowed us to separate the analyses to produce data corresponding to glial and neuronal parameters. Thus, as captured images from each section included grey matter regions, we used the neuronal analysis parameters to ascertain amount of DAB stain in nuclear and cytoplasmic compartments in these identified cells. Given our

interest in evaluating HMGB1 translocation from nuclear to cytoplasmic compartments, and bias inherent in subjective assessment, we found this to be an acceptable tool for this purpose. I devised this algorithm with help from the technical experts at Aperio/ Leica Biosystems, and they are now taking this forward for further validation in-house.

4.5 Statistical Analysis

Statistical analyses were carried out using GraphPad Prism software, V5. Differences across multiple groups were assessed using the Kruskall-Wallis test with Dunn's post-hoc correction for multiple groups, or the Mann-Whitney U test if pairs of groups were compared. Single measure intraclass correlation coefficients using an absolute agreement definition and based on a two-way random effects model were calculated using IBM SPSS Statistics Version 22, and were performed with the help of a statistician (Dr Peter Nightingale).

4.6 Results

4.6.1 HMGB1 expression is increased in active lesional tissue in patients with progressive MS compared to non-MS controls

This series of lesions within the designated 'AL' tissue blocks comprised material taken from patients with chronic MS but who still demonstrated ongoing inflammatory, demyelinating lesional pathology. LFB/ Class II staining identified the lesion in the diagnostic slides and our assessment demonstrates positive MBP staining in the context of CD68-positive cells. Whilst lipophages were evident, they were less prominent, appearing around and within lesions, thus classifying all the plaques in this series as late active or chronic active lesions. Cytoplasmic translocation was evident in macrophages/activated microglia, with characteristic short, fattened processes and rounded/ amoeboid cell bodies. In accordance with the findings from Andersson et al (2008), figure 4.1 demonstrates low IR in the white matter of non-MS control patients which was consistent across all subjects, with both frontal and temporal lobe regions being assessed.

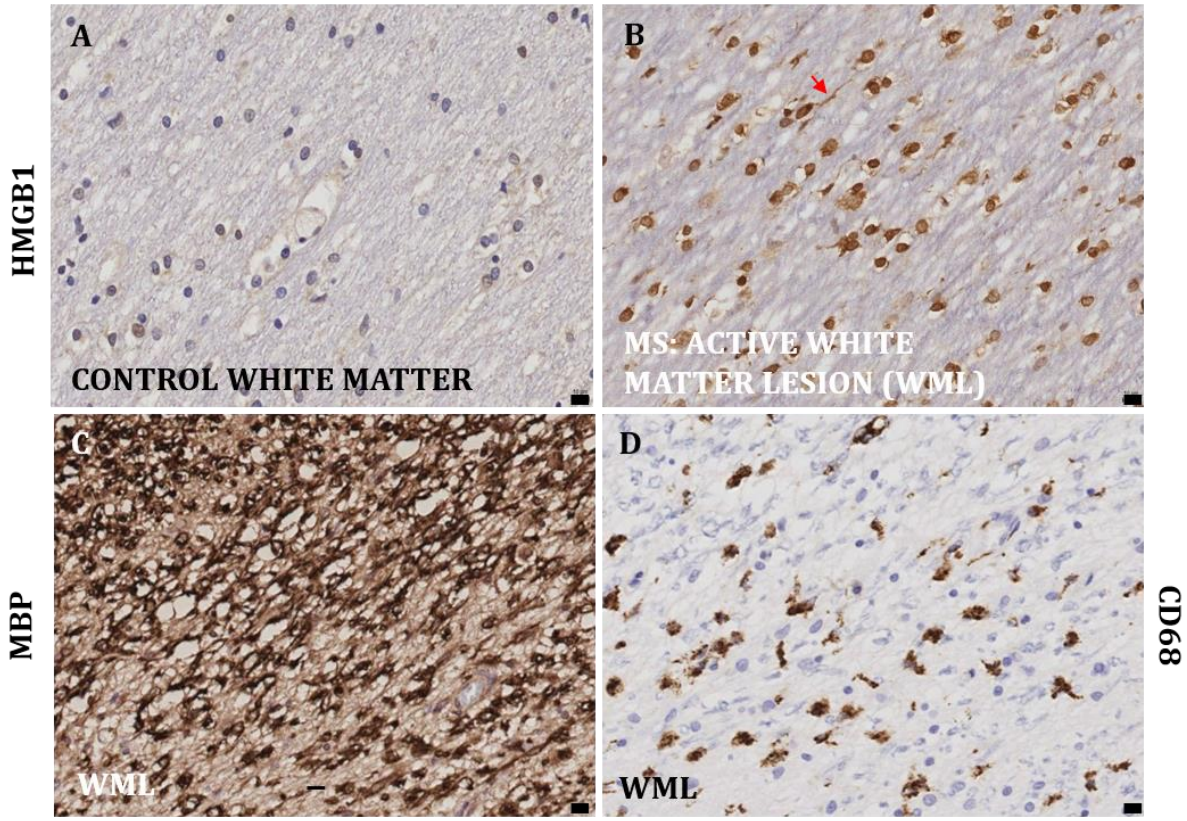

Figure 4.1. HMGB1 expression is increased in active white matter lesions in patients with SPMS (A) shows anti-HMGB1 expression pattern in a non-MS control subject, where comparative staining intensity in white matter is reduced. (B) anti-HMGB1 staining in the same region demonstrates increased expression, with delineation of cells appearing to be of macrophage/ microglial lineage (arrow). (C) anti-MBP IHC staining pattern demonstrating fragmentation of myelin prior to frank demyelination. (D) anti-CD68 IHC expression shows activated cells, with short, fat processes, and numerous lipophages which predominantly appear to be macrophages, morphologically. Original scale bar = 10μm.

4.6.2 HMGB1 expression is increased in non-lesional white matter compared to non-MS controls

Figure 4.2 demonstrates normal myelination patterns in the control tissue with some CD68-positive cells evident. These predominantly had ramified morphology suggestive of resting microglial cells, with occasional perivascular macrophages seen. Most CD68+ cells also appeared to HMGB1+,, although dedicated co-localisation analysis is required to confirm this. In the inset of figure 4.2G, HMGB1 staining is also seen in the nucleus of oligodendrocytes, as suggested by their

density, roundedness and presence of tissue artefact around them- giving them a characteristic 'halo' appearance- and their staining pattern is relatively weak. Stromal intensity was higher in one of the control subjects, but the cellular staining remained relatively weak in both the white and grey matter.

In contrast to this, when assessing tissue from both the NAWM and AL tissue blocks, HMGB1 staining was consistently increased, most obviously affecting oligodendrocytes. In addition, shrunken OGD with an intense IR staining pattern were frequently seen in non-lesional regions of both NAWM and AL tissue blocks (figure 4.2H; inset). Occasionally, apparent evidence of cytoplasmic translocation in OGD was also seen (figure 4.2H; inset).

When assessing staining intensity, late active and chronic active scores were combined due to their similar staining patterns in non-lesional regions. The visual differences described above were reflected in the semi-quantitative analysis, where increased anti-HMGB1 IR scores in MS vs non-MS controls were consistently seen, and this difference was statistically significant ($p=0.0005$). The majority of NAWM blocks also showed increased HMGB1 staining, although this did not reach statistical significance. Possible reasons for this are discussed below.

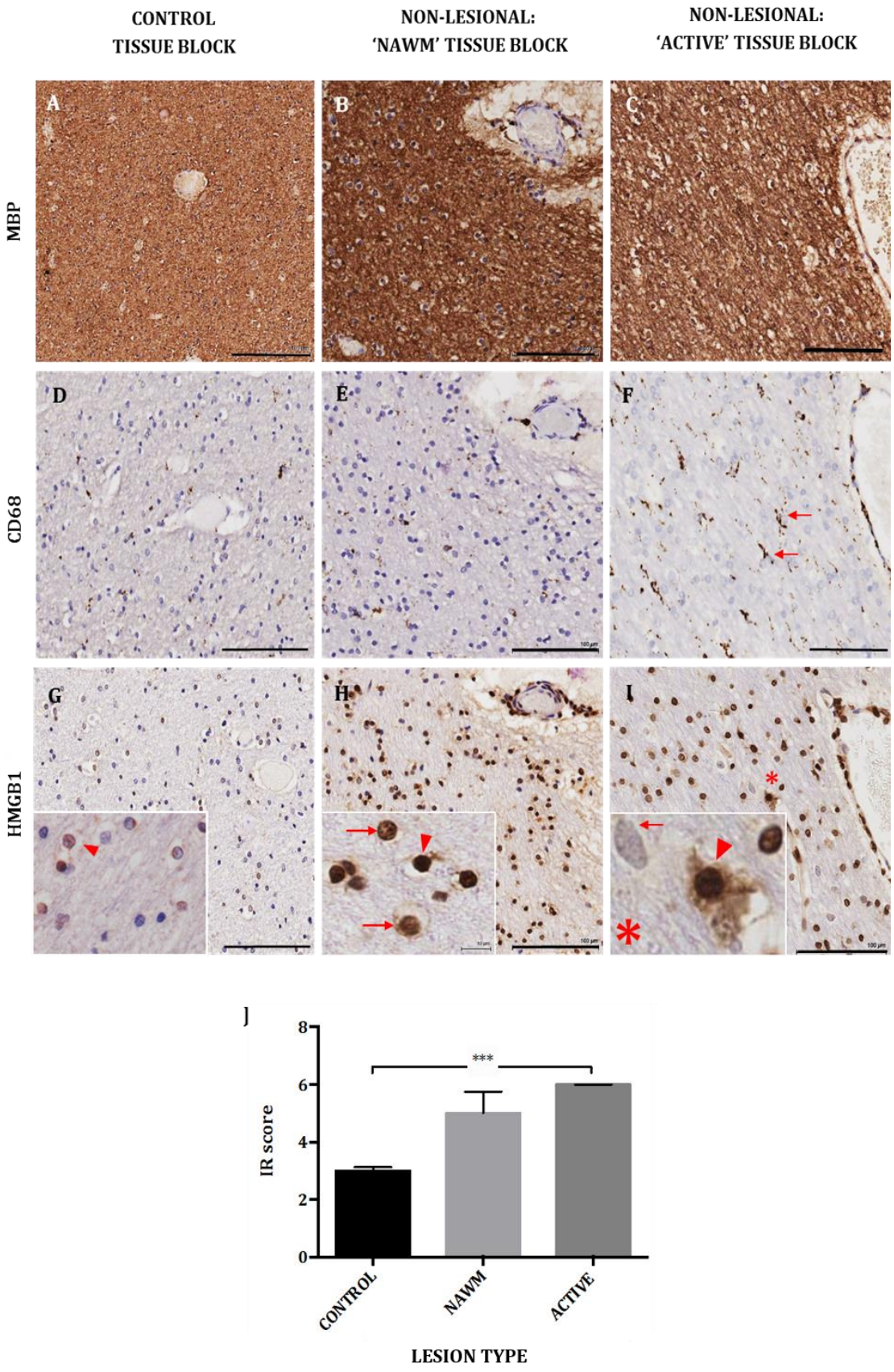

Figure 4.2. HMGB1 expression is increased in non-lesional white matter compared to non-MS controls. (*Continued overleaf).*

Figure 4.2. HMGB1 expression is increased in non-lesional white matter compared to non-MS controls *(continued)*. (A-C) Anti-MBP immunoreactivity (IR); (D-F) Anti-CD68 IR; (G-I) Anti- HMGB1 IR.
(A, D, G): Control tissue block. A normal myelination pattern is evident in 4.2A, with a few CD68-positive cells including perivascular macrophages. Anti-HMGB1 immunoreactivity (IR) is evident in figure 4.2G, particularly in OGD (inset, arrowhead) but intensity is weak. ***(B, E, H) MS: NAWM tissue block***. (B) normal myelination pattern is evident with slightly higher numbers of CD68-positive macrophages/ microglia seen in I, although most demonstrate a ramified morphology. CD68-positive cells are generally HMGB1 positive (H) but OGD in particular show increased expression. The inset demonstrates the presence of both morphologically normal (arrow) and possibly apoptotic (arrowhead) OGD. ***(C, F and I) MS: AL tissue block*** show the staining pattern in non-lesion region from a block containing active lesions. The myelination pattern is normal but there are numerous CD68-positive cells throughout the parenchyma (arrows). The HMGB1 staining is increased as seen in the NAWM blocks (4.2H and –I), particularly in OGD. The inset shows an intensely staining OGD with evidence of cytoplasmic translocation. The adjacent cell is likely to be another glial cell, possibly an astrocyte as demonstrated on GFAP staining on sequential sections. ***(J) semi-quantitative IR scoring***: demonstrated IR scores from each tissue block with significant differences across the groups, particularly between AL and control tissue blocks. NB 'active' refers to both active and chronic active lesional tissue blocks- see text *Statistical analysis: Kruskal-Wallis with Dunn's post-hoc correction. ***p=0.0005*. *Scale bars=100μm.*

4.6.3 HMGB1 expression is increased in non-lesional grey matter compared to non-MS controls

Normal myelination patterns are shown in these cortical regions, taken from layer 3 of the pyramidal cortex. The IR in control tissue was consistently low across all non-MS control patients. The most obvious difference in MS tissue was the presence of intensely positive 'satellite' oligodendrocytes, in their classic configuration in close proximity to pyramidal neurons, as shown in the insets in figures 4.3H and 4.3I. Translocation of HMGB1 into the neuronal cytoplasm was also seen, where long cytoplasmic processes were often noted- a finding not observed in the control tissue. There was greater variability in the NAWM blocks, with some patients demonstrating less intense staining than others, but the overall intensity was consistently greater than non-MS controls.

Further examination of this staining pattern at both low and at higher magnifications revealed striking differences in sub-cellular localisation, as shown in figure 4.4. We observed clear anti-HMGB1 IR in neuronal nuclei of non-MS control patients, where molecules of HMGB1 were observed in close association with chromatin (4.4C; inset, arrowhead). The cause of death for this non-MS control patient shown was acute arrhythmia and chronic myocardial ischaemia. The finely granular, perinuclear blush of anti-HMGB1 IR may represent cytoplasmic staining although subsequent immunofluorescent analysis of control tissue also demonstrated autofluorescence suggestive of lipofuscin-related artefact. In the grey matter of the NAWM block shown in figure 4.4D, clearly increased IR is shown, with some cells displaying cytoplasmic staining with very little nuclear IR (arrowhead), where others showed intense nuclear IR and relatively less cytoplasmic staining (arrow). The presence of HMGB1 in the cytoplasm likely represents translocated HMGB1 from the nucleus into the cytoplasm. Again, oligodendrocytes demonstrated consistently increased IR in close apposition with neurons. In non-lesional regions of AL blocks, many neurons demonstrated cytoplasmic translocation, often with extended axonal processes as shown in figures 4.4E-H. However, unlike the neuronal dystrophy observed in the early active lesions seen in Chapter 3, this was rarely seen in this cohort of progressive patients.

The presence of HMGB1-positive cells likely to represent endothelial cells is also shown in figure 4.4H (asterisk), where anti-CD68, -CD3 and –GFAP reactivity are absent. It is unclear whether this represents expression or uptake of HMGB1 and further in-situ hybridisation studies are required.

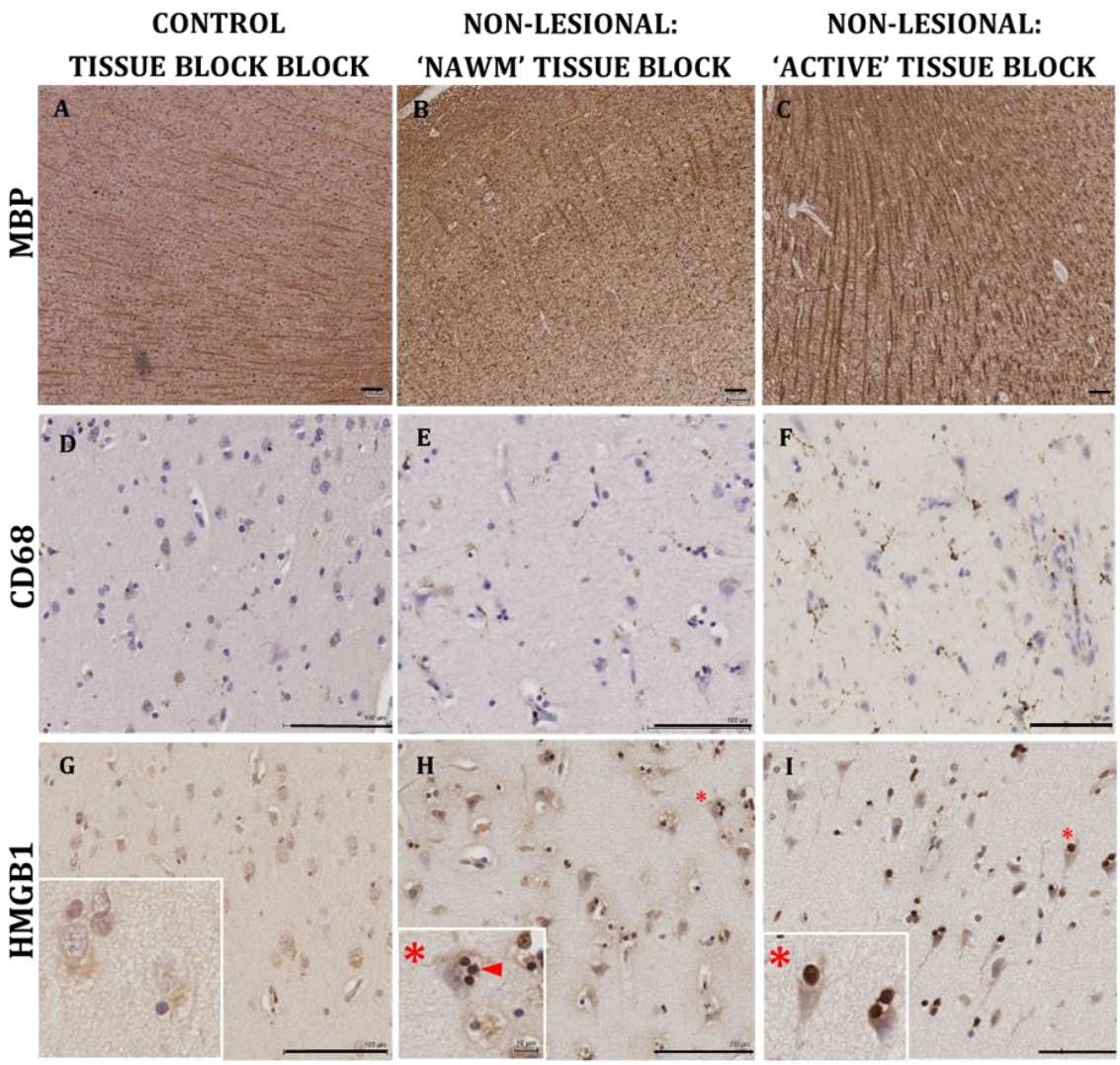

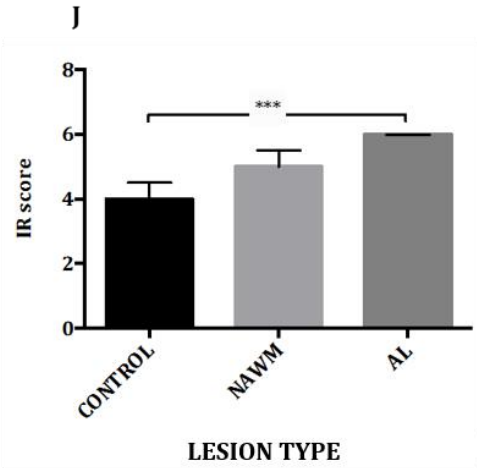

Figure 4.3. HMGB1 expression is increased in non-lesional grey matter compared to non-MS controls. ***(A, D, G): control tissue***. Normal myelination pattern evident, with rare CD68-positive cells. HMGB1 staining is weakly evident in 4.3G (inset). ***(B, E, H): NAWM tissue***. (B) normal myelination pattern with occasional CD68-positive microglia evident in (E). (H) demonstrates increased HMGB1 expression, particularly in satellite oligodendrocytes. ***(C, F and I): active lesional tissue***, whilst the myelination pattern was normal, there are numerous CD68-positive cells throughout the parenchyma. There was greater evidence of cytoplasmic translocation in HMGB1-positive neurons in AL tissue blocks than in NAWM. (J) semi-quantitative IR scoring shown in each tissue block, with significant differences across the groups, particularly between AL and control tissue blocks. *Statistical analysis: Kruskal-Wallis with Dunn's post-hoc correction. ***p=0.0004. Scale bars=100µm.*

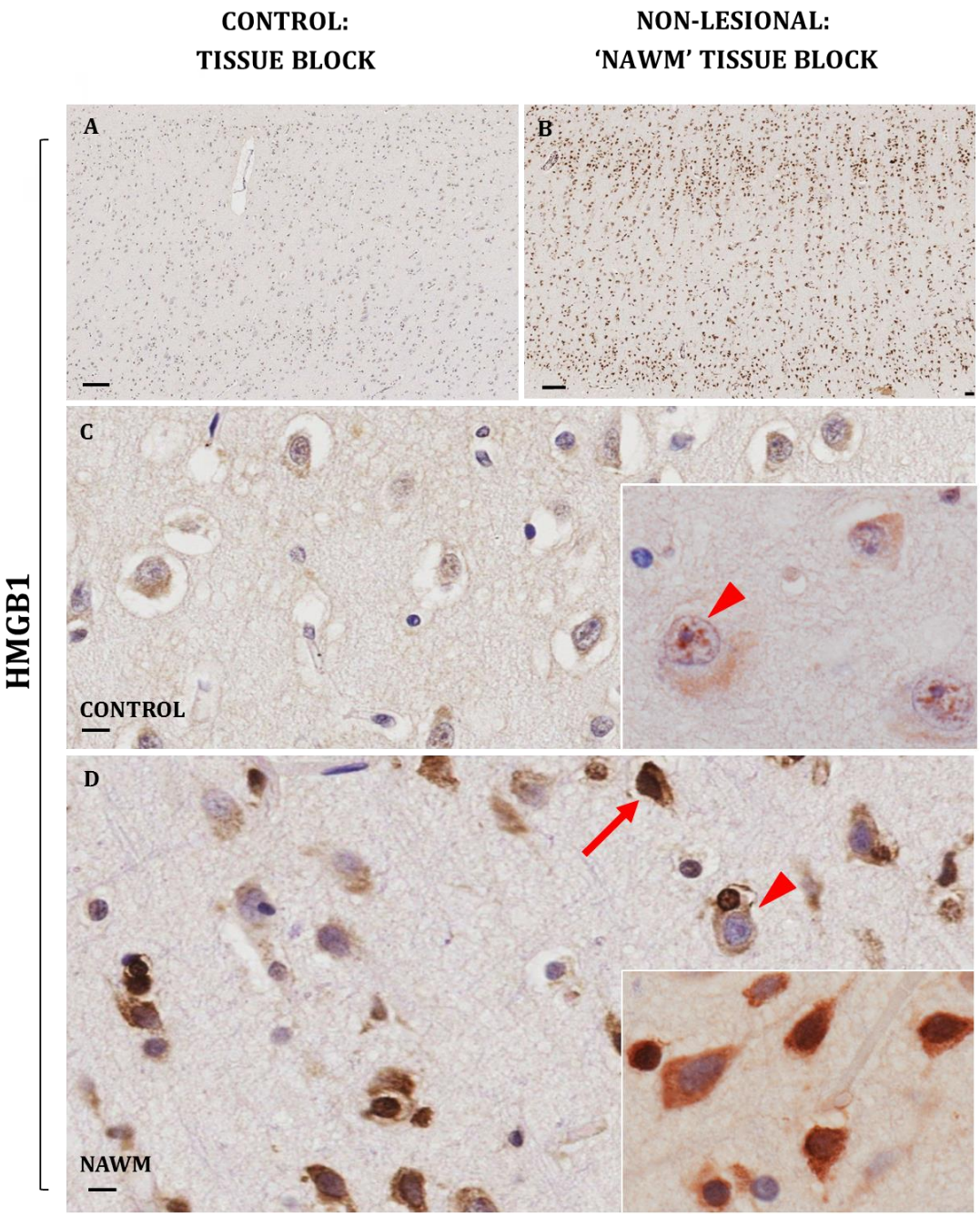

Figure 4.4 (A-D). HMGB1-positive cells in MS cortex demonstrate significantly greater cytoplasmic staining vs non-MS control tissue. ***(A, C) Control tissue; (B, D) NAWM tissue block.*** (A) Low power magnification demonstrates that HMGB1 IR is reduced across all layers of non-MS control cortex compared to MS cortex (B). (C) demonstrates a predominantly nuclear HMGB1 staining pattern, in close association with the chromatic structure (arrowhead). (D) shows differential staining pattern in NAWM tissue blocks with some neurons displaying increased nuclear stain but relatively little cytoplasmic staining (arrow), whereas others showed minimal nuclear staining but more prominent cytoplasmic staining (arrowhead). In all cases, intense HMGB1 IR was observed in OGD, especially in satellite cells *(continued overleaf).*

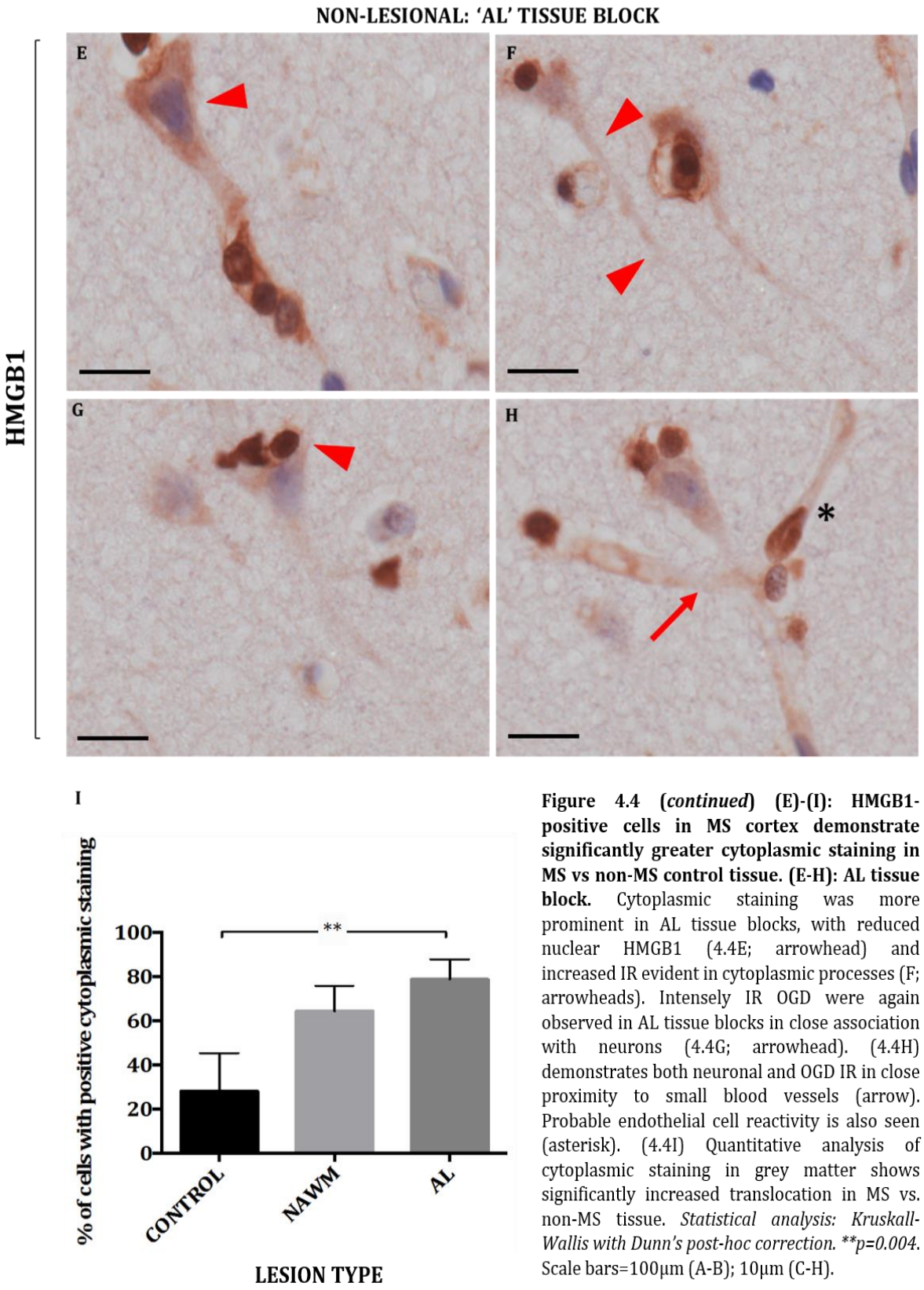

Figure 4.4 (*continued*) (E)-(I): HMGB1-positive cells in MS cortex demonstrate significantly greater cytoplasmic staining in MS vs non-MS control tissue. (E-H): AL tissue block. Cytoplasmic staining was more prominent in AL tissue blocks, with reduced nuclear HMGB1 (4.4E; arrowhead) and increased IR evident in cytoplasmic processes (F; arrowheads). Intensely IR OGD were again observed in AL tissue blocks in close association with neurons (4.4G; arrowhead). (4.4H) demonstrates both neuronal and OGD IR in close proximity to small blood vessels (arrow). Probable endothelial cell reactivity is also seen (asterisk). (4.4I) Quantitative analysis of cytoplasmic staining in grey matter shows significantly increased translocation in MS vs. non-MS tissue. *Statistical analysis: Kruskall-Wallis with Dunn's post-hoc correction. **p=0.004.* Scale bars=100µm (A-B); 10µm (C-H).

Quantitative analysis of cytoplasmic translocation using Leica IA software showed this pattern in active lesional blocks was increased compared to non-MS controls (p=0.004), (figure 4.4I). As discussed, the analysis parameters were set to detect larger objects with heterogenous nuclei (representative of the prominent nucleolus of neurons) and so the majority of cells assessed represented neurons. Thus, the difference focusses mainly on assessing neuronal cytoplasmic translocation, which is increased in MS vs control tissue.

4.6.4 HMGB1 expression is decreased in demyelinated vs. myelinated regions of the brain

We compared the HMGB1 expression in myelinated regions of MS tissue with non-MS control tissue and, as reported earlier, increased IR was observed in both the grey and white matter of MS tissue as seen in figure 4.5A-D. Interestingly, however, chronically demyelinated regions of the white and grey matter (Figure 4.5E-F) showed a return to basal levels of HMGB1, even lower than that seen in non-MS control patients. MBP-staining in controls was also carried out, and did not reveal demyelination in the regions assessed, therefore this was unlikely to be contributing to the reduced expression in these subjects. In the grey matter, the reduction in HMGB1 staining in MS tissue was not related to type of tissue block i.e. active or NAWM, and related solely to signs of chronic demyelination. OGD with increased expression were rarely noted, as were macrophage/ microglial-type cells. This discrepant pattern in the grey-matter often occurred within the same section, as shown in figure 4.5D and 4.5F. Interestingly, regions of subpial demyelination sometimes demonstrated deep sulcal meningeal blood vessels, full of HMGB1-positive cells (4.5F, inset), which were CD68+CD3+ (data not shown).

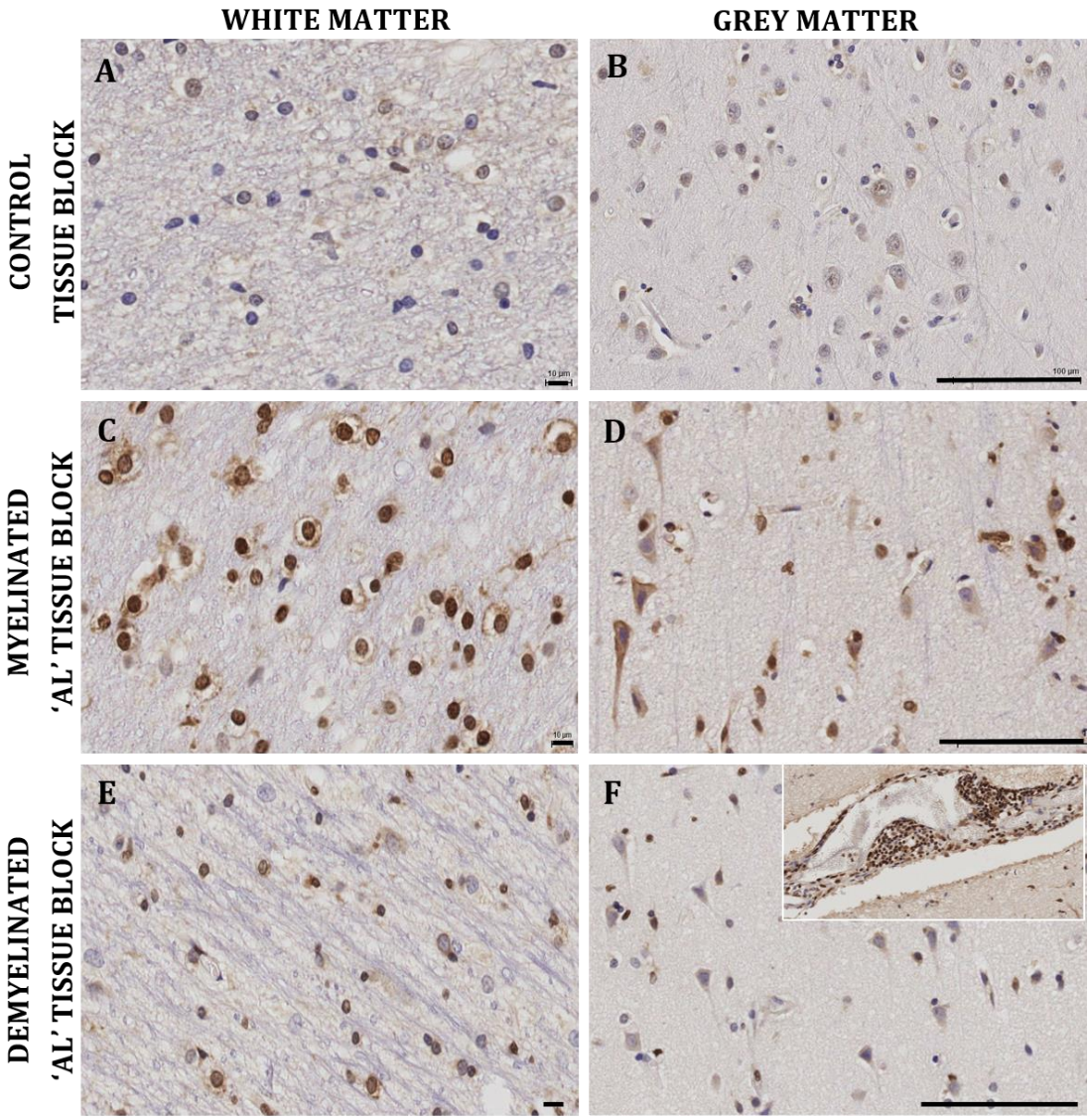

Figure 4.5. HMGB1 expression is decreased in demyelinated regions of MS brain tissue. (A,B) Control tissue: demonstrates low basal expression of HMGB1. (C,D) non lesional region of 'AL' tissue block demonstrates increased HMGB1 IR in both white and grey matter. I shows a demyelinated region **within the same section** containing an AL, with reduction in cell density overall evident. HMGB1 IR is reduced in this setting. (F) Cortical demyelinating lesions (type III, subpial in this case) demonstrate decreased HMGB1 IR also, in contrast to (D), which is a myelinated region within the same section. Inset demonstrates the presence of deep sulcal meningeal blood vessels which show florid infiltration of HMGB1-positive cells. (A, C, E)=white matter; (B, D, F)= grey matter. *Scale bars A, C, E=10µm; B, D, F=100 µm.*

4.6.5 CD68-positive cells are increased in normal-appearing white matter (NAWM) and active lesional tissue blocks in MS patients

Given the known relationship between HMGB1 and macrophage/ microglial cells, we sought to determine whether proportion of CD68-positive cells differed between tissue types in non-lesional regions. We found that proportion of CD68-positive cells was found to correlate with semi-quantitative IR scores as shown in figure 4.6. In addition, proportion of CD68-positive cells was markedly increased in non-lesional tissue within active lesional blocks ($p<0.0001$) and also in NAWM tissue blocks ($p=0.03$) compared to non-MS control tissue, as shown in 4.7. Interestingly, the proportion of CD68-positive cells in CAL was similar to the values found in non-MS control tissue, and significantly lower than in NAWM and AL tissue blocks (4.7G; images not shown). Of note, all CD68-positive cells were counted and no distinction was made on the basis of morphology. However, we did observe the presence of so-called 'microglial nodules', in both myelinated regions of AL tissue blocks as well as NAWM blocks (4.7C; inset).

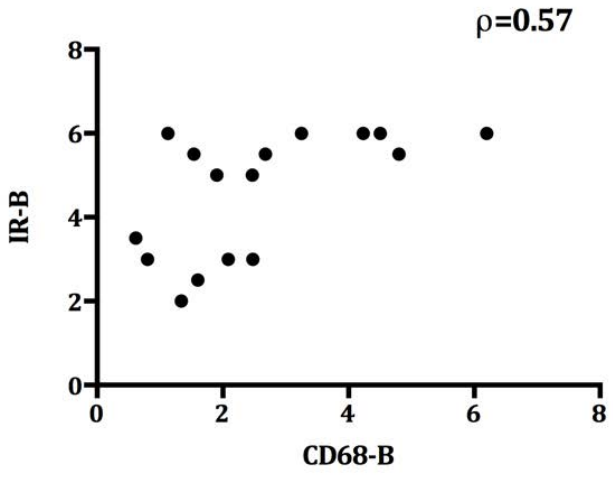

Figure 4.7. HMGB1 IR correlates with proportion of CD68-positive cells in non-lesional white matter. *Statistical analysis: Spearman's rank correlation. p=0.02*

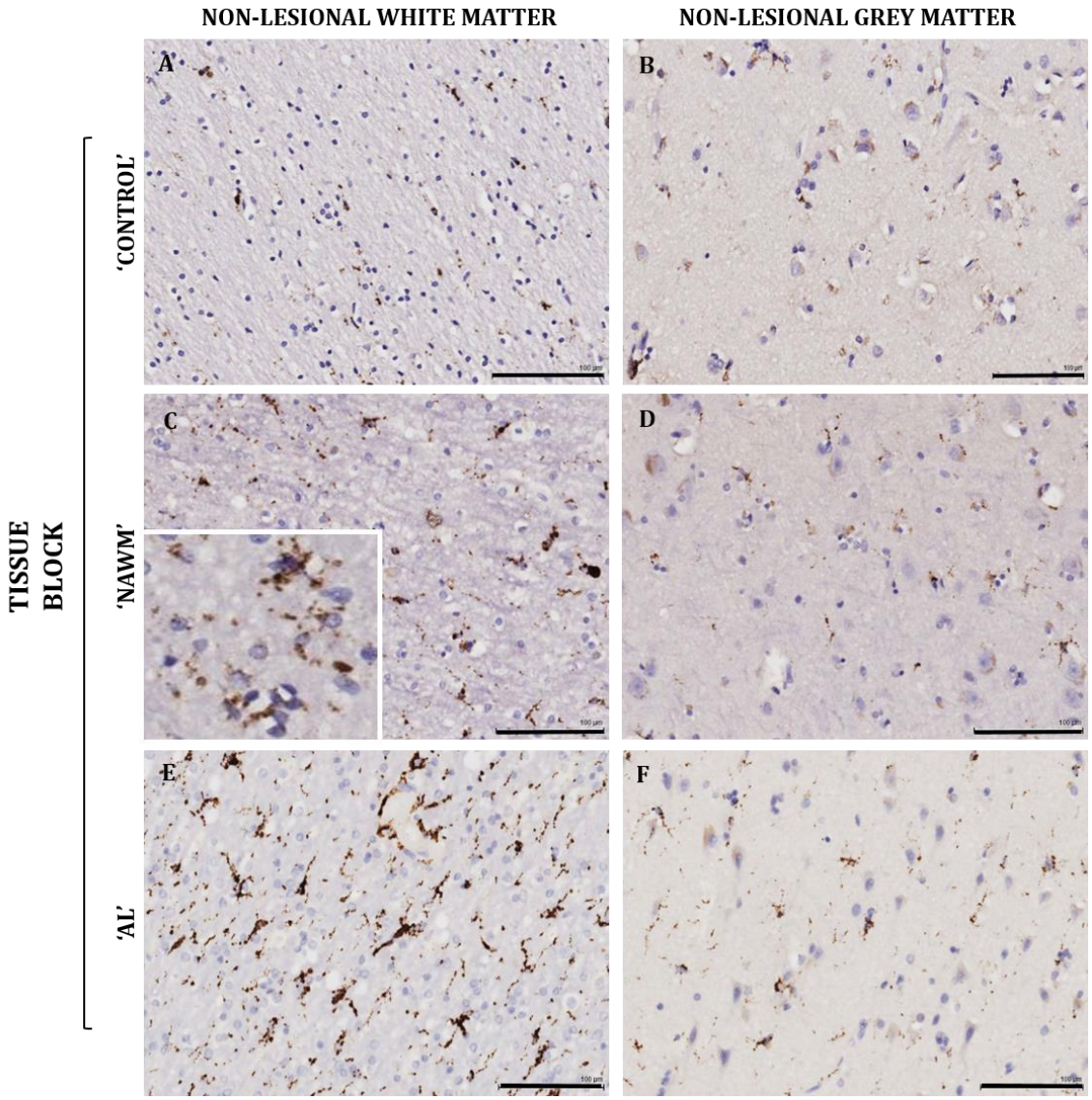

G

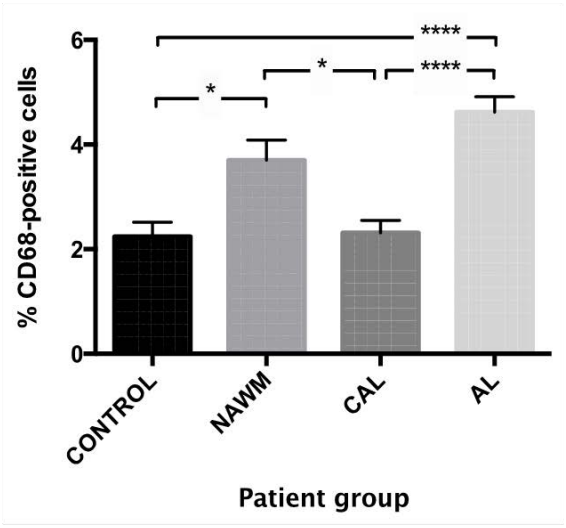

Figure 4.7. Comparison of CD68-positive cellular staining between different tissue types in human neuropathological tissue. Proportion of CD68-positive cells is significantly increased in non-lesional regions of AL and NAWM tissue blocks in MS patients (C-F) vs. non-MS controls (A-B). Of note, CD68-positive 'microglial nodules' were observed in both AL and NAWM tissue blocks (C, inset). Quantitative differences in CD68-positive cell count between all of the tissue blocks examined is shown in (G). *Statistical analysis: Kruskal-Wallis with Dunn's post-hoc correction. *p<0.05; ****p<0.0001*. Scale bars=100µm

4.7 Discussion

4.7.1 Increased HMGB1 expression in active MS lesions in SPMS patients highlights ongoing inflammation-related damage in chronic disease

It is well-known that patients with chronic disease have active lesions and the data presented here also demonstrates this. This is borne out by the fact that both longitudinal analysis of MS brain tissue using MRI, and pathological studies have shown that lesions continuously arise and regress during the long course of the disease. The profound destruction following inflammatory cell infiltration from the periphery is well-documented and gives rise to classical inflammatory, demyelinating MS lesions. We have confirmed the findings by Andersson et al, and our own findings in Chapter 3; that HMGB1 IR was clearly increased in active MS WML compared to non-MS control white matter.

HMGB1 reactivity in endothelial cells was also noted in both active lesional and non-lesional regions. Previous work has shown that HMGB1 acts upon endothelial cells via RAGE and that this can lead to upregulation of ICAM-1 and VCAM, leading to adherence of inflammatory cells (Fiuza et al. 2003). In addition, it is now established that HMGB1 can complex with CXCL12, acting at CXCR4 to propagate T-cell recruitment through the BBB. Anti-HMGB1 monoclonal antibody therapy has been used to attenuate ischaemia-related neuroinflammation by reducing blood-brain barrier permeability, suppressing microglial activation, matrix metalloproteinase-9 activity and cytokine release by immune cells such as IL-17 (Liu et al. 2007; Zhang et al. 2011). All of these pathological processes are relevant to MS and amelioration of clinical signs were observed when using a monoclonal antibody to HMGB1 in EAE (A Uzawa et al. 2013). These authors postulated that anti-HMGB1 therapy could be used clinically during relapses, when the BBB is

known to be more permeable, allowing penetration of anti-HMGB1 Ig molecules into the CNS and exert its anti-inflammatory function.

4.7.2 HMGB1 expression is increased in non-lesional regions of MS brain compared to non-MS control tissue

Despite the changes above, what remains unclear is the nature of the earliest alterations within MS brain tissue which go on to form this archetypal lesion. MRI studies have shown that not all early alterations in brain texture suggestive of MS-related pathology go on to become classical MS lesions, as discussed in chapter 1. This suggests that at some level, there is intrinsic regulation, which can limit lesion formation at the earliest stages. Understanding this process better may allow development of therapeutic strategies that could augment this endogenous, protective response.

In this context, our finding of increased HMGB1 IR in non-lesional regions is profoundly important in furthering our understanding of the molecular changes taking place in these areas of MS brain tissue. The changes were markedly different compared to non-MS control patients in both NAWM and AL tissue blocks, although the latter showed strikingly consistent increase in IR whereas there was more heterogeneity in the NAWM tissue. This is reflected when comparing IR between groups, where difference in semi-quantitative scoring between controls and MS patients was strongly significant in the AL tissue group but not in the NAWM group. This is likely to be due to greater heterogeneity within patients as discussed but also to smaller numbers in this group (NAWM n=5 vs. AL/CAL n=10). Despite this, IR was greater in all MS patients vs controls, highlighting a potential disease-specific effect. We would need to carefully examine white matter regions from patients with neurological diseases other than

MS in order to ascertain this, but IR staining patterns in this series clearly differentiates between MS and non-MS control patients.

4.7.3 HMGB1 expression in OGD is significantly upregulated in MS brain tissue compared to non-MS controls

Aside from macrophages as already reported (Andersson et al, 2008), it was particularly interesting to note that the main cell type demonstrating these differences were oligodendrocytes, assessed morphologically. Given the increased IR in NAWM tissue blocks in particular- technically at least 1cm from identified white matter lesions- this may reflect endogenous HMGB1 expression in OGD. Its function in this context may be different to those resulting from exposure to exogenous HMGB1 released by macrophages/microglia, for example.

HMGB1 has been shown to be expressed in both neurons and OGD, in an early report describing amphoterin expression, as it was then known, in rats (M M Daston & Ratner 1994). It is fascinating to note that in this study, HMGB1 expression in OGD was most intense in early postnatal development i.e. in immature OGD-lineage cells, whereas in adults, expression of positive cells was more widely scattered and less intensely immunoreactive. Of additional interest was the finding that amphoterin-positive cells did not co-localise with GFAP-positive cells, thus independently confirming both our findings and those of Andersson et al. The authors concluded that amphoterin/ HMGB1 was involved in neuron-glial interactions (adhesion) in the developing CNS, by enabling pre-myelinating OGD to act as a permissive substrate for fasciculation of neurites, or may have a role in the segregation of axons by developing OGD. Given the

profound upregulation in immature OGD, they also suggested that amphoterin/ HMGB1 be used as a novel marker of OGD development.

The widespread increase in oligodendroglial anti-HMGB1 IR in MS brain tissue, as opposed to non-MS control tissue, raises the possibility that the phenotype of some of these cells may be relatively immature. It is well-known that re-expression of developmental pathways often occur under conditions of cellular stress. NG2 cells, for example, have been shown to clear β-amyloid peptide via endocytosis and augment autophagy (W. Li et al. 2013). In MS itself (John et al. 2002), OGD precursor cells (OPCs) are known to accumulate in and adjacent to MS lesions (Guus Wolswijk 1998; Chang et al. 2000a) but it is unclear how widespread the presence of these cells is. Further co-localisation work using established markers e.g. NG2 or –O1 for immature cells and –O4, Nogo and CAII for mature cells would be of particular interest in ascertaining at what developmental stage HMGB1 expression is closest to. Whether our observation of widespread HMGB1 IR in OGD is reflective of a similar process in MS is unexplored.

Given the widespread expression pattern in MS tissue, it is also possible that OGD themselves are producing HMGB1. Certainly, microglial cells in proximity to OGD contain the receptors required for transduction of HMGB1-mediated signalling, such as TLRs and RAGE if this reached the extracellular space (Bsibsi et al. 2002). This action may reflect chronic damage affecting oligodendrocytes as a result of other proinflammatory cytokines diffusing from local activated microglia or distal lesional regions, activating receptors for HMGB1 on OGD and thus producing a pro-inflammatory cytokine 'wave' through the MS brain. Alternatively, it may be an endogenous response to an unknown trigger, stimulating production of

HMGB1 in OGD. Given the well-known difficulty in visualising cytoplasmic processes of OGD, it is unclear from which sub-cellular compartment this increased production would arise.

Our work also demonstrates that semi-quantitative HMGB1 IR scores were positively correlated with proportion of CD68-positive cells in myelinated white matter, suggesting that they may be related to pathological processes occurring in non-lesional as well as lesional tissue. Their role in this context may not be the same as the highly reactive macrophage/ lipophages observed in the EAL in chapter 3, and again M1/M2 phenotyping would be of interest here.

Oligodendroglial abnormalities in non-lesional tissues have been noted in numerous previous reports and were discussed in Chapter 1 (section 1.2.7) (Amor et al. 2010; Jack van Horssen et al. 2012; Van Noort et al. 2010; Singh et al. 2013; Van der Valk & Amor 2009; van Noort et al. 2010; Zeis et al. 2008; Graumann et al. 2003; Ingram et al. 2014; Bsibsi et al. 2013b; Barnett et al. 2009). The overall consensus at present is that oligodendroglial activity in non-lesional regions of MS brain is largely protective. Graumann et al performed microarray analysis and quantitative PCR to screen for upregulated genes using carefully characterised NAWM blocks from the same source as our tissue, the UK MSBB (Graumann et al. 2003). They found significant upregulation of genes related to maintenance of cellular homeostasis, in addition to neuroprotective mechanisms induced upon ischemic preconditioning. This was exemplified by the upregulation of the transcription factor HIF-1α, members of its associated PI3K/Akt signalling pathways and the latter's target genes such as VEGF-receptor-1, although it is important to note that HIF-1α is not purely anti-inflammatory in its function. They postulated the pattern highlights a general neuroprotective reaction against

oxidative stress which they discussed could either be a response to chronic damage or else a trigger to subsequent pathology. Interestingly, HMGB1 expression was also found to be upregulated in 6 out of 11 MS subjects, but overall failed to reach statistical significance. They pointed out that subsequent quantitative PCR of promising candidate genes revealed the microarray data to significantly underestimate the upregulation found, and may be why HMGB1 upregulation failed to reach significance. In reality, however, this lack of significant gene upregulation is unsurprising in the particular case of HMGB1 as under physiological conditions, constitutive levels of the protein itself are already high with at least $1x10^6$ molecules within the nucleus alone. It may be that it is the mobilisation and subsequent function of this large amount of stored HMGB1, either as a transcription factor within the nucleus or else within the cytoplasm or indeed extracelluar space, that is pathologically relevant and will be discussed further, below.

Zeis et al (Zeis et al. 2008) extended the findings above and screened similar tissue from the same brain bank and found other genes upregulated in NAWM tissue, including STAT6, JAK1, IL-10 and IL-4R in addition to Hif-1α as shown previously. Whilst these mediators do not have purely anti-inflammatory effects, taken together the authors postulate a protective phenotype overall. Pro-inflammatory genes such as STAT4, IL-1β and MCSF were also upregulated but less consistently. Immunofluorescence colocalisation analysis of human brain tissue demonstrated oligodendroglial expression of STAT6, JAK1, IL-13R and IL-4R and whilst STAT4 expression was predominantly found in microglia. These findings further reinforced the concept that a CNS-specific inflammatory reaction takes place

throughout the whole of the white matter in MS brain tissue, and that OGD were important in mediating anti-inflammatory or protective strategies.

Other work examining NAWM changes has shown increased expression of alpha-B-crystallin, a small heat-shock protein also known as HSPB5, as discussed in Chapter 1. Several groups have documented up to 20-fold increased expression of HSPB5 in multiple sclerosis brain and its absence in control brain tissue. It was also found to be a target of CD4+ T-cell-mediated damage to the myelin sheath (Ousman et al. 2007a). Further work demonstrated it was a potent negative regulator of pro-inflammatory pathways in both the immune system and CNS. Compared to wild-types, HSPB5 -/- mice demonstrated worse clinical outcomes in EAE during both acute and progressive phases,with higher Th1 and Th17 cytokine secretion from T cells and macrophages, and generally more profound CNS inflammation. Potential anti-apoptotic functions were also shown and antibodies to HSPB5 were detected in CSF from MS patients and in sera from EAE mice. Lastly, administration of recombinant HSPB5 improved clinical EAE outcomes (Ousman et al. 2007b).

Recent work has shown that 'stressed' OGD produce HSPB5 (Duvanel et al. 2004; van Noort et al. 2010), which acts as an intracellular chaperone, attenuating the effects of oxidative stress. Secreted HSPB5 then activates microglia within 'microglial nodules' or 'pre-active lesions' in close proximity to OGD, to produce widespread TLR2-mediated anti-inflammatory or protective responses throughout the normal-appearing brain tissue during MS (Van Noort et al. 2010; Bsibsi et al. 2014). In addition to TLR2, microglia were shown to express HSPB5 receptors TLR1, CD14 and other markers including multiple antiviral genes,

including RIG-1. These were induced by HSPB5 stimulation, all of which are otherwise inducible by type 1 interferons. Whilst the authors tentatively suggest that the type 1 INF-like response induced may be mimicked by IFN-β treatment in patients, it is likely that the IFN signature in MS brain overall is not anti-inflammatory. However, the critically important finding from this body of work is the identification that the immunoregulatory environment maintained by OGD-microglial interaction is subject to change upon exposure to mediators such as IFN-γ from circulating T-cells, for example. Here, the microglial response changes sharply to a pro-inflammatory, destructive phenotype. This may explain in part, why there appears to be a precarious balance between protective and destructive mechanisms in non-lesional brain tissue, and further argues that changes in these regions precede frankly demyelinating lesions.

Both HMGB1 and heat shock proteins are thought to be DAMPs, released in response to cellular stress as outlined above (Tsan & Gao 2004; Tsan 2011; Bianchi 2007). An important study linking HSP function with HMGB1 in the context of autophagy and mitophagy has recently been reported (Tang et al. 2011a). The authors reiterated that targeted deletion of HMGB1 (e.g. using shRNA transfection to produce HMGB1-/- cells) leads to mitochondrial fragmentation, deficits in mitochondrial respiration and ATP synthesis. These changes were similarly observed with disruption of the HSPB1 gene in embryonic fibroblasts, and forced HSPB1 expression in HMGB1 knock-out cells reversed the phenomenon. As discussed in Chapter 1, previous reports had identified the critically important role that HMGB1 plays in autophagic surveillance and mitochondrial quality control (Tang et al. 2010). However, this study identified

that nuclear HMGB1 acts as a master regulator of HSPB1 levels at the transcriptional level, and that the latter was the downstream effector molecule delivering the pro-autophagic directives of HMGB1 (Tang et al. 2011b). Whilst the work in MS has dealt predomominantly with the role of HSPB5 in NAWM, all of the small HSPs have been shown to be involved in regulation of cell survival and death (Acunzo et al. 2012). Thus, it is possible that HMGB1 interacts with HSPB5 also, in orchestrating autophagic responses. Molecular work of this complexity regarding HMGB1 function has not been carried out in oligodendroglial-like cells, but it would be of great interest to investigate the effects of HMGB1 on regulating levels of HSPB5, for example.

A final and purely speculative possibility alludes to HMGB1's role as a promiscuous sensor of viral proteins, discussed in Chapter 1, where chronic (vs. acute) infection of some OGD may engage HMGB1 to orchestrate specific anti-viral responses via HSPs, and produce an immunoregulatory environment.

Regardless of the cause of OGD stress, the widespread expression and hence similarity to other molecules such as HSPB5, suggests that HMGB1 may also serve as a protective mediator in the NAWM of MS brain tissue. However, we can speculate that upon exposure to pro-inflammatory cytokines such as IFN-γ, the switch to a pro-inflammatory environment may induce HMGB1 to take on a more damaging role, as demonstrated in active lesions, or else be secreted from infiltrating macrophages and function entirely independently from endogenous HMGB1, expressed by CNS-resident cells.

4.7.4 HMGB1 expression is reduced in demyelinated regions of both grey and white matter

HMGB1 IR was reduced in demyelinated regions of MS brain tissue. This may be due to reduced cell numbers overall, which is an accepted pathological consequence of chronic demyelination over time, giving rise to an apparent reduction as observed in both our work and by Andersson et al (Andersson et al. 2008). However, as seen in Chapter 3, IR was also significantly reduced in demyelinated regions of biopsy tissue taken from a patient at an early stage of the disease. Thus, reduced cell density of HMGB1-expressing cells over time may be insufficient to explain reduced IR, and instead may reflect a dynamic reduction in expression. Of particular interest was the fact that deep sulcal meningeal blood-vessels were sometimes overlying subpial demyelinated regions. A florid inflammatory cell infiltrate could be observed in this situation,and the majority of cells were HMGB1+ and CD68+ and/ or CD3+ using sequential staining (latter data not shown).

4.7.5 HMGB1 expression patterns demonstrate widespread abnormality in non-lesional grey matter regions of MS brain tissue

HMGB1 was previously identified as a promoter for neurite outgrowth in developing neurons, and enhances neuronal survival (Huttunen et al. 2000; Rouhiainen et al. 2000). It is well established that in pathological settings, processes usually restricted to CNS development can re-emerge in an effort to maintain neuroprotection. This may be the case for HMGB1, and unlike the heavily post- translationally modified, extracellular HMGB1 released from macrophages which is pro-inflammatory (see Chapter 1), endogenously produced HMGB1 in settings of chronic neuronal damage may well be tuned to repair rather than

destruction, as alluded to earlier in this chapter. However, the post-translational phenotype of HMGB1 molecules in this setting has not been explored in detail in brain tissue as yet.

The finding of increased anti-HMGB1-IR in OGD/ satellite cell expression in MS NAGM was striking, in their classic configuration in apposition with neurons. OGD are known to provide trophic support to neurons (Wilkins et al. 2003; Wilkins et al. 2001) (Lee et al. 2012). In addition to direct cell-cell contact, many studies have shown that OGD- or OPC-conditioned media provide soluble factors which are essential for normal neuronal functioning, such as BDNF (Ghosh et al. 1994) and IGF-1 (Wilkins et al. 2001).

Intense OGD IR was often associated with cytoplasmic translocation in neuronal somata in non-lesional GM. This pattern in AL and also in a number of NAWM tissue blocks was significantly different to that observed in non-MS control tissue. It was rarely observed in chronically demyelinated regions however as outlined above, suggesting that these changes occurred early in the disease process. As in the case of NAWM, whether these NAGM changes represent a distal effect of cortical and/ or white matter lesions, or precede their development is not clear.

The consequences of cytoplasmic translocation are unclear, and it is also not established whether it is released from the cell in MS. In the necrotic core of murine models of ischaemic stroke, neurons were shown to rapidly empty their nuclear and then cytoplasmic cellular content of HMGB1 into the surrounding tissue (Qiu et al. 2007). Interestingly, peri-lesional neurons- unlike those cells at the necrotic core- were shown to translocate HMGB1 from the nucleus but then retain it within the cytoplasm for an extended period and did not release it into the media. They did not further explore the reason for this, but subsequent studies

highlighting the critically important role of HMGB1 in autophagy and bioenergetic preservation of compromised cells, as delineated above and in Chapter 1, may contribute to the explanation. Clearly, neurons are under significant metabolic stress in the context of demyelination in MS, exacerbated by the redistribution of sodium channels and subsequent energy inefficiencies in these large cells. It was particularly interesting to note that large pyramidal neurons were more likely to demonstrate cytoplasmic translocation than smaller neurons in the internal and external granular layers- which are responsible for synapsing over relatively shorter distances. We have not explored this further as yet but it is an important observation that warrants further investigation. In addition, non-lesional grey matter in NAWM tissue blocks sometimes showed intense nuclear expression of HMGB1 but cytoplasmic translocation was relatively less pronounced. This suggests a temporal sequence, where increased nuclear expression is followed by cytoplasmic translocation and this in turn is followed by globally reduced HMGB1 expression in the context of chronic demyelination, possibly because the HMGB1 has 'emptied' from the cell and not been replenished. This is highly speculative and needs further verification by additional techniques such as in-situ hybridisation. However,it raises interesting possibilities as to the development of neuronal changes over time in MS brain tissue. The lack of association of CD68-positive cells and HMGB1 IR scores in this tissue type further supports an independent mechanism of HMGB1-related activity between neurons and OGD in progressive MS patients. Again, its role here may in fact be important in mediating protective responses in this dysfunctional CNS environment.

4.8 Limitations of study

Autopsy tissue is well-known to produce artefact when examining protein expression. Both post-mortem interval and formalin fixation have an impact in both under and over-expression of antigens. In addition, age also has an impact on antigen expression and detection, which is especially difficult in the setting of MS research, as patients are relatively young when they die and control subjects are usually elderly. Finally, sex-specific effects cannot be ruled out but again, MS research is hindered in this respect due to the female preponderance of the disease. It was not possible to fully control for these factors, therefore their potential impact must be taken into consideration. Larger studies and age/ sex-matching would be required in future studies to ensure any differences were not related to these factors.

Despite a great deal of research into NABT in MS, no consistent definition has been reached neuropathologically, as to what constitutes 'normal' tissue in MS brain. A distance of 1500μm from the lesion border was chosen in this study based on appearances within the tissue sections overall using a variety of stains and IHC (*F. Roncaroli, personal communication*) and in accordance with other published papers and theses, where a minimum of 900 μm has been used. With regards to image selection, only one image was used for scoring but raters were also given low power views to place this image into context when scoring, with these views covering a large area of approximately $1mm^2$.

IR scoring is a subjective assessment of antigen expression, and as mentioned previously, the DAB reaction used in this study is not stoichiometric and therefore absolute expression cannot be calculated. Despite this, the methodology has been used in a number of other studies, to semi-quantitatively reflect the pattern of IR in the whole group and not just in the images presented. In this study, three

different raters, experienced in neuropathological assessment of tissue and blinded to the clinical history, were used to provide a robust analysis and the resultant correlation between rating scores was good.

The manual counting of CD68-positive cells is subject to obvious limitation as 2-dimensional counting of objects can introduce inaccuracy. However, any errors were likely to be applied to all sections assessed, as one rater was used to count.

Assessment of cytoplasmic translocation using the Leica IA software was novel and, therefore the technique has not undergone an established standardisation process. In addition, it was not possible to identify which cell types demonstrated the greatest cytoplasmic translocation, which was responsible for the final calculation. Thus, it required this tool to be used in conjunction with visual assessment to identify which cells in a particular tissue type (GM vs. WM) were likely to have contributed to this the most when interpreting the results. Nonetheless, it provides an objective assessment of translocation and further work is currently being done to develop this within Leica Biosystems.

Finally, whilst it appeared that HMGB1 IR was prominent in OGD, this was based on morphological appearance in the white matter especially and by classical configurations in the grey matter, in close apposition to neurons. The only way to confirm that these are indeed OGD would be to perform co-localisation studies with established markers such olig2, using immunofluorescence techniques. In addition, in-situ hybridisation studies would demonstrate mRNA expression of HMGB1, confirming expression of the molecule in specific cell types. This work is planned and will be undertaken as discussed in 'Future work'; section 7.3.

4.9 Conclusions

I have performed a detailed examination of HMGB1-related neuropathological changes occurring in NABT of MS patients and shown that anti-HMGB1 IR is profoundly increased in non-lesional regions of both GM/WM in this series of MS patients compared to non-MS controls. The fact that expression was increased in NAWM tissue potentially refutes our original hypothesis of HMGB1 reflecting centrifugal diffusion from the lesion core to the surrounding perilesional tissue. Oligodendrocytes clearly expressed HMGB1 in non-lesional WM and in satellite cells in close apposition with neurons in myelinated GM. Increased endogenous HMGB1 expression may upregulate downstream molecules such as HSPs in OGD, which are also known to have roles in autophagy and mitochondrial quality control. Neurons in grey matter demonstrated evidence of cytoplasmic translocation of HMGB1 which may also signify autophagic rather than destructive effects, given the established role of HMGB1 here. In addition, the possibility that marked anti-HMGB1 IR in OGD may reflect widespread alterations in their developmental phenotype, also warrants further exploration.

Given the potentially beneficial role of HMGB1 in pre-lesional MS pathology therefore, a simple HMGB1-blocking approach as seen in the EAE work may not be successful in the long-term treatment of MS patients. Similar caution was raised in the work by Andersson et al (Andersson et al. 2008). It is theoretically feasible, however, that drugs targeting very specific post-translational modifications, such as the disulphide-linked form of heavily oxidised, extracellular HMGB1, could be used therapeutically in active disease.

5.

Cerebrospinal fluid biomarkers of damage, inflammation and degeneration in Multiple Sclerosis

5.1 Introduction

5.1.1 CSF biomarkers in MS

The use of biomarkers such as MRI have profoundly changed our understanding and management of neurological illness, but tissue confirmation of disease processes remains the gold-standard. CSF sampling can therefore be viewed as a 'liquid biopsy', as its proximity to the brain substance is the often the best chance clinicians have in capturing disease processes in real-time (Giovannoni 2006).

A biomarker in body fluids is 'a characteristic that is objectively measured and evaluated as an indicator of normal..(and) pathogenic processes, or pharmacological responses to a therapeutic intervention' (Floyd & McShane 2004.). A 'perfect' biomarker in MS would reflect neuropathological changes occurring in MS lesions and then be validated in patients with neuropathologically confirmed MS. It would also have a high specificity and sensitivity for prediction of neurodisability and should be reliable, non-invasive, simple to use, and cheap.

Accurate diagnosis, prognostication and monitoring of disease progression are critical in our management of MS patients. Although MR imaging has emerged as our greatest tool to facilitate this to date, it has inherent drawbacks including the fact that traditional metrics are poorly correlated with disability outcomes and generally measure late disease processes (Fisniku et al. 2008b). Body fluid biological markers are potentially of great use as they can aid prognostication and responsiveness to treatment [Teunissen 2012]. Molecular biomarkers may reflect disease-specific mechanisms (Deisenhammer et al. 2009) and are thus of added value.

However, despite an explosive effort in the search for appropriate biomarkers in MS, there remains a dearth of genuinely useful molecules which could be used for monitoring or prognosticating disease progression more accurately for use in daily practice.

5.1.1.1 Free-light chain levels are established markers of intrathecal inflammation in MS

As detailed, we collected a large series of CSF samples from MS patients and a range of non- MS control subjects. In order to assess whether this was a representative cohort of patients to analyse, we chose to assess CSF free-light chain levels as this is an established marker of MS (Presslauer et al. 2014; Presslauer et al. 2008; Senel et al. 2014). As discussed in the General Introduction, chapter 1, whilst T-cells are critically important in MS-related pathology, meningeal ectopic B cell follicles and plasmablasts in the CSF are also likely to contribute to the pathology of MS (Aloisi et al. 2010; Meinl et al. 2006). These CNS-resident B cells produce intrathecal immunoglobulin, allowing detection of CSF-specific oligoclonal bands that continue to be an important component of the diagnostic pathway for MS (Katsavos and Anagnostouli, 2013; Tumani et al. , 2009). During active antibody production, FLC are also produced and so serve as markers of this process.

Interestingly, plasma cells release HMGB1 into the extracellular milieu following LPS-stimulated maturation (Vettermann et al. 2011). This demonstrates a potentially pro-inflammatory effect in autoimmune disease and chronic inflammation although other studies have also suggested that the primary role in the setting of chronic inflammation is to promote immunosuppression (G. Li,

Liang, et al. 2013). However, as FLC reflect antibody production, it may be that they are correlated with HMGB1 production also and we wished to examine this.

5.1.1.2 Neurofilament proteins are established markers of neuroaxonal damage

Neurofilament proteins are widely regarded as the most reliable protein biomarker for neurodegeneration (Teunissen & Khalil 2012; Teunissen et al. 2005; Petzold et al. 2010). Their importance in potentially delineating pathological processes as well as their utility in clinical trials and routine laboratory practice is being increasingly recognised (Petzold et al. 2010).

They are the predominant axonal cytoskeleton proteins and comprise three elements that differ in molecular size: the light chain (NfL)- 68 kDa, the intermediate chain (NfM)- 150 kDa, and the heavy chain (NfH) of 190–210 kDa (Petzold 2005). The NfL is the 'backbone' to which NfH and NfM chains attach to form polymerised neurofilaments. The degree of filamenous phosphorylation alters the axonal diameter, as the more phosphorylated it is, the broader the diameter (Fuchs 1998). Non-phosphorylated neurofilament has been observed within active MS lesions (Trapp et al. 1998) and in murine and primate models early during EAE pathology. Following axonal injury, they are released into the extracellular space, and subsequently into the CSF and peripheral blood (Petzold 2005). Thus analysis of CSF or serum NF levels is accepted as a valuable tool to estimate extent of axonal damage in patients with MS.

A number of studies have shown increased NfL levels in the CSF of patients within all MS subgroups (Norgren et al. 2003; Lycke et al. 1998; Teunissen et al. 2009), and they have demonstrated their potential utility in monitoring therapeutic

efficacy (Gunnarsson et al. 2011) as well as serving as possible outcome measures in clinical trials (Romme Christensen et al. 2014). These will be discussed in more detail in the discussion, section 4.4.2, below as we wished to corroborate these findings to ensure that our cohort is representative of MS and non-MS patient groups. In addition, given its detection in patients at early stages of MS, we wished to examine the relationship of this sensitive marker of degeneration to other inflammatory markers such as cell count or indeed FLC, as the correlation between these two established markers of different components of MS-related pathology has not been reported before.

5.1.1.3 HMGB1 is potentially a novel CSF biomarker in MS

As presented in Chapters 3 and 4, we found widespread expression of HMGB1 throughout the MS brain, in both lesional and non-lesional regions. Western blotting analysis originally demonstrated the presence of HMGB1 in the CSF in two MS patients whereas it was not detected in 2 control patients (Andersson et al. 2008). The lack of a quantitative assay curtailed further exploration of these promising findings until IBL-International developed a commercial assay for the detection of free HMGB1 in body fluids (Yamada 2003). Since then, reports of its utility in numerous diseases including MS have been reported and will be discussed further in section 5.6.3 of this chapter, in the discussion.

Many of the HMGB1+ cells in the early active biopsy lesion in particular were perivascular macrophages and we know that HMGB1 is classically produced by these cells (Andersson et al. 2008; Wang 1999). There is limited information of HMGB1 function and production by lymphocytes in the literature (I E Dumitriu et al. 2005; Sundberg et al. 2009), but our observation of probable CD3+ HMGB1+

lymphocytes suggests that these cells may also have the capability to produce HMGB1 in this setting. In the context of BBB compromise, infiltrating HMGB1+ leukocytes may enter the CNS space and thus serve as a source of secreted HMGB1 in CSF. CXCL12 and CXCL13 are detected in the CSF (Krumbholz et al. 2006), and these may be involved in HMGB1 function both directly and indirectly. CXCL12 directly associates with HMGB1 and acts via CXCR4 to increase leukocyte chemotactic activity (Schiraldi et al. 2012), whilst CXCL13 is a powerful T- and B-cell chemoattractant and is implicated in MS pathology (Krumbholz et al. 2006). In addition, given recent work suggesting that CSF production may reflect parenchymal changes to a greater degree than previously thought, it is possible that it may also be secreted from the great numbers of HMGB1+ CNS-resident cells. This latter source may be more relevant in the remission phase of the disease, as we know from the observations in the neuropathology work that HMGB1 expression is increased even in non-lesional tissue, and in patients who have ceased to actively relapse.

5.2 Hypotheses

1. Classical (FLC and NfL) and non-classical (HMGB1) molecules associated with MS pathology are increased in the CSF of MS vs. non-MS patients
2. HMGB1 and FLC levels are correlated due to production by B-cells
3. The increase in HMGB1 levels is likely to be more marked in the earlier, inflammatory disease phase (i.e. CIS/ RRMS), even in non-actively relapsing patients

5.3 Aims

1. To establish a well-characterised clinical cohort comprising both MS and non-MS control patients

2. Evaluation of this cohort using two well-established protein markers in MS: k and λ free-light chain (FLC) and neurofilament-light (NfL) levels

3. To investigate CSF levels of a relatively novel biomarker, HMGB1, using a quantitative ELISA assay in this patient cohort

5.4 Materials and methods

5.4.1 Study Subjects

Ethical approval for the study was obtained via the Human Biorepository Research Centre (HBRC), University of Birmingham and all subjects provided written informed consent to participate in this study. Between February 2011 and September 2013, matched serum and CSF samples were prospectively collected from 170 patients who underwent routine diagnostic lumbar puncture as elective cases on the neurological investigations day-case unit at University Hospital, Birmingham (UHB). The latter represents the main referral centre for the region; 86% of the cases were referred from peripheral hospitals for diagnostic LP at QEHB. CSF and serum samples from a further 13 patients were collected from University Hospital of North Staffordshire (UHNS) for the free-light chain study, following local ethical approval.

The following diagnostic groups were established: CIS (n=24), RRMS (n=27) and primary progressive MS (PPMS) (n=13)- fulfilling the criteria of dissemination in space and time for diagnosis of MS according to recent criteria (Polman et al. 2005)- see table 5.1. The majority of MS patients were not receiving any disease-modifying treatment at time of LP except 1 PPMS patient who was taking methotrexate. 1 RRMS patient had been on TYSABRI® but had not received it in the 30 days prior to LP due to concerns over possible PML, which were disproven following the LP. As part of the HBRC ethics, this same patient had provided biopsy material whose clinical history and neuropathological findings have already been reviewed in chapters 3 and 4. Two of the MS patients (1 CIS and 1 RRMS) had received a course of steroid therapy in the month prior to CSF collection.

Patient group	n	Gender M:F	Age	OCB status+ (%)
Clinically-isolated syndrome (CIS)	24	8:16	38 (21-70)	21/24 (88)
Primary-progressive MS (PPMS)	13	5:8	51 (43-72)	10/12* (83)
Relapsing-remitting MS (RRMS)	28	4:24	41 (19-72)	24/26* (92)
Other neurological disease (OND)	100	33:67	43 (17-85)	1/87* (1)
Other neurological inflammatory disease (ONID)	18	10:8	44 (24-83)	1/17* (6)

Table 5.1. Demographic data from MS and non-MS patients: median (range). MS patients were classified into three clinical subgroups: CIS, RRMS and PPMS. Non-MS patients were classified according to diagnosis of other inflammatory neurological disease (ONID) or other non-inflammatory neurological disease (OND). *denotes patients with either missing data or matched bands in the serum and CSF.

In addition, other neurological inflammatory diseases (ONID) (n=18) and other neurological diseases (OND) (n=100) comprised the non-MS patient groups. We wished to create a detailed database and so carefully reviewed all patient records in order to give as accurate a diagnosis at time of review as possible. The breakdown of diagnoses in the OND group are shown in figure 5.1.

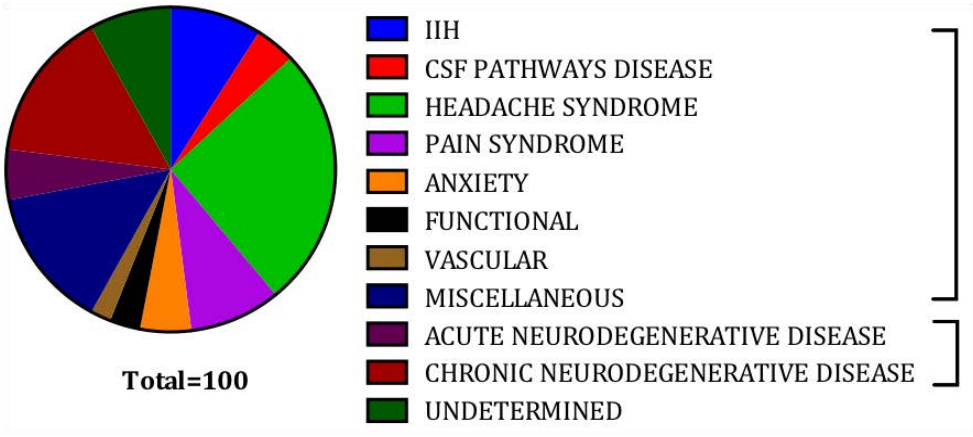

Figure 5.1. Diagnoses comprising 'other neurological diseases' (OND), n=100. OND-control (OND-C) refers to patients with non-degenerative disease and OND-D includes patients with ongoing degenerative disease.

Where indicated, extensive diagnostic work-up with clinical/ structural (brain+/-spinal MRI)/ laboratory/ functional (EEG/EMG) tests were carried out before the majority of patients were given a diagnosis of headache syndrome comprising both tension and migrainous headache, or else pain, anxiety or functional syndromes. 'Vascular' diagnoses comprised samples collected many months after the initial insult, but whose symptoms were in keeping with chronic sequelae from this. The miscellaneous group included diagnoses such as fibromyalgia, chronic fatigue syndrome, vasovagal syncope and convergent spasm. 'CSF pathways disease' collectively referred to patients whose CSF was collected by the neurosurgical team for therapeutic drainage to manage symptoms relating to syringes. These subgroups of patients are referred to collectively as 'OND-control' or OND-C in the NfL analyses, as it was important to differentitate between degenerative and non-degenerative patient groups (see NfL section 5.3.2), given the knowledge that NfL levels are increased in some neurodegenerative diseases. Excluding IIH, these patients were likely to be as close to 'normal' CSF as possible, although they would not be classified as 'healthy controls'. The 'acute degenerative' subgroup comprised motor neurone

disease (n=1), rapidly progressive presentation of normal pressure hydrocephalus (n=1), subacute compressive spinal disease +/- myelopathy (n=2) and multiple system atrophy (n=1). Chronic neurodegenerative diseases included hereditary disorders such as Friedrich's ataxia, Charcot-Marie tooth disease and other long-standing conditions such as axonal neuropathy secondary to previous chemotherapy use, or cervical spondylitic lesions. The degenerative diagnoses were collectively referred to as 'OND-degenerative' (OND-D) for the reasons outlined above.

Patients categorised with 'undetermined' diagnoses were designated thus due to (i) the prospective nature of the data collection i.e. insufficient evidence was available in order to make a firm diagnosis by the referring/ reviewing clinicians at the time when the diagnostic classifications for this study were being generated and (ii) some patients moved away or were lost to follow-up at the local hospital, prematurely curtailing a full diagnostic work-up.

ONID diagnoses comprised anti-phospholipid syndrome (n=1), Behcet's disease (n=2), inflammatory neuropathy (n=4), Compressive myelitis (n=2), Neuroretinitis (n=1), Sjogren's syndrome (n=1), idiopathic transverse myelitis (n=3), aseptic meningitis (n=1) and Neurosarcoid (n=3).

5.4.2 Data management

Given the number of patients included in the study, a systematic approach was adopted to establish data integrity. In line with national guidelines, all data collected through the HBRC was anonymised, and a unique set of codes (total=7) were assigned to each patient, corresponding to serum (x1), EDTA blood (x5) and CSF (x1) samples. Patient information was accessed via the Clinical Portal system

of University Hospital Birmingham or if obtained from peripheral hospitals, any correspondence regarding patient data was obtained using anonymised codes, via 'NHS.net' or secure local hospital email addresses. If patients' care was not based at UHB, MR imaging from peripheral hospitals was transferred over to the UHB 'PACS' system in order to centralise access. Data on patient names, hospital numbers and clinical information was carefully filed and stored in a locked office in the Centre for Translational Inflammation Research, which nominated clinical assessors (GHS and MD) were able to access. Datasets using the anonymised patient identifiers were compiled on excel spread-sheets.

5.4.3 Preparation of CSF and serum

Samples were prepared as outlined in the methods section in Appendix 1.

Samples were also analysed for cell counts, protein and glucose concentrations and oligoclonal band (OCB) status as part of the clinical laboratory diagnostic work-up. Cell counts were analysed in the clinical laboratories by experienced technicians using accepted clinical laboratory protocols. In brief, this comprised adding two drops of well-mixed CSF to a tube containing 0.1% toluidine blue solution. The sample was left for 1 minute to reconstitute with the stain. Capillary action was then used to introduce the sample to fill the Kova Glassitic Slide-10 counting chamber, without introducing bubbles. The number of polymorphonuclear, mononuclear and red blood cells were counted by eye using the guide shown in figure 5.2, multiplying the final count by the dilution factor if this had been necessary.

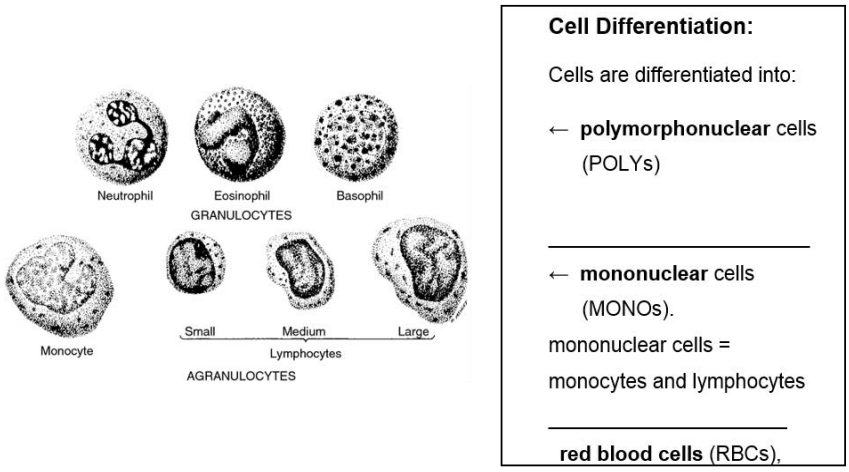

Figure 5.2. Cell differentiation guide (Clinical Microbiology laboratories, University Hospital Birmingham (UHB)). Reproduced from documentation kindly provided by Yvonne Brocklehurst- Senior laboratory manager, Microbiology department, UHB.

5.4.4 Analytical procedures

5.4.4.1 Nephelometric free light-chain (FLC) quantification

The methods for this part of the chapter are detailed in Appendix 1.

5.4.4.2 Neurofilament-light (NfL) quantification.

NfL (predominantly unphosphorylated form) was measured by quantitative enzyme-linked immunosorbance assay (ELISA), purchased commercially from Uman Diagnostics (Umeå, Sweden, lot #*70189*) on a total of 117 samples. Assays were performed on the same day using carefully designed 96-well plate schemata in order to include control and index samples on each plate to account for batch-to-batch variability. All standards, samples and positive controls were thawed on ice on the day of the assay and analysed in duplicate. The intra-assay and inter-assay variability were determined to be <6% and <9% respectively. The detection level for the kit is set at 31ng/L, defined as the mean of blank samples+2SD. The assay was performed as outlined in General Methods, chapter 2, according to

manufacturer's instructions and using digital multichannel pipettes to minimise pipetting error.

5.4.4.3 HMGB1 quantification

HMGB1 was measured in 117 samples by quantitative enzyme-linked immunosorbance assay (ELISA), purchased commercially from IBL International (Hamburg, Germany). Assays were performed on the same day and all samples thawed on ice on the day of the assay as above. As the assay is designed for analysis of serum samples, we used the 'high-sensitivity' standard curve analysis option, given the likelihood of low HMGB1 levels in the CSF of this cohort of patients. The intra- and inter-assay variability using the high sensitive range were determined to be 3.2-10.2% and 1.3-10.7% respectively. The detection limit or analytical sensitivity for the high-sensitivity assay is set at 0.2ng/mL, whilst the limit of quantification i.e. the functional sensitivity is set to 0.1ng/ml.

5.5 Statistical Analysis

Data were analysed using GraphPad Prism 5 (GraphPad Software Inc., CA, USA). Non-parametric analyses were used and data represented as medians, with multiple comparisons performed using a Kruskal-Wallis test with Dunn's post-hoc correction. Two-group comparisons were performed using a Mann-Whitney *U* test for unpaired continuous measures. Spearman's rank correlation coefficient was used to evaluate the statistical dependency of two variables

5.6 Results

5.6.1 Free-light chain levels are elevated in the CSF of MS patients but not in other inflammatory/non-inflammatory neurological diseases

The results from this section of work are presented within the paper attached to the Appendix, section 1 as described earlier.

5.6.2 Neurofilament light chain levels in the CSF from patients with different neurological diseases

For the purposes of this analysis, the OND group was subdivided into OND-Control (OND-C) and OND-degenerative (OND-D). The OND-C group comprised patients with a diagnosis of headache disorder, CSF pathways disease, IIH, pain syndrome, anxiety, functional and miscellaneous groups. The latter group was included as none of the patients in this group had evidence of degenerative disease. The OND-D group represented patients with diagnoses of chronic or acute neurodegenerative diseases as described in section 5.4.1. Median values and range are presented in table 5.2.

Patient group	NfL levels, median (ng/ml) (range)
CIS*	1362 (664-10000)
PP-MS	1389 (1028-3235)
RR-MS	2475 (1014-10000)
ONID	1400 (487-4902)
OND-C	905 (262-1912)
OND-D	1628 (613-10000)

Table 5.2. Comparson of median and range of NfL values in different patient groups. **CIS, clinically isolated syndrome; PPMS, primary-progressive MS; RRMS, relapsing-remitting MS; OND-C, other neurological disease (OND)- OND-control; OND-D, other neurological disease (OND)- OND- degenerative; ONID, other neurological inflammatory disease*.

Neurofilament levels were increased in all MS groups compared to the OND-C but not the OND-D patient groups, as shown in figure 5.3 and table 5.2. This was most

apparent when comparing the RRMS vs OND-C group (p<0.0001) and the CIS vs OND-C (p=0.003), whilst comparison between PPMS vs OND-C did not reach statistical significance (p=0.05). This difference primarily reflects median values between the groups, and levels were highest in the RRMS group as compared to CIS and PPMS patients. PPMS median values showed the tightest range, whilst the OND-D group demonstrated the largest.

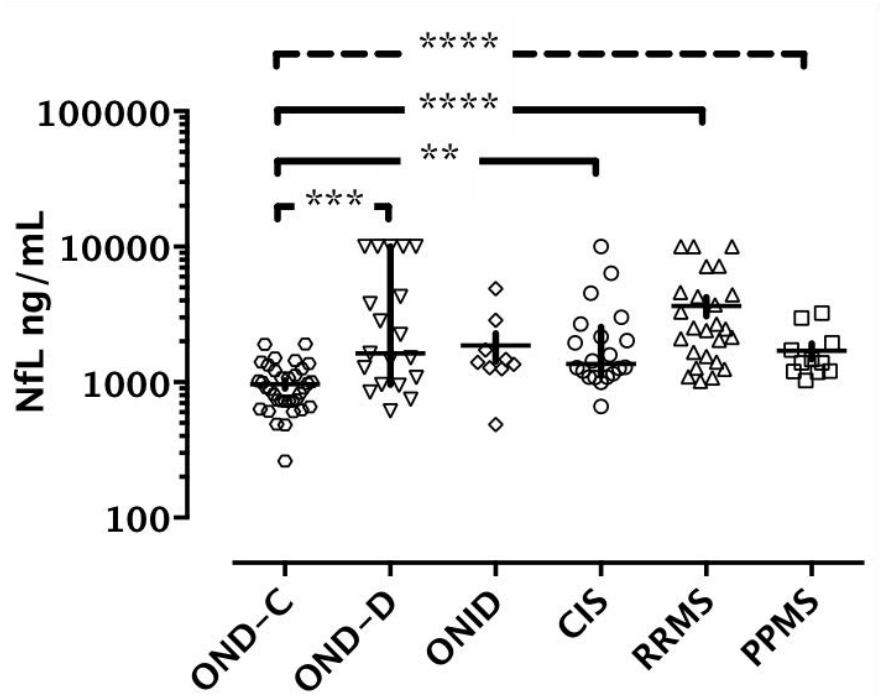

Figure 5.3 Neurofilament-light (NfL) levels are elevated in the cerebrospinal fluid (CSF) in patients with MS and degenerative diseases. Non-inflammatory and non-degenerative CSF samples (OND-C), showed the lowest NfL levels. *CIS, clinically isolated syndrome; RRMS, relapsing-remitting MS; PPMS, primary progressive MS; OND, other neurological disease; OND-C, OND-control; OND-D, OND-degenerative; ONID, other neurological inflammatory disease. Statistical analysis: Kruskall-Wallis multiple group comparison with Dunn's post-test; **p<0.003; ***p<0.0005; ****p<0.0001. All other comparisons were not significant.*

After the RRMS group, median values were highest in the OND-D then ONID groups. However differences between the ONID and the other groups failed to reach significance despite this, and may reflect either similar median values such

as in the PPMS group or else higher absolute values in the other groups over a wider range. The OND-D groups comprised patients with chronic and acute neurogenerative diseases. Within this group there was a significant difference between median values, with higher values in the acute degenerative group ($p<0.005$). Sub-group comparison revealed that median NfL levels were not significantly different between RRMS patients- with the highest median values- and OND-D patients.

Age is thought to influence NfL detection and a mild-moderate positive correlation of neurofilament levels with age when including all patients was observed ($r=0.29$; $p=0.002$), shown in table 4.5. Sub-group analysis in order to consider the correlation with age in the MS patients alone removed this association ($r=-0.07$; $p=0.61$), whereas when considering the OND group as a whole, a strong correlation was demonstrated, with a corresponding increase in its statistical significance ($r=0.71$; $p<0.0001$).

NfL is thought to represent degenerative processes in the CNS, and given the importance of understanding how these may interact with inflammation in MS, we also sought to correlate NfL levels from the whole cohort with a variety of indices representing different aspects of inflammation. Lymphocyte concentration/ml as determined by FACS analysis showed a strong correlation with cell count as determined by clinical laboratory analysis ($r=0.63$; $p<0.0001$) (data not shown). However, although increasing lymphocyte count/ml was mildly correlated ($r=0.25$; $p=0.01$), total cell count measured by lab analysis and encompassing all types of inflammatory cells, was better correlated with increasing NfL levels ($r=0.33$; $p=0.0003$).

As described previously, protein measurements in the CSF are important as they may indicate endothelial barrier breakdown, allowing more protein to enter the otherwise tightly controlled CNS, and we found that levels were moderately correlated with NfL values (r=0.37; 0.0001). Finally, a novel correlation was identified between kappa and lambda free light chains and NfL (r=0.29; p=0.003 and r=0.38; p<0.0001 respectively). This was further enhanced by the removal of the 'acute degenerative' subgroup of patients, who had outlying levels of NfL (see brackets in table 5.3), on the basis that they are likely to demonstrate increased NfL levels according to current literature, but are unlikely to demonstrate increased FLC thus potentially biasing any association. Whilst this artificial analysis has some limitations, the strength of association for both κ and λ FLC and their statistical significance (r=0.38; p=0.0001 and r=0.49; p<0.0001 respectively) were increased.

Variable	Correlation coefficient I	p-value
Age: overall*	0.29	0.002
Lymphocyte count/ml	0.25	0.01
Cell count/ ml	0.33	0.0003
Protein level (g/l)	0.37	0.0001
kFLC	0.29 (0.38)	0.003 (0.0001)
λFLC	0.38 (0.49)	<0.0001 (<0.0001)

Table 5.3. Correlation of NfL levels with demographic and inflammatory data. * A subgroup analysis for age (MS vs non-MS) was also performed, see text. Statistical analysis: Spearman's rank correlation.

5.6.3 HMGB1 levels are elevated in the CSF of CIS and ONID patients compared to other patient groups.

CSF HMGB1 levels were undetectable using this assay in a number of patients, as shown in table 5.6, when using the minimum requirement of the blank standard as a cut-off for presence of HMGB1. In all plates, the equivalent OD of the blank equated to a mean of 116pg/ml, similar to the manufacturer's 'functional sensitivity' i.e. limit of quantification of 100pg/ml. The patients with levels consistently above the level of detection were the CIS and ONID groups, and this reflects their higher median levels compared to the other groups as shown in table and figure 5.4.

Patient group	Patients with detectable* HMGB1 levels (%)	Detectable HMGB1 levels, median (pg/ml) (range)
CIS	90	243 (148-518)
PP-MS	73	221 (151-1131)
RR-MS	84	193 (142-5216)
OND	75	179 (105-461)
ONID	100	267 (237-467)

Table 5.4. Comparison of patients with detectable levels of HMGB1 levels (pg/ml) in patient groups, in addition to median values and range in those with detectable levels. *detectable defined as >116pg/ml. *CIS, clinically isolated syndrome; PPMS, primary-progressive MS; RRMS, relapsing-remitting MS; OND, other neurological disease (OND); ONID, other neurological inflammatory disease.*

Comparison of HMGB1 levels between patient groups revealed increased levels in patients with RRMS and ONID patients when compared with OND patients, as seen in figures 5.8 A and B., There was a marginally higher statistical significance in RRMS vs OND (0.01) than in ONID vs OND (0.02), although both comparisons were weakly significant. All other comparisons including between CIS and ONID, and when examining OND subgroups (OND-C and OND-D- see 5.3.1) and MS or ONID groups (data not shown), were not statistically different.

Analysis of correlation between HMGB1 levels and total cell count showed a mild association which was statistically significant (r=0.25; p=0.0085), whilst correlation with lymphocyte count showed a weak association, which was not statistically significant (p=0.05; data not shown). Correlation with any other variable did not reach statistical significance.

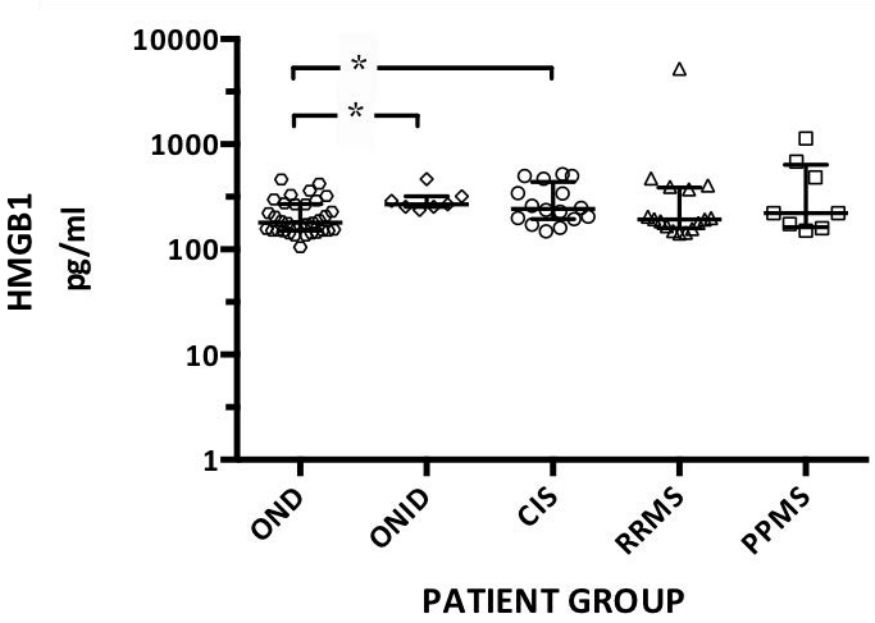

Figure 5.4. HMGB1 levels (pg/ml) are increased in both clinically isolated syndrome (CIS) and other neurological inflammatory diseases (ONID) compared to other neurological disease (OND) patient groups. Median values were highest in CIS and ONID patients. *Statistical analysis: Mann-Whitney U test. *p<0.05*

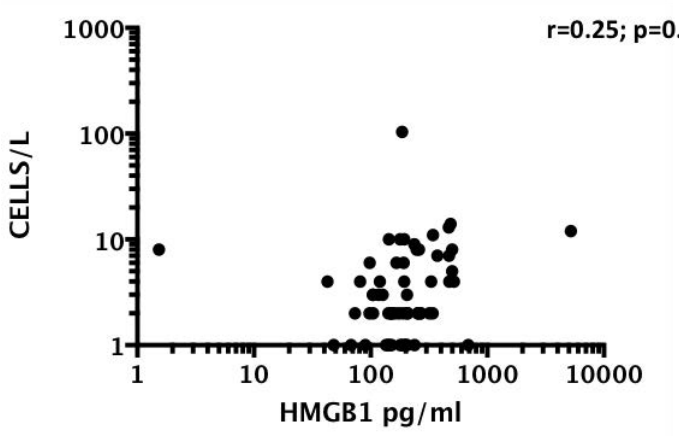

Figure 5.5 HMGB1 levels (pg/ml) showed a positive correlation with cerebrospinal fluid (CSF) cell count/ l, which was statistically significant. *Statistical analysis: Spearman's correlation.*

5.7 Discussion

Particular strengths of this chapter relate to the collection of a large cohort of carefully diagnosed patients, resulting in clearly delineated patient groups. This enabled us to examine subgroups of patients and explore correlations which have not been performed before. Below I have discussed the results of the three main components of this chapter, namely CSF analysis of FLC, NfL and HMGB1 levels.

5.7.1 Measurement of CSF kappa free light chain levels alone is a sensitive and specific diagnostic marker for patients with MS, and does not require blood/ CSF index measurements.

The FLC findings have been discussed in the attached paper in Appendix 1, and can be read in conjunction with this section of the thesis. An additional point of discussion outlined below relating to further characterisation of an outlying FLC-negative MS patient is described.

One outlying RRMS patient had previously been treated with natalizumab a month prior to CSF sampling and showed marked suppression of FLC levels, a finding

which has been reported with NfL levels whilst on the drug, but not FLC levels (Gunnarsson et al. 2011). This suggests that natalizumab may alter B-cell function, given that FLC levels had not started to rise despite being off the drug for one month. This is in accordance with a previously published report which found that OCBs 'disappeared' in a proportion of natalizumab-treated patients who had initial and follow-up LPs undertaken for the same reason as in our patient, to rule out PML (von Glehn et al. 2012). A larger series of 76 patients treated with natalizumab went on to find that 16% of previously OCB-positive patients became negative following treatment, and the proportion of patients with an intrathecal synthesized fraction in the normal range increased from 20 to 45% (Harrer et al. 2013). Of particular interest, this patient's OCB status was negative at the time of diagnosis and was not re-sent with this LP. His MS was previously highly aggressive, necessitating a brain biopsy at diagnosis due to the fulminant clinical presentation. His disease progression, however, was ultimately stabilised by early natalizumab therapy, which he received as soon as the biopsy results demonstrated demyelinating disease, and when he was still technically a CIS patient. Given the superiority of FLC analysis and the ease with which the assay can be performed over OCB analysis, it would be interesting to include FLC levels as an outcome measure in natalizumab-related clinical trials in particular.

5.7.2 CSF NfL levels are increased in MS patients, and correlate with λFLC

We have shown that CSF NfL levels are increased in patients with all subtypes of MS, particularly RRMS and CIS. The difference was most marked when comparing RRMS vs. patients with non-degenerative OND. The absolute levels of NfL in our cohort of patients is in keeping with the published literature, but are higher in the

MS subgroups, considering most are in remission. Without a perfect biomarker for disease, clinical diagnosis and classification cannot be correct 100% of the time, but our diagnostic grouping was a rigorous process, and we sought to make every effort to accurately classify all disease groups and sub-groups. This may be reflective of the high proportion of OCB+ patients in the MS groups, as higher NfL levels have been shown to correlate with OCB status. (Norgren et al. 2003).

As described in section 4.1, several studies have shown increased NfL levels in the CSF of patients with all MS subgroups (Malmeström et al. 2003; Lycke et al. 1998; Norgren et al. 2003; Teunissen et al. 2009). Patients relapsing have up to 10-fold higher levels than those in remission although levels overall were higher in RRMS patients vs healthy controls (Malmeström et al. 2003). Our cohort of patients were predominantly in remission, and we also found NfL levels were increased when comparing MS patients with the OND-C group. The latter is likely to have included patients with levels close to the healthy controls, given the normality of their investigations.

NfL concentrations in MS patients have also been found to be independent of age and can be either high or low with increasing age (Khademi et al. 2013) (Khalil et al. 2013). In accordance with this, we did not find a correlation with age in the MS group either. However, we found a strong correlation between age and NfL in the OND group, as also reported previously (Khalil et al. 2013), and probably reflects ongoing neurodegeneration in normally aging subjects. It also highlights the likely 'normality' of our OND control group.

NfL levels in patients with ONID were also high, although this did not reach statistical significance when comparing other groups. This may be due to our relatively small cohort and thus may not be able to detect true differences. Another possible explanation would be that the type of axonal damage occurring in MS is more diffuse, thus enabling higher absolute levels as the acute inflammatory damage occurring in active lesions is superimposed upon this aberrant background, which may not be as marked in ONID cases.

However, increased NfL levels have been reported in other CNS inflammatory disorders, notably SLE (Trysberg et al. 2003), cerebral vasculitis (Nylén et al. 2002) and paediatric opsoclonus-myoclonus syndrome (Pranzatelli et al. 2014). In the Trysberg paper, 4 of the 'other inflammatory neurological disease' group of patients were defined as having demyelinating disease, but comparative data between the groups was not presented or commented upon. Similarly, data directly comparing non-MS inflammatory neurological diseases with MS patients is relatively sparse, considering the implications this has on interpreting the sensitivity and specificity of the test. One early study demonstrated lower NfL levels in patients with ONID compared to MS patients, but they also found that levels were greatest in patients with progressive disease vs earlier in the disease course, in RRMS patients (Semra et al. 2002). The latter findings in particular have not been replicated and may be related to use of different ELISA methods or indeed differences in disease activity in the patients studied, leading to differential phosphorylation of the NfL proteins and hence detectable levels.

Of particular interest is the moderately positive correlation between CSF pleiocytosis and NfL levels. This has been reported previously (Khalil et al. 2013;

Norgren et al. 2003; Norgren et al. 2004), and highlights the important link between NfL levels i.e. acute axonal injury and inflammatory disease activity. The fact that this relationship is maintained in patients who are not actively relapsing underlines the ongoing nature of disease activity in MS, irrespective of relapses. Interestingly, the lymphocyte count as determined by sensitive FACS analysis, was less strongly correlated than the total cell count as reported in the laboratory indices (see figure 5.2). This may be related to the limited range of cell numbers in the laboratory counts, inadvertently skewing the association. On the other hand, they may represent a genuine biological difference, with monocytes, e.g. macrophages, contributing more to the correlation than lymphocytes alone.

Other notable correlations with NfL levels included increased CSF protein, again reflecting its relevance in the active stage of the disease, with breach of the CNS endothelium in the context of active inflammation. As before, the fact that the majority of patients were not relapsing is of interest although due to relatively low clearance, accumulated protein during previous relapses may take some time to clear. This association has been noted before (Khalil et al. 2013), although not in other reports (Norgren et al. 2003; Norgren et al. 2004). Variations in local laboratory analysis may account for some of this discrepancy, and again heterogenous patient cohorts are likely to contribute.

A novel finding from this part of the study has been the observation of an association between FLC and NfL. The correlation is stronger with λFLC levels, suggesting that NfL may reflect processes occurring slightly later in the disease course, possibly when inflammation-related damage is peaking.

The relationship between these two important biomarkers has not been fully explored. Interestingly, the outlying RRMS patient whose FLC levels were not detectable and who had previously been taking natalizumab one month earlier, demonstrated persistently elevated NfL levels (4602.44ng/ml). The reduction in NfL levels has been reported to occur 6 months after natalizumab therapy is commenced (Gunnarsson et al. 2011) thus at one month off treatment, it is possible that CSF levels were already climbing back up, in a patient who was known to have an aggressive disease phenotype, as described in Chapter 3 and earlier in this chapter (5.4.1). A recent open-label study also found that NfL levels decreased following natalizumab therapy over 60 weeks follow-up in a small cohort of patients with progressive MS, along with levels of osteopontin and other inflammatory markers (Romme Christensen et al. 2014). However, the potential dissociation of the sustained inflammatory suppression in this one patient, as shown by persistently suppressed FLC levels but continuing neurodegeneration, is informative. Clearly, these observations require replication in a larger cohort but generate interesting questions nonetheless.

Although FLC levels have not been considered in relation to NfL, another mediator thought to reflect B-cell pathology, CXCL13 has been examined in this context in optic neuritis patients (Modvig et al. 2013). However, no correlation was seen in this group of MS patients, and may reflect the patient cohort at an early stage of MS (optic neuritis). In addition it also potentially highlights different aspects of B-cell pathology as CXCL13 is chemotactic for B cells, whereas FLC are specific to antibody-secreting B-cells. Thus, understanding the relationship between FLC and NfL may be more instructive in furthering our understanding of disease

mechanisms, as it may shed light on the relationship between neurodegeneration and B-cell mediated inflammation.

The final point of interest is the finding of greatly elevated NfL levels in patients with 'acute' neurodegenerative disease. The findings are not novel, with motor neurone disease, normal pressure hydrocephalus and multiple system atrophy (MSA) all demonstrating high levels of NfL (Norgren et al. 2003; Rosengren et al. 1996; Rosengren et al. 2002; Tortelli et al. 2012; Tortelli et al. 2014; Pyykkö et al. 2014; Jeppsson et al. 2013). The latter is particularly interesting, as higher levels are observed in MSA and progressive supranuclear palsy (PSP) than in the classical extrapyramidal disorder Parkinson's disease (PD), and are thought to be due to the extensive deposition of aggregrates throughout the putamen, pallidum, pyramids and tracts, brainstem, cerebellum and spinal cord, rather than the restricted striato-nigral pathway located deep within the brain tissue, which is predominantly affected in PD. The high levels in ALS are also thought to reflect the large diameter and extended axons of the pyramidal tract, where neurodegenerative changes unsurprisingly liberate large quantities of NfL. There is relatively less data on NfL levels in cases of cervical compression leading to myelopathy, but it is expected that levels would be elevated in this context also.

Thus the observation that FLC levels correlated with NfL level suggests that inflammation and neurodegeneration may occur in concert from the earliest stages of MS and are not necessarily directly linked to relapse status.

5.7.3 CSF HMGB1 levels are elevated in both CIS patients and in other inflammatory neurological diseases, compared to non-inflammatory control subjects

We found increased HMGB1 levels in the CSF of patients with CIS and ONID as compared to OND. This implicates HMGB1 in the earlier phase of MS. However, there were methodological issues when analysing the ELISA results, mainly attributable to the poor sensitivity of the assay at the lower levels of detection. On the other hand, our findings were consistent with the guidance from the manufacturers, as we also found that the lower limit of detection was approximately 100pg/ml. This ELISA is the only assay currently available for quantitative measurement of HMGB1 protein levels in body fluids. It states itself that it is designed for measurement of HMGB1 levels in serum, cell culture supernatants and BALF, and that assessment of levels in other body fluids would need be interpreted carefully in light of this. Accordingly, the majority of reports have concentrated on measurement of HMGB1 using the IBL-International ELISA, in the plasma (Ito et al. 2011; Sapojnikova et al. 2014). However, there are increasing reports in the CSF also, as shown in table 5.5.

Neurological disorder	**Findings**	**Reference**
H1N1-related encephalopathy	High levels of serum, not CSF HMGB1 correlate with poor outcome	(Momonaka et al. 2014)
Paediatric TBI	High levels of CSF HMGB1 correlate with poor outcome	(Au et al. 2012)
Post-cardiac arrest	High levels of CSF, not serum HMGB1 correlate with poor outcome	(Oda et al. 2012)
Canine encephalitis	HMGB1 detected in CSF of encephalitic dogs	(Miyasho et al. 2011)
Encephalopathy, meningitis, non-CNS febrile controls	High levels of CSF HMGB1 in patients with bacterial/ aseptic meningitis but not encephalitis	(Asano et al. 2011)
SAH	High levels of CSF HMGB1 correlate with poor outcome	(Nakahara et al. 2009)

Table 5.5. Studies reporting CSF HMGB1 levels using the IBL-International ELISA assay in different neurological disorders.

The most promising current use of the assay is its utility in identifying cases and prognosis of bacterial meningitis (Asano et al. 2011), and this is supported by

western blotting analysis of CSF HMGB1 levels also (Höhne et al. 2013b). Other reports have identified its potential importance as a prognostic marker in other diseases (Momonaka et al. 2014; Au et al. 2012; Oda et al. 2012; Nakahara et al. 2009). Interestingly, the recent study by Momonaka et al reported that serum HMGB1 levels were most useful as a prognostic marker in encephalopathy, whereas outcome following successful resuscitation following cardiac arrest is best predicted using CSF HMGB1 levels, rather than serum. The former may reflect the accepted role of HMGB1 in the systemic inflammatory response (Wang et al. 1999), whereas the latter may reflect the profound neurodegenerative sequelae of cardiac arrest. Identification of HMGB1 in the CSF of MS patients was originally identified by Andersson et al, who performed western blotting analysis on ultrafiltrated CSF samples from 2 MS patients and 2 controls and found increased expression in the former (Andersson et al. 2008). Since then, quantitative determination of HMGB1 levels using the IBL-International ELISA in MS patients have only recently been reported in the literature and are summarised in table 5.6.

Study	**Plasma/ CSF**	**HMGB1 levels (ng/ml)**			**Reference**
		MS	***NMO***	***Control***	
1	Plasma/ CSF	NA	ND	NA	(Glasnović et al. 2014)

2	Plasma	1.33*	3.99*	ND	(Wang et al. 2012)
3	**CSF**	**1.9 ± 1.26**	**2.34± 1.29***	**1.26 ± 0.49***	(Wang et al. 2013)
4	Plasma	2.94 ± 2.78	2.65± 3.91	1.55 ± 2.07	(Akiyuki Uzawa et al. 2013)
	CSF	**1.43 ± 0.82**	**3.56± 3.76**	**0.85 ± 0.21**	

Table 5.6. Studies reporting HMGB1 levels using the IBL-International ELISA assay in MS and NMO/ control patients. The source fluid (plasma and/ or CSF) in which HMGB1 levels were measured is highlighted in column one. If absolute HMGB1 levels were reported, this is also shown and describes mean values apart from study (1), which reports median values. CSF levels are shown in bold. *indicates significant difference between patient groups as highlighted by asterisk. *NA- not available. ND- analysis not performed.*

Wang et al examined plasma HMGB1 levels in remission-phase MS (n=20) and neuromyelitis optica (NMO) (n=29) patients but did not include a control group (Wang et al. 2012). They found that levels were significantly higher in the NMO group than in the MS patients, whilst univariate logistic regression analysis showed a significant association of HMGB1 levels with NMO diagnosis. Despite the relatively small sample size, they used an HMGB1 cut-off of ≥2 ng/ml to generate a sensitivity of 89.7% and specificity of 95.0% for the diagnosis of NMO over MS. This may have a clinical application as although the initial presentation is often very similar, the management and prognosis of these two diagnoses is very different, thus any discriminatory investigations are of great use.

Another group then repeated this patient group comparison but using CSF, and found no significant difference in HMGB1 levels between MS and NMO patients (Wang et al. 2013). However, NMO levels were significantly higher vs. control (non-inflammatory neurological disease) samples, although MS levels were not. Of note, the MS/ NMO patients included in this study were actively relapsing, but had not received any immunosuppression at the time of sampling. This may explain why the absolute levels are relatively high compared to our cohort,

although it is interesting to note that the controls (ALS (n = 2), MSA (n= 3), sciatica (n = 4), and cervical spondylosis (n = 5)) themselves had relatively high levels of HMGB1 (see table 5.8). We did not see any association between HMGB1 level and these diagnoses (as represented by the acute and chronic degenerative subgroups in our cohort) although there may be variation in clinical presentation which might account for these differences.

A third group has also examined HMGB1 levels using the ELISA, but in both plasma and CSF and comparing MS/ NMO groups with a non-inflammatory control group (ALS n=11, spinocerebellar degeneration n=10, PD n=5 and PSP n=4). Again, all the MS/ NMO patients were relapsing and had not received acute treatment at time of sampling, although 30% of the MS patients were on DMT or oral prednisolone (dose not specified). In addition, there appeared to be considerable clinical heterogeneity within the groups, with a median EDSS score of 6.8 for the NMO (range: 1.5-9.0) and 3.5 (range 1.0-7.5) for the RRMS patients. They found that NMO patients had higher HMGB1 levels than both MS and control patients ($p<0.001$ in both cases). They also found that MS patients had higher serum ($p=0.002$) and CSF ($p<0.001$) values vs. control patients, although once again the latter had a high mean value of 0.85 ± 0.21ng/ml. Similar to our findings, they also found a positive correlation between cell counts and HMGB1 levels, although demonstrated a stronger association ($r=0.8$; $p<0.01$), perhaps due to the fact that the patients were actively relapsing in this cohort. The high CSF HMGB1 levels in relapsing NMO patients also had evidence of severe blood-brain barrier disruption, with corresponding increases in CSF protein and Qalb and correlating with the CSF cell count, thus facilitating access of anti-AQP4 antibodies to astrocytes (Akiyuki Uzawa et al. 2013). The difference in HMGB1 levels in NMO vs

MS were attributed primarily to the fulminance of this inflammatory reaction, which is usually more severe in NMO. In addition, they postulated that another source of HMGB1 release would be during cell death processes, either via apoptosis or necrosis. The positive correlation between CSF GFAP and HMGB1 suggested that astroctyes may provide this, given their known derangement in this condition (Howe et al. 2014). In keeping with our findings and others (Andersson et al. 2008), HMGB1 expression in astrocytes is less marked in the context of MS and would explain why they are unlikely to contribute to CSF levels compared to NMO.

The fourth and final study is a recent report by Glasnovic et al (Glasnović et al. 2014). They describe no difference in CSF HMGB1 levels between MS patients and control subjects. The patients had RRMS (2010 McDonald criteria), with a mean EDSS of 3.0±0.7 suggesting a reasonable degree of disability given they were described at 'disease onset'. They state that samples were taken '..during the diagnostic procedure at the disease onset..' and before receiving any immunosuppressive or immunomodulatory treatment. It is not clear how long the patients had been symptomatic, or indeed whether they were relapsing at time of CSF sampling. The control group had been taken from patients undergoing epidural anaesthesia prior to lower extremity surgery, although no detail is given of co-morbidities in this group. The data is presented graphically and whilst the absolute values are therefore not available for review, the median values seem to be lower in both control and MS patient groups compared to previous reports. The authors report that this is the first investigation of CSF HMGB1 levels in MS patients at 'clinical onset '. Our group of non-relapsing CIS patients represents an even earlier time-point in the disease course, and this is where we found the

difference between patients and controls. In accordance with the correlation with cell count, this supports the notion that HMGB1 is secreted by monocytes, including macrophages (Andersson et al. 2008). These are present in greater number during the early phase of the disease when inflammation dominates as well as during relapses, as shown by the reports presented above and in the biopsy findings as discussed in chapter 3.

The possibility that other cell types may be releasing HMGB1 bears consideration. Unlike NMO, this is unlikely to be from astrocytes in MS, as shown in previous studies (Andersson et al. 2008) and in our own work as shown in Chapter 3 and 4. Given the profound neuropathological changes in neuronal cells observed in the earlier chapters, it is possible that dying or damaged neurones may also be releasing HMGB1 into the CSF.

This is of particular interest when considering the high values of some the 'control' groups as described earlier, and may reflect the fact that many of these cases had profound neurodegenerative disease e.g. ALS. It is conceivable that HMGB1 is released from either inflammatory cells involved in ALS pathogenesis, or else from dying neurones themselves, with parenchymal HMGB1 finding its way to the CSF as described earlier (Hwang et al. 2013; Casula et al. 2011). Our OND group represented a larger cohort than these other studies, with a greater number of non-degenerative cases. Whilst sub-group analysis did not show any significant differences between degenerative and non-degenerative cases, it may still be underpowered to detect any differences, especially as they are likely to be relatively small. Certainly, the levels measured in these studies is far lower than the values generated in trauma or SAH for example.

Of note, none of these studies have included an 'inflammatory' neurological disease group, other than MS or NMO, which is surprising given the clear association between inflammatory cell count and HMGB1 levels. We actively sought to identify this group and found a statistically significant increase in CSF HMGB1 levels in this group within a relatively narrow range. This again may reflect the contribution of inflammatory cells in the generation of extracellular HMGB1, and indicates that CSF levels are not specific for MS.

5.8 Limitations of CSF study

The clinical cohort is heterogenous but carefully categorised, therefore will serve as an important resource for future studies also. However, the cross-sectional nature of the study is a limitation and further clinical outcome data would have been useful in order to allow prognostication in some of the patient groups. This will be done in the future as sufficient time has elapsed since the first recruited patients. In addition, further clinical data would have been helpful such as EDSS but this was not performed either in the initial consultation prior to LP or at time of LP as most patients had not been diagnosed with demyelinating disorder at point of sampling. This is related to the design of the study where patients were referred by Neurologists, usually from peripheral hospitals to UHB, and diagnosis of MS made at subsequent clinic visits. In addition, the relatively small numbers in some of the groups eg ONID and PPMS made it difficult to perform meaningful statistical analyses in some instances.

The HMGB1 assay in particular had limitations when examining CSF levels in these patient groups. These include poor sensitivity of the assay at low HMGB1 concentrations, which was relevant for many of the cases (table 5.6). It would be

worthwhile generating a standard curve with extra values at lower concentrations, in order to confirm accuracy of interpolated values. As it stands, , the HMGB1 ELISA assay is not optimised for measuring the relatively low concentrations in the CSF.

In addition, since the assay was developed, the field of HMGB1 research has moved on a great deal and amount of HMGB1 as a stand-alone molecule is less informative than its modified self. Redox state, acetylation, methylation and other post-translational modifications are critically important in understanding what function HMGB1 may be performing in this extracellular position. Thus, western blotting in order to detect acetylated protein, for example, would be worthwhile as it would demonstrate qualitative differences that are functionally more informative. One may postulate that the HMGB1 measured would be oxidised and acetylated, although this would need verification in future studies.

5.9 Summary

We collected a large, detailed cohort of CSF samples, which will serve as an excellent resource for future studies. Both FLC and NfL data demonstrated that the subjects are representative of MS and non-MS cohorts, due to similarity with published reports. Novel findings included identification of superiority of kFLC levels over OCB in detection of some MS cases, and was found to have a sensitivity of 96.2% and a specificity of 98.1% for diagnosing MS. In addition, unlike previous reports, we found that an index serum/CSF measurement was not required as specificity and sensitivity are maintained when evaluating levels of kFLC. A novel association between FLC and NfL was also observed, highlighting the possible association between B-cell mediated inflammation and degenerative processes in

MS. Finally, our efforts to investigate HMGB1 as a novel biomarker in MS demonstrated levels are indeed significantly increased in CIS vs OND control patients. However, levels were also significantly increased in the ONID patient group and positively correlated with cell count. This suggests that increased CSF HMGB1 levels may reflect inflammatory cell production rather than MS-specific pathological processes per se. In addition, the HMGB1 measured is not modified in any way, which we know has major implications in directing its function. Finally, the absolute levels measured were relatively low in this cohort, reflective of normal clinical practice as most LPs will not be performed during acute relapse. However, the assay is not designed to measure at these low CSF levels, so for all of these reasons, we would conclude that the HMGB1 ELISA is not optimised to be used as a biomarker in clinical management of MS patients, but it does provide useful data for research purposes.

6.

Exploration of the relationship between the LRRIg molecules and HMGB1 in MS

6.1 Introduction

The widespread increase in HMGB1 expression in MS patients demonstrated in the previous chapters adds to our understanding of the changes taking place

throughout brain tissue during the course of the disease process. The CSF studies detailed in Chapter 5 demonstrate that HMGB1 is elevated in the CSF of early MS vs. control patients and that levels correlate with inflammatory cell count, despite this being a non-relapsing cohort of patients. Thus, along with release from damaged cells, it may also be secreted by inflammatory cells and subsequently find its way to the extracellular space to exert pro-inflammatory functions as previously suggested (Andersson et al. 2008).

In addition, I have demonstrated increased HMGB1 expression in non-lesional regions compared to non_MS control patients. This raises the possibility that another facet of HMGB1 expression may reflect endogenous protective mechanisms in OGD. This is due in part to the large number of cells demonstrating increased expression of HMGB1, in addition to recent reports suggesting this function, although there is likely to be a delicate balance between protective and destructive function (T Zeis et al. 2009; Zeis et al. 2008; Bsibsi et al. 2013b).

As discussed in Chapter 1, the biology of HMGB1 is complex and its eventual function depends on both post-translational modification and sub-cellular localisation. Thus, a simple knock-down solution is unlikely to result in disease modification in MS, although it may be used in relapse akin to steroids, as suggested by others (Andersson et al. 2008; A Uzawa et al. 2013). My work suggests that HMGB1 may also serve as a 'flag' of disease activity, which we have shown takes place distal to the active lesions and involves CNS-resident cells.

Given that its expression and/or release can trigger a cascade of variable outcomes, in this final body of work we wished to take these observations forward using an in-vitro model to explore possible sequelae following HMGB1 stimulation

alongside other mediators. In addition, we focussed our attention on a novel family of CNS-enriched molecules associated with cell survival and function, some of which are linked to HMGB1, in an effort to hone in on more specific events linked to HMGB1 biology. These are the LRRIg molecules- AMIGO-1, -2 and -3 and LINGO-1. As discussed in Chapter 1, General introduction, AMIGO-1 and -2 have been shown to have important roles in neurite fasciculation, neuronal signalling and survival (Zhao et al. 2011; Kuja-Panula et al. 2003; Ono et al. 2003b; Peltola et al. 2011; Rabenau et al. 2004; Ono et al. 2009b), whilst AMIGO-3 and LINGO-1 both appear to bind to the NgR1, potentiating neurodegenerative pathways via RhoA activation (Mi et al. 2004; Ahmed et al. 2013).

As the most striking changes in HMGB1 expression described in chapters 3 and 4 were observed in OGD- a critically important cell in MS biology- we used the immortalised MO3.13 OGD-like cell line (McLaurin et al. 1995) in the first part of this chapter. This enabled us to model expression patterns of HMGB1 in response to pro-inflammatory and anti-inflammatory stimuli in this cell type, to simulate aspects of the micro-environment in the MS brain. We also explored the association between HMGB1 and the LRRIg molecules in this setting, in addition to examining whether other pro/anti-inflammatory cues influenced LRRIg expression. In the latter part of the chapter, we examined novel expression patterns of the AMIGO family of molecules using both autopsy and actively demyelinating, human biopsy tissue.

In summary, the purpose of this chapter of work was to examine potential downstream effectors of HMGB1 function and was primarily concerned with hypothesis generation

6.2 Hypotheses

1. HMGB1 influences expression of LINGO-1 and the AMIGO family of proteins.

2. AMIGO-1 and AMIGO-2 expression is reduced in a pro-inflammatory environment whereas AMIGO-3 and LINGO-1 expression is increased

6.3 Aims

1. To examine factors influencing the expression of HMGB1 in an in-vitro model using the immortalised MO3.13 OGD cell-line

2. To compare the impact of HMGB1 stimulation vs. other pro- and anti-inflammatory mediators on expression of LRRIg molecules in MO3.13 cells

3. To perform a novel investigation of LRRIg molecule expression patterns in human brain tissue, comparing non-inflamed control (non-MS) vs. MS patients

6.4 Methods

6.4.1 MO3.13 cell culture

The immortalised human-human hybrid cell line expressing phenotypic characteristics of primary oligodendrocytes was used in this chapter of work (McLaurin et al. 1995) and has been discussed in Chapter 2, General Methods. In brief, cells were cultured in high glucose formulation of DMEM supplemented with 10% Fetal Bovine Serum Gold, with added Pen/Strep (1X). Cells were maintained in 75cm^2 tissue-culture flasks (Greiner Bio-One, Frickenhausen,Germany) at 37^0C (humidified) with 5% CO_2 and passaged at 70% confluency. Approximately $5x10^5$ cells were added to each well in 6-well plates and left for 24h to allow adherence. Media was then replaced with low-serum DMEM, (0.5% serum) and left for a further 24h. Serum reduction was employed as it has been reported that this led to the expression of the mature oligodendrocyte marker (GST-π) in this cell line (Haq et al. 2003).

6.4.2 Cell culture treatments

A variety of pro-/anti-inflammatory treatments were used to stimulate the MO3.13 OGD-like cell line. HMGB1 was used for the first time and further background detailing its use in other cell types is given below. All cell culture treatments were stimulated for 24h and used at a standard concentration of 10ng/ml cytokine in low-serum DMEM (0.5%) apart from bvHMGB1 where we used a range of doses.

Baculoviral (bv) HMGB1

HMGB1 was identified as a potent proinflammatory mediator when applied exogenously (Wang 1999), but the original recombinant protein used in these studies was bacterially-derived from *E.Coli*. Further work compared this form of the protein to that derived following expression of the protein in a baculoviral system, producing a more pure form of the peptide (Parkkinen et al. 1993; Rouhiainen et al. 2007). They demonstrated that whilst the purified peptide isolated from eukaryotic cells can itself still elicit TNFα and nitric oxide production from mononuclear cells, the proinflammatory activity is much reduced when compared to HMGB1 produced from bacterially-produced HMGB1. This difference between baculoviral and bacterially-derived HMGB1 was explained by the fact that the HMGB1 molecule is well-known to avidly complex with other molecules, particularly the bacterially-derived lipophilic polypeptides present in *E.Coli*.

To consider the effects of HMGB1 itself as opposed to highly inflammatory contaminants; we chose to use bvHMGB1 in our treatments (Novus Biologicals: NBC1-18488). We performed dose response relationships as there is limited data concerning standard HMGB1 stimulation doses in cell culture conditions.

6.4.3 RNA extraction and RT-PCR

Cell supernatant was removed and RNA extracted from cultured cells using the RNEasy Mini Kit (Qiagen, Hilden, Germany) as described in the General Methods, Chapter 2. Concentration was then determined at OD_{260} using a NanoDrop ND-2000 UV spectrophotometer (Thermofishes, Surrey, UK). 1µg of RNA was used for generation of cDNA using the High Capacity cDNA Archive kit (Applied Biosystems, Warrington, UK).

6.4.4 Real-time (RT) PCR

As detailed previously, target and house-keeping (GAPDH) gene expression was determined using Applied Biosystem "assay on demand" primer-probes along with Lightcycler® 480 Probes Master reagents for the RT reaction mixture (Roche Diagnostics, Switzerland). Samples were added to the RT reaction mixture to a total volume of 5µl and loaded in duplicate in multiplex format (i.e. target and house-keeping gene in each well) into white 384-well plates. C_t values were generated by the LightCycler 480 machine (Roche Diagnostics, Switzerland), and ΔCT values calculated with reference to GAPDH. As outlined previously, arbitrary units (AU) [AU = 1000 x ($2^{-\Delta Ct}$)] and fold-change (R/Q) [R/Q = $2^{-\Delta\Delta Ct}$) using treatment – control condition ΔC_t values to generate $\Delta\Delta C_t$ values, were then calculated. Genes and NCBI reference are shown in table 6.1.

GENE	**NCBI REFERENCE (*HUMAN*)**	**ABI ASSAY REF**
GAPDH	NM_002046.3	Hs02758991_g1
HMGB1	NM_002128.4	Hs01590761_g1
AMIGO-1	NM_020703.2	Hs00827030_g1
AMIGO-2	NM_001143668.1	Hs00406170_g1
AMIGO-3	NM_198722.2	Hs03055344_s1
LINGO-1	NM_032808.5	Hs00262326_s1
RAGE	NM_001136.4	Hs00542584_g1
TLR-4	NM_138554.3	Hs00152939_m1

Table 6.1. List of genes used for RT-PCR with corresponding NCBI and Applied Biosystems reference codes.

6.4.5 Protein extraction and determination of concentration

Cells were harvested, pelleted and cell culture supernatants removed. Pellets were then lysed using RIPA buffer (Sigma R0278) with added protease inhibitor

cocktail (PIC) (Roche Diagnostics, Basel, Switzerland), centrifuged and the clarified protein supernatant collected as outlined in the General Methods, chapter 2. Protein concentrations were then determined using the BioRad$_{DC}$ kit (Bio-Rad, Hemel Hempstead, UK).

6.4.6 Immunoblotting

Immunoblotting was used to determine total protein expression of HMGB1 and the LRRIg molecules under differing cell culture conditions using Novex® NuPage® 4-12% Bis-Tris protein gels under reducing conditions (Invitrogen, Paisley, UK). Proteins were transferred to PVDF membranes using the Trans-Blot® Turbo™ machine (Bio-Rad, Hemel Hempstead, UK).

Primary antibodies were all polyclonal antibodies raised in rabbit, with anti-HMGB1, anti-AMIGO-1, anti-AMIGO-2, anti-AMIGO-3 from Abcam (Cambridge, UK) whilst anti-LINGO-1 antibody was from Upstate (Dundee, UK). All antibodies were used at a dilution of 1:500, except HMGB1 which was used at a dilution of 1:1000. Secondary antibodies used for HMGB1 and LRRIg primary antibodies were against rabbit, at 1:5000. Membranes were stripped and re-probed for HRP-conjugated β-actin 1:5000 (Genscript, New Jersey, USA). Bands were visualised using the ECL detection kit (GE Healthcare, Bucks, UK) and bands visualised using the ChemiDoc™ XRS system. Densitometry was calculated using the in-built software.

6.4.7 Immunohistochemistry

6.4.7.1 Patient demographics

As described in detail in chapter 4 tissue blocks were obtained from the UK MS Brain Bank. Specific patient characteristics are demonstrated in table 6.2.

	AGE	SEX	MS SUBTYPE	DISEASE DURATION (Y)	PMI (H)	CAUSE OF DEATH
MS						
	42	F	PP	6	11	BRONCHOPNEUMONIA
	57	M	PR	33	21	MULTIPLE SCLEROSIS
	50	M	SP	NK	24	BRONCHOPNEUMONIA
	73	M	PP	52	20	LEFT VENTRICULAR FAILURE, BRONCHOPNEUMONIA
	39	F	SP	21	18	BRONCHOPNEUMONIA
	44	F	SP	19	20	URINARY TRACT INFECTION; SEPSIS
	53	M	SP	33	14	SEPTICAEMIA DUE TO UTI
	77	M	SP	39	19	BRONCHOPNEUMONIA; MYOCARDIAL INFARCTION
	40	M	SP	16	27	BRONCHOPNEUMONIA
CONTROL						
	82	M	N/A	N/A	21	NK
	78	F	N/A	N/A	33	MYELOID LEUKAEMIA
	67	F	N/A	N/A	33	ACUTE ARRHYTHMIA, INTESTINAL OBSTRUCTION
	71	F	N/A	N/A	24	ACUTE BRONCHITIS

Table 6.2. Demographic data for patient used in LRRIg neuropathological study. *PR= progressive relapsing; SP= secondary progressive; PP= primary progressive; NK= not known*

6.4.7.2 Immnunohistochemical(IHC) analysis

IHC analysis was performed as described in Chapter 2, Materials and Methods, and was carried out using the Leica Bondmax automated stainer. Antibodies used were anti-MBP, -CD68, -CD3, -GFAP and –HMGB1 as described in table 2.1, and anti-AMIGO-1, -2 (10µg/ml) and–LINGO-1 (100 µg/ml) as described above. The AMIGO-3 antibody was raised in mouse following in-house design, with a peptide sequence taken from the extracellular signalling sequence as the immunogen, with monoclonal specificity. All antibodies were extensively optimised in order to achieve an acceptable balance between signal: noise. Sequential sections were

used to delineate lesion borders and cellularity by staining with H&E, MBP and CD68 in order to verify presence of 'active' and 'chronic active' lesions in-house. This was also useful for ascertaining whether there was evidence of demyelination (GM/ WM) in the 'normal-appearing white-matter' tissue blocks in our hands, as well as in non-MS control tissue. Comparative IR staining intensity was not assessed between the different molecules, partly due to the differing concentrations of antibodies used, but was assessed within different tissue types.

6.5 Statistical analysis

Prism for Mac Version 5.0 (La Jolla, California, USA) was used to perform statistical analysis. For in-vitro work, both ΔC_t and fold-change values used for PCR work and densitometric protein band analysis were used in statistical tests. In-vitro data was normally distributed and comparisons between multiple treatments were analysed using one-way analysis of variance (ANOVA) with Tukey's post-hoc multiple comparison test used to account for type 1 errors. Continuous data was expressed as mean and standard error of the mean (SEM). The threshold for statistical significance was set at $p<0.05$.

6.6 Results

IN-VITRO DATA

6.6.1 HMGB1 is expressed in the MO3.13 cell line, although its receptors TLR4 and RAGE are weakly detectable at baseline.

At baseline, HMGB1 mRNA expression is evident, consistent with its ubiquitous expression in most cells (Yang et al. 2013). However, basal levels of its two key receptors, TLR4 and RAGE were barely detectable.

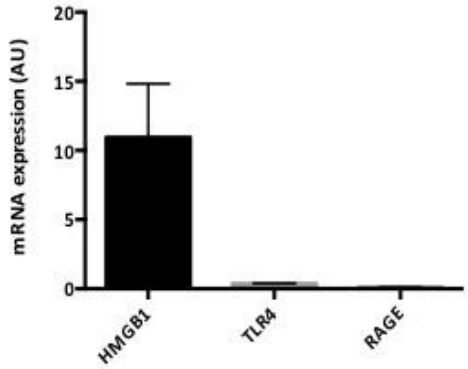

Figure 6.1. Baseline mRNA expression of HMGB1 and its receptors in the oligodendroglial cell line, MO3.13. Total mRNA expression for each of the genes is presented as arbitrary units (AU). *Data are expressed as mean ± SEM. n=3.*

6.6.2 Stimulation of MO3.13 cells with TGF-β1 increases HMGB1 mRNA expression but total protein levels are unchanged

TGF-β1 significantly increased HMGB1 mRNA expression as compared to IFNγ or IL-1β (p=0.005 and P=0.016 respectively) as shown in figure 6.2A. However, this phenomenon was not observed at the total protein level using immunoblotting (figure 6.2B) as semi-quantitative densitometry did not show any significant difference between the control and the same range of mediators (figure 6.2C).

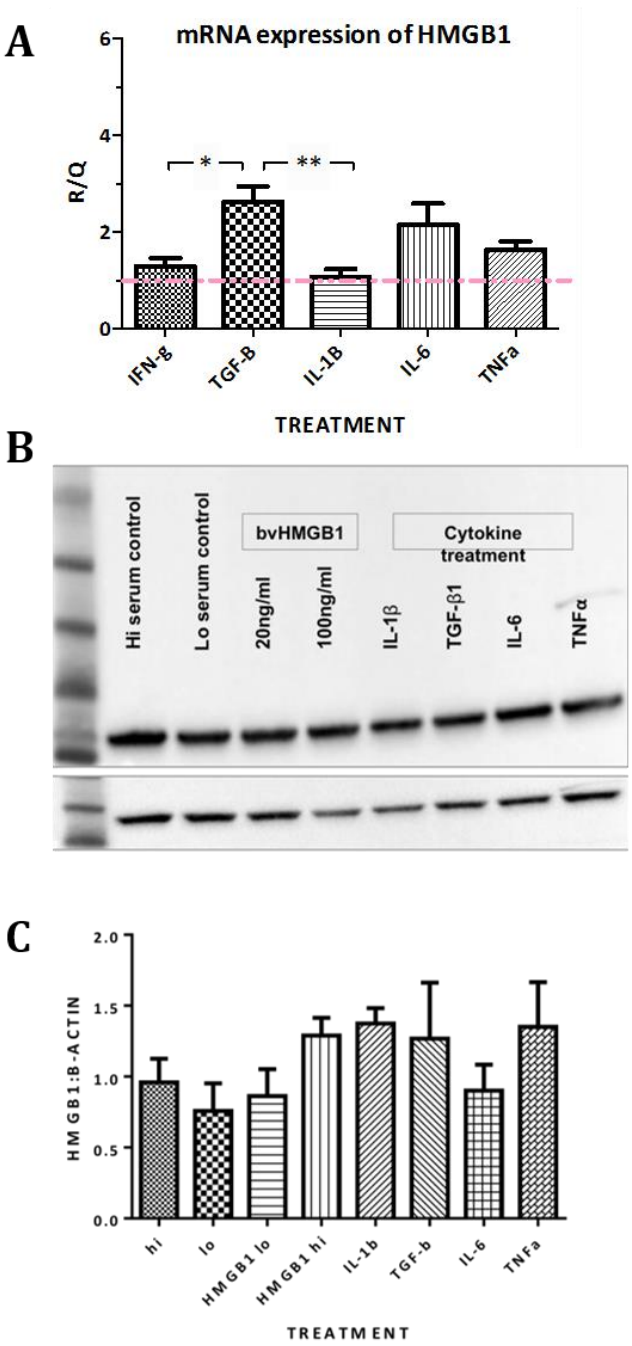

Figure 6.2. TGFβ increases mRNA expression of HMGB1 in oligodendroglial-like cells, but total protein expression is unchanged following cytokine stimulation. (A) Relative mRNA expression of HMGB1 as compared to untreated control MO3.13 cells normalised to GAPDH, after 24h exposure to cytokine. Dashed line represents mRNA expression fold-change of 1 i.e. no change. Expression is significantly increased following TFGβ stimulation compared to treatment with IL-1b ($p=0.005$) and IFNγ ($p=0.016$). This finding was not replicated at the total protein level, as no significant difference in expression was identified following cytokine stimulation using western blotting (B). (C) demonstrates semi-quantitative densitometry of (B), normalised to values of the loading control (β-actin) using 'Chemidoc' software, Biorad Laboratories. Data are expressed as mean ± SEM (A) (n=6); (B, C) (n=3). *Statistical test used: ANOVA with Tukey's post-hoc multiple comparison test.*

6.6.3 HMGB1 receptors, RAGE and TLR4 are significantly upregulated following HMGB1 stimulation of MO3.13 cells.

MO3.13 cells demonstrate mRNA expression of the HMGB1 receptors, RAGE and TLR4, upon stimulation with bvHMGB1 (figure 6.3). Interestingly, TGF-β1 also significantly increased RAGE mRNA expression compared to the other mediators, similar to HMGB1. However, TLR4 demonstrated marked sensitivity to bvHMGB1 stimulation, whilst treatment with the other mediators did not produce a significant change in expression compared to control.

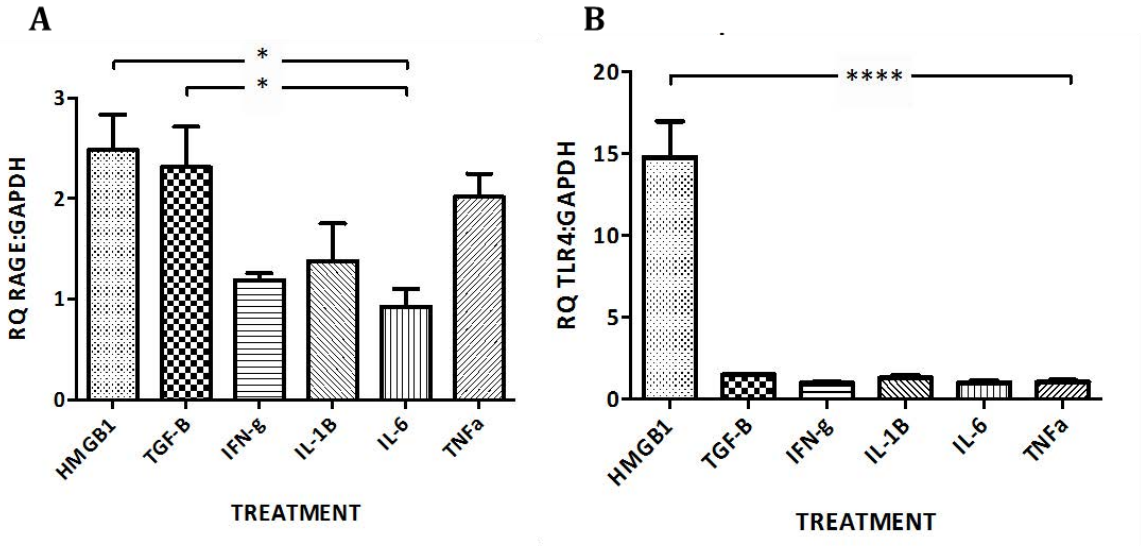

Figure 6.3. mRNA expression of RAGE and TLR4 is significantly upregulated in MO3.13 cells following exposure to bvHMGB1. Relative mRNA expression of (A) RAGE and (B) TLR4 as compared to untreated control MO3.13 cells after 24h exposure to cytokine. (A) Weakly significant increase in RAGE expression was observed following HMGB1 (20ng/ml) and TFG-β1 (10ng/ml)stimulation compared to treatment with IL-6 (p=0.04). (B) However, HMGB1 markedly induced TLR4 mRNA expression, which was strongly statistically significant. Data are expressed as mean ± SEM (n=3-6). All cytokine treatments were administered in low serum conditions. *Statistical test used: ANOVA with Tukey's post-hoc multiple comparison test.*

The effect on RAGE expression was maintained at total protein with HMGB1 treatment compared to other treatments, but was lost with TGF-β1 stimulation. Classically pro-inflammatory stimuli appeared to reduce expression compared to

control (figure 6.4A). Assessment of TLR4 expression using western blotting was not possible due to poor antibody specificities.

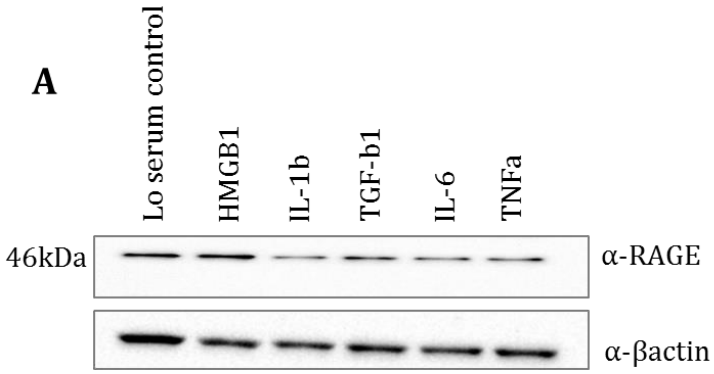

Figure 6.4. Total protein expression of RAGE following exposure to multiple cytokines in oligodendroglial-like cells. (A) shows a representative western blot and semi-quantitative densitometric analyses demonstrating that expression of RAGE in MO3.13 cells is increased at the total protein level by HMGB1 stimulation, and this was weakly significant. All cytokine treatments were normalised to low serum control values. *Data are expressed as mean ± SEM (n=3)*

6.6.4 Expression of LRRIg molecules is responsive to treatment with HMGB1 in MO3.13 cells

6.6.4.1 AMIGO-1 expression is increased by high doses of HMGB1 at both mRNA and total protein level

As shown in figure 6.5, HMGB1 stimulation of MO3.13 cells showed a dose-dependent increase in AMIGO-1 mRNA expression, with a peak fold-change at 100ng/ml. This same pattern was replicated at the protein level using western blotting analysis and interestingly, all other cytokines appeared to suppress AMIGO-1 expression at the tested doses as compared to control.

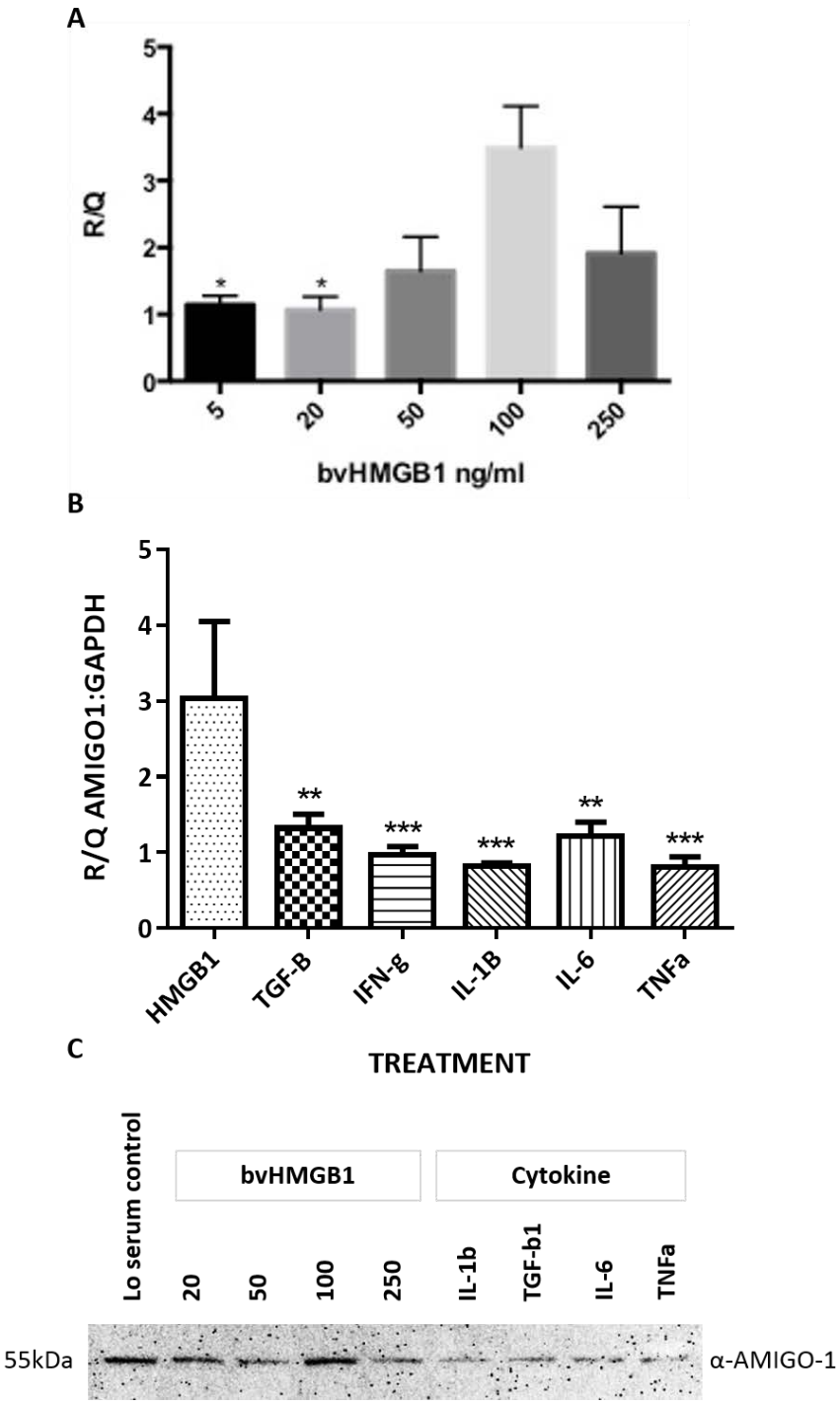

Figure 6.5. High-dose bvHMGB1 stimulation increases AMIGO-1 mRNA and total protein levels. (A) Dose-response curve demonstrating increased effect of bvHMGB1 on AMIGO-1 mRNA expression at 100ng/ml vs. 5 or 20ng/ml (n=3; *p<0.05*). (B) mRNA levels of AMIGO-1 following stimulation by a panel of cytokines (n=6). (C) total protein levels of AMIGO-1 following stimulation by a panel of cytokines, as assessed by western blotting. bvHMGB1 dose units = ng/ml. Asterisks denote significance of bvHMGB1 treatment vs cytokine treatment. **p<0.05 **p<0.005 ***p<0.0005 Statistical test used: ANOVA with Holm-Sidak post-hoc multiple comparison test.* Data are expressed as mean±SEM (n=3-6).

6.6.4.2 AMIGO-2 mRNA expression is increased following HMGB1 stimulation

As shown in figure 6.6A, high levels of AMIGO-2 mRNA expression were evident at all doses of bvHMGB1 stimulation. Despite an apparent trend towards lower doses stimulating greater expression of AMIGO-2, there is variability in the data as shown by the error bars. When comparing total mRNA levels of AMIGO-2 following stimulation by our panel of cytokines, expression was reduced compared to control in response both pro-and anti-inflammatory cytokine treatments, particularly IL-6 and TNFα, where the latter appeared to entirely supress expression. However, once again there appears to be an HMGB1-specific response, where expression is upregulated compared to all other treatments, and this is weakly significant as shown on in figure 6.6B. The HMGB1 dose used in this experiment was 100ng/ml, as this showed the least variability in dose-response.

However, expression of total protein levels of AMIGO-2 using western blotting demonstrated that the situation was more complex. Multiple bands at differing molecular weights were observed, with a faint band at the expected MW of 55kDa. A more prominent band at approximately 30kDa was consistently evident, although the significance of this is unclear.

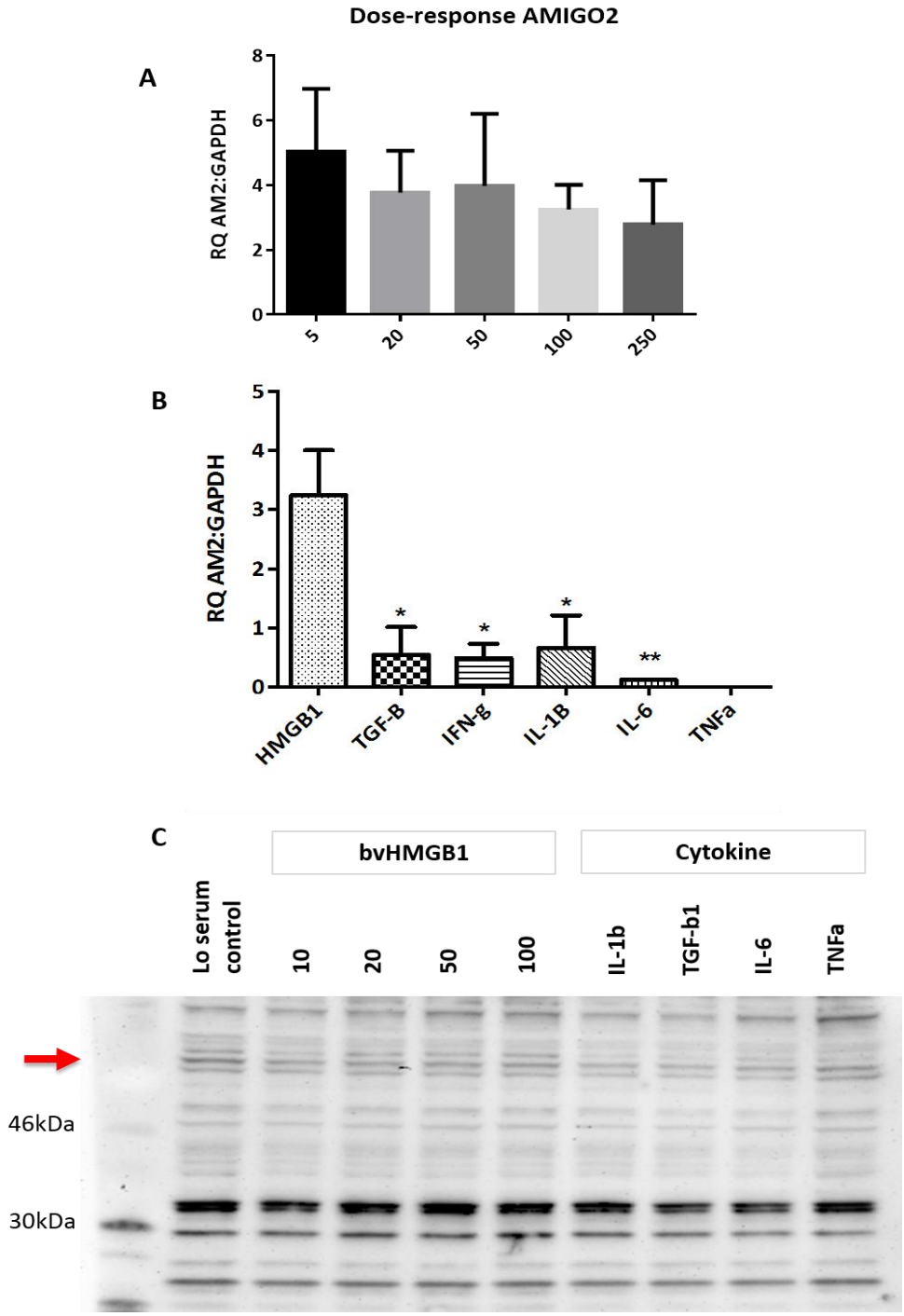

Figure 6.6. HMGB1 increases AMIGO-2 mRNA levels, but less obviously at the protein level. (A) Dose-response curve demonstrating effect of bvHMGB1 on AMIGO-2 mRNA expression. (B) mRNA levels of AMIGO-2 following stimulation by a panel of cytokines. (C) total protein levels of HMGB1 following stimulation by a panel of cytokines, as assessed by western blotting (arrow: expected band at 55kDa). bvHMGB1 dose units = ng/ml. Asterisks denote significance of bvHMGB1 treatment vs cytokine treatment.***p<0.005 ***p<0.0005. Statistical test used: ANOVA with Holm-Sidak post-hoc multiple comparison test. Data are expressed as mean ± SEM (n=3-6).*

6.6.4.3 AMIGO-3 expression is increased by low doses of bvHMGB1

In contrast to AMIGO-1 data, AMIGO-3 mRNA expression levels were highest at lower doses of bvHMGB1 stimulation, as shown in figure 6.7A. Compared to the other cytokines used, the bvHMGB1-stimulated response produced a significantly greater effect on mRNA expression as demonstrated in figure 6.7B.

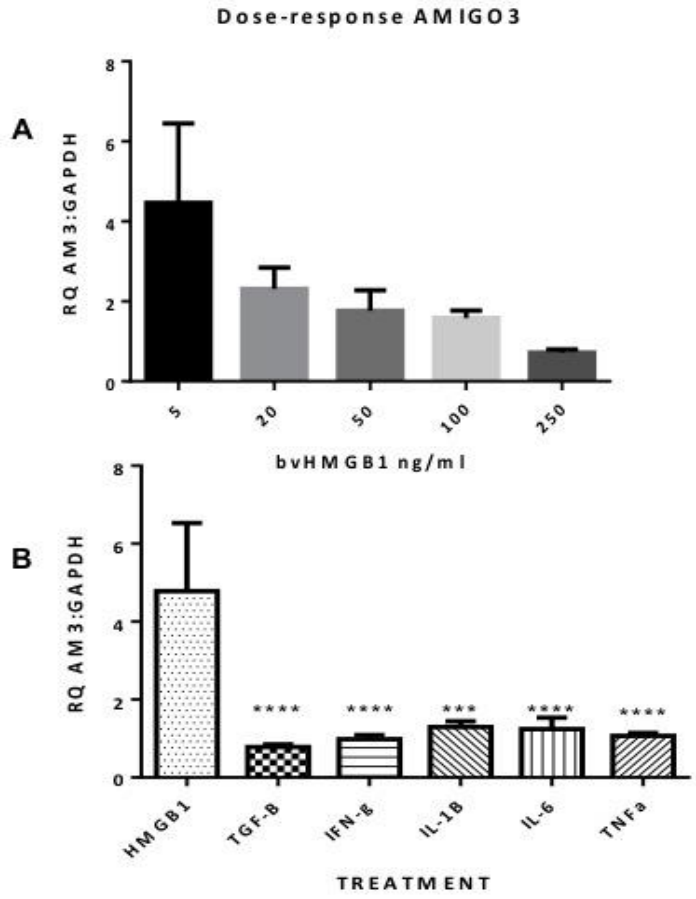

Figure 6.7. bvHMGB1 treatment increases mRNA expression of AMIGO3. (A) Dose-response curve demonstrating expression of AMIGO3 with increasing doses of bvHMGB1, (B) AMIGO3 expression is unchanged by either pro- or anti-inflammatory cytokine treatments. However, as noted with its two homologues, expression is upregulated following stimulation by bvHMGB1 compared to all other treatments. HMGB1 dose used: 5ng/ml. Asterisks denote significance of bvHMGB1 treatment vs cytokine treatment.****p=0.0001 ****p<0.0001Statistical test used: ANOVA with Holm-Sidak post-hoc multiple comparison test. Data are expressed as mean ± SEM (n=3-6).*

Unfortunately, it was not possible to perform western blotting to assess this effect at the protein level as a variety of antibodies tested failed to produce positive bands.

6.6.4.4 LINGO-1 expression is increased by bvHMGB1 stimulation.

bvHMGB1 consistently increased expression of LINGO-1 mRNA compared to control at all doses (figure 6.8A). It also stimulated almost 5-times greater fold-change expression of LINGO-1 than the other cytokines used.

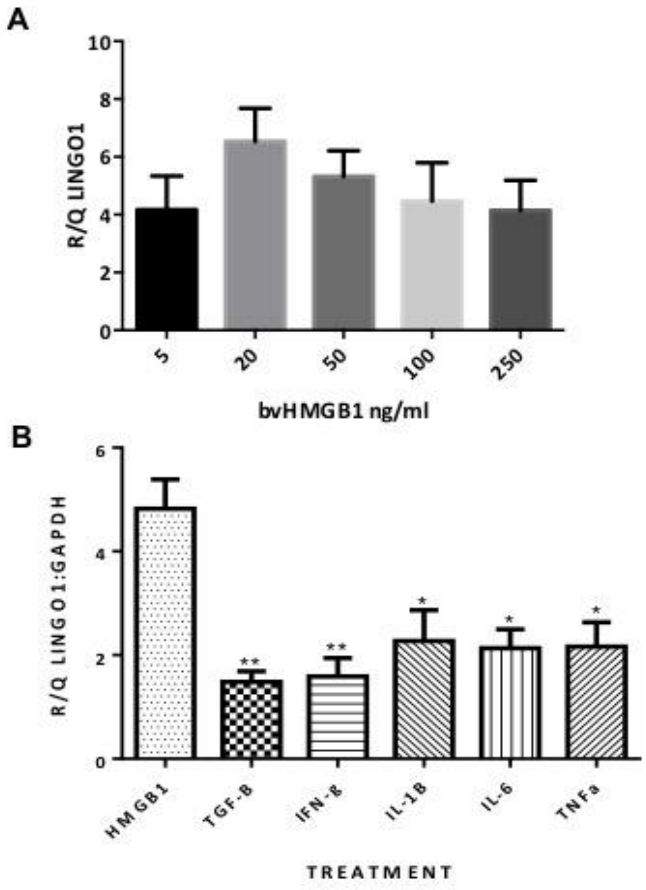

Figure 6.8. bvHMGB1 treatment significantly increases mRNA expression of LINGO-1. (A) LINGO-1 mRNA expression is increased compared to control at all treatment doses of bvHMGB1 (B) LINGO1 expression is significantly increased following stimulation by bvHMGB1 compared to other treatments. HMGB1 dose used in (B): 20ng/ml. Asterisks denote significance of bvHMGB1 treatment vs cytokine treatment.**p<0.05 **p<0.008Statistical test used: ANOVA with Holm-Sidak post-hoc multiple comparison test. Data are expressed as mean±SEM (n=3-6).*

Interestingly however, stimulation with IL-1β, IL-6 and TNFα also appeared to increase its expression approximately two-fold, with the difference between bvHMGB1-stimulated expression and these mediators being of correspondingly weaker significance ($p<0.05$) than between bvHMGB1 and IFNγ and TGFβ1 ($p<0.08$).

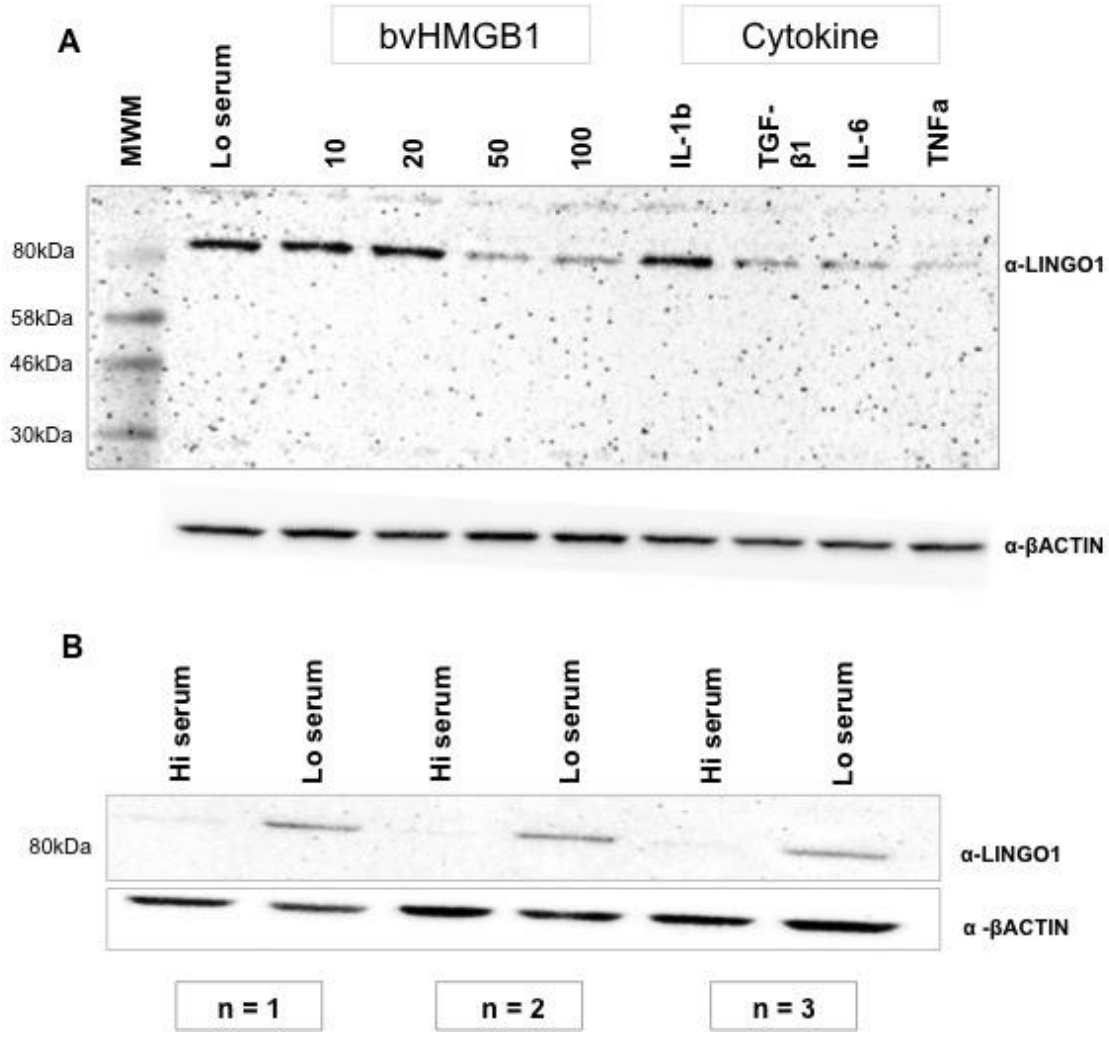

Figure 6.9. Expression of LINGO-1 is increased in low-serum conditions and by bvHMGB1 and IL-1β stimulation. (A) demonstrates that low-dose bvHMGB1 stimulation increased LINGO1 expression compared to higher doses, with IL-1β also consistently inducing expression compared to the other cytokines tested (B)LINGO-1 expression is reduced in high-serum and induced when placed in low-serum conditions. *(n=3).*

When assessing total protein levels, expression of LINGO-1 was similar to control at lower doses of bvHMGB1 as shown in figure 6.9A, but appeared to be suppressed at higher doses. In addition, expression was consistently induced by IL-1β in particular, but was suppressed by both pro-inflammatory (TNFα, IL-6) and anti-inflammatory (TGF-β1) mediators. Interestingly, serum is known to contain TGF-β and the expression of LINGO-1 is similarly reduced in high-serum conditions as with TGF- β1 stimulation. This suggests a specific role for HMGB1 and IL-1β in inducing expression of LINGO-1.

I then decided to compare the expression pattern of LINGO-1 in high vs. low-serum conditions to test whether global cellular stress precipitated by this change in treatment conditions produced differential LINGO-1 expression patterns. The results were striking, as LINGO-1 expression was barely detectable in high serum conditions and clearly induced in low-serum conditions, as shown in figure 6.9B. Possible reasons for this are discussed in section 6.7.

NEUROPATHOLOGICAL EXPRESSION OF LRRIg PROTEINS

I performed a preliminary analysis of the expression pattern of these novel molecules in human brain. Using tissue from the UK MS Brain Bank as described in Chapter 4, expression patterns in non-MS control brain and in MS lesional and non-lesional tissue were assessed.

6.6.5 Neuronal and stromal expression of AMIGO-1 and AMIGO-2 is robust in non-MS control brain tissue but markedly reduced in non-lesional MS brain tissue

Immunohistochemical analysis of non-MS control brain tissue revealed the expression of AMIGO-1 and AMIGO-2 was most prominent in neurons within the grey matter (GM), where a characteristic, punctate staining pattern was evident (Figure 6.10A and 6.11A), reminiscent of the neuronal staining pattern observed in mice- Chapter 1, General introduction figure 1.8 (Peltola et al. 2011). In the MS tissue, both staining intensity and frequency of positively staining neurons were reduced. In the control white matter (WM), staining in OGD was discernible, though faint and in both GM and WM, stromal staining was prominent. However, in both NAWM and non-lesional regions of AL tissue blocks from MS patients, expression appeared to be reduced overall, with minimal staining, if any, in the white matter.

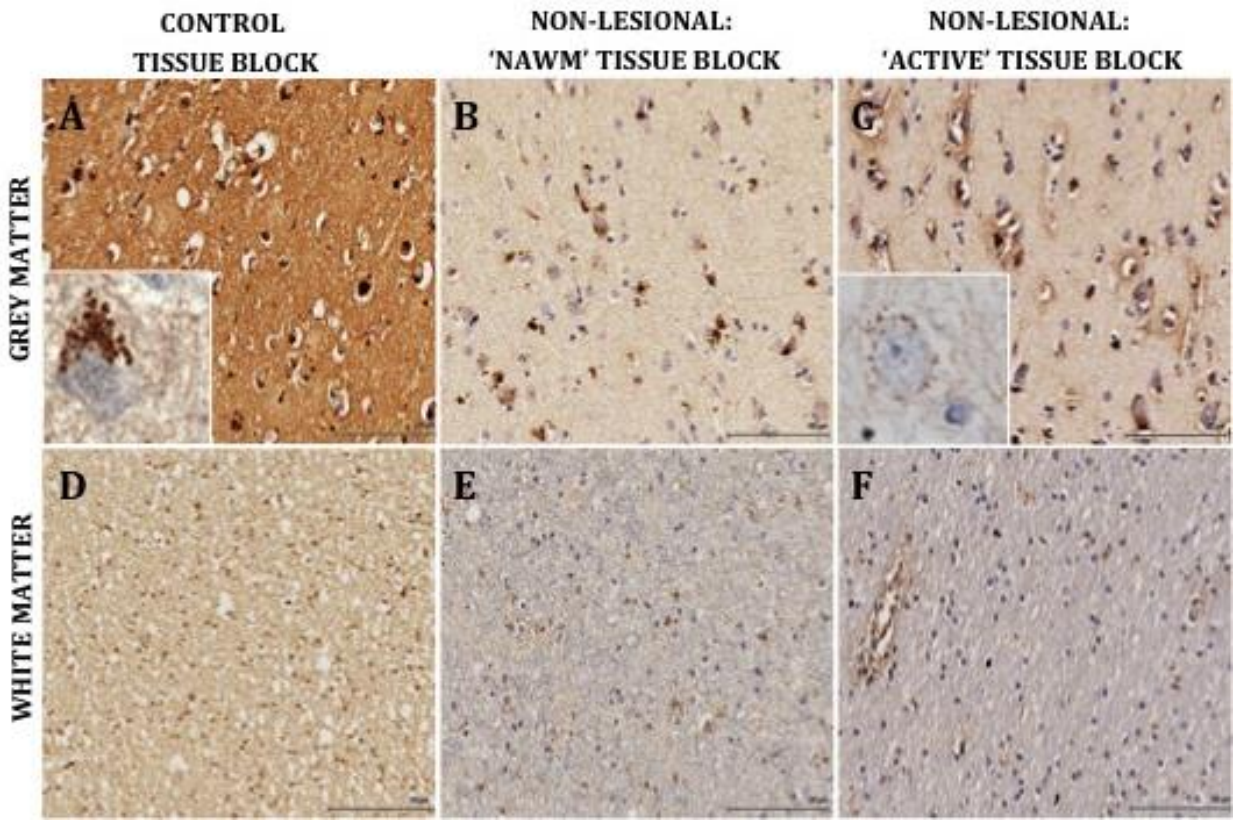

Figure 6.10 AMIGO-1 expression pattern in post-mortem human brain tissue. Expression demonstrated in both grey and white-matter as indicated in non-MS control (A, D), normal-appearing white matter (NAWM) (B,E) and non-lesional regions of active lesional (AL) tissue blocks (C,F). Inset in (A) and (C) illustrate IR in neurons (x63). *Tissue blocks taken from inferior/ superior frontal gyri. Scale bar = 100 μm.*

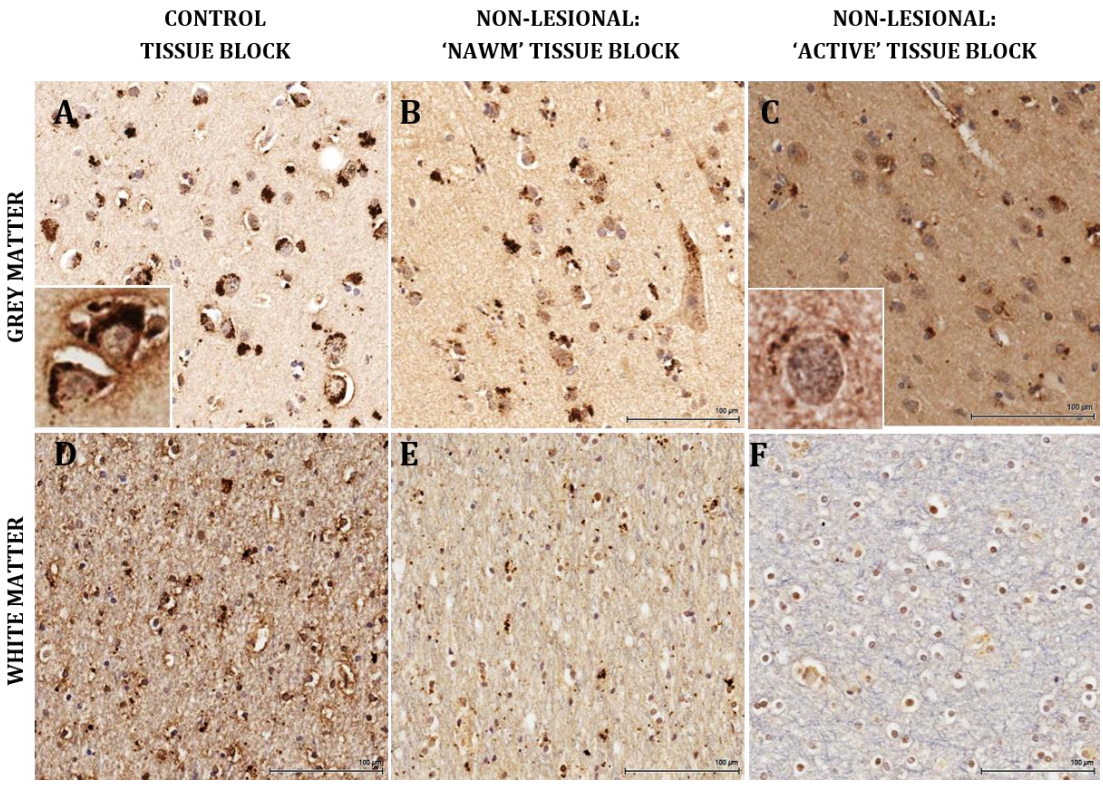

Figure 6.11. AMIGO-2 expression pattern in post-mortem human brain tissue. Expression demonstrated in both grey and white-matter as indicated in non-MS control (A, E), normal-appearing white matter (NAWM) (B,E) and non-lesional regions of active lesional (AL) tissue blocks (G,F). Inset in (A) and (C) illustrate IR in neurons (x63). *Tissue blocks taken from inferior/ superior frontal gyri. Scale bar = 100 μm.*

6.6.6 AMIGO-3 expression is induced at low levels in active lesional MS tissue but is undetectable in non-MS control tissue.

In contrast to AMIGO-1 and -2, AMIGO-3 was not expressed in non-MS control tissue. Conversely, in AL tissue blocks, expression was evident in glial cells in the AL and in non-lesional WM, which morphologically appeared to be activated microglia (figure 6.12F; arrowhead). In the GM of AL tissue blocks, neuronal nuclei displayed evidence of faint IR, with weak staining also evident in the cytoplasm (figure 6.12C; arrow).

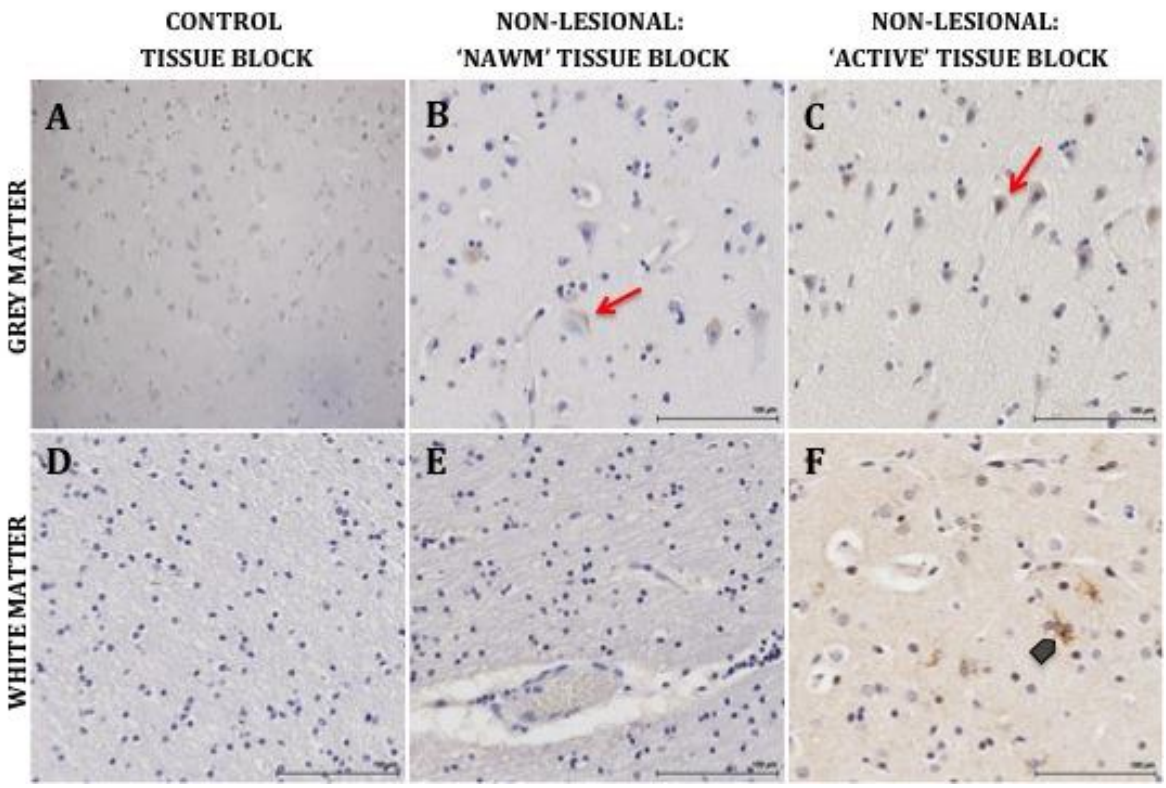

Figure 6.12. AMIGO-3 expression pattern in post-mortem human brain tissue. Non-MS control (A, D), normal-appearing white matter (NAWM) (B,E) and non-lesional regions of active lesional (AL) tissue blocks (C,F). AMIGO-3 expression is undetectable in all tissue types, except faint IR in MS grey matter. However, the fine granularity and cresenteric appearance in neurons, (figure 6.12B; arrow), means we cannot exclude the possibility that this pattern of IR may represent lipofuscin staining. In MS white matter, AMIGO-3 positive cells with probably microglial morphology could be seen (arrowhead). *Tissue blocks taken from inferior/ superior frontal gyri. Scale bar = 100 μm.*

6.6.7 LINGO-1 is robustly expressed in non-MS control patients, but is relatively reduced in MS patients in post-mortem tissue

The most consistent difference between control and MS patients was in the neuronal expression pattern of LINGO-1 in the GM. This was characterised by an intensely immunoreactive, punctate appearance in neurons in the non-MS control cortex, evident over the neuronal soma and proximal dendrites, as seen in figure 6.13D. The pattern was similar to the changes observed in AMIGO-1 and -2 staining. Interestingly, this staining pattern was evident in the GM of NAWM tissue

blocks although there appeared to be fewer cells displaying it (figure 6.13E). In both demyelinated (data not shown) and non-lesional regions of the cortex, this characteristic pattern was clearly different as virtually all cells demonstrated a more homogenous staining pattern with fine granularity evident at higher power, as seen in 6.13F. In addition, increased IR along axons themselves was seen in the GM (inset).

In the lesional white matter, as shown by the dotted line in figure 6.13C, LINGO-1 staining was greatly reduced. This may reflect reduced expression within the stroma, but also may highlight reduction of axonal/ cellular expression, as the designated 'AL' tissue blocks were in fact late active or chronic actively demyelinating lesions.

In non-lesional WM the degree of stromal staining was greater in non-MS control> MS NAWM> MS AL tissue blocks, as shown in figures 6.13G-I. However, it did not appear as if OGD themselves expressed LINGO-1 in the nucleus or cytoplasm (6.13G; inset) and instead, a punctate pattern throughout the stroma was seen.

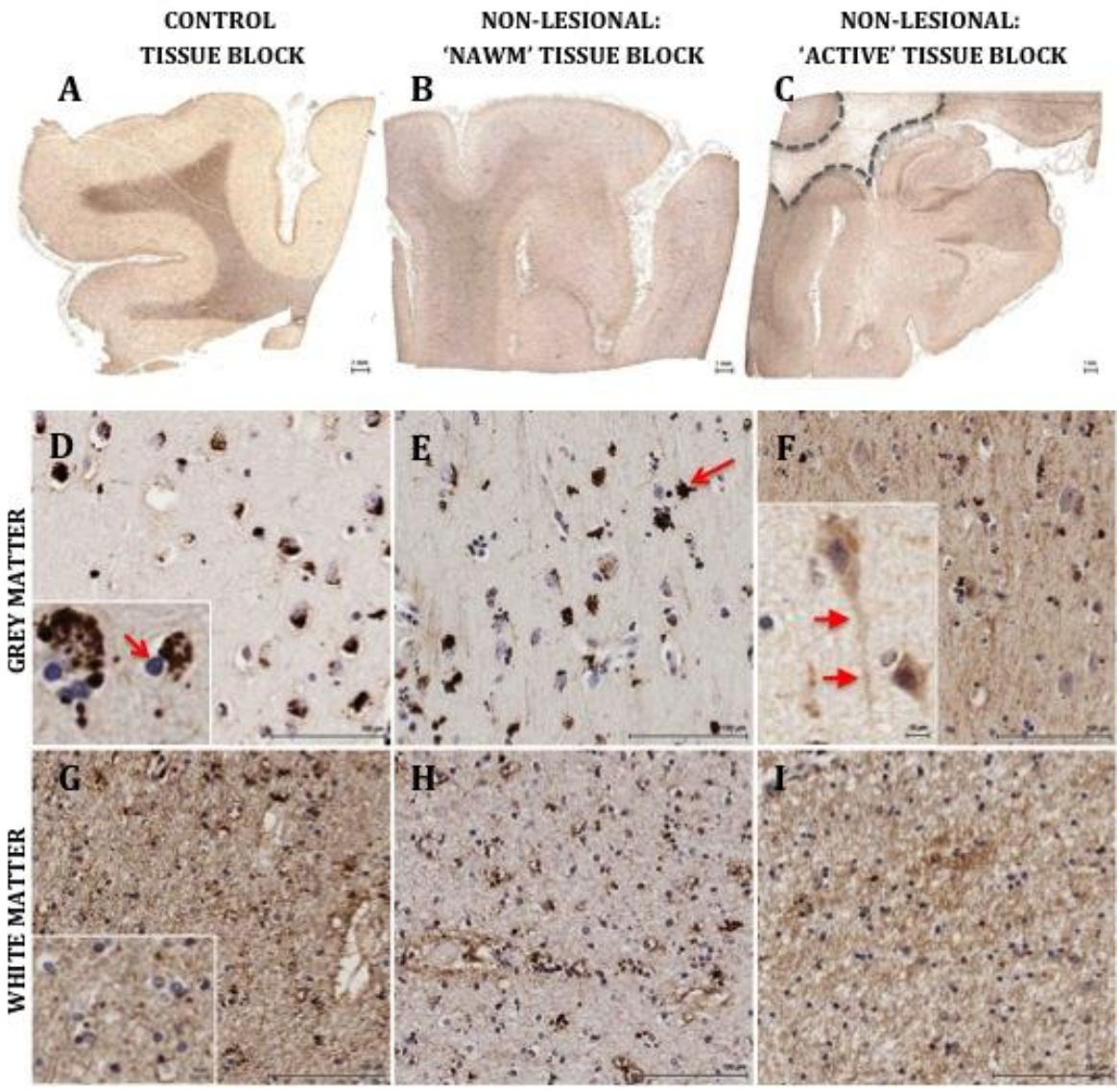

Figure 6.13. LINGO- expression pattern in post-mortem human brain tissue. Expression demonstrated in both grey and white-matter as indicated in non-MS control (A, D, E), normal-appearing white matter (NAWM) (B,E,H) and non-lesional regions of active lesional (AL) tissue blocks (C, F, I). (A-C) Low magnification view. NB In figure 6.14C, the dotted lines represent a lesional region of active/ chronic active demyelination. (D) All neuronal cells demonstrate punctate staining pattern; inset- located around neuronal soma and proximal dendrites. Arrow- OGD do not demonstrate IR. (E) Similar staining pattern in NAWM but fewer positive cells (F) Punctate staining pattern significantly reduced. Inset: staining pattern around soma more diffuse with clear axonal staining. *Tissue blocks taken from inferior/ superior frontal gyri. Scale bar (A-C) = 1mm; (D-I) = 100μm; inset in (D) and (F) = 10μm.*

6.6.8 LRRIg expression pattern in early active lesional (EAL) tissue, from a biopsy sample in a patient with clinically isolated syndrome (CIS).

The tissue characteristics of this biopsy sample have been addressed in detail in chapter 3. In figure 6.14A-D, the demonstration of florid inflammatory cell infiltrate with evidence of myelin fragmentation as opposed to demyelination per se (data not shown), illustrates the characterisation of this as an early inflammatory lesion as per ICDNS classification (www.icdns.org). In figure 6.15A, AMIGO-1 expression pattern is weak overall, although the finely spiculated appearance in lipophages may be attributable to myelin breakdown products, suggesting that AMIGO-1 may be expressed on the myelin sheath. In figure 6.15B, the background stromal staining pattern of AMIGO-2 is relatively increased, as is cell-specific staining in OGD and in macrophages. Interestingly it is relatively weaker in lipophages, suggesting that different types of macrophages/ microglia may express AMIGO-2.

AMIGO-3 staining is undetectable in non-MS control autopsy tissue, and faintly evident in AL tissue blocks (figure 6.12). However, when comparing post-mortem and early active lesional biopsy tissue, expression was profoundly different. In spite of caveats relating to comparison between biopsy and autopsy tissue as discussed, the staining pattern in the early active lesional biopsy tissue was markedly increased using the in-house mouse monoclonal anti-AMIGO-3 antibody. Once again isotype control antibody testing did not reveal evidence of non-specific IR. The predominant subcellular localisation was nuclear, and evident in macrophage, oligodendrocytes and–strikingly- neuronal nuclei. Anti-AMIGO-3 IR overall was greater in the active lesional regions shown in figure

6.15C. In non-lesional white matter it demonstrates a punctate pattern adjacent to OGD (figure 6.16C; inset). The latter demonstrated clear IR around the chromatin structure within the nuclei of virtually all neuronal subtypes throughout the cortex and was particularly noticeable in large pyramidal nuclei. Despite the propensity of HMGB1 to translocate to the neuronal cytoplasm, its predominant staining pattern in non-lesional grey matter neurons was also nuclear as shown below in figure 6.19. LINGO-1 IR also shows increased stromal staining with a prominent, punctate pattern evident in lipophages- again suggesting myelin breakdown products. In addition, increased IR in OGD-like cells are also seen in this tissue type, which is further illustrated in figure 6.16, below.

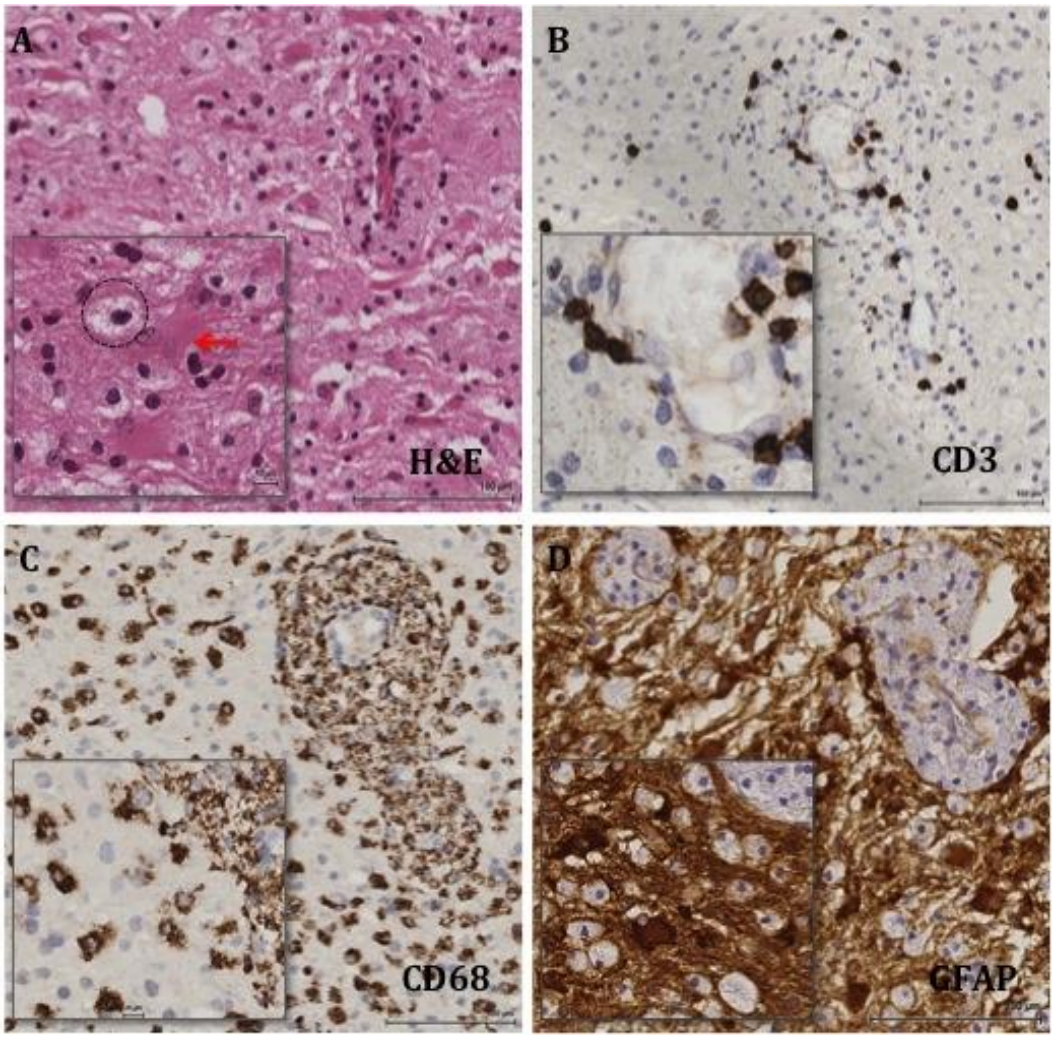

Figure 6.14. Characterisation of early active lesional tissue, taken from a biopsy sample in a patient with clinically isolated syndrome (CIS). (A)-(D) demonstrate the basic staining pattern in this tissue block. (A) cytoarchitectural pattern as shown using H&E staining;inset- gemistoctic astrocytes with mitotic nuclei are evident (arrow), immediately adjacent to foamy macrophages (circle). (B) anti-CD3-positive cells demonstrating presence of lymphocytes in both a perivascular distribution and occasional cells migrating into the parenchyma. (C) numerous anti-CD68-positive cells are evident, predominantly lipophages morphologically (D) anti-GFAP-positivity is evident, demonstrating both gemistocytic astrocytes and the intense background glial fibrillary reaction in this lesion type. *Scale bar = 100μm.*

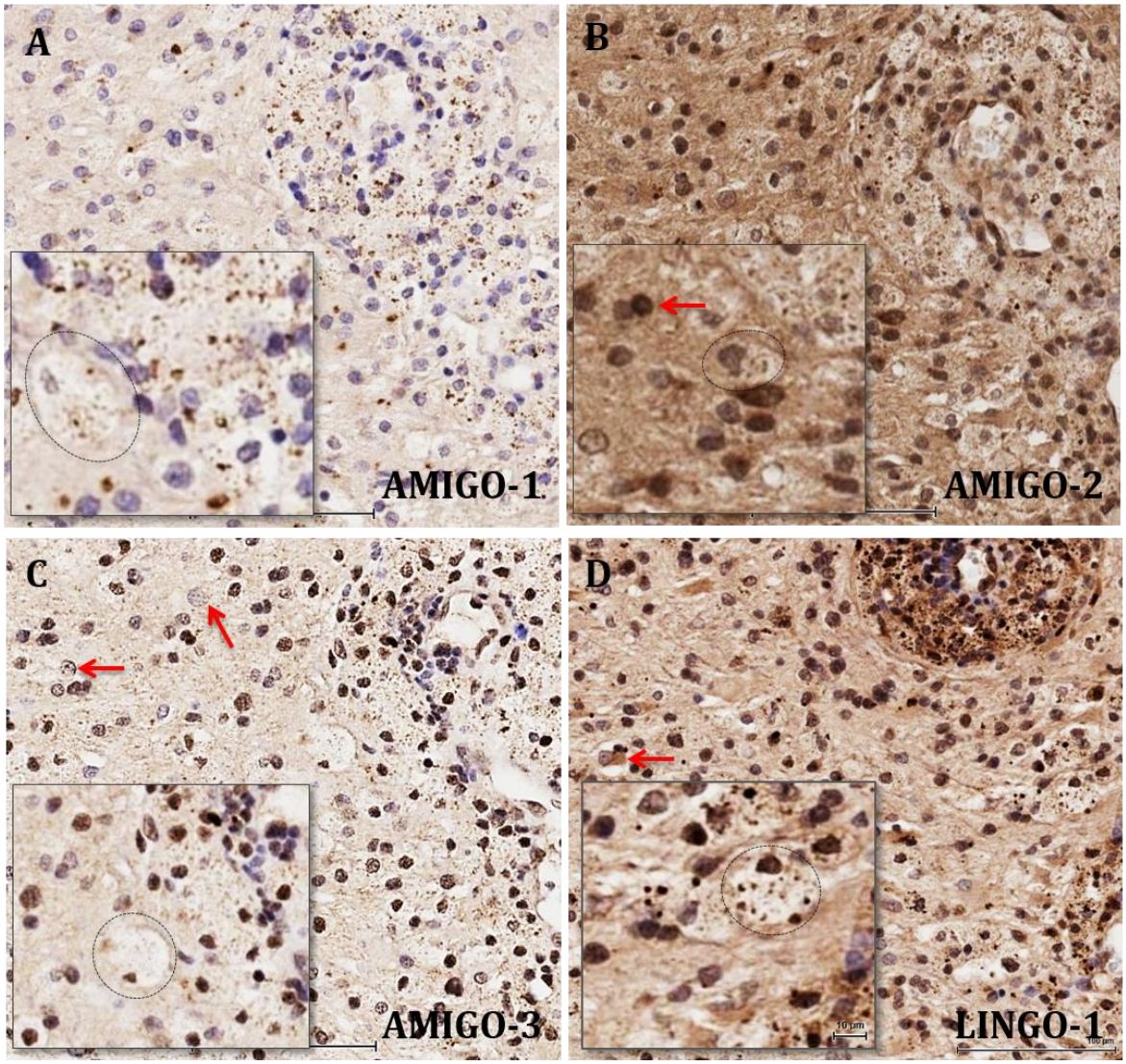

Figure 6.15. LRRIg expression pattern in early active lesional tissue, taken from a biopsy sample in a patient with clinically isolated syndrome (CIS). (A)-(D) LRRIg expression pattern in this block. (A) shows minimal cell-specific or stromal AMIGO-1 IR, including in lipophages (inset; circle) although a punctate staining pattern is evident in the latter suggestive of myelin breakdown products. (B) AMIGO-2 IR is evident in the nuclei of cells including oligodendrocytes (arrow) but not in lipophages per se (circle). (C) AMIGO-3 IR appears to be predominantly nuclear, particularly in macrophages whilst IR is not evident in astrocytes (arrows) (D) LINGO-1 IR demonstrates a similar staining pattern to AMIGO-3 although pale, cytoplasmic IR can also be seen in astrocytes (arrow). *Scale bar = 100μm.*

6.6.9 LRRIg expression pattern in non-lesional white matter, from an early active lesional tissue block

As discussed in chapter 3 and 4, non-lesional regions were initially classified as being ≥7mm from the lesion border, with an intact myelin pattern and lack of significant inflammatory cell infiltrate or perivascular lymphocytic cuffing.

In this context, once again AMIGO-1 IR was weak, with an occasional OGD-like cell displaying evidence of staining as seen in the inset in figure 6.16A. AMIGO-2 IR, however, clearly demonstrated OGD expression, as shown in figure 6.16B and stromal IR was also stronger than that observed in the autopsy material. Once again, the AMIGO-3 staining pattern was markedly different in this tissue type, shown in figure 6.16C. Both OGD and macrophages appear to express AMIGO-3 and staining was apparently upregulated in those OGD which demonstrated shrinkage in size and nuclear condensation- possibly highlighting pyknosis (inset; arrow). Anti-LINGO-1 IR in a punctate pattern along axons was evident in figure 6.16D, but in addition, apparent cell-specific IR was also seen in OGD. This was in contrast to the findings in post-mortem tissue, where stromal and axonal IR was prominent but staining of the OGD cell body or processes were not clearly seen.

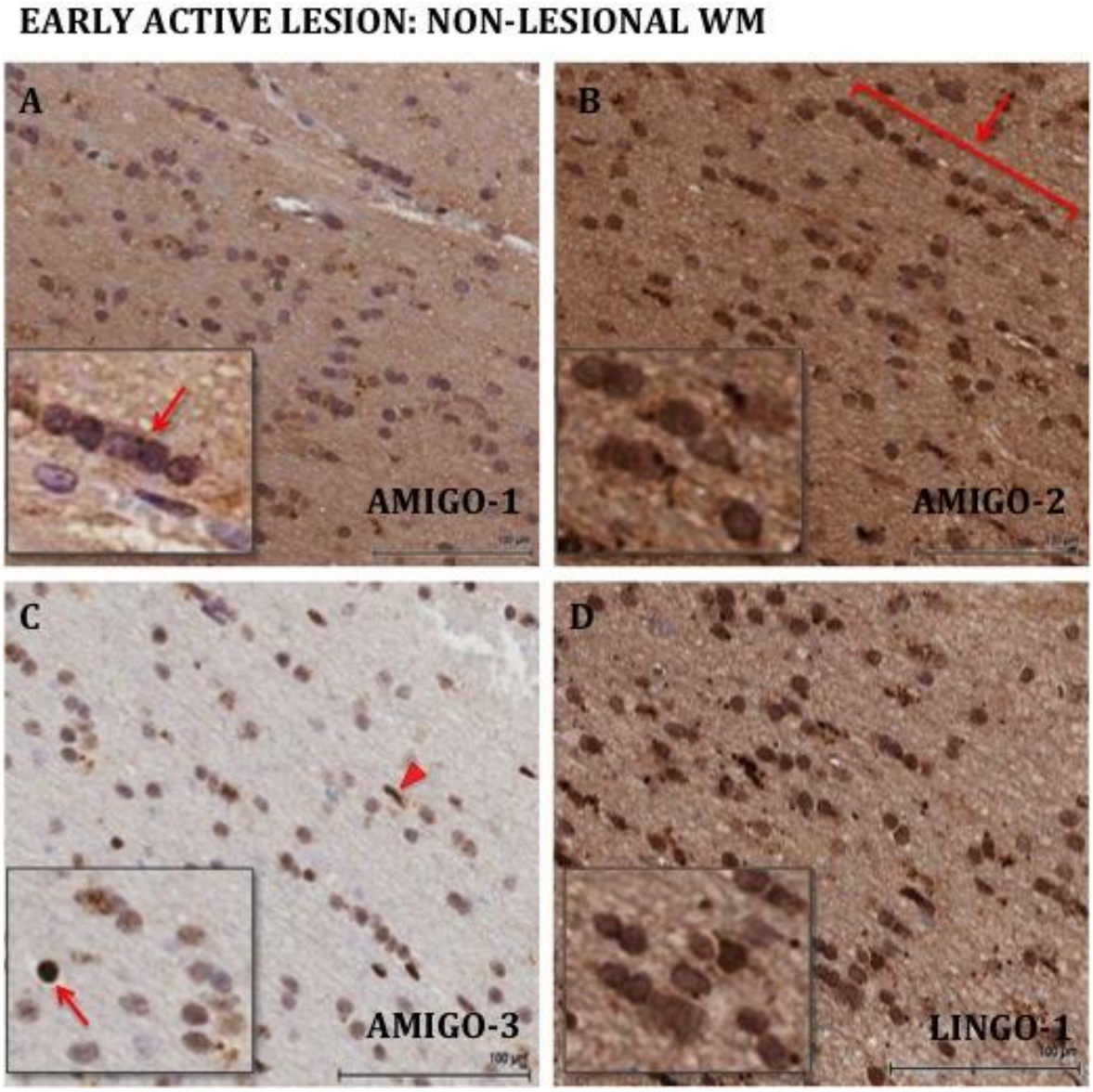

Figure 6.16. LRRIg expression pattern in non-lesional white matter adjacent to early active lesional tissue, taken from a biopsy sample in a patient with clinically isolated syndrome (CIS). (A) AMIGO-1 IR is low, similar to the pattern seen in figure 6.15, above. Occasional punctate staining in OGD is evident (arrow). (B) AMIGO-2 IR is increased in non-lesional white matter, particularly in OGD as demonstrated lining up along the axon (arrow). A punctate staining pattern is clearly evident adjacent to these cells (inset). (C) AMIGO-3 IR is evident predominantly in macrophages, some of which demonstrate a rod-shaped appearance (arrowhead) and in OGD with variable IR. Those cells with condensed nuclei and which may represent apoptosing cells appear to stain more intensely. (D) LINGO-1 IR is evident in OGD and along the axon. *Scale bar = 100μm.*

6.6.10 LRRIg expression pattern in non-lesional grey matter, from an early active lesional tissue block

Figures 6.17A & -B demonstrate similar AMIGO-1 and AMIGO-2 IR patterns, in that neuronal expression is weak overall with a diffuse IR around the soma. Once again however, AMIGO-2 stromal staining was prominent. As seen in figure 6.17C, AMIGO-3 IR was again significantly different compared to autopsy tissue (figure 6.12C), and this change was most striking in the non-lesional grey matter. Here, AMIGO-3 displays clear neuronal nuclear IR (inset), with occasional cytoplasmic expression in pyknotic neurons. In AMIGO-molecules, satellite cell (OGD) reactivity was not clearly discernible, though was evident in LINGO-1-positive cells (inset).

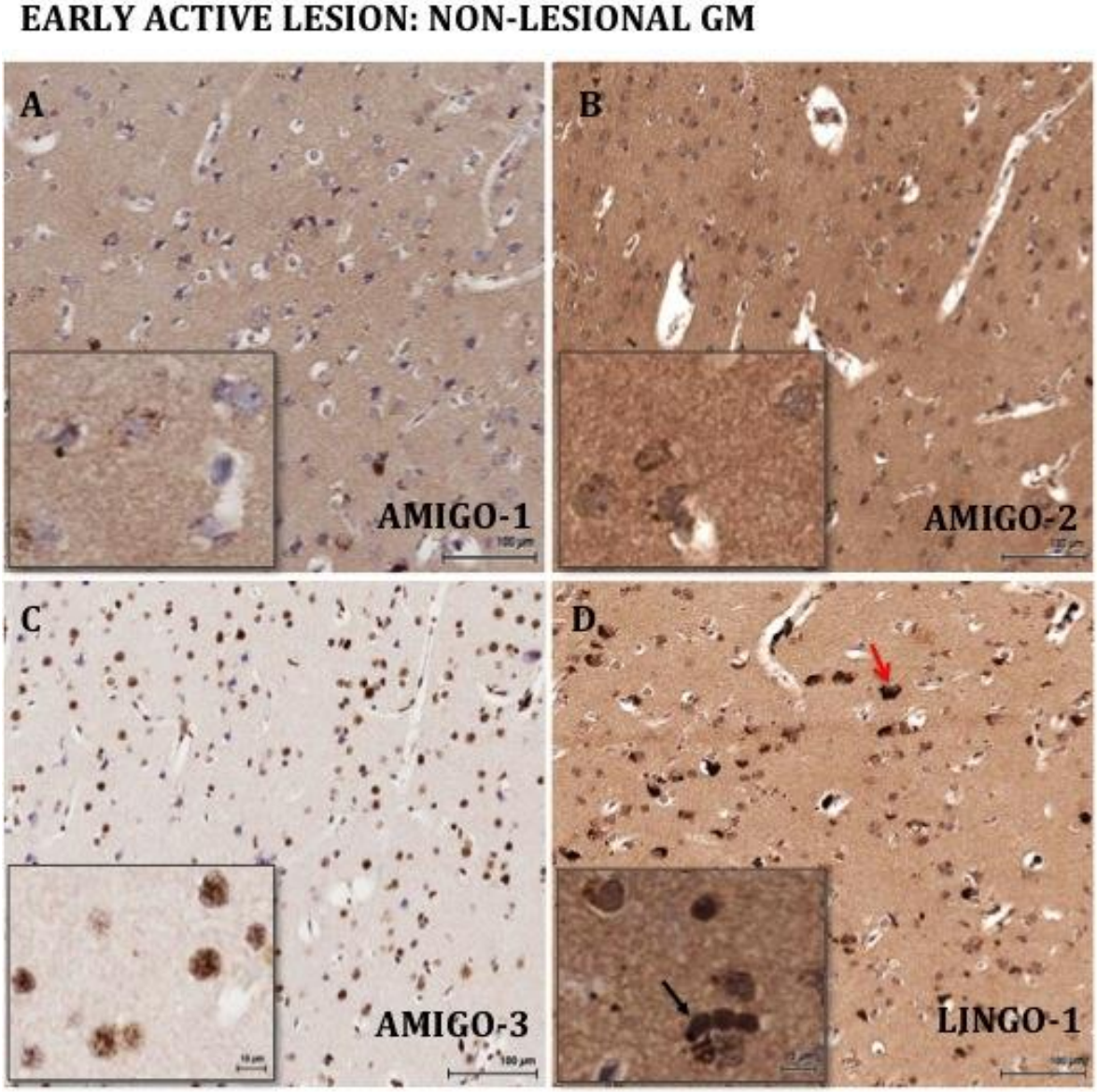

Figure 6.17 LRRIg expression pattern in non-lesional grey matter adjacent to early active lesional tissue, taken from a biopsy sample in a patient with clinically isolated syndrome (CIS). (A) AMIGO-1 IR is low although occasional punctate staining in neurons is evident. (B) AMIGO-2 demonstrates a similar IR staining pattern to (A) in non-lesional grey matter, where IR overall is weak, although the stromal IR is relatively greater than in AMIGO-1 (C) AMIGO-3 IR is clearly evident in neuronal nuclei, with occasional cytoplasmic staining seen in pyknotic neurons (not shown) (D) LINGO-1 IR is seen with a similar frequency and intensity of positively stained neurons to those in NAWM tissue blocks in the autopsy series, as shown in figure 6.13. *Scale bar = 100 μm.*

Finally, co-localisation studies are required to confirm cell-specific expression, with support from in-situ hybridisation and would need to be performed in future work. However, neuropathological assessment of cell types based on characteristic morphological appearances enables a preliminary assessment of this, and is summarised in Table 6.3, below. Control tissue was used although if certain expression patterns were increased/ decreased in this cell type in EAL tissue, this is indicated by arrows in superscript.

	MACROPHAGE/ MICROGLIA	ASTROCYTE	OLIGODENDROCYTE	NEURON
AMIGO-1	±	-	±	+++$^{\downarrow}$
AMIGO-2	+$^{\uparrow}$	+	+$^{\uparrow}$	+++$^{\downarrow}$
AMIGO-3	±$^{\uparrow}$	-	-$^{\uparrow}$	-$^{\uparrow}$
LINGO-1	++$^{\uparrow}$	+$^{\uparrow}$	+$^{\uparrow}$	+++

Table 6.3. Summary of cell-specific expression of LRRIg proteins in early active lesional (EAL) biopsy tissue. Arrows denote the comparative staining intensity in early active lesional MS biopsy tissue. $^{\uparrow}$=increased; $^{\downarrow}$=decreased**.** *± = weak; + = moderate; ++ = strong staining intensity.*

6.7 Discussion

In chapters 3 and 4, I demonstrated increased expression of HMGB1 in macrophages/microglia and OGD, and in chapter 5 reported that HMGB1 levels in the CSF were elevated in MS patients vs. controls, correlating with inflammatory cell count. It is plausible that it may therefore be released into the extracellular space and act as a pro-inflammatory mediator here.

In this context, one of the aims of this chapter was to model aspects of the oligodendroglial response; both in terms of cues augmenting endogenous HMGB1 expression in addition to the effects of exogenous HMGB1 stimulation on expression of putatively associated mediators such as the LRRIg molecules, in the MO3.13, OGD-like immortalised cell line.

In addition, I also discuss neuropathological observations in both autopsy and biopsy tissue sampled *in vivo*. Clearly, comparing expression patterns between post-mortem and biopsy tissue is subject to a number of caveats, not least stability of the molecule relating to post-mortem interval and length of fixation time. Biopsy tissue is more likely to preserve antigen, due to quicker time to fixation, and relatively less time spent in formalin which may mask epitopes. Comparison with non-MS control biopsy tissue is thus most important and we are currently collecting material for exactly this purpose. As this was a preliminary study, these factors were not controlled for, and any observations reported below must be viewed in this context. In spite of this, the findings are novel and raise interesting scientific questions which are discussed below.

6.7.1 HMGB1 mRNA levels are increased by TGF-β1 stimulation but not by classically pro-inflammatory cytokines

The rationale behind using different cytokine mediators to stimulate OGD-like cells is to recapitulate the pathological microenvironment of EAE or MS and examine subsequent responses in this setting. Thus, MO3.13 cells were treated using a range of cytokines simulating exposure from pro-inflammatory sources e.g Th1 (IFNγ), Th17 (IL-6) cells and macrophages (IL-1β, TNFα), vs. anti-inflammatory stimulation using TGF-β1 (Qin et al. 2009; Rhodes et al. 2006a; Moransard et al. 2011).

As shown in figure 6.1, HMGB1 is expressed at baseline in the MO3.13 cell line as would be expected by this near ubiquitous protein (Muller et al. 2004; Yao et al. 2012), and as seen in the neuropathology work in chapters 3 and 4 in MS and non-MS control OGD.

Interestingly, our preliminary results show that TGF-β1 stimulation significantly increased HMGB1 mRNA expression compared to the other, classically pro-inflammatory cytokines. This raises the possibility that endogenous expression of HMGB1 in this OGD-like cell is more sensitive to anti-inflammatory as opposed to pro-inflammatory stimuli.

Recent work has highlighted the role of TGF-β released from the 'alternative' microglial phenotype (M2), and associated with anti-inflammatory function in the CNS (Pittet et al. 2013; Zhou et al. 2012). Induced M2 macrophages were also shown to produce anti-inflammatory cytokines such as IL-10 and TGF-β and their adoptive transfer into injured spinal cord stimulated local resulted in decreased spinal cord lesion volume, increased remyelination and preservation of neurons,

with significant functional improvement (Ma et al. 2014). As seen in chapter 4, there were increased numbers of CD68-positive cells in MS patients (lesional and non-lesional), vs. controls. M1/ M2 phenotypic characterisation was not performed, but recent work has demonstrated that M2 cells are present in non-lesional MS brain tissue, and thus may be the source of exogenous TGF-β in these regions of MS brain tissue (J van Horssen et al. 2012; Singh et al. 2013).

TGF-β signaling is principally mediated through receptor-activated Smad proteins. Olig1- an important transcription factor determining OGD linage (Xin et al. 2005)- is also a Smad 2/3 cofactor involved in TGF-β-induced cell motility in OGD and remyelination (Motizuki et al. 2013) (Kachar et al. 1986). Thus exogenous TGF-β may enhance OGD myelination and whether this is facilitated by HMGB1 needs to be determined in functional studies.

6.7.2 HMGB1 stimulation upregulates expression of its receptors, TLR4 and RAGE, potentially creating an autocrine loop

The work described above demonstrates HMGB1 and its receptors are expressed in the MO3.13 cells and therefore may also be expressed in OGD. The presence of exogenous HMGB1 increases expression of its receptors, likely contributing to a feed-forward loop whereby HMGB1-related responses in these OGD-like cells are propagated. Although the HMGB1 receptors, TLR4 and RAGE are expressed at very low levels at baseline, they appear to be highly sensitive to induction by exogenous bvHMGB1, as seen in figure 6.3. Oligodendrocytes are known to express TLR4, activating the MyD88 pathway and OPCs demonstrate JNK phosphorylation following direct ligation of TLR4, suggesting this signalling machinery is functionally active (Taylor et al. 2010). However, they are not

thought to secrete TNF or other pro-inflammatory cytokines via NFκB signaling as classically occurs in macrophages following TLR4 ligation for example (Yao et al. 2010; Balabanov et al. 2007). In-vivo injection of LPS in mice demonstrated profound upregulation of NG2-positive cells, thought to be OPCs, up to a distance of 6500μm in the surrounding regions in response to this. LPS-related signalling is likely to take place via TLR4 and so it is tempting to speculate that HMGB1 in the extracellular space may stimulate a similar response in upregulating immature OGD. Interestingly, this marked NG2+ upregulation started as early as 2h post-injection and preceded the arrival of macrophages from the periphery (Rhodes et al. 2006b). The authors postulated that demyelinating lesions opened the BBB, allowing platelet-derived factors entry and NG2-cell proliferation, in order to promote regenerative responses. The mechanism of NG2-cell positivity 'spreading' across the parenchyma was not specifically addressed but given my findings in the neuropathology work in non-lesional regions, this is particularly interesting.

In addition, TGF-β1 stimulation also significantly increased RAGE mRNA expression, although this was not observed with TLR4 expression. TGF-β1 stimulation has been shown to increase RAGE expression in different cell types, including articular chondrocytes where it induces a phenotypic switch to encourage hypertrophy (Narcisi et al. 2012). In addition, the role of TGF-β and RAGE signalling in cell proliferation has also been examined with some reports suggesting that their promotion is related to STAT5 signalling (Brizzi et al. 2004). Thus, the increased mRNA levels of RAGE in oligodendroglial-like MO3.13 cells following stimulation by HMGB1 and TGF- β1 may represent an effort to promote

cell proliferation, although specific signalling machinery activated following their ligation needs to be identified.

Further work has also demonstrated that the interaction between HMGB1 and TGF-β1 can have reparative function in general. In an alveolar cell injury model, wounded epithelial cell monolayers released HMGB1, which accelerated wound closure in the distal lung epithelium via the IL-1β-mediated activation of TGF-β1, and was postulated to be important in resolution of acute lung injury by promoting repair (Pittet et al. 2013). The authors further suggested that after injury, a controlled inflammatory response may have enhanced tissue repair and restoration of function, therefore a complete inhibition of this response by anti-inflammatory agents may have an adverse effect on lung epithelial repair. They described that if this inflammatory response becomes uncontrolled and maladaptive because of the severity or frequency of repeated insults, it may become an important mechanism in the development of lung fibrosis, for example. These same principles could be applied to CNS pathology, and as discussed in chapter 1, it may be that exogenous HMGB1's initial role is to stimulate regenerative processes, including in OGD cells.

Western blotting analysis demonstrated that total protein levels of RAGE also increased following stimulation by HMGB1, but interestingly were downregulated by all other mediators. Some of these mediators may not be directly linked to RAGE expression, hence lack of protein expression in response to their stimulation.

In summary, our work supports the contention that OGD-like cells appear to have a more active role in innate immunity than previously thought, clearly responding to stimulation by bvHMGB1 in particular.

6.7.3 AMIGO-1 expression is attenuated in a pro-inflammatory environment

AMIGO-1 and -2 appear to be involved with neuroprotective responses (Chen et al. 2006; Zhao et al. 2014b; Laeremans et al. 2013) whereas AMIGO-3 and LINGO-1 apparently augment neurodegenerative responses (Ahmed et al. 2013; Lee et al. 2014; Rudick et al. 2008). Thus, we wished to investigate LRRIg expression profiles in the first instance, and their relation with exogenously applied HMGB1. We know that HMGB1 induces expression of AMIGO-1 in developing neurites and wanted to test whether a similar situation was evident in OGD-like cells.

AMIGO-1 mRNA and protein levels are moderately increased by high doses of bvHMGB1 stimulation, but are unchanged compared to control by lower doses, as shown in figure 6.5. Expression at the total protein level is similarly evident at higher doses of bvHMGB1 stimulation but profoundly reduced by pro-inflammatory cytokines in particular, and indeed by low-dose HMGB1. These changes suggest that AMIGO-1 expression is either unchanged or downregulated when exposed to pro-inflammatory mediators in this cell type, although caution needs to be exercised in extrapolating this to the in-vivo setting.

The in-vitro findings thus inform the neuropathology work as AMIGO-1 expression was weak in the generally proinflammatory environment of the white

matter lesion. In non-overtly lesional WM, AMIGO-1 staining is also weakly seen in OGD and microglia/ macrophages, but not obviously in astrocytes.

However, this has implications in the context of MS where the tissue micro-environment is likely abnormal in both lesional and non-lesional regions, as discussed at length in this thesis. The main literature relating to AMIGO-1 highlights its apparent beneficial role in CNS function, with involvement in neurite growth/ survival in development (Kuja-Panula et al. 2003; Ono et al. 2003b; Zhao et al. 2014b; Chen et al. 2011). Thus, based on my work and the available literature, the possibility that reduction in AMIGO-1 levels in MS patients may result in loss of neuroprotective function warrants further exploration.

6.7.4 Neuronal AMIGO-1 expression in non-MS controls is reminiscent of Kv2.1 channel pattern of expression

In the post-mortem series, AMIGO-1 is robustly expressed in human brain tissue. It is predominantly expressed in neuronal and some perivascular cells in chronic/late active lesional tissue. Interestingly, the stromal background was significantly stronger in all non-MS control subjects, as was cell-specific staining in the GM. Expression patterns appear to be specific as both IgG controls and omission of the primary antibody demonstrate negative or weak staining only.

The neuronal staining pattern demonstrated a characteristic, punctate appearance around the neuronal soma and proximal dendrites. This was reminiscent of the pattern of AMIGO-1 expression described by Zhao et al in animal studies where it co-localised with Kv2.1 in specific clusters at the plasma membrane. Further experiments also suggested binding of AMIGO-1 to Kv2.1 (Chen et al. 2011; Zhao et al. 2014b) as well as functional dependence *in vivo*. They

were found to colocalise in mature but not early developing brain, suggesting that established function of AMIGO-1 in extension of developing neurites may not be its only role in mature brain. These findings led the authors to propose that AMIGO1 be regarded as an auxiliary subunit of the Kv2.1 channel and likely plays a role in central neuronal signalling.

Given this, the reduction in expression of AMIGO-1 in MS patients in our work is intriguing. Work by Jukkola et al demonstrated somatodendritic Kv2.1 channels significantly decrease with increasing severity of EAE (Jukkola et al. 2012). If AMIGO-1 was found to co-localise with Kv2.1 in humans as in zebrafish and mice, the findings in EAE corroborate our findings of apparent decreased expression AMIGO-1 in our MS patients. It is worth noting that AMIGO-1 expression was consistently observed in large pyramidal neurons in particular, which is consistent with the known expression pattern of Kv2.1 (Murakoshi & Trimmer 1999). We did not perform neuronal subpopulation analysis but it would be informative to perform a more detailed study examining this. Interestingly, in the early active lesion taken from a biopsy specimen in a patient with clinically-isolated syndrome, the staining pattern was similarly reduced, suggesting that this downregulation in AMIGO-1 expression may actually occur early in the disease course. This would also be consistent with the Kv2.1 pattern of expression in EAE, however, where expression was found to be reduced at peak relapse in a relapsing-remitting EAE model, but normalised in the remission phase (Jukkola et al. 2012).

Voltage-gated K+ channels (Kv channels) are a broad family of K+- selective ion channels that are critically important in the regulation of excitability in numerous

cells throughout the body. Kv2.1 channels form prominent clusters in somatodendritic regions of cortical/ hippocampal pyramidal neurons and spinal cord motor neurons (O'Connell et al. 2010; Misonou et al. 2004). It has a high threshold for activation and primarily regulates excitability during high-frequency firing in pyramidal neurons in response to excitatory stimuli (e.g., glutamate and increased cytoplasmic Ca2+) and cell stress. In this situation, it can alter punctate clustering into a more diffuse pattern over the neuronal soma (figure 6.18.) although whether this is driving pathology or represents a compensatory mechanism remains unclear.

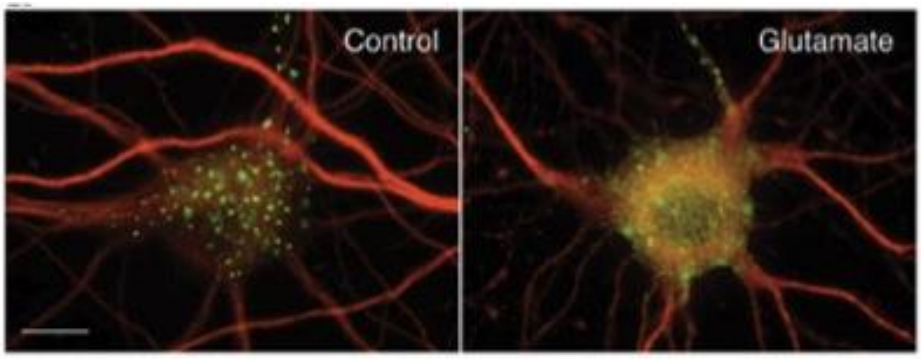

Figure 6.18. Kv2.1 expression changes from a clustered to a diffuse localisation upon stimulation with glutamate. Cultured neurons were incubated with 10 μM glutamate for 10 min at 37 °C. The cells were then fixed and stained for Kv2.1 (green) and MAP-2 (red). *Scale bar, 10 μm. Adapted from* (Misonou et al. 2004)

MS has been considered as a type of 'channelopathy', due to the dysregulation of many different ion channels in the disease (Schattling et al. 2014). Dalfampridine is a broad potassium channel inhibitor and is currently used as a symptomatic treatment in MS to enhance walking ability with modest success, primarily through enhanced conduction through demyelinated lesions (Jensen et al. 2014). However, use in routine clinical practice is limited by small gains in function and the development of adverse side-effects including-interestingly, trigeminal

neuralgia (Birnbaum & Iverson 2014). It is possible that the latter may result following inhibition of ion channels such as Kv2.1, which would normally serve to damp down neuronal hyperactivity.

Intracellular accumulation of sodium via channel dysfunction has also been extensively studied (Craner et al. 2004), but clinical trials employing sodium channel blockers have not been universally successful yet (Hayton et al. 2012). However, deeper understanding of the role of ion channels in MS pathology is an important aspect of future neuroprotective strategies and more recent studies have demonstrated early success with this, examining the role of acid-sensing ion channels (ASICs) (Arun et al. 2013). Their potential interaction with AMIGO-1 has not been studied before and would be of interest.

6.7.5 AMIGO-2 expression is suppressed by pro-inflammatory cytokines in vitro but expression is increased in active lesional MS tissue

Whilst AMIGO-2 is implicated in pathological processes such as tumour biology (Rabenau et al. 2004), in the CNS it appears to promote cellular survival (Ono et al. 2003a). AMIGO-2 mRNA levels were suppressed by pro-inflammatory cytokine stimulation such as IL-6 and TNF-α in particular (figure 6.8). However, at the total protein level, AMIGO-2 is not expressed at the expected 55kDa weight, and instead multiple faint bands at differing molecular weights are observed. This may represent lack of antibody specificity, but a lower MW product is consistently observed at 30kDa. Further work using stimulated fibroblasts have also shown that its expression is induced by TGF-β stimulation, but instead of multiple bands evident as in my work, 2 bands at 50kDa and 30kDa are consistently observed.

These independent findings possible cleavage of the molecule upon stimulation with TGF-β and warrant further exploration.

Neuropathological analysis of non-MS control tissue demonstrates robust AMIGO-2 staining, with a punctate staining pattern in the soma and proximal dendrites of neurons as seen with AMIGO-1. Although DAB reactivity is not stoichiometric as discussed, staining is particularly intense in control GM. As shown in figure 6.11 however, there is a reduction in staining intensity in MS brain tissue compared to non-MS control. Reduced neuronal staining persists in both post-mortem and biopsy tissue taken from the patient presenting with CIS.

In contrast, AMIGO-2 expression throughout the biopsy tissue is generally upregulated, particularly in OGD. Thus, although AMIGO-2 expression in neurons appeared to be reduced, the ready expression in OGD in this tissue suggests that it is induced in a pro-inflammatory microenvironment. Given the observation *in-vitro* that pro-inflammatory mediators suppress AMIGO-2 mRNA expression, this is unexpected and may relate to the unusual immunoblotting pattern evident in figure 6.6C. The antibody is specific to a 15 a.a peptide sequence near the c-terminal residues of the protein, therefore may represent a cleaved peptide from the cytoplasmic region, as alluded to earlier. Thus, whilst mRNA expression may be downregulated by pro-inflammatory mediators, this cytoplasmic region may be involved in pathophysiological processes. This is speculative and requires further investigation, which is underway.

The other important observation is that AMIGO-2 IR appeared to be both nuclear and membrane-bound. This distribution was similarly described by Ono et al in their original description of AMIGO2 or alivin-1 (Ono et al. 2003b), identifying its

crucial role in the depolarisation-dependent survival of cerebellar neurons. Cues for upregulation included Ca^{2+} signalling and expression was markedly reduced prior to apoptosis-related cell death, highlighting its importance in cell survival. Its nuclear and membrane-bound subcellular localisation was explained by other similar examples whereby signal-transducing receptors meant to be located at the plasma membrane are in fact located in the nucleus, such as EGFR and FGF receptors (Marti et al. 2001; Maher 1996). Curiously, they display transactivator activity and may function as transcription factors (Brosenitsch & Katz 2001). There is no evidence yet that AMIGO-2 may perform this function but its subcellular localisation warrants further evaluation of this.

In addition, they do not present images or directly refer to the characteristic punctate clustering around the soma and proximal dendrites that we observed in the human tissue, although they do describe AMIGO-2 expression in this exact location in neurons.

Thus, as with AMIGO-1 which displayed a similar pattern described above, its function may be related to cell survival against environmental stressors. Loss of expression may indicate impending cell death as described by Ono et al. However, it is also possible that the molecule is cleaved and this has pathogenic effects in non-neuronal cells, hence its upregulation in early active lesions. In-situ hybridisation would thus be particularly revealing in this context and forms the basis of future work.

6.7.6 AMIGO-3 expression is increased in an active inflammatory environment

The in-vitro work demonstrated that upregulation of AMIGO-3 was sensitive to all doses of bvHMGB1 stimulation, but particularly at lower doses, as seen in figure 6.9A. This suggests that OGD cells might upregulate AMIGO-3 in the presence of small amounts of extracellular HMGB1. The significance of this is unknown, but the importance of AMIGO-3 acting at the NgR/p75 receptor complex on axonal surfaces to activate RhoA signalling and potentiate neurodegenerative processes has been reported (Ahmed et al. 2013). It is tempting to speculate that extracellular HMGB1- presumably oxidised and hence pro-inflammatory- released by activated M1 phenotype macrophages/ microglia may potentiate neurodegenerative processes via this pathway, providing a potential mechanistic link between inflammatory and neurodegenerative processes. It is also worth noting that although levels of HMGB1 were significantly higher in the CSF of MS patients vs. controls in chapter 5, absolute levels detectable by the assay were low. Despite the fact that local HMGB1 levels in the parenchyma would be higher than those detectable in the CSF, the correlation with inflammatory cell numbers suggests that these relatively low levels would be more in keeping with inflammatory cell secretion vs necrotic release. The latter are seen in cases of trauma or bacterial infection for example, where CSF concentrations reach microgram levels. Thus, sensitivity to low levels of exogenous HMGB1 is an important finding and may well have pathological significance as described above.

Interestingly, other pro-inflammatory mediators appeared to have no effect on AMIGO-3 expression, suggesting an HMGB1-specific response. Further work is required to examine this in greater detail but it is an entirely novel and exciting avenue to further explore.

AMIGO-3 staining is undetectable in non-MS control autopsy tissue, and faintly evident in AL tissue blocks (figure 6.12). However, expression was markedly increased in biopsy tissue, in both early active lesions and in surrounding non-lesional grey and white-matter. Once again, a range of control conditions failed to reveal evidence of non-specific IR. Increased expression in active lesional regions may be linked to its function at the NgR complex on the axonal membrane to activate RhoA signalling in the presence of myelin proteins (Ahmed et al. 2013). However, anti-AMIGO-3 IR is also seen in the non-lesional white matter in a punctate pattern adjacent to OGD (figure 6.16C; inset), which may also be relevant in this context, despite the lack of overt demyelination. Certainly, myelin proteins present in the outer surface of the myelin sheath and adjacent to the axonal surface, such as MAG, act at this receptor complex suggesting that these changes may occur early in the pathology.

The predominant subcellular localisation was nuclear; in macrophages, OGD and–most-strikingly- neuronal nuclei. The latter demonstrated clear anti-AMIGO-3 IR around the chromatin structure within virtually all neuronal nuclei. The apparent similarity with the HMGB1 neuronal staining pattern in this active lesional tissue (figure 3.4G; inset) is of further interest as HMGB1 is known to act as a facilitator of transcription due to its ability to alter chromatin structure (Müller et al. 2004). Whether AMIGO-3 also demonstrates this function and whether it is beneficial or detrimental to the cell is unclear at present.

Unlike the AMIGO-1 and -2 rabbit polyclonal antibodies which were commercially produced, the AMIGO-3 antibody was a mouse monoclonal antibody, produced following our design of the peptide sequence used for mouse immunisation (*MD,*

personal communication). The AMIGO-1 and -2 antibodies used short peptide sequences from the cytoplasmic regions as immunogens, whereas the AMIGO-3 antibody included the signal sequence in the extracellular domain, suggesting that its nuclear presence reflects the whole molecule being present here, or else possibly cleavage of this domain.

6.7.7 The relationship between HMGB1 and LINGO-1 may reflect direct interaction between inflammatory and degenerative processes

A similar pattern to that observed with AMIGO-3 was noted in LINGO-1 analyses, as this was also sensitive to upregulation of mRNA levels by HMGB1 at all doses used. In addition, proinflammatory cytokines upregulated mRNA expression of LINGO-1, but this response was significantly less when compared to bvHMGB1 as seen in figure 6.8. Using Western blotting, low dose bvHMGB1 appeared to stimulate LINGO-1 expression, with 20ng/ml consistently producing increased levels at both the mRNA and protein levels, whilst IL-1β also reliably induced LINGO-1 expression. Factors influencing expression of LINGO-1 itself have not been explored in great detail however, and the observation that both exogenous HMGB1 and IL-1β appear to increase total protein levels of LINGO-1 is relatively novel. Activated, pro-inflammatory microglia/ macrophages are well- known to release both of these molecules, and so may in fact serve as another link between inflammatory and degenerative processes in MS.

The standard protocol for management of MO3.13 cells requires low serum conditions, but I compared expression of LINGO-1 in both high and low-serum conditions. The results were remarkably consistent, in that LINGO-1 total protein expression was consistently induced in a low-serum setting, with virtually none

detectable in high serum conditions. Whilst this finding requires further investigation, it provides interesting insight into this molecule. It suggests that global cellular stress, as represented by lower serum conditions, also stimulates the expression of LINGO-1. At the same time however, the specific purpose of serum depletion is to encourage MO3.13 cell differentiation toward a more mature OGD phenotype, and that cellular differentiation itself is a bioenergetically demanding process, placing the cell under metabolic stress. Serum depletion classically induces cells to withdraw from the proliferative cell cycle and enter the quiescent G_0/G_1 phase, facilitating differentiation (Van Rechem et al. 2010; Pirkmajer & Chibalin 2011). Thus, this observation likely reflects the fact that mature OGD are known to express LINGO-1 (Mi et al. 2005; Mi et al. 2007), although the possibility that it represents sensitivity to more global cellular stressors cannot be excluded and could be further explored.

It has also been shown that LINGO-1 is not directly implicated in specific, adaptive neuroimmune aspects of MOG-induced EAE, but rather reflects CNS-specific processes. For example, the induction phase of EAE in LINGO-1 knock-out (KO) mice showed no difference when compared to wild-type mice (Mi et al. 2007). In addition, T-cell function was similar between the two groups, as shown by cytokine profile produced by encephalitogenic T-cells of LINGO-1 KO rodents and by the ability of the latter cells to induce EAE following adoptive transfer. However, the reverse of this i.e. adoptive transfer of encephalitogenic T-cells from wild-type rodents into LINGO-1 KO's attenuated the signs and symptoms of EAE. Thus, LINGO-1 blockade either using Lingo-1 KO's or by direct antagonism using a specific IgG antagonist produced CNS-specific benefits; with improved

functional outcomes of lower EAE scores in addition to physiological parameters such as diffusion tensor imaging (DTI), where fibre tract integrity was superior in LINGO-1 KO's vs. wild-types. In addition, both myelin staining using toluidine-blue and electron microscopy confirmed the presence of enhanced remyelination.

The relationship between HMGB1 and LINGO-1 in particular is novel and has not been explored previously. The sensitivity of both AMIGO-3 and LINGO-1 to exogenous HMGB1 is of particular interest when considering our CSF work, whereby levels were higher in MS patients vs. controls but otherwise low in absolute terms, as discussed above with respect to AMIGO-3 sensitivity to exogenous HMGB1. Thus, extracellular HMGB1 may behave in a classically pro-inflammatory manner, and so upregulation of down-stream molecule expression such as LINGO-1 and AMIGO-3 especially may be an indicator of potentially damaging, pro-inflammatory processes classically associated with MS. Thus, this in-vitro work identifies an important potential link between pro-inflammatory processes occurring in MS and ensuing degenerative signalling pathways which may be activated as a result.

6.7.8 LINGO-1 expression may be upregulated in OGD in early active lesional tissue but not in non-MS control or chronic MS brain tissue

In non-MS control tissue, neuronal expression in the grey matter was clearly evident, with a similarly punctate staining pattern around the neuronal soma and proximal dendrites observed with AMIGO-1 and -2 IR. It is expressed in a similar pattern in the grey matter of 'NAWM' tissue blocks, although subjectively it appeared that fewer cells demonstrated this pattern. The staining intensity in non-lesional grey matter of AL blocks was reduced and the majority of neurons

demonstrated a more homogenous cytoplasmic pattern of expression, frequently highlighting axonal expression as shown in figure 6.15D. This suggests that chronic lesion activity may exhaust LINGO-1 expression, as most of the lesions were late or chronic active lesions in the autopsy series. In addition, the more diffuse expression pattern observed over the neuronal soma suggests that LINGO-1 may also redistribute its characteristically punctate clusters of protein along the cell surface, as discussed earlier with respect to AMIGO-1. The normal association of LINGO-1 with ion channel physiology has not been described before, and certainly not reported in human brain.

It also consistently appears that LINGO-1 expression was increased in the white matter of non-MS control subjects, although- importantly- this was predominantly within the stroma or along axons and was not directly expressed in the OGD cell body. In contrast, WM expression was generally reduced in MS patients from the autopsy series, as shown in the low power views in figure 6.13A-C. However, IR was clearly evident in OGD cell bodies as well as astrocytes in both lesional and non-lesional white matter in the early active lesional biopsy tissue, as well as the punctate staining throughout the stroma as seen in the post-mortem tissue. In addition, we observed a markedly spiculated appearance of foamy macrophages, suggesting that LINGO-1 was staining positively for myelin breakdown products, possibly derived from myelin stripped from axons. Thus, we can speculate that LINGO-1 is expressed along the myelin sheath in human brain, ready to interact with the NgR at the axonal surface, as has been shown in animal work (Mi et al. 2005; Mi et al. 2004). In-situ hybridisation studies would be of great interest here in particular, as it may be that lipophages themselves don't express LINGO-1, and

instead reflects uptake of cellular debris from damaged cells. Recent work has shown that foamy macrophages are anti-inflammatory in their behaviour (Boven et al. 2006) and it is possible that these macrophages are attempting to curb degenerative activity involving LINGO-1 and RhoA signalling, and this acts as a cue for subsequent phagocytosis. These changes suggest that LINGO-1 is clearly upregulated in the early stages of MS, both in and around active lesions.

LINGO-1 expression has been examined in human brain before, and some aspects of our findings in human brain are consistent this work (Satoh et al. 2007). Theirs was a smaller series of 5 MS patients but with 10 non-MS control patients, although they do not present IHC evidence of the staining pattern in the latter group of patients. They found prominent staining in astrocytes and macrophages, in addition to neurons, but questioned the data from Mi et al (Mi et al. 2005), as they did not find LINGO-1 expression in OGD. In addition, their western blotting data suggests that total protein expression is generally downregulated in MS tissue, compared to non-MS neurological control tissue. However, the tissue used for analysis by this group was chronic active lesional tissue, and I have similarly shown that there is a general down-regulation of LINGO-1 expression in this setting. In contrast, my findings in the early active lesional biopsy tissue reveal that LINGO-1 likely has an important role in the acute stages of lesion formation, and found clear evidence of OGD staining as described above.

Interestingly, the expression pattern in neurons was also slightly different in our study compared to the work by this group. Although we rarely observed the characteristic, punctate staining pattern seen in non-MS control tissue in MS brains, we observed relatively weak staining with diffuse IR over the soma and

into the axon. The work by Satoh et al also demonstrated smooth cytoplasmic staining around a particular subgroup of pontine neurons. We used exactly the same antibody as used in this study, and so different antibody specificities are not attributable to differences. They do not state where in the pons these neurons are located but those forming part of the locus coeruleus, in the posterior area of the rostral pons, comprise the nucleus pigmentosus pontis i.e. 'heavily pigmented nucleus of the pons'. Although we did not have samples from a similar area, we have seen in our own work that in basal ganglia regions, pigmented neurons have this exact appearance, regardless of antibody specificity. For this reason, we did not include these areas for own analysis. Thus, it is possible that melanin pigmentation may have contributed to the strongly IR, cytoplasmic staining pattern rather than specific IR per se. On the other hand, this smooth appearance may reflect similar changes to those observed by ourselves, albeit at a greater intensity. This would presumably be due to the same process as described earlier, from a punctate staining pattern to a more diffuse one. For the rest of the analyses, they presented tissue taken from frontal lobe regions, and it would have been of interest to compare their LINGO-1 staining in these regions with our expression pattern, particularly in their non-MS control subjects, as we analysed tissue predominantly located in these regions also.

In summary, it is likely that LINGO-1 has an important role early in MS-related pathology and so any analysis of human material would need to take this into account. Our in-vitro work suggests that exogenous HMGB1 increased expression of LINGO-1 both at the mRNA and total protein level in OGD-like MO3.13 cells. The higher levels of HMGB1 observed in the CSF of MS patients as described in chapter

5, may reflect its secretion by immune cells and thus propagate LINGO-1 mediated neurodegenerative processes within active lesional regions. It is thus possible that this represents a link between neuroinflammatory and degenerative processes in MS.

6.8 Limitations

In vitro work: Immortalised cell lines can be obtained relatively easily for use in multiple experiments, giving an idea of how the equivalent cell might behave *in-vivo*. However, potential drawbacks include their transformed nature as they are in the proliferative cell cycle stage, and this can skew results. To minimise potential confounders, we ensured that they were passaged when no more than 70% confluent, all experiments were performed at low passage numbers and used identical culturing conditions including when repeating experiments for 'n' numbers. We also performed experiments at n≥3, in order to reduce the chance of random observations. However, results can only be interpreted within this model; using a primary cell line would recapitulate responses closer to the *in vivo* environment, although animal models and human tissue analysis (see below) would give a greater understanding of the disease specific biology.

Ex vivo (neuropathology) work: General limitations when using both biopsy and autopsy material have been discussed in chapters 3 and 4. In this chapter of work, no attempt was made to semi-quantitate observed IR, and thus was a purely descriptive study. This introduces obvious bias but due to the novel nature of the examination of these molecules in human brain tissue, the main purpose was simply to observe findings that would inform a more detailed study going forward. The same principle holds for the fact that relatively few patients were examined

in both control and MS subjects, and findings would need replication in a larger study.

In-situ hybridisation studies would be of interest in order to confirm the presence of mRNA expression of the molecules. Co-localisation studies, preferably using fluorescent-IHC would also be particularly helpful in identifying which cell types express the relevant molecules with greater certainty.

6.9 Summary

HMGB1 and its receptors are expressed in the MO3.13 OGD-like cell line, and potentially demonstrate autocrine behaviour to propagate sensitivity to exogenous HMGB1. HMGB1 also appears to directly upregulate mRNA and/ or protein expression of all LRRIg molecules, compared to a range of other pro- and anti-inflammatory mediators in this cell line, which is a novel finding and supports our original hypotheses.

I have also examined AMIGO molecule expression for the first time in human brain tissue. AMIGO-1 and AMIGO-2 expression demonstrated similar patterns, with characteristically punctate clusters of expressed protein, situated around the neuronal soma and in the proximal dendrites. This pattern has been seen before in association with AMIGO-1, with Kv2.1 ion channel expression in neurons. I found that IR was reduced in neurons in MS brain tissue, as also seen with Kv2.1 expression in EAE (Jukkola et al. 2012), raising the intriguing possibility that AMIGO molecule expression in MS highlights neuronal stress, resulting from either Wallerian degeneration as a result of distal demyelination or local neuronal metabolic stress. Thus, augmenting AMIGO-1 activity in particular may have

therapeutic implications as part of a neuroprotective strategy but further work is required to take forward our preliminary findings.

AMIGO-3 expression was virtually undetectable in the post-mortem tissue but demonstrated striking changes in the early active lesional biopsy tissue, particularly in neurons, as did LINGO-1 expression. Thus AMIGO-3 and LINGO-1 are clearly upregulated in an acutely inflamed microenvironment. In addition, the in-vitro work demonstrated that both AMIGO-3 and LINGO-1 appear to be particularly sensitive to low-dose HMGB1 stimulation; a finding which is potentially relevant when considering the relatively low levels of HMGB1 detected in the CSF of MS patients, albeit significantly higher when compared to control subjects. Given their known interaction at the NgR and potentiation of neurodegenerative processes, this phenomenon may highlight a novel link between inflammatory and neurodegenerative processes. In addition, the expression profile in non-lesional regions suggests that this process can occur more widely in MS brain tissue. The results thus support the suggestion that blockade of LINGO-1 may be beneficial in MS (Pepinsky et al. 2014) but we would also add that inhibiting the activity of AMIGO-3 is another potential neuroprotective, therapeutic strategy which warrants further investigation.

7

General Discussion

The need to understand the basis of disease progression in MS remains unmet. Disease modifying therapies have significantly changed how MS is managed, due to the relative suppression of relapses on treatment. However, the evidence that progression of disability is halted by these treatments is inconclusive, despite this aspect of the disease generating profound morbidity and socio-economic burden. Evidence derived from biomarkers such as MRI and CSF analysis have suggested that disease processes driving MS are ongoing, in between relapses that affect clinically eloquent regions. This is reflected neuropathologically, as isolated inflammatory lesions are not the only manifestation of MS-related pathology. Thus, this PhD project investigated MS-related disease processes distal to classical inflammatory lesions in the neuropathological study and changes occurring predominantly in non-relapsing MS patients in the CSF study. The potential implications of these findings are considered in the series of questions, below.

7.1 Does exogenous HMGB1 activate degenerative pathways in MS?

The novel finding arising from this project is that HMGB1 expression was increased throughout the brain tissue of MS patients, vs non-MS controls, as seen in Chapters 3 and 4. CD68-positive, HMGB1-positive macrophages were clearly evident in early and late-active MS lesions as well as in non-lesional regions in both autopsy tissue from patients with progressive MS and in biopsy tissue taken *in-vivo* from a patient with a clinically isolated syndrome (CIS). In addition, as seen in Chapter 5, CSF HMGB1 levels were increased in MS patients at an early stage of disease vs. non-inflammatory control patients. However, absolute levels are much lower compared to those seen in the setting of CNS trauma and cellular necrosis for example, raising the possibility that secreted HMGB1 from either immune cells

or from the parenchyma itself may be contributing. The best-characterised role of HMGB1 is its pro-inflammatory effects upon release from activated macrophages as discussed in detail in Chapter 1, General Introduction (Wang et al., 1999), therefore its presence in the extracellular space may result in deleterious consequences.

In Chapter 6, exogenous HMGB1 stimulation in-vitro upregulated expression of its receptors in OGD-like cells (MO3.13 cell line), potentially propagating chronic inflammation and damage to OGD. As discussed below, expression of the LRRIg molecules, AMIGO-3 and LINGO-1 is also significantly increased by bvHMGB1 compared to other pro-inflammatory mediators. These molecules have both been reported to propagate neurodegenerative processes by signalling through the p75/NTR/ NgR complex (Mi et al. 2004; Ahmed et al. 2013). It is therefore tempting to suggest that exogenous HMGB1 may influence degenerative processes via AMIGO-3 and LINGO-1-associated RhoA signalling. Their expression in non-lesional regions early-on in CIS brain tissue, also suggests that pathological processes are taking place globally in MS brain tissue, and thus treatments targeting these may have a greater impact on disability.

Anti-LINGO1 trials are already underway as a novel MS therapy. It has recently been reported that 1st line disease-modifying agents are cost-effective and may slow progression of disease as assessed at 6y-follow up using robust statistical models (Palace et al. 2015). However, caution when interpreting this data should be used in certain instances. For example, censoring of patients when they switched to a non-scheme drug would probably select out the patients with more severe disease, potentially reducing disability progression estimates over time.

The importance of accurate assessment of treatment impact upon disability outcomes across the board are highlighted by this, and neuroprotective drugs such as anti-LINGO agents are attempting to address this. Phase I trials using anti-LINGO-1 agents demonstrated an equivalent incidence of side-effects compared to placebo, with no adverse events (Tran et al. 2014). More recently, a phase II trial examining the effects of high-dose anti-LINGO1 infusion on optic neuritis outcomes (the 'RENEW' trial; NCT01721161) demonstrated superiority over placebo as it was associated with a 34% recovery of optic nerve latency vs. placebo, but not with secondary outcomes such as change in the thickness of retinal layers or with improved visual function itself (http://www.biogenidec.com/research_product_pipeline.aspx?ID=5778). Whilst the improvements are modest in the primary outcome over 24 weeks, with no benefit in secondary outcomes, it is a landmark trial due to its novelty. It marks a departure from traditional immunomodulatory therapeutic approaches which have dominated the scene in MS over the past 25 years. The 'SYNERGY' trial using varying anti-LINGO-1 doses is ongoing, recruiting patients with both RRMS and SPMS and is due to complete in 2016. This will be a more detailed examination of outcome measures and its findings will be of significant interest. However, the modest benefits as seen in RENEW suggest that anti-LINGO-1 therapy is likely the first in a long line of future neuroprotective therapies. Our findings of increased AMIGO-3 expression in the context of an actively inflamed MS lesion from a biopsy specimen suggests that it has role at the earliest stage of disease. This, along with previously published data (Ahmed et al. 2013), suggests that AMIGO-3 antagonism may also demonstrate therapeutic potential and warrants further exploration.

7.2 Does endogenous HMGB1 act as a protective agent in MS?

We postulated earlier that exogenous HMGB1 may contribute to neurodegeneration via the LRRIg molecules. However, it is possible that endogenous HMGB1 expression in CNS cells reflects different cellular processes and further consideration of this forms the basis of future work.

Upregulation of genes involved in ischaemic pre-conditioning, in normal-appearing white matter (NAWM) have been demonstrated, suggesting that the background brain parenchyma in MS is under stress and that OGD themselves express multiple members of the STAT6 signalling pathway. This suggests an anti-inflammatory, potentially protective phenotype in these cells. Protective responses in OGD have also been suggested in other studies, where their secretion of damage-related molecules, such as αB-crystallin have been shown to trigger an immunoregulatory response in surrounding macrophage/ microglial cells (Amor et al. 2010; Jack van Horssen et al. 2012; Van Noort et al. 2010; Singh et al. 2013; Van der Valk & Amor 2009; van Noort et al. 2010; Zeis et al. 2008; Graumann et al. 2003; Ingram et al. 2014; Bsibsi et al. 2013b; Barnett et al. 2009). In the nucleus, HMGB1 acts as a master-regulator of small heat-shock protein expression, of which αB-crystallin/ HSPB5, is an example. Thus, HMGB1 may be linked to the processes described above, in driving protective responses in OGD via αB-crystallin/ HSPB5 expression upon the appropriate cues.

As discussed in section 1.4 of the General Introduction, redox modification relating to intensity of cellular stress, generally dictates the subsequent function

of HMGB1. Despite the apparently precarious balance between protective and destructive pathways in non-lesional MS brain tissue (Zeis et al. 2008), the degree of tissue stress is likely to be moderate in these regions. In this context, HMGB1 may be secreted from its normal position in the nucleus into the cytosol, in a reduced form (figure 1.6). It is unknown whether this redox configuration of HMGB1 induces an immunoregulatory profile in surrounding microglia/ macrophages akin to αB-crystallin, and would be of great interest to further explore. However, reduced HMGB1 is known to augment autophagic pathways, and we know that it has multi-functional roles in this process (figure 1.5), both in the cytoplasm and extracellularly. It was not possible to reliably discern cytoplasmic translocation using brightfield microscopy in this study as OGD have scant cytoplasm evident in their cell bodies. Despite this, occasional cells were seen which may have demonstrated this in the brain tissue (Section 4.5.2; figure 4.2), and in preliminary in-vitro fluorescence-ICC experiments using stimulated MO3.13 cells (data not shown). HMGB1 also has an important role in autophagy within the nucleus itself, and so even if the increased OGD expression of HMGB1 in MS patients vs. controls reflects nuclear vs. cytoplasmic subcellular localisation, this may reflect autophagic processes in any case. Thus, one mechanism of OGD protection may be related to potentiation of autophagic pathways in MS brain tissue. Given the critically important role of HMGB1 in mediating autophagy, this may be relevant to the findings presented in this thesis.
Autophagy pathways in MS have not been explored in detail before, although autophagic activity in T-cells has been reported, contributing to chronicity of infection (Pua et al. 2007). Basal levels of autophagy are low in non-diseased brain tissue using the GFP-LC3 autopahgy mouse model (Mizushima et al. 2004) but as

discussed in chapter one, section 1.4.5.5, its upregulation in other neurological diseases is increasingly recognised (Frake et al. 2015). Interestingly, it has also recently been reported that mTOR/p70S6K signalling can distinguish between routine, maintenance-level autophagy from autophagic cell death during influenza-A infection (Datan, E et al. 2015). LC3 is critically important for transport and maturation of the autophagosome. A recent study found that its expression was significantly upregulated in surviving OGD in Nasu-Hakola disease (NHD)- a rare autosomal recessive disorder characterized by sclerosing leukoencephalopathy, using IHC in human brain (Satoh et al. 2014). In contrast, expression was not detected in OGD in the lesional rim of chronic demyelinating lesions in MS patients, although was evident in Iba-1-positive microglia/ macrophages. As I have demonstrated in this work, expression of HMGB1 was lower in similar chronic lesional/ peri-lesional areas and we can speculate that this is related to exhaustion of autophagic pathways. Accordingly, analysis of LC3-II expression in our acutely demyelinating biopsy tissue specimen would be of great interest in taking this forward.

In vivo studies utilising the Long–Evans shaker (*les*) rat model with severe CNS dysmyelination and subsequent demyelination during development have also revealed autophagic changes specifically affecting OGD (Kwiecien et al. 1998). Oligodendrocytes from *les* rats have been shown to accumulate cytoplasmic vesicles and electron microscopic studies have characterised these as early and late autophagosomes, along with an increase in autophagy markers using IHC and Western blotting (Smith et al. 2013). Interestingly, upregulating autophagy promoted membrane extensions in *les* oligodendrocytes *in vitro*. *In vivo,*

intermittent fasting promoted autophagy and increased the proportion of myelinated axons as well as myelin sheath thickness in both *les* and control rats. Thus this work identified an important role for autophagy in promoting the survival and function of oligodendrocytes, which may be relevant in MS.

The potential importance of autophagy is readily apparent in neurodegenerative diseases, where helping clearance of intracellular protein aggregates may improve cellular function. Both in vitro and in vivo work using mouse models has demonstrated that upregulation of autophagy results in clearance of a wide range of aggregate-prone molecules, particularly smaller, soluble aggregates (Chen et al. 2012; Winslow et al. 2010). Statins are thought to augment autophagic processes amongst other roles (Ghavami et al. 2012), and have recently been shown to ameliorate whole-brain atrophy measures and some disability outcomes in patients with progressive MS- a clinical cohort who have traditionally been refractory to disease modulation. This seminal study demands more pre-clinical work be done to investigate the mechanisms behind these observations, but we can speculate that potentiation of autophagy may be one aspect of this apparently neuroprotective effect. More recently, the specific peptide sequence of the functionally-relevant domain of the pro-autophagic molecule beclin-1 has been identified. This peptide has been modified to enhance cellular penetration and directly augment autophagic clearance of intracellular aggregates, with relevance to diseases such as Huntington's (Shoji-Kawata et al. 2013).

We can thus speculate that one aspect of increased HMGB1 expression in oligodendrocytes found in this study may be reflecting autophagic processes in

MS vs. non-MS control brain tissue. Whilst MS is by no means a classical neurodegenerative disease with known intranuclear inclusion proteins, it would be of interest to further explore its potential role here in more detail, given the importance of HMGB1 in autophagy. Certainly, if further evidence is presented which suggests that autophagy is relevant to the pathogenesis, this would represent an entirely novel therapeutic avenue of MS research.

Further work demonstrated that autophagic clearance of protein aggregates were identified in OGD precursors (NG2 cells) in Alzheimer's disease mouse models (W. Li et al. 2013). NG2 cells have established roles in neuroprotection and immune modulation, particularly in the setting of myelinogenesis but also in neuronal survival (for review, see: Boda & Buffo 2014). Intense anti-amphoterin /HMGB1 immunoreactivity (IR) in OGD of relatively immature phenotype were seen in the developing rodent (M. M. Daston & Ratner 1994). Morphologically, they were reminiscent of NG2 cells, although not specifically tested for, and adult rodents showed much weaker IR in comparison. My work in human tissue found that OGD were weakly HMGB1-positive in some non-MS control subjects, but IR was profoundly increased in MS brain tissue in comparison. This also raises the possibility that subpopulations of OGD may demonstrate immature cell characteristics in MS patients as discussed earlier. We know that OGD precursor cells (OPCs) are numerous, certainly in peri-lesional regions of MS brain (G Wolswijk 1998; Chang et al. 2000a). The presence of myelin proteins is traditionally thought to create an inhibitory environment and to halt differentiation into mature OGD (Mi et al. 2007). However, a potential explanation for the widespread increase in anti-HMGB1 IR in MS patients might be that the

brain has an endogenous strategy for dealing with cellular stress; by employing widespread changes within OGD themselves. One mechanism may be via re-expression of developmental pathways (John et al. 2002; Chang et al. 2000b) and/ or by increasing cellular proliferation rate (Pua et al. 2007). HMGB1 is known to have an important role in proliferation, and its deletion by the use of RNAi lentiviral vectors has been shown to significantly decrease cell proliferation (Song et al. 2012). In addition, deletion of HMGB1 rendered cells vulnerable to apoptosis induced by oxaliplatin and mediated by the caspase-3 pathway. Whether this occurs in OGD is purely speculative, and relatively little experimental evidence exists at present to support or refute the notion.

A final explanation for increased anti-HMGB1-IR is that HMGB1 may be sensing direct infection within the CNS by bacterial or viral pathogens. We know that HMGB1 is a promiscuous sensor of many different pathogens, viruses in particular (Yanai et al.2009), and it is possible that OGD are either infected themselves or else are responding to signals released by other cells e.g. macrophages/microglia. This hypothesis is purely speculative, and direct assay of infective antigens using novel sequencing techniques could be performed to further investigate this.

7.3 Is AMIGO-1 involved in regulating neuronal excitability in MS brain tissue?

This family of molecules have multiple CNS-specific roles including cell adhesion, fasciculation and myelination. I have demonstrated that their expression is upregulated by HMGB1 in the MO3.13, OGD-like cell-line, particularly in the case of AMIGO-3 and LINGO-1. The latter two molecules have both been reported to propagate neurodegenerative processes by signalling through the p75/NTR/ NgR

complex (Mi et al. 2004; Ahmed et al. 2013), with potential pathological relevance as described above. However, the changes in expression of AMIGO-1 in particular highlight potential mechanisms of cellular stress in MS brain tissue compared to control. Whilst expressed robustly in neurons of non-MS control patients in a classically punctate pattern, I found that this was significantly reduced in both post-mortem and biopsy MS tissue. The expression of AMIGO-1 has been intimately linked to the expression and function of the potassium channel kv2.1 (Peltola et al. 2011). The redistribution of ion channels may be influenced by demyelinating insult due to the metabolic changes resulting in the cell, or else reflect intrinsic neuronal dysfunction. The changes in AMIGO-1 expression pattern may be reflecting similar pathology, although dedicated co-localisation studies examining Kv2.1 with AMIGO-1 would thus be informative.

7.4 Conclusion

The purpose of this project was to further explore novel markers of disease in MS. Generalised pathology in MS brain tissue is increasingly recognised to occur at early stages of disease, but the molecular mechanisms underlying these changes are not completely understood. HMGB1 is a well-characterised molecule, known to act as a link between sterile damage and innate immune mechanisms. My analysis of HMGB1 expression patterns in human subjects with and without MS, in non-lesional regions of tissue in neuropathological work, and in non-relapsing patients with respect to the CSF study, demonstrated novel findings. The significantly increased expression of HMGB1 in non-lesional regions in the neuropathological work lends support to the concept of MS as a generalised CNS disorder, rather than a disease characterised by development of focal,

inflammatory lesions alone. As these changes were noted early-on in the disease course in chapter 3, this suggests that these widespread pathological changes do not necessarily occur exclusively in progressive MS patients. Despite the majority of MS patients being in remission rather than relapse, higher HMGB1 CSF concentrations were found in MS patients vs. controls, further suggesting that the disease process is ongoing in between relapses, as supported by the FLC and NfL data also.

The finding that exogenous HMGB1 stimulation significantly upregulates AMIGO-3 and LINGO-1 expression in OGD-like cells suggests that it may influence neurodegenerative processes, thus acting as a potential link between neurodegenerative and inflammatory pathways. However, endogenously expressed HMGB1 is likely to be in a different redox state to oxidised, pro-inflammatory, extracellular HMGB1. In this setting, it may augment neuroprotective pathways, possibly by participating in autophagic processes within OGD. We remain hopeful that neuroprotective therapeutic approaches may yield greater benefit for patients with progressive MS than those currently available.

7.5 Future perspectives

7.5.1 Further HMGB1 expression analysis in MS brain tissue

Whilst I have presented a comprehensive assessment of HMGB1 expression in MS and non-MS control patients, and between different sub-types of tissue, further work in this area would help to confirm these findings. Using snap-frozen non-MS control and MS human brain tissue, further studies include:

(i) Determination of HMGB1 mRNA expression in different cell types using in-situ hybridisation analysis

(ii) Confirmation of cell types expressing HMGB1 with co-localisation studies using IHC-Fl. Cell markers would include olig2/ Nogo-A for OGD, CD68 for macrophages/ microglia, CD3 for pan T- lymphocytes, CD20 for (immature) B-cells, NeuN for neurons, GFAP for astrocytes and NG2 for OPC.

(iii) Compare HMGB1 staining pattern in a range of non-MS and non-neurological control subjects using biopsy material

(iv) Western-blotting (WB) analysis to assess total expression of HMGB1 in MS vs non- MS brain tissue. Pre-screening of each block with MBP/ oil-red O to assess extent of demyelination in all tissue blocks would be essential. Performing sub-cellular localisation studies would be useful; for example, a lower nuclear: cytoplasmic anti-HMGB1 expression ratio in MS vs control tissue would suggest cytoplasmic translocation and the associated implications with pathology in MS tissue. In addition, examination of post-translational modifications of HMGB1 such as acetylation status in the non-MS vs MS control subjects would also be of great interest, although assessment of redox status would ultimately be most informative.

7.5.2 HMGB1, autophagy and MS

A novel area of research relates to the potential role of autophagy in MS, and how HMGB1 may be implicated, given its established role in this cellular process. Neuropathological tissue analysis of LC3, for example, would be of interest in the biopsy tissue in particular. To address this in-vitro, MO3.13 cells and primary OGD cultures could be used to investigate:

(i) basal levels of autophagy e.g. measuring LC3B or LC3 I:LC3II ratios

(ii) whether these levels change if HMGB1 is knocked-down e.g. using RNAi lentiviral vectors ($HMGB1^{-/-}$) or if it is stably over-expressed.

(iii) the effect of these changes on cellular viability; for example using a triplex assay to measure cell viability, cytotoxicity and apoptosis in the same sample.

This experimental set-up can then be used to investigate the effects of cellular stress e.g. following hypoxia/ starvation on autophagy markers and cell viability in wild-type or $HMGB1^{-/-}$ OGD. Once this model is established, selected pro-autophagic drugs could be screened to determine whether autophagy is augmented in OGD, whether they affect cell viability and how any changes compare to manipulations in HMGB1 expression.

Further in-vivo studies could be designed on the basis of data arising from the above experiments.

7.5.3 LRRIg molecules and MS

This is also a novel area and there are a number of potential avenues of research arising from this project. The following suggestions explore research questions arising from the project directly and indirectly:

(i) Confirmation of cell types expressing each of the LRRIg molecules with co-localisation studies using IHC-Fl, as outlined in 7.5.1(i)

(ii) Determination of LRRIg mRNA expression in different cell types using in-situ hybridisation analysis

(iii) Compare LRRIg staining pattern in a range of non-MS and non-neurological control subjects using biopsy material, in particular AMIGO-3

(iv) Co-localisation studies of AMIGO-1 and Kv2.1 in human brain tissue using in-situ hybridisation and IHC-Fl

(v) In-vitro work using primary neuronal cell cultures, for example:

a. To perform sub-cellular localisation studies to examine levels of AMIGO-3 expression under different experimental conditions to further investigate the nuclear localisation of AMIGO-3 seen in the NAGM in the biopsy tissue work

b. Investigate whether AMIGO-3 knock-down e.g. using RNAi lentivial vectors alters cell viability using the triplex assay as described above

(vi) In-vivo work using the EAE rodent model of MS to investigate whether AMIGO-3 antagonism ameliorates clinical outcomes

REFERENCES

Acunzo, J., Katsogiannou, M. & Rocchi, P., 2012. Small heat shock proteins HSP27 (HspB1), αB-crystallin (HspB5) and HSP22 (HspB8) as regulators of cell death. *The international journal of biochemistry & cell biology*, 44(10), pp.1622–31.

Ahmed, Z. et al., 2013. AMIGO3 is an NgR1/p75 co-receptor signalling axon growth inhibition in the acute phase of adult central nervous system injury. *PloS one*, 8(4), p.e61878.

Albert, M. et al., 2007. Extensive Cortical Remyelination in Patients with Chronic Multiple Sclerosis. *Brain Pathology*, 17(2), pp.129–138.

Allen, I. V & McKeown, S.R., 1979. A histological, histochemical and biochemical study of the macroscopically normal white matter in multiple sclerosis. *Journal of the neurological sciences*, 41(1), pp.81–91.

Aloisi, F. et al., 2010. Detection of Epstein-Barr virus and B-cell follicles in the multiple sclerosis brain: what you find depends on how and where you look. *Brain : a journal of neurology*, 133(Pt 12), p.e157.

Amor, S. et al., 2010. Inflammation in neurodegenerative diseases. *Immunology*, 129, pp.154–169.

Andersson, Å. et al., 2008. Pivotal Advance: HMGB1 expression in active lesions of human and experimental multiple sclerosis. *Journal of Leukocyte Biology*, 84(5), pp.1248–1255.

Andersson, U. & Tracey, K.J., 2011. HMGB1 is a therapeutic target for sterile inflammation and infection. *Annual review of immunology*, 29, pp.139–62.

Anon, Vitamin D and Multiple sclerosis: Are we still in the dark? Available at: http://m.neurology.org/content/82/10_Supplement/P6.144

Arun, T. et al., 2013. Targeting ASIC1 in primary progressive multiple sclerosis: evidence of neuroprotection with amiloride. *Brain : a journal of neurology*, 136(Pt 1), pp.106–15.

Asano, T. et al., 2011. High mobility group box 1 in cerebrospinal fluid from several neurological diseases at early time points. *The International journal of neuroscience*, 121(8), pp.480–4.

Au, A.K. et al., 2012. Cerebrospinal fluid levels of high-mobility group box 1 and cytochrome C predict outcome after pediatric traumatic brain injury. *Journal of neurotrauma*, 29(11), pp.2013–21.

Babbe, H. et al., 2000. Clonal expansions of CD8(+) T cells dominate the T cell infiltrate in active multiple sclerosis lesions as shown by micromanipulation and single cell polymerase chain reaction. *The Journal of experimental medicine*, 192(3), pp.393–404.

Balabanov, R. et al., 2007. Interferon-gamma-oligodendrocyte interactions in the regulation of experimental autoimmune encephalomyelitis. *The Journal of neuroscience : the official journal of the Society for Neuroscience*, 27(8), pp.2013–24.

Barker, P.A., 2004. p75NTR is positively promiscuous: novel partners and new insights. *Neuron*, 42(4), pp.529–33.

Barkhof, F., 2002. The clinico-radiological paradox in multiple sclerosis revisited. *Current opinion in neurology*, 15(3), pp.239–45.

Barnett, M.H. et al., 2009. Immunoglobulins and complement in postmortem multiple sclerosis tissue. *Annals of neurology*, 65(1), pp.32–46.

Barnett, M.H. & Prineas, J.W., 2004. Relapsing and remitting multiple sclerosis: Pathology of the newly forming lesion. *Annals of Neurology*, 55(4), pp.458–468.

Barnett, M.H. & Prineas, J.W., 2004. Relapsing and remitting multiple sclerosis: pathology of the newly forming lesion. *Ann Neurol*, 5, pp.458–468.

Barsness, K.A. et al., 2004. Hemorrhage-induced acute lung injury is TLR-4 dependent. *American journal of physiology. Regulatory, integrative and comparative physiology*, 287(3), pp.R592–9.

Beck, R.W. et al., 1993. The effect of corticosteroids for acute optic neuritis on the subsequent development of multiple sclerosis. The Optic Neuritis Study Group. *The New England journal of medicine*, 329(24), pp.1764–9.

Berger, T. et al., 1997. Experimental autoimmune encephalomyelitis: the antigen specificity of T lymphocytes determines the topography of lesions in the central and peripheral nervous system. *Laboratory investigation; a journal of technical methods and pathology*, 76(3), pp.355–64.

Bhakar, A.L. et al., 2003. Apoptosis induced by p75NTR overexpression requires Jun kinase-dependent phosphorylation of Bad. *The Journal of neuroscience : the official journal of the Society for Neuroscience*, 23(36), pp.11373–81.

Bianchi, M.E., 2007. DAMPs, PAMPs and alarmins: all we need to know about danger. *Journal of leukocyte biology*, 81(1), pp.1–5.

Birnbaum, G. & Iverson, J., 2014. Dalfampridine may activate latent trigeminal neuralgia in patients with multiple sclerosis. *Neurology*, 83(18), pp.1610–2.

Bjartmar, C. et al., 2001. Axonal loss in normal-appearing white matter in a patient with acute MS. *Neurology*, 57, pp.1248–1252.

Bloomgren, G. et al., 2012. Risk of natalizumab-associated progressive multifocal leukoencephalopathy. *The New England journal of medicine*, 366(20), pp.1870–80.

Bo, L. et al., 2003. Subpial demyelination in the cerebral cortex of multiple sclerosis patients. *J Neuropathol Exp Neurol*, 62, pp.723–732.

Boda, E. & Buffo, A., 2014. Beyond cell replacement: unresolved roles of NG2-expressing progenitors. *Frontiers in neuroscience*, 8, p.122.

Bogie, J.F.J., Stinissen, P. & Hendriks, J.J.A., 2014a. Macrophage subsets and microglia in multiple sclerosis. *Acta neuropathologica*.

Bogie, J.F.J., Stinissen, P. & Hendriks, J.J.A., 2014b. Macrophage subsets and microglia in multiple sclerosis. *Acta neuropathologica*.

Bonaldi, T. et al., 2003. Monocytic cells hyperacetylate chromatin protein HMGB1 to redirect it towards secretion. *Embo J*, 22(20), pp.5551–5560.

Boven, L.A. et al., 2006. Myelin-laden macrophages are anti-inflammatory, consistent with foam cells in multiple sclerosis. *Brain : a journal of neurology*, 129(Pt 2), pp.517–26.

Brettschneider, J. et al., 2010. The chemokine CXCL13 is a prognostic marker in clinically isolated syndrome (CIS). C. Kleinschnitz, ed. *PloS one*, 5(8), p.e11986.

Brizzi, M.F. et al., 2004. RAGE- and TGF-beta receptor-mediated signals converge on STAT5 and p21waf to control cell-cycle progression of mesangial cells: a possible role in the development and progression of diabetic nephropathy. *FASEB journal : official publication of the Federation of American Societies for Experimental Biology*, 18(11), pp.1249–51.

Brosenitsch, T.A. & Katz, D.M., 2001. Physiological patterns of electrical stimulation can induce neuronal gene expression by activating N-type calcium channels. *The Journal of neuroscience : the official journal of the Society for Neuroscience*, 21(8), pp.2571–9.

BROWNELL, B. & HUGHES, J.T., 1962. The distribution of plaques in the cerebrum in multiple sclerosis. *Journal of neurology, neurosurgery, and psychiatry*, 25, pp.315–20.

Bsibsi, M. et al., 2013a. Alpha-B-crystallin induces an immune-regulatory and antiviral microglial response in preactive multiple sclerosis lesions. *Journal of neuropathology and experimental neurology*, 72(10), pp.970–9.

Bsibsi, M. et al., 2013b. Alpha-B-crystallin induces an immune-regulatory and antiviral microglial response in preactive multiple sclerosis lesions. *Journal of neuropathology and experimental neurology*, 72(10), pp.970–9.

Bsibsi, M. et al., 2002. Broad expression of Toll-like receptors in the human central nervous system. *Journal of neuropathology and experimental neurology*, 61(11), pp.1013–21.

Bsibsi, M. et al., 2014. Demyelination during multiple sclerosis is associated with combined activation of microglia/macrophages by IFN-γ and alpha B-crystallin. *Acta neuropathologica*, 128(2), pp.215–29.

Buntinx, M. et al., 2004. Cytokine-induced cell death in human oligodendroglial cell lines. II: Alterations in gene expression induced by interferon-gamma and tumor necrosis factor-alpha. *Journal of neuroscience research*, 76(6), pp.846–61.

Bustin, M., 1999. Regulation of DNA-dependent activities by the functional motifs of the high-mobility-group chromosomal proteins. *Mol Cell Biol*, 19(8), pp.5237–5246.

Cabarrocas, J. et al., 2003. Effective and selective immune surveillance of the brain by MHC class I-restricted cytotoxic T lymphocytes. *European journal of immunology*, 33(5), pp.1174–82.

Calabresi, P.A., 2011. Inflammation in multiple sclerosis--sorting out the gray matter. *The New England journal of medicine*, 365(23), pp.2231–3.

Calogero, S. et al., 1999. The lack of chromosomal protein Hmg1 does not disrupt cell growth but causes lethal hypoglycaemia in newborn mice. *Nature genetics*, 22(3), pp.276–80.

Carswell, R., 1838. *Pathological anatomy: illustrations of the elementary forms of disease*,

Casula, M. et al., 2011. Toll-like receptor signaling in amyotrophic lateral sclerosis spinal cord tissue. *Neuroscience*, 179(0), pp.233–243.

Chang, A. et al., 2000a. NG2-positive oligodendrocyte progenitor cells in adult human brain and multiple sclerosis lesions. *The Journal of neuroscience : the official journal of the Society for Neuroscience*, 20(17), pp.6404–12.

Chang, A. et al., 2000b. NG2-positive oligodendrocyte progenitor cells in adult human brain and multiple sclerosis lesions. *The Journal of neuroscience : the official journal of the Society for Neuroscience*, 20(17), pp.6404–12.

Charcot, J., 1868. Histologie de la sclérose en plaques.

Chard, D. & Miller, D., 2009. Is multiple sclerosis a generalized disease of the central nervous system? An MRI perspective. *Current Opinion in Neurology*, 22(3), pp.214–218.

Chen, M.S. et al., 2000. Nogo-A is a myelin-associated neurite outgrowth inhibitor and an antigen for monoclonal antibody IN-1. *Nature*, 403(6768), pp.434–439.

Chen, S. et al., 2012. Autophagy dysregulation in amyotrophic lateral sclerosis. *Brain pathology (Zurich, Switzerland)*, 22(1), pp.110–6.

Chen, Y. et al., 2006. AMIGO and friends: An emerging family of brain-enriched, neuronal growth modulating, type I transmembrane proteins with leucine-rich repeats (LRR) and cell adhesion molecule motifs. *Brain Research Reviews*, 51(2), pp.265–274.

Chen, Y., Hor, H.H. & Tang, B.L., 2011. AMIGO is expressed in multiple brain cell types and may regulate dendritic growth and neuronal survival. *Journal of Cellular Physiology*.

Chertoff, M. et al., 2011. Neuroprotective and neurodegenerative effects of the chronic expression of tumor necrosis factor α in the nigrostriatal dopaminergic circuit of adult mice. *Experimental neurology*, 227(2), pp.237–51.

Coisne, C., Lyck, R. & Engelhardt, B., 2013. Live cell imaging techniques to study T cell trafficking across the blood-brain barrier in vitro and in vivo. *Fluids and barriers of the CNS*, 10(1), p.7.

Comi, G. et al., 2001. Effect of early interferon treatment on conversion to definite multiple sclerosis: a randomised study. *The Lancet*, 357(9268), pp.1576–1582.

Compston, A., 1988. The 150th anniversary of the first depiction of the lesions of multiple sclerosis. *Journal of neurology, neurosurgery, and psychiatry*, 51(10), pp.1249–52.

Confavreux, C. et al., 2000. Relapses and progression of disability in multiple sclerosis. *The New England journal of medicine*, 343(20), pp.1430–8.

Cook, S. ed., *Handbook Of Multiple Sclerosis Third Edition* 3rd ed.,

Craner, M.J. et al., 2004. Molecular changes in neurons in multiple sclerosis: Altered axonal expression of Nav1.2 and Nav1.6 sodium channels and Na+/Ca2+ exchanger. *Proceedings of the National Academy of Sciences of the United States of America*, 101(21), pp.8168–8173.

Crews, F.T. et al., 2013. High mobility group box 1/Toll-like receptor danger signaling increases brain neuroimmune activation in alcohol dependence. *Biological psychiatry*, 73(7), pp.602–12.

Daston, M.M. & Ratner, N., 1994. Amphoterin (P30, HMG-1) and RIP are early markers of oligodendrocytes in the developing rat spinal cord. *Journal of Neurocytology*, 23(5), pp.323–332.

Daston, M.M. & Ratner, N., 1994. Amphoterin (P30, HMG-1) and RIP are early markers of oligodendrocytes in the developing rat spinal cord. *Journal of neurocytology*, 23(5), pp.323–32.

Dean, G. & Elian, M., 1997. Age at immigration to England of Asian and Caribbean immigrants and the risk of developing multiple sclerosis. *Journal of neurology, neurosurgery, and psychiatry*, 63(5), pp.565–8.

Degryse, B. et al., 2001. The high mobility group (HMG) boxes of the nuclear protein HMG1 induce chemotaxis and cytoskeleton reorganization in rat smooth muscle cells. *The Journal of cell biology*, 152(6), pp.1197–206.

Deisenhammer, F. et al., 2009. EFNS guidelines on disease-specific CSF investigations. *European journal of neurology : the official journal of the European Federation of Neurological Societies*, 16(6), pp.760–70.

Dumitriu, I.E. et al., 2005. Release of high mobility group box 1 by dendritic cells controls T cell activation via the receptor for advanced glycation end products. *J Immunol*, 174(12), pp.7506–7515.

Dumitriu, I.E. et al., 2005. Requirement of HMGB1 and RAGE for the maturation of human plasmacytoid dendritic cells. *European journal of immunology*, 35, pp.2184–2190.

Duvanel, C.B. et al., 2004. Tumor necrosis factor-alpha and alphaB-crystallin up-regulation during antibody-mediated demyelination in vitro: a putative protective mechanism in oligodendrocytes. *Journal of neuroscience research*, 78(5), pp.711–22.

Dyment, D.A. et al., 2004. An extended genome scan in 442 Canadian multiple sclerosis-affected sibships: a report from the Canadian Collaborative Study Group. *Human molecular genetics*, 13(10), pp.1005–15.

Ebers, G.C. et al., 2004. Parent-of-origin effect in multiple sclerosis: observations in half-siblings. *Lancet*, 363(9423), pp.1773–4.

Edinger, A.L. & Thompson, C.B., 2004. Death by design: apoptosis, necrosis and autophagy. *Current opinion in cell biology*, 16(6), pp.663–9.

Engelhardt, B., 2008. The blood-central nervous system barriers actively control immune cell entry into the central nervous system. *Current pharmaceutical design*, 14(16), pp.1555–65.

Engelhardt, B., Wolburg-Buchholz, K. & Wolburg, H., 2001. Involvement of the choroid plexus in central nervous system inflammation. *Microscopy research and technique*, 52(1), pp.112–29.

Evangelou, N., 2001. Size-selective neuronal changes in the anterior optic pathways suggest a differential susceptibility to injury in multiple sclerosis. *Brain*, 124(9), pp.1813–1820.

Evangelou, N., 2012. The only way to manage neurodegeneration in MS is to prevent it with effective anti-inflammatory therapy: yes. *Multiple sclerosis (Houndmills, Basingstoke, England)*, 18(12), pp.1680–1.

Fan, J. et al., 2007. Hemorrhagic shock induces NAD(P)H oxidase activation in neutrophils: role of HMGB1-TLR4 signaling. *Journal of immunology (Baltimore, Md. : 1950)*, 178(10), pp.6573–80.

Fang, P., Schachner, M. & Shen, Y.Q., 2012. HMGB1 in Development and Diseases of the Central Nervous System. *Mol Neurobiol*, 45(3), pp.499–506.

Feinstein, A. et al., 1992. Clinically isolated lesions of the type seen in multiple sclerosis: a cognitive, psychiatric, and MRI follow up study. *Journal of neurology, neurosurgery, and psychiatry*, 55(10), pp.869–76.

Felts, P.A. et al., 2005. Inflammation and primary demyelination induced by the intraspinal injection of lipopolysaccharide. *Brain : a journal of neurology*, 128(Pt 7), pp.1649–66.

Filippi, M. et al., 2001. Diffusion tensor magnetic resonance imaging in multiple sclerosis. *Neurology*, 56(3), pp.304–11.

Filippi, M. & Rocca, M.A., 2005. MRI evidence for multiple sclerosis as a diffuse disease of the central nervous system. *Journal of neurology*, 252 Suppl , pp.v16–24.

Filippi, M., Tortorella, C. & Bozzali, M., 1999. Normal-appearing white matter changes in multiple sclerosis: the contribution of magnetic resonance techniques. *Multiple sclerosis (Houndmills, Basingstoke, England)*, 5(4), pp.273–82.

Filippini, G. et al., 2013. Immunomodulators and immunosuppressants for multiple sclerosis: a network meta-analysis. *The Cochrane database of systematic reviews*, 6, p.CD008933.

Fisniku, L.K. et al., 2008a. Disability and T2 MRI lesions: a 20-year follow-up of patients with relapse onset of multiple sclerosis. *Brain : a journal of neurology*, 131(Pt 3), pp.808–17.

Fisniku, L.K. et al., 2008b. Disability and T2 MRI lesions: a 20-year follow-up of patients with relapse onset of multiple sclerosis. *Brain : a journal of neurology*, 131(Pt 3), pp.808–17.

Fiuza, C. et al., 2003. Inflammation-promoting activity of HMGB1 on human microvascular endothelial cells. *Blood*, 101(7), pp.2652–2660.

Florez-McClure, M.L. et al., 2004. The p75 neurotrophin receptor can induce autophagy and death of cerebellar Purkinje neurons. *The Journal of neuroscience : the official journal of the Society for Neuroscience*, 24(19), pp.4498–509.

Floyd, E. & McShane, T.M., Development and use of biomarkers in oncology drug development. *Toxicologic pathology*, 32 Suppl 1, pp.106–15.

Fournier, A.E., GrandPre, T. & Strittmatter, S.M., 2001. Identification of a receptor mediating Nogo-66 inhibition of axonal regeneration. *Nature*, 409(6818), pp.341–6.

Frake, R.A. et al., 2015. Autophagy and neurodegeneration. *Journal of Clinical Investigation*, 125(1), pp.65–74.

Fu, M. et al., 2004. Acetylation of nuclear receptors in cellular growth and apoptosis. *Biochemical pharmacology*, 68(6), pp.1199–208.

Fuchs, E., 1998. A Structural Scaffolding of Intermediate Filaments in Health and Disease. *Science*, 279(5350), pp.514–519.

Gallo, A. et al., 2005. Diffusion-tensor magnetic resonance imaging detects normal-appearing white matter damage unrelated to short-term disease activity in patients at the earliest clinical stage of multiple sclerosis. *Archives of neurology*, 62(5), pp.803–8.

Gao, H.M. et al., 2011. HMGB1 acts on microglia Mac1 to mediate chronic neuroinflammation that drives progressive neurodegeneration. *J Neurosci*, 31(3), pp.1081–1092.

Gava, G. et al., 2014. Long-term influence of combined oral contraceptive use on the clinical course of relapsing-remitting multiple sclerosis. *Fertility and sterility*, 102(1), pp.116–22.

Geurts, J.J.G. et al., 2003. Altered expression patterns of group I and II metabotropic glutamate receptors in multiple sclerosis. *Brain : a journal of neurology*, 126(Pt 8), pp.1755–66.

Ghavami, S. et al., 2012. Apoptosis, autophagy and ER stress in mevalonate cascade inhibition-induced cell death of human atrial fibroblasts. *Cell death & disease*, 3, p.e330.

Ghosh, A., Carnahan, J. & Greenberg, M.E., 1994. Requirement for BDNF in activity-dependent survival of cortical neurons. *Science (New York, N.Y.)*, 263(5153), pp.1618–23.

Glasnović, A. et al., 2014. Decreased Level of sRAGE in the Cerebrospinal Fluid of Multiple Sclerosis Patients at Clinical Onset. *Neuroimmunomodulation*, 21(5), pp.226–33.

Von Glehn, F. et al., 2012. Disappearance of cerebrospinal fluid oligoclonal bands after natalizumab treatment of multiple sclerosis patients. *Multiple sclerosis (Houndmills, Basingstoke, England)*, 18(7), pp.1038–41.

Goodin, D.S. et al., 2012. Cause of death in MS: long-term follow-up of a randomised cohort, 21 years after the start of the pivotal IFNβ-1b study. *BMJ open*, 2(6), p.e001972–.

Hayakawa, K., Qiu, J. & Lo, E.H., 2010. Biphasic actions of HMGB1 signaling in inflammation and recovery after stroke. *Annals of the New York Academy of Sciences*, 1207, pp.50–7.

Hayton, T. et al., 2012. Longitudinal changes in magnetisation transfer ratio in secondary progressive multiple sclerosis: data from a randomised placebo controlled trial of lamotrigine. *Journal of neurology*, 259(3), pp.505–14.

He, Z. et al., 2012. HMGB1 promotes the differentiation of Th17 via up-regulating TLR2 and IL-23 of CD14+ monocytes from patients with rheumatoid arthritis. *Scandinavian journal of immunology*, 76(5), pp.483–90.

Hedström, A.K. et al., 2009. Tobacco smoking, but not Swedish snuff use, increases the risk of multiple sclerosis. *Neurology*, 73(9), pp.696–701.

Hendriks, J.J. et al., 2005. Macrophages and neurodegeneration. *Brain Res Brain Res Rev*, 48, pp.185–195.

Hernán, M.A., Olek, M.J. & Ascherio, A., 2001. Cigarette smoking and incidence of multiple sclerosis. *American journal of epidemiology*, 154(1), pp.69–74.

Hickman, S.J., 2003. Corticosteroids do not prevent optic nerve atrophy following optic neuritis. *Journal of Neurology, Neurosurgery & Psychiatry*, 74(8), pp.1139–1141.

Höhne, C. et al., 2013a. High mobility group box 1 prolongs inflammation and worsens disease in pneumococcal meningitis. *Brain : a journal of neurology*, 136(Pt 6), pp.1746–59.

Höhne, C. et al., 2013b. High mobility group box 1 prolongs inflammation and worsens disease in pneumococcal meningitis. *Brain : a journal of neurology*, 136(Pt 6), pp.1746–59.

Hori, O. et al., 1995. The Receptor for Advanced Glycation End Products (RAGE) Is a Cellular Binding Site for Amphoterin. *Journal of Biological Chemistry*, 270(43), pp.25752–25761.

Van Horssen, J. et al., 2012. Clusters of activated microglia in normal-appearing white matter show signs of innate immune activation. *J Neuroinflammation*, 9, p.156.

Van Horssen, J. et al., 2012. Clusters of activated microglia in normal-appearing white matter show signs of innate immune activation. *Journal of neuroinflammation*, 9, p.156.

Hou, W. et al., 2013. Strange attractors: DAMPs and autophagy link tumor cell death and immunity. *Cell death & disease*, 4, p.e966.

Goodwin, G.H., Sanders, C. & Johns, E.W., 1973. A new group of chromatin-associated proteins with a high content of acidic and basic amino acids. *Eur J Biochem*, 38(1), pp.14–19.

Graumann, U. et al., 2003. Molecular changes in normal appearing white matter in multiple sclerosis are characteristic of neuroprotective mechanisms against hypoxic insult. *Brain Pathol*, 13, pp.554 – 73.

Greenberg, B.M. et al., 2013. Interferon beta use and disability prevention in relapsing-remitting multiple sclerosis. *JAMA neurology*, 70(2), pp.248–51.

Greenfield's Neuropathology. Volume I; 8th Ed.

De Groot, C.J. et al., 2001. Post-mortem MRI-guided sampling of multiple sclerosis brain lesions: increased yield of active demyelinating and (p)reactive lesions. *Brain*, 124, pp.1635–1645.

Gunnarsson, M. et al., 2011. Axonal damage in relapsing multiple sclerosis is markedly reduced by natalizumab. *Annals of neurology*, 69(1), pp.83–9.

Haq, E. et al., 2003. Molecular mechanism of psychosine-induced cell death in human oligodendrocyte cell line. *Journal of Neurochemistry*, 86(6), pp.1428–1440.

Harrer, A. et al., 2013. Cerebrospinal fluid parameters of B cell-related activity in patients with active disease during natalizumab therapy. *Multiple sclerosis (Houndmills, Basingstoke, England)*, 19(9), pp.1209–12.

Hassan-Smith, G. & Douglas, M.R., 2011. Epidemiology and diagnosis of multiple sclerosis. *British journal of hospital medicine (London, England : 2005)*, 72(10), pp.M146–51.

Hauser, S.L., Chan, J.R. & Oksenberg, J.R., 2013. Multiple sclerosis: Prospects and promise. *Annals of neurology*, 74(3), pp.317–27.

Hayakawa, K., Pham, L.-D.D., et al., 2012. Astrocytic high-mobility group box 1 promotes endothelial progenitor cell-mediated neurovascular remodeling during stroke recovery. *Proceedings of the National Academy of Sciences of the United States of America*, 109(19), pp.7505–10.

Hayakawa, K., Miyamoto, N., et al., 2012. High-mobility group box 1 from reactive astrocytes enhances the accumulation of endothelial progenitor cells in damaged white matter. *Journal of neurochemistry*.

Hayakawa, K., Nakano, T., et al., 2010. Inhibition of reactive astrocytes with fluorocitrate retards neurovascular remodeling and recovery after focal cerebral ischemia in mice. *Journal of cerebral blood flow and metabolism : official journal of the International Society of Cerebral Blood Flow and Metabolism*, 30(4), pp.871–82.

Howe, C.L. et al., 2014. Neuromyelitis optica IgG stimulates an immunological response in rat astrocyte cultures. *Glia*, 62(5), pp.692–708.

Huang, Q. & Figueiredo-Pereira, M.E., 2010. Ubiquitin/proteasome pathway impairment in neurodegeneration: therapeutic implications. *Apoptosis : an international journal on programmed cell death*, 15(11), pp.1292–311.

Huseby, E.S. et al., 2001. A pathogenic role for myelin-specific CD8(+) T cells in a model for multiple sclerosis. *The Journal of experimental medicine*, 194(5), pp.669–76.

Huttunen, H.J. et al., 2000. Coregulation of neurite outgrowth and cell survival by amphoterin and S100 proteins through receptor for advanced glycation end products (RAGE) activation. *The Journal of biological chemistry*, 275(51), pp.40096–105.

Huttunen, H.J. & Rauvala, H., 2004. Amphoterin as an extracellular regulator of cell motility: from discovery to disease. *Journal of Internal Medicine*, 255(3), pp.351–366.

Hwang, C.-S. et al., 2013. Elevated serum autoantibody against high mobility group box 1 as a potent surrogate biomarker for amyotrophic lateral sclerosis. *Neurobiology of disease*, 58, pp.13–8.

Ingram, G. et al., 2014. Complement activation in multiple sclerosis plaques: an immunohistochemical analysis. *Acta neuropathologica communications*, 2, p.53.

Ito, I., Fukazawa, J. & Yoshida, M., 2007. Post-translational methylation of high mobility group box 1 (HMGB1) causes its cytoplasmic localization in neutrophils. *The Journal of biological chemistry*, 282(22), pp.16336–44.

Ito, Y. et al., 2011. Increased levels of cytokines and high-mobility group box 1 are associated with the development of severe pneumonia, but not acute encephalopathy, in 2009 H1N1 influenza-infected children. *Cytokine*, 56(2), pp.180–7.

Jacobs, L.D. et al., 2000. Intramuscular interferon beta-1a therapy initiated during a first demyelinating event in multiple sclerosis. CHAMPS Study Group. *The New England journal of medicine*, 343(13), pp.898–904.

Jayaraman, L. et al., 1998. High mobility group protein-1 (HMG-1) is a unique activator of p53. *Genes & Development*, 12(4), pp.462–472.

Jensen, H.B. et al., 2014. 4-Aminopyridine for symptomatic treatment of multiple sclerosis: a systematic review. *Therapeutic advances in neurological disorders*, 7(2), pp.97–113.

Jeppsson, A. et al., 2013. Idiopathic normal-pressure hydrocephalus: pathophysiology and diagnosis by CSF biomarkers. *Neurology*, 80(15), pp.1385–92.

Ji, B. et al., 2006. LINGO-1 antagonist promotes functional recovery and axonal sprouting after spinal cord injury. *Molecular and cellular neurosciences*, 33(3), pp.311–20.

John, G.R. et al., 2002. Multiple sclerosis: re-expression of a developmental pathway that restricts oligodendrocyte maturation. *Nature medicine*, 8(10), pp.1115–21.

Jube, S. et al., 2012. Cancer cell secretion of the DAMP protein HMGB1 supports progression in malignant mesothelioma. *Cancer research*, 72(13), pp.3290–301.

Jukkola, P.I. et al., 2012. K+ channel alterations in the progression of experimental autoimmune encephalomyelitis. *Neurobiology of disease*, 47(2), pp.280–93.

Kabat, E.A., Moore, D.H. & Landow, H., 1942. AN ELECTROPHORETIC STUDY OF THE PROTEIN COMPONENTS IN CEREBROSPINAL FLUID AND THEIR RELATIONSHIP TO THE SERUM PROTEINS. *The Journal of clinical investigation*, 21(5), pp.571–7.

Kachar, B., Behar, T. & Dubois-Dalcq, M., 1986. Cell shape and motility of oligodendrocytes cultured without neurons. *Cell and Tissue Research*, 244(1).

Kajander, T. et al., 2011. Crystal Structure and Role of Glycans and Dimerization in Folding of Neuronal Leucine-Rich Repeat Protein AMIGO-1. *Journal of Molecular Biology*, 413(5), pp.1001–1015.

Kapoor, R. et al., 2010. Lamotrigine for neuroprotection in secondary progressive multiple sclerosis: a randomised, double-blind, placebo-controlled, parallel-group trial. *Lancet neurology*, 9(7), pp.681–8.

Kazama, H. et al., 2008. Induction of Immunological Tolerance by Apoptotic Cells Requires Caspase-Dependent Oxidation of High-Mobility Group Box-1 Protein. *Immunity*, 29(1), pp.21–32.

Khademi, M. et al., 2013. Intense inflammation and nerve damage in early multiple sclerosis subsides at older age: a reflection by cerebrospinal fluid biomarkers. *PloS one*, 8(5), p.e63172.

Khalil, M. et al., 2013. CSF neurofilament and N-acetylaspartate related brain changes in clinically isolated syndrome. *Multiple sclerosis (Houndmills, Basingstoke, England)*, 19(4), pp.436–42.

Kim, J.-B. et al., 2006. HMGB1, a novel cytokine-like mediator linking acute neuronal death and delayed neuroinflammation in the postischemic brain. *The Journal of neuroscience : the official journal of the Society for Neuroscience*, 26(24), pp.6413–21.

Kim, S.-W. et al., 2012. Glycyrrhizic acid affords robust neuroprotection in the postischemic brain via anti-inflammatory effect by inhibiting HMGB1 phosphorylation and secretion. *Neurobiology of disease*, 46(1), pp.147–56.

Kobe, B., 2001. The leucine-rich repeat as a protein recognition motif. *Current Opinion in Structural Biology*, 11(6), pp.725–732.

Krumbholz, M. et al., 2006. Chemokines in multiple sclerosis: CXCL12 and CXCL13 up-regulation is differentially linked to CNS immune cell recruitment. *Brain : a journal of neurology*, 129(Pt 1), pp.200–11.

Kuja-Panula, J. et al., 2003. AMIGO, a transmembrane protein implicated in axon tract development, defines a novel protein family with leucine-rich repeats. *The Journal of Cell Biology*, 160(6), pp.963–973.

Kutzelnigg, A. et al., 2005. Cortical demyelination and diffuse white matter injury in multiple sclerosis. *Brain : a journal of neurology*, 128(Pt 11), pp.2705–12.

Kwiecien, J.M. et al., 1998. Morphological and morphometric studies of the dysmyelinating mutant, the Long Evans shaker rat. *Journal of neurocytology*, 27(8), pp.581–91.

Laeremans, A. et al., 2013. AMIGO2 mRNA expression in hippocampal CA2 and CA3a. *Brain structure & function*, 218(1), pp.123–30.

Laird, M.D. et al., 2014. High mobility group box protein-1 promotes cerebral edema after traumatic brain injury via activation of toll-like receptor 4. *Glia*, 62(1), pp.26–38.

Landtblom, A.-M. et al., 2010. The first case history of multiple sclerosis: Augustus d'Esté (1794-1848). *Neurological sciences : official journal of the Italian Neurological Society and of the Italian Society of Clinical Neurophysiology*, 31(1), pp.29–33.

Lassmann, H., 2008. Mechanisms of inflammation induced tissue injury in multiple sclerosis. *Journal of the neurological sciences*, 274(1-2), pp.45–7.

Leal, M.C. et al., 2013. Interleukin-1β and tumor necrosis factor-α: reliable targets for protective therapies in Parkinson's Disease? *Frontiers in cellular neuroscience*, 7, p.53.

Lee, D.H.S., Strittmatter, S.M. & Sah, D.W.Y., 2003. Targeting the Nogo receptor to treat central nervous system injuries. *Nature reviews. Drug discovery*, 2(11), pp.872–8.

Lee, S.C. & Raine, C.S., 1989. Multiple sclerosis: oligodendrocytes in active lesions do not express class II major histocompatibility complex molecules. *Journal of neuroimmunology*, 25(2-3), pp.261–6.

Lee, X. et al., 2014. LINGO-1 regulates oligodendrocyte differentiation by inhibiting ErbB2 translocation and activation in lipid rafts. *Molecular and cellular neurosciences*.

Lee, X. et al., 2007a. NGF regulates the expression of axonal LINGO-1 to inhibit oligodendrocyte differentiation and myelination. *The Journal of neuroscience : the official journal of the Society for Neuroscience*, 27(1), pp.220–5.

Lee, X. et al., 2007b. NGF regulates the expression of axonal LINGO-1 to inhibit oligodendrocyte differentiation and myelination. *The Journal of neuroscience : the official journal of the Society for Neuroscience*, 27(1), pp.220–5.

Lee, Y. et al., 2012. Oligodendroglia metabolically support axons and contribute to neurodegeneration. *Nature*, 487(7408), pp.443–448.

Lehnardt, S. et al., 2003. Activation of innate immunity in the CNS triggers neurodegeneration through a Toll-like receptor 4-dependent pathway. *Proceedings of the National Academy of Sciences of the United States of America*, 100(14), pp.8514–9.

Lehnardt, S. et al., 2002. The Toll-Like Receptor TLR4 Is Necessary for Lipopolysaccharide-Induced Oligodendrocyte Injury in the CNS. *J. Neurosci.*, 22(7), pp.2478–2486.

Levin, L.I. et al., 2005. Temporal relationship between elevation of epstein-barr virus antibody titers and initial onset of neurological symptoms in multiple sclerosis. *JAMA : the journal of the American Medical Association*, 293(20), pp.2496–500.

Li, G., Liang, X. & Lotze, M.T., 2013. HMGB1: The Central Cytokine for All Lymphoid Cells. *Frontiers in immunology*, 4, p.68.

Li, G., Tang, D. & Lotze, M.T., 2013. Ménage à Trois in stress: DAMPs, redox and autophagy. *Seminars in cancer biology*, 23(5), pp.380–90.

Li, S. et al., 2004. Blockade of Nogo-66, Myelin-Associated Glycoprotein, and Oligodendrocyte Myelin Glycoprotein by Soluble Nogo-66 Receptor Promotes Axonal Sprouting and Recovery after Spinal Injury. *The Journal of Neuroscience*, 24(46), pp.10511–10520.

Li, W. et al., 2004. A Neutralizing Anti-Nogo66 Receptor Monoclonal Antibody Reverses Inhibition of Neurite Outgrowth by Central Nervous System Myelin. *Journal of Biological Chemistry*, 279(42), pp.43780–43788.

Li, W. et al., 2013. Autophagy is involved in oligodendroglial precursor-mediated clearance of amyloid peptide. *Molecular neurodegeneration*, 8(1), p.27.

Lindersson, E. et al., 2004. Proteasomal inhibition by alpha-synuclein filaments and oligomers. *The Journal of biological chemistry*, 279(13), pp.12924–34.

Linington, C. et al., 1988. Augmentation of demyelination in rat acute allergic encephalomyelitis by circulating mouse monoclonal antibodies directed against a myelin/oligodendrocyte glycoprotein. *The American journal of pathology*, 130(3), pp.443–54.

Lisak, R.P. et al., 2012. Secretory products of multiple sclerosis B cells are cytotoxic to oligodendroglia in vitro. *Journal of neuroimmunology*, 246(1-2), pp.85–95.

Liu, K. et al., 2007. Anti-high mobility group box 1 monoclonal antibody ameliorates brain infarction induced by transient ischemia in rats. *FASEB journal : official publication of the Federation of American Societies for Experimental Biology*, 21(14), pp.3904–16.

Llufriu, S. et al., 2014. Magnetic resonance spectroscopy markers of disease progression in multiple sclerosis. *JAMA neurology*, 71(7), pp.840–7.

Loizou, C.P. et al., 2014. Quantitative texture analysis of brain white matter lesions derived from T2-weighted MR images in MS patients with clinically isolated syndrome. *Journal of neuroradiology. Journal de neuroradiologie*.

Lu, B. et al., 2012. Novel role of PKR in inflammasome activation and HMGB1 release. *Nature*, 488(7413), pp.670–4.

Lucchinetti, C. et al., 2000. Heterogeneity of multiple sclerosis lesions: Implications for the pathogenesis of demyelination. *Annals of Neurology*, 47(6), pp.707–717.

Lucchinetti, C.F. et al., 2011a. Inflammatory cortical demyelination in early multiple sclerosis. *The New England journal of medicine*, 365(23), pp.2188–97.

Lucchinetti, C.F. et al., 2011b. Inflammatory cortical demyelination in early multiple sclerosis. *The New England journal of medicine*, 365(23), pp.2188–97.

Lycke, J.N. et al., 1998. Neurofilament protein in cerebrospinal fluid: a potential marker of activity in multiple sclerosis. *Journal of Neurology, Neurosurgery & Psychiatry*, 64(3), pp.402–404.

Ma, S.-F. et al., 2014. Adoptive transfer of M2 macrophages promotes locomotor recovery in adult rats after spinal cord injury. *Brain, behavior, and immunity*.

Magliozzi, R. et al., 2007a. Meningeal B-cell follicles in secondary progressive multiple sclerosis associate with early onset of disease and severe cortical pathology. *Brain : a journal of neurology*, 130(Pt 4), pp.1089–104.

Magliozzi, R. et al., 2007b. Meningeal B-cell follicles in secondary progressive multiple sclerosis associate with early onset of disease and severe cortical pathology. *Brain : a journal of neurology*, 130(Pt 4), pp.1089–104.

Maher, P.A., 1996. Nuclear Translocation of fibroblast growth factor (FGF) receptors in response to FGF-2. *The Journal of cell biology*, 134(2), pp.529–36.

Malmeström, C. et al., 2003. Neurofilament light protein and glial fibrillary acidic protein as biological markers in MS. *Neurology*, 61(12), pp.1720–5.

Marik, C. et al., 1997. Lesion genesis in a subset of patients with multiple sclerosis: a role for innate immunity? *Brain*, 130, pp.2800–2815.

Maroso, M. et al., 2011. Interleukin-1 type 1 receptor/Toll-like receptor signalling in epilepsy: the importance of IL-1beta and high-mobility group box 1. *Journal of internal medicine*, 270(4), pp.319–26.

Maroso, M. et al., 2010. Toll-like receptor 4 and high-mobility group box-1 are involved in ictogenesis and can be targeted to reduce seizures. *Nature medicine*, 16(4), pp.413–9.

Marti, U. et al., 2001. Nuclear localization of epidermal growth factor and epidermal growth factor receptors in human thyroid tissues. *Thyroid : official journal of the American Thyroid Association*, 11(2), pp.137–45.

Martinez-Vicente, M. et al., 2010. Cargo recognition failure is responsible for inefficient autophagy in Huntington's disease. *Nature neuroscience*, 13(5), pp.567–76.

Massa, P.T., Ozato, K. & McFarlin, D.E., 1993. Cell type-specific regulation of major histocompatibility complex (MHC) class I gene expression in astrocytes, oligodendrocytes, and neurons. *Glia*, 8(3), pp.201–7.

McKerracher, L. et al., 1994. Identification of myelin-associated glycoprotein as a major myelin-derived inhibitor of neurite growth. *Neuron*, 13(4), pp.805–811.

McLaurin, J. et al., 1995. A human glial hybrid cell line differentially expressing genes subserving oligodendrocyte and astrocyte phenotype. *Journal of neurobiology*, 26(2), pp.283–93.

Meinl, E., Krumbholz, M. & Hohlfeld, R., 2006. B lineage cells in the inflammatory central nervous system environment: migration, maintenance, local

antibody production, and therapeutic modulation. *Annals of neurology*, 59(6), pp.880–92.

Merkler, D. et al., 2006. A new focal EAE model of cortical demyelination: multiple sclerosis-like lesions with rapid resolution of inflammation and extensive remyelination. *Brain*, 129(8), pp.1972–1983.

Metz, I. et al., 2014. Pathologic heterogeneity persists in early active multiple sclerosis lesions. *Annals of neurology*, 75(5), pp.728–38.

Mi, S. et al., 2007. LINGO-1 antagonist promotes spinal cord remyelination and axonal integrity in MOG-induced experimental autoimmune encephalomyelitis. *Nature medicine*, 13(10), pp.1228–33.

Mi, S. et al., 2004. LINGO-1 is a component of the Nogo-66 receptor/p75 signaling complex. *Nat Neurosci*, 7(3), pp.221–228.

Mi, S. et al., 2005. LINGO-1 negatively regulates myelination by oligodendrocytes. *Nat Neurosci*, 8(6), pp.745–751.

MILLER, H., NEWELL, D.J. & RIDLEY, A., 1961. Multiple sclerosis. Treatment of acute exacerbations with corticotrophin (A.C.T.H.). *Lancet*, 2(7212), pp.1120–2.

Mina Son, E.K. and J.-S.S., 2012. Role of HMGB1 in TLR3-mediated inflammation -- Son et al. 188 (1001): 180.10 -- The Journal of Immunology. *journal of Immunology*. Available at: http://www.jimmunol.org/cgi/content/meeting_abstract/188/1_MeetingAbstracts/180.10 .

Miron, V.E. et al., 2013. M2 microglia and macrophages drive oligodendrocyte differentiation during CNS remyelination. *Nature neuroscience*, 16(9), pp.1211–8.

Misonou, H. et al., 2004. Regulation of ion channel localization and phosphorylation by neuronal activity. *Nature neuroscience*, 7(7), pp.711–8.

Mistry, N. et al., 2014. Cortical lesion load correlates with diffuse injury of multiple sclerosis normal appearing white matter. *Multiple sclerosis (Houndmills, Basingstoke, England)*, 20(2), pp.227–33.

Mitsouras, K. et al., 2002. The DNA architectural protein HMGB1 displays two distinct modes of action that promote enhanceosome assembly. *Molecular and cellular biology*, 22(12), pp.4390–401.

Miyasho, T. et al., 2011. High mobility group box 1 (HMGB1) protein is present in the cerebrospinal fluid of dogs with encephalitis. *The Journal of veterinary medical science / the Japanese Society of Veterinary Science*, 73(7), pp.917–22.

Mizushima, N. et al., 2004. In vivo analysis of autophagy in response to nutrient starvation using transgenic mice expressing a fluorescent autophagosome marker. *Molecular biology of the cell*, 15(3), pp.1101–11.

Modvig, S. et al., 2013. Relationship between cerebrospinal fluid biomarkers for inflammation, demyelination and neurodegeneration in acute optic neuritis. *PloS one*, 8(10), p.e77163.

Moisy, D. et al., 2012. HMGB1 protein binds to influenza virus nucleoprotein and promotes viral replication. *Journal of virology*, 86(17), pp.9122–33.

Moll, N.M. et al., 2011. Multiple sclerosis normal-appearing white matter: pathology-imaging correlations. *Annals of neurology*, 70(5), pp.764–73.

Momonaka, H. et al., 2014. High mobility group box 1 in patients with 2009 pandemic H1N1 influenza-associated encephalopathy. *Brain & development*, 36(6), pp.484–8.

Moransard, M. et al., 2011. NG2 expressed by macrophages and oligodendrocyte precursor cells is dispensable in experimental autoimmune encephalomyelitis. *Brain : a journal of neurology*, 134(Pt 5), pp.1315–30.

Motizuki, M. et al., 2013. Oligodendrocyte transcription factor 1 (Olig1) is a Smad cofactor involved in cell motility induced by transforming growth factor-β. *The Journal of biological chemistry*, 288(26), pp.18911–22.

Mowry, E.M. et al., 2009. Clinical predictors of early second event in patients with clinically isolated syndrome. *Journal of neurology*, 256(7), pp.1061–6.

Muller, S., Ronfani, L. & Bianchi, M.E., 2004. Regulated expression and subcellular localization of HMGB1, a chromatin protein with a cytokine function. *Journal of Internal Medicine*, 255(3), pp.332–343.

Müller, S., Ronfani, L. & Bianchi, M.E., 2004. Regulated expression and subcellular localization of HMGB1, a chromatin protein with a cytokine function. *Journal of Internal Medicine*, 255(3), pp.332–343.

Murakoshi, H. & Trimmer, J.S., 1999. Identification of the Kv2.1 K+ channel as a major component of the delayed rectifier K+ current in rat hippocampal neurons. *The Journal of neuroscience : the official journal of the Society for Neuroscience*, 19(5), pp.1728–35.

Nair, A., Frederick, T.J. & Miller, S.D., 2008. Astrocytes in multiple sclerosis: a product of their environment. *Cellular and molecular life sciences : CMLS*, 65(17), pp.2702–20.

Nakahara, T. et al., 2009. High-mobility group box 1 protein in CSF of patients with subarachnoid hemorrhage. *Neurocritical care*, 11(3), pp.362–8.

Narcisi, R. et al., 2012. TGF β-1 administration during ex vivo expansion of human articular chondrocytes in a serum-free medium redirects the cell phenotype toward hypertrophy. *Journal of cellular physiology*, 227(9), pp.3282–90.

Nixon, R.A. et al., 2005. Extensive involvement of autophagy in Alzheimer disease: an immuno-electron microscopy study. *Journal of neuropathology and experimental neurology*, 64(2), pp.113–22.

Nixon, R.A., 2013. The role of autophagy in neurodegenerative disease. *Nature medicine*, 19(8), pp.983–97.

Van Noort, J.M. et al., 2010. Alpha b-crystallin is a target for adaptive immune responses and a trigger of innate responses in preactive multiple sclerosis lesions. *J Neuropathol Exp Neurol*, 7, pp.694–703.

Van Noort, J.M. et al., 2010. Alphab-crystallin is a target for adaptive immune responses and a trigger of innate responses in preactive multiple sclerosis lesions. *Journal of neuropathology and experimental neurology*, 69(7), pp.694–703.

Norgren, N. et al., 2004. Neurofilament and glial fibrillary acidic protein in multiple sclerosis. *Neurology*, 63(9), pp.1586–1590.

Norgren, N., Rosengren, L. & Stigbrand, T., 2003. Elevated neurofilament levels in neurological diseases. *Brain Research*, 987(1), pp.25–31.

Nylén, K. et al., 2002. Cerebrospinal fluid neurofilament and glial fibrillary acidic protein in patients with cerebral vasculitis. *Journal of neuroscience research*, 67(6), pp.844–51.

O'Connell, K.M.S., Loftus, R. & Tamkun, M.M., 2010. Localization-dependent activity of the Kv2.1 delayed-rectifier K+ channel. *Proceedings of the National Academy of Sciences of the United States of America*, 107(27), pp.12351–6.

Oda, Y. et al., 2012. Prediction of the neurological outcome with intrathecal high mobility group box 1 and S100B in cardiac arrest victims: a pilot study. *Resuscitation*, 83(8), pp.1006–12.

Oh, Y.J. et al., 2009. HMGB1 is phosphorylated by classical protein kinase C and is secreted by a calcium-dependent mechanism. *Journal of immunology (Baltimore, Md. : 1950)*, 182(9), pp.5800–9.

Oksenberg, J.R. et al., 2008. The genetics of multiple sclerosis: SNPs to pathways to pathogenesis. *Nature reviews. Genetics*, 9(7), pp.516–26.

Okuma, Y. et al., 2012. Anti-high mobility group box-1 antibody therapy for traumatic brain injury. *Annals of neurology*, 72(3), pp.373–84.

Ono, T. et al., 2003a. Alivin 1, a novel neuronal activity-dependent gene, inhibits apoptosis and promotes survival of cerebellar granule neurons. *The Journal of neuroscience : the official journal of the Society for Neuroscience*, 23(13), pp.5887–96.

Ono, T. et al., 2003b. Alivin 1, a novel neuronal activity-dependent gene, inhibits apoptosis and promotes survival of cerebellar granule neurons. *The Journal of neuroscience : the official journal of the Society for Neuroscience*, 23(13), pp.5887–96.

Ono, T. et al., 2009a. Mice deficient in alivin1/amigo2 show enhanced locomotor activity. *Neuroscience Research*, 65(65), p.S228.

Ono, T. et al., 2009b. Mice deficient in alivin1/amigo2 show enhanced locomotor activity. *Neuroscience Research*, 65(65), p.S228.

Ousman, S.S. et al., 2007a. Protective and therapeutic role for alphaB-crystallin in autoimmune demyelination. *Nature*, 448(7152), pp.474–9.

Ousman, S.S. et al., 2007b. Protective and therapeutic role for alphaB-crystallin in autoimmune demyelination. *Nature*, 448(7152), pp.474–9.

Palace, J. et al., 2015. Effectiveness and cost-effectiveness of interferon beta and glatiramer acetate in the UK Multiple Sclerosis Risk Sharing Scheme at 6 years: a clinical cohort study with natural history comparator. *The Lancet. Neurology*, 14(5), pp.497–505.

Park, J.B. et al., 2005. A TNF Receptor Family Member, TROY, Is a Coreceptor with Nogo Receptor in Mediating the Inhibitory Activity of Myelin Inhibitors. *Neuron*, 45(3), pp.345–351.

Parkkinen, J. et al., 1993. Amphoterin, the 30-kDa protein in a family of HMG1-type polypeptides. Enhanced expression in transformed cells, leading edge localization, and interactions with plasminogen activation. *The Journal of biological chemistry*, 268(26), pp.19726–38.

Peltola, M.A. et al., 2011. AMIGO is an auxiliary subunit of the Kv2.1 potassium channel. *EMBO reports*, 12(12), pp.1293–9.

Pepinsky, R.B. et al., 2014. Structure of the LINGO-1-anti-LINGO-1 Li81 antibody complex provides insights into the biology of LINGO-1 and the mechanism of action of the antibody therapy. *The Journal of pharmacology and experimental therapeutics*, 350(1), pp.110–23.

Petzold, A. et al., 2010. Neurofilament ELISA validation. *Journal of immunological methods*, 352(1-2), pp.23–31.

Petzold, A., 2005. Neurofilament phosphoforms: surrogate markers for axonal injury, degeneration and loss. *Journal of the neurological sciences*, 233(1-2), pp.183–98.

Pirkmajer, S. & Chibalin, A. V, 2011. Serum starvation: caveat emptor. *American journal of physiology. Cell physiology*, 301(2), pp.C272–9.

Pittas, F. et al., 2009. Smoking is associated with progressive disease course and increased progression in clinical disability in a prospective cohort of people with multiple sclerosis. *Journal of neurology*, 256(4), pp.577–85.

Pittet, J.-F. et al., 2013. HMGB1 accelerates alveolar epithelial repair via an IL-1β- and αvβ6 integrin-dependent activation of TGF-β1. *PloS one*, 8(5), p.e63907.

Polman, C.H. et al., 2006. A randomized, placebo-controlled trial of natalizumab for relapsing multiple sclerosis. *The New England journal of medicine*, 354(9), pp.899–910.

Polman, C.H. et al., 2005. Diagnostic criteria for multiple sclerosis: 2005 revisions to the "McDonald Criteria". *Annals of neurology*, 58(6), pp.840–6.

Polman, C.H. et al., 2011. Diagnostic criteria for multiple sclerosis: 2010 revisions to the McDonald criteria. *Annals of neurology*, 69(2), pp.292–302.

Pranzatelli, M.R. et al., 2014. CSF neurofilament light chain is elevated in OMS (decreasing with immunotherapy) and other pediatric neuroinflammatory disorders. *Journal of neuroimmunology*, 266(1-2), pp.75–81.

Presslauer, S. et al., 2008. Elevated levels of kappa free light chains in CSF support the diagnosis of multiple sclerosis. *Journal of neurology*, 255(10), pp.1508–14.

Presslauer, S. et al., 2014. Kappa free light chains: diagnostic and prognostic relevance in MS and CIS. P. Villoslada, ed. *PloS one*, 9(2), p.e89945.

Pua, H.H. et al., 2007. A critical role for the autophagy gene Atg5 in T cell survival and proliferation. *The Journal of experimental medicine*, 204(1), pp.25–31.

Pyykkö, O.T. et al., 2014. Cerebrospinal fluid biomarker and brain biopsy findings in idiopathic normal pressure hydrocephalus. *PloS one*, 9(3), p.e91974.

Qin, H. et al., 2009. TGF-beta promotes Th17 cell development through inhibition of SOCS3. *Journal of immunology (Baltimore, Md. : 1950)*, 183(1), pp.97–105.

Qiu, J. et al., 2007. Early release of HMGB-1 from neurons after the onset of brain ischemia. *J Cereb Blood Flow Metab*, 28(5), pp.927–938.

Rabenau, K.E. et al., 2004. DEGA/AMIGO-2, a leucine-rich repeat family member, differentially expressed in human gastric adenocarcinoma: effects on ploidy,

chromosomal stability, cell adhesion/migration and tumorigenicity. *Oncogene*, 23(29), pp.5056–67.

Rauvala, H. et al., 1988. The adhesive and neurite-promoting molecule p30: analysis of the amino-terminal sequence and production of antipeptide antibodies that detect p30 at the surface of neuroblastoma cells and of brain neurons. *The Journal of cell biology*, 107(6 Pt 1), pp.2293–305.

Rauvala, H. & Pihlaskari, R., 1987. Isolation and some characteristics of an adhesive factor of brain that enhances neurite outgrowth in central neurons. *J Biol Chem*, 262(34), pp.16625–16635.

Ravizza, T. et al., 2006. The IL-1beta system in epilepsy-associated malformations of cortical development. *Neurobiology of disease*, 24(1), pp.128–43.

Van Rechem, C. et al., 2010. Differential regulation of HIC1 target genes by CtBP and NuRD, via an acetylation/SUMOylation switch, in quiescent versus proliferating cells. *Molecular and cellular biology*, 30(16), pp.4045–59.

Redwine, J.M., Buchmeier, M.J. & Evans, C.F., 2001. In vivo expression of major histocompatibility complex molecules on oligodendrocytes and neurons during viral infection. *The American journal of pathology*, 159(4), pp.1219–24.

Rhodes, K.E., Raivich, G. & Fawcett, J.W., 2006a. The injury response of oligodendrocyte precursor cells is induced by platelets, macrophages and inflammation-associated cytokines. *Neuroscience*, 140(1), pp.87–100.

Rhodes, K.E., Raivich, G. & Fawcett, J.W., 2006b. The injury response of oligodendrocyte precursor cells is induced by platelets, macrophages and inflammation-associated cytokines. *Neuroscience*, 140(1), pp.87–100.

Rice, C.M. et al., 2013. Primary progressive multiple sclerosis: progress and challenges. *Journal of neurology, neurosurgery, and psychiatry*, 84(10), pp.1100–6.

Rivers, T.M. & Schwentker, F.F., 1935. ENCEPHALOMYELITIS ACCOMPANIED BY MYELIN DESTRUCTION EXPERIMENTALLY PRODUCED IN MONKEYS. *The Journal of experimental medicine*, 61(5), pp.689–702.

Romme Christensen, J. et al., 2014. Natalizumab in progressive MS: Results of an open-label, phase 2A, proof-of-concept trial. *Neurology*, 82(17), pp.1499–507.

Rosengren, L.E. et al., 2002. Patients with Amyotrophic Lateral Sclerosis and Other Neurodegenerative Diseases Have Increased Levels of Neurofilament Protein in CSF. *Journal of Neurochemistry*, 67(5), pp.2013–2018.

Rosengren, L.E. et al., 1996. Patients with amyotrophic lateral sclerosis and other neurodegenerative diseases have increased levels of neurofilament protein in CSF. *Journal of neurochemistry*, 67(5), pp.2013–8.

Rouhiainen, A. et al., 2000. Occurrence of amphoterin (HMG1) as an endogenous protein of human platelets that is exported to the cell surface upon platelet activation. *Thrombosis and haemostasis*, 84(6), pp.1087–94.

Rouhiainen, A. et al., 2007. Pivotal advance: analysis of proinflammatory activity of highly purified eukaryotic recombinant HMGB1 (amphoterin). *Journal of leukocyte biology*, 81(1), pp.49–58.

Rouhiainen, A. et al., 2004. Regulation of monocyte migration by amphoterin (HMGB1). *Blood*, 104(4), pp.1174–1182.

Rudick, R.A., Mi, S. & Sandrock, A.W., 2008. LINGO-1 antagonists as therapy for multiple sclerosis: in vitro and in vivo evidence. *Expert opinion on biological therapy*, 8(10), pp.1561–70.

Sadovnick, A.D. et al., 1996. Evidence for genetic basis of multiple sclerosis. The Canadian Collaborative Study Group. *Lancet*, 347(9017), pp.1728–30.

Salminen, A. et al., 2013. Impaired autophagy and APP processing in Alzheimer's disease: The potential role of Beclin 1 interactome. *Progress in neurobiology*, 106-107, pp.33–54.

Sapojnikova, N. et al., 2014. Correlation between MMP-9 and extracellular cytokine HMGB1 in prediction of human ischemic stroke outcome. *Biochimica et biophysica acta*, 1842(9), pp.1379–1384.

Satoh, J. et al., 2007. TROY and LINGO-1 expression in astrocytes and macrophages/microglia in multiple sclerosis lesions. *Neuropathology and Applied Neurobiology*, 33(1), pp.99–107.

Satoh, J.-I. et al., 2014. LC3, an autophagosome marker, is expressed on oligodendrocytes in Nasu-Hakola disease brains. *Orphanet journal of rare diseases*, 9, p.68.

Sawcer, S., Franklin, R.J.M. & Ban, M., 2014. Multiple sclerosis genetics. *The Lancet. Neurology*, 13(7), pp.700–9.

Scaffidi, P., Misteli, T. & Bianchi, M.E., 2002. Release of chromatin protein HMGB1 by necrotic cells triggers inflammation. *Nature*, 418(6894), pp.191–195.

Scalfari, A. et al., 2013. Mortality in patients with multiple sclerosis. *Neurology*, 81(2), pp.184–92.

Schattling, B., Eggert, B. & Friese, M.A., 2014. Acquired channelopathies as contributors to development and progression of multiple sclerosis. *Experimental neurology*, 262PA, pp.28–36.

Schiraldi, M. et al., 2012. HMGB1 promotes recruitment of inflammatory cells to damaged tissues by forming a complex with CXCL12 and signaling via CXCR4. *The Journal of Experimental Medicine*, 209(3), pp.551–563.

Schnaar, R.L. & Lopez, P.H.H., 2009. Myelin-associated glycoprotein and its axonal receptors. *Journal of Neuroscience Research*, 87(15), pp.3267–3276.

Schwartz, M. & Raposo, C., 2014. Protective Autoimmunity: A Unifying Model for the Immune Network Involved in CNS Repair. *The Neuroscientist : a review journal bringing neurobiology, neurology and psychiatry*, 20(4), pp.343–358.

Semino, C. et al., 2005. NK/iDC interaction results in IL-18 secretion by DCs at the synaptic cleft followed by NK cell activation and release of the DC maturation factor HMGB1. *Blood*, 106(2), pp.609–16.

Semino, C. et al., 2007. The maturation potential of NK cell clones toward autologous dendritic cells correlates with HMGB1 secretion. *Journal of leukocyte biology*, 81(1), pp.92–9.

Semra, Y.K., Seidi, O.A. & Sharief, M.K., 2002. Heightened intrathecal release of axonal cytoskeletal proteins in multiple sclerosis is associated with progressive disease and clinical disability. *Journal of neuroimmunology*, 122(1-2), pp.132–9.

Sena, A. et al., 2012. Oral contraceptive use and clinical outcomes in patients with multiple sclerosis. *Journal of the neurological sciences*, 317(1-2), pp.47–51.

Senel, M. et al., 2014. Cerebrospinal fluid immunoglobulin kappa light chain in clinically isolated syndrome and multiple sclerosis. *PloS one*, 9(4), p.e88680.

Seo, J.H. et al., 2013. Oligodendrocyte precursors induce early blood-brain barrier opening after white matter injury. *The Journal of clinical investigation*, 123(2), pp.782–6.

Serafini, B. et al., 2004. Detection of ectopic B-cell follicles with germinal centers in the meninges of patients with secondary progressive multiple sclerosis. *Brain pathology (Zurich, Switzerland)*, 14(2), pp.164–74.

Shao, Z. et al., 2005. TAJ/TROY, an Orphan TNF Receptor Family Member, Binds Nogo-66 Receptor 1 and Regulates Axonal Regeneration. *Neuron*, 45(3), pp.353–359.

Shi, Y. et al., 2012. Enhanced HMGB1 expression may contribute to Th17 cells activation in rheumatoid arthritis. *Clinical & developmental immunology*, 2012, p.295081.

Shirani, A. et al., 2012. Association between use of interferon beta and progression of disability in patients with relapsing-remitting multiple sclerosis. *JAMA : the journal of the American Medical Association*, 308(3), pp.247–56.

Shoji-Kawata, S. et al., 2013. Identification of a candidate therapeutic autophagy-inducing peptide. *Nature*, 494(7436), pp.201–6.

Singh, S. et al., 2013. Microglial nodules in early multiple sclerosis white matter are associated with degenerating axons. *Acta neuropathologica*, 125(4), pp.595–608.

Smith, C.M., Mayer, J.A. & Duncan, I.D., 2013. Autophagy promotes oligodendrocyte survival and function following dysmyelination in a long-lived myelin mutant. *The Journal of neuroscience : the official journal of the Society for Neuroscience*, 33(18), pp.8088–100.

Song, B. et al., 2012. Effect of HMGB1 silencing on cell proliferation, invasion and apoptosis of MGC-803 gastric cancer cells. *Cell biochemistry and function*, 30(1), pp.11–7.

Sterner, R., Vidali, G. & Allfrey, V.G., 1979. Studies of acetylation and deacetylation in high mobility group proteins. Identification of the sites of acetylation in HMG-1. *Journal of Biological Chemistry* , 254 (22), pp.11577–11583.

Su, Z. et al., 2011. HMGB1 blockade attenuates experimental autoimmune myocarditis and suppresses Th17-cell expansion. *European journal of immunology*, 41(12), pp.3586–95.

Sundberg, E. et al., 2009. High mobility group box chromosomal protein 1 acts as a proliferation signal for activated T lymphocytes. *Immunobiology*, 214(4), pp.303–9.

Takahashi, N., Takahashi, Y. & Putnam, F.W., 1985. Periodicity of leucine and tandem repetition of a 24-amino acid segment in the primary structure of leucine-rich alpha 2-glycoprotein of human serum. *Proceedings of the National Academy of Sciences of the United States of America*, 82(7), pp.1906–10.

Takata, K. et al., 2004. High mobility group box protein-1 inhibits microglial Abeta clearance and enhances Abeta neurotoxicity. *Journal of neuroscience research*, 78(6), pp.880–91.

Takata, K. et al., 2003. Role of high mobility group protein-1 (HMG1) in amyloid-β homeostasis. *Biochemical and Biophysical Research Communications*, 301(3), pp.699–703.

Tang, D. et al., 2008. A pilot study to detect high mobility group box 1 and heat shock protein 72 in cerebrospinal fluid of pediatric patients with meningitis. *Critical care medicine*, 36(1), pp.291–5.

Tang, D. et al., 2010. Endogenous HMGB1 regulates autophagy. *The Journal of Cell Biology*, 190(5), pp.881–892.

Tang, D. et al., 2011a. High-mobility group box 1 is essential for mitochondrial quality control. *Cell metabolism*, 13(6), pp.701–11.

Tang, D. et al., 2011b. High-mobility group box 1 is essential for mitochondrial quality control. *Cell metabolism*, 13(6), pp.701–11.

Taylor, D.L. et al., 2010. Attenuation of proliferation in oligodendrocyte precursor cells by activated microglia. *Journal of neuroscience research*, 88(8), pp.1632–44.

Teunissen, C.E. et al., 2009. Combination of CSF N-acetylaspartate and neurofilaments in multiple sclerosis. *Neurology*, 72(15), pp.1322–9.

Teunissen, C.E., Dijkstra, C. & Polman, C., 2005. Biological markers in CSF and blood for axonal degeneration in multiple sclerosis. *Lancet neurology*, 4(1), pp.32–41.

Teunissen, C.E. & Khalil, M., 2012. Neurofilaments as biomarkers in multiple sclerosis. *Multiple sclerosis (Houndmills, Basingstoke, England)*, 18(5), pp.552–6.

Thallmair, M. et al., 1998. Neurite growth inhibitors restrict plasticity and functional recovery following corticospinal tract lesions. *Nature neuroscience*, 1(2), pp.124–31.

The IFNB Multiple Sclerosis Study Group, 1993. Interferon beta-1b is effective in relapsing-remitting multiple sclerosis: I. Clinical results of a multicenter, randomized, double-blind, placebo-controlled trial. *Neurology*, 43(4), pp.655–655.

Tian, J. et al., 2007. Toll-like receptor 9-dependent activation by DNA-containing immune complexes is mediated by HMGB1 and RAGE. *Nature immunology*, 8(5), pp.487–96.

Tintor??, M. et al., 2008. Do oligoclonal bands add information to MRI in first attacks of multiple sclerosis? *Neurology*, 70(13 PART 2), pp.1079–1083.

Tortelli, R. et al., 2014. Cerebrospinal fluid neurofilament light chain levels: marker of progression to generalized amyotrophic lateral sclerosis. *European journal of neurology : the official journal of the European Federation of Neurological Societies*.

Tortelli, R. et al., 2012. Elevated cerebrospinal fluid neurofilament light levels in patients with amyotrophic lateral sclerosis: a possible marker of disease severity and progression. *European journal of neurology : the official journal of the European Federation of Neurological Societies*, 19(12), pp.1561–7.

Traboulsee, A. et al., 2003. Disability in multiple sclerosis is related to normal appearing brain tissue MTR histogram abnormalities. *Multiple sclerosis (Houndmills, Basingstoke, England)*, 9(6), pp.566–73.

Tran, J.Q. et al., 2014. Randomized phase I trials of the safety/tolerability of anti-LINGO-1 monoclonal antibody BIIB033. *Neurology® neuroimmunology & neuroinflammation*, 1(2), p.e18.

Trapp, B.D. et al., 1998. Axonal Transection in the Lesions of Multiple Sclerosis. *New England Journal of Medicine*, 338(5), pp.278–285.

Trapp, B.D. & Stys, P.K., 2009. Virtual hypoxia and chronic necrosis of demyelinated axons in multiple sclerosis. *Lancet neurology*, 8(3), pp.280–91.

Trojano, M. et al., 2009. Real-life impact of early interferon beta therapy in relapsing multiple sclerosis. *Annals of neurology*, 66(4), pp.513–20.

Trysberg, E. et al., 2003. Neuronal and astrocytic damage in systemic lupus erythematosus patients with central nervous system involvement. *Arthritis and rheumatism*, 48(10), pp.2881–7.

Tsan, M.-F., 2011. Heat shock proteins and high mobility group box 1 protein lack cytokine function. *Journal of leukocyte biology*, 89(6), pp.847–53.

Tsan, M.-F. & Gao, B., 2004. Endogenous ligands of Toll-like receptors. *Journal of leukocyte biology*, 76(3), pp.514–9.

Uzawa, A. et al., 2013. Anti-high mobility group box 1 monoclonal antibody ameliorates experimental autoimmune encephalomyelitis. *Clinical and experimental immunology*, 172(1), pp.37–43.

Uzawa, A. et al., 2013. CSF high-mobility group box 1 is associated with intrathecal inflammation and astrocytic damage in neuromyelitis optica. *Journal of neurology, neurosurgery, and psychiatry*, 84(5), pp.517–22.

Van der Valk, P. & Amor, S., 2009. Preactive lesions in multiple sclerosis. *Curr Opin Neurol*, 3, pp.207–213.

Vandeputte, D.A.A. et al., 2002. Expression and distribution of id helix-loop-helix proteins in human astrocytic tumors. *Glia*, 38(4), pp.329–38.

Venereau, E. et al., 2012. Mutually exclusive redox forms of HMGB1 promote cell recruitment or proinflammatory cytokine release. *The Journal of experimental medicine*, 209(9), pp.1519–28.

Vettermann, C. et al., 2011. Proteome profiling suggests a pro-inflammatory role for plasma cells through release of high-mobility group box 1 protein. *Proteomics*, 11(7), pp.1228–37.

Villar, L.M. et al., 2012. High levels of cerebrospinal fluid free kappa chains predict conversion to multiple sclerosis. *Clinica chimica acta; international journal of clinical chemistry*, 413(23-24), pp.1813–6.

Vogel, D.Y.S. et al., 2013. Macrophages in inflammatory multiple sclerosis lesions have an intermediate activation status. *Journal of neuroinflammation*, 10(1), p.35.

Vourc'h, P. & Andres, C., 2004. Oligodendrocyte myelin glycoprotein (OMgp): evolution, structure and function. *Brain research. Brain research reviews*, 45(2), pp.115–24.

Vrenken, H. et al., 2006. Normal-Appearing White Matter Changes Vary with Distance to Lesions in Multiple Sclerosis. *AJNR Am. J. Neuroradiol.*, 27(9), pp.2005–2011.

Wang, H. et al., 2013. Cerebrospinal fluid high-mobility group box protein 1 in neuromyelitis optica and multiple sclerosis. *Neuroimmunomodulation*, 20(2), pp.113–8.

Wang, H., 1999. HMG-1 as a Late Mediator of Endotoxin Lethality in Mice. *Science*, 285(5425), pp.248–251.

Wang, H. et al., 1999. Proinflammatory cytokines (tumor necrosis factor and interleukin 1) stimulate release of high mobility group protein-1 by pituicytes. *Surgery*, 126(2), pp.389–92.

Wang, K.C. et al., 2002. p75 interacts with the Nogo receptor as a co-receptor for Nogo, MAG and OMgp. *Nature*, 420(6911), pp.74–78.

Wang, K.-C. et al., 2012. Elevated plasma high-mobility group box 1 protein is a potential marker for neuromyelitis optica. *Neuroscience*, 226, pp.510–6.

Weinstock-Guttman, B. et al., 2011. Vitamin D metabolites are associated with clinical and MRI outcomes in multiple sclerosis patients. *Journal of neurology, neurosurgery, and psychiatry*, 82(2), pp.189–95.

Werring, D.J. et al., 1999. Diffusion tensor imaging of lesions and normal-appearing white matter in multiple sclerosis. *Neurology*, 52(8), pp.1626–32.

Wild, C.A. et al., 2012. HMGB1 conveys immunosuppressive characteristics on regulatory and conventional T cells. *International immunology*, 24(8), pp.485–94.

Wilkins, A. et al., 2003. Oligodendrocytes Promote Neuronal Survival and Axonal Length by Distinct Intracellular Mechanisms: A Novel Role for Oligodendrocyte-Derived Glial Cell Line-Derived Neurotrophic Factor. *J. Neurosci.*, 23(12), pp.4967–4974.

Wilkins, A., Chandran, S. & Compston, A., 2001. A role for oligodendrocyte-derived IGF-1 in trophic support of cortical neurons. *Glia*, 36(1), pp.48–57.

Williams, A., Piaton, G. & Lubetzki, C., 2007. Astrocytes--friends or foes in multiple sclerosis? *Glia*, 55(13), pp.1300–12.

Winslow, A.R. et al., 2010. α-Synuclein impairs macroautophagy: implications for Parkinson's disease. *The Journal of cell biology*, 190(6), pp.1023–37.

De Wit, J. et al., 2011. Role of Leucine-Rich Repeat Proteins in the Development and Function of Neural Circuits. *Annual Review of Cell and Developmental Biology*, 27(1), pp.697–729.

Witte, M.E. et al., 2014. Mitochondrial dysfunction contributes to neurodegeneration in multiple sclerosis. *Trends in molecular medicine*, 20(3), pp.179–87.

Wolswijk, G., 1998. Chronic Stage Multiple Sclerosis Lesions Contain a Relatively Quiescent Population of Oligodendrocyte Precursor Cells. *The Journal of Neuroscience*, 18(2), pp.601–609.

Wolswijk, G., 1998. Chronic stage multiple sclerosis lesions contain a relatively quiescent population of oligodendrocyte precursor cells. *The Journal of neuroscience : the official journal of the Society for Neuroscience*, 18(2), pp.601–9.

Wraith, D.C. & Nicholson, L.B., 2012. The adaptive immune system in diseases of the central nervous system. *The Journal of clinical investigation*, 122(4), pp.1172–9.

Xin, M. et al., 2005. Myelinogenesis and axonal recognition by oligodendrocytes in brain are uncoupled in Olig1-null mice. *The Journal of neuroscience : the official journal of the Society for Neuroscience*, 25(6), pp.1354–65.

Yamada, S., 2003. High Mobility Group Protein 1 (HMGB1) Quantified by ELISA with a Monoclonal Antibody That Does Not Cross-React with HMGB2. *Clinical Chemistry*, 49(9), pp.1535–1537.

Yamasaki, R. et al., 2014. Differential roles of microglia and monocytes in the inflamed central nervous system. *The Journal of experimental medicine*.

Yanai, H. et al., 2009. HMGB proteins function as universal sentinels for nucleic-acid-mediated innate immune responses. *Nature*, 462(7269), pp.99–103.

Yang, D. et al., 2007. High mobility group box-1 protein induces the migration and activation of human dendritic cells and acts as an alarmin. *J Leukoc Biol*, 81(1), pp.59–66.

Yang, H. et al., 2010. A critical cysteine is required for HMGB1 binding to Toll-like receptor 4 and activation of macrophage cytokine release. *Proceedings of the National Academy of Sciences*, 107(26), pp.11942–11947.

Yang, H. et al., 2013. The many faces of HMGB1: molecular structure-functional activity in inflammation, apoptosis, and chemotaxis. *Journal of Leukocyte Biology* , 93 (6), pp.865–873.

Yao, S. et al., 2010. LPS mediated injury to oligodendrocytes is mediated by the activation of nNOS: relevance to human demyelinating disease. *Nitric oxide : biology and chemistry / official journal of the Nitric Oxide Society*, 22(3), pp.197–204.

Yao, S.-Y., Natarajan, C. & Sriram, S., 2012. nNOS mediated mitochondrial injury in LPS stimulated oligodendrocytes. *Mitochondrion*, 12(2), pp.336–44.

Yu, S.H. & Spring, T.G., 1977. The interaction of nonhistone chromosomal proteins HMG1 and HMG2 with subfractions of H1 histone immobilized on agarose. *Biochimica et biophysica acta*, 492(1), pp.20–8.

Zeis, T. et al., 2009. Molecular changes in white matter adjacent to an active demyelinating lesion in early multiple sclerosis. *Brain Pathol*, 19, pp.459–466.

Zeis, T. et al., 2009. Molecular changes in white matter adjacent to an active demyelinating lesion in early multiple sclerosis. *Brain pathology (Zurich, Switzerland)*, 19(3), pp.459–66.

Zeis, T. et al., 2008. Normal-appearing white matter in multiple sclerosis is in a subtle balance between inflammation and neuroprotection. *Brain*, 131, pp.288–303.

Zeis, T. & Schaeren-Wiemers, N., 2008. Lame ducks or fierce creatures? The role of oligodendrocytes in multiple sclerosis. *Journal of molecular neuroscience : MN*, 35(1), pp.91–100.

Zhang, J. et al., 2011. Anti-high mobility group box-1 monoclonal antibody protects the blood-brain barrier from ischemia-induced disruption in rats. *Stroke; a journal of cerebral circulation*, 42(5), pp.1420–8.

Zhao, X. et al., 2014a. Amigo adhesion protein regulates development of neural circuits in zebrafish brain. *The Journal of biological chemistry*, 289(29), pp.19958–75.

Zhao, X. et al., 2014b. Amigo adhesion protein regulates development of neural circuits in zebrafish brain. *The Journal of biological chemistry*, 289(29), pp.19958–75.

Zhao, X. et al., 2011. High Mobility Group Box-1 (HMGB1; Amphoterin) Is Required for Zebrafish Brain Development. *Journal of Biological Chemistry*, 286(26), pp.23200–23213.

Zhou, X., Spittau, B. & Krieglstein, K., 2012. TGFβ signalling plays an important role in IL4-induced alternative activation of microglia. *Journal of neuroinflammation*, 9, p.210.

Zou, J.Y. & Crews, F.T., 2014. Release of Neuronal HMGB1 by Ethanol through Decreased HDAC Activity Activates Brain Neuroimmune Signaling. *PloS one*, 9(2), p.e87915.

Zurolo, E. et al., 2011. Activation of Toll-like receptor, RAGE and HMGB1 signalling in malformations of cortical development. *Brain*, 134(Pt 4), pp.1015–1032.

APPENDIX 1

APPENDIX 2

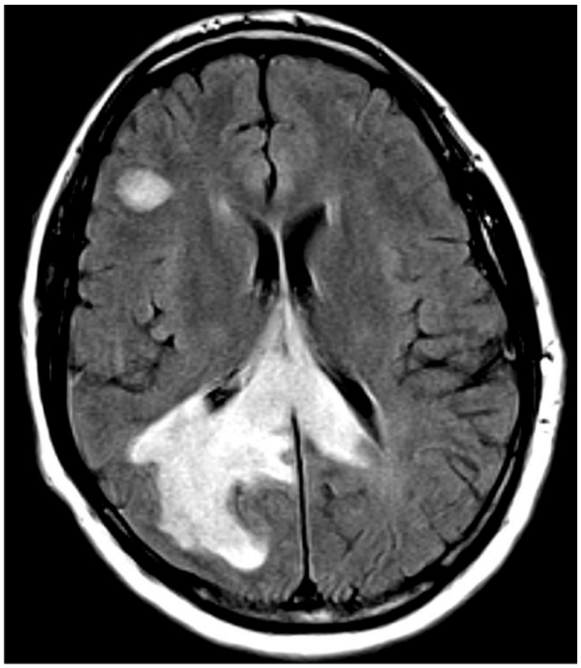

Figure A1. Patient MS1. T2-weighted Axial FLAIR MRI - taken from presenting scan performed at referring hospital, demonstrating multifocal parenchymal changes in the right occipital lobe extending into the corpus callosum, as well as a juxtacortical lesion in the right frontal lobe. *MRI- magnetic resonance imaging*

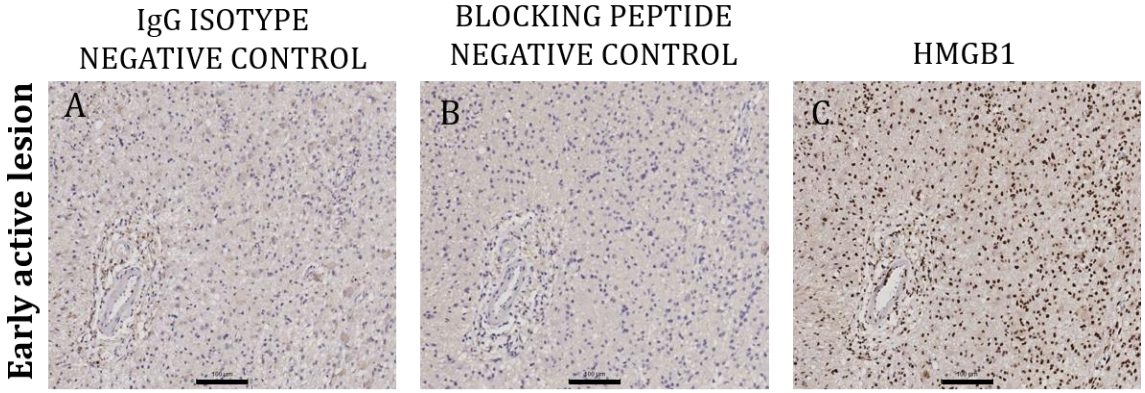

Figure A2. HMGB1-positive staining is specific when compared to the staining pattern using negative controls. Negative controls were performed by (A) using affinity-purified rabbit polyclonal IgG isotype control (B) using preimmune serum from the rabbit immunised with the specific HMGB1 peptide sequence, at a dilution of 1:400. The staining is markedly reduced in the negative control data as compared to the positive anti-HMGB1 staining pattern as shown in (C) for comparison. Scale bar = 100μm